High Integrity Map Matching Algorithms for Advanced Transport Telematics Applications

Article · January 2006

CITATIONS
108

READS
3,230

1 author:

Mohammed Quddus
Imperial College London
163 PUBLICATIONS **12,678** CITATIONS

SEE PROFILE

High Integrity Map Matching Algorithms for Advanced Transport Telematics Applications

Mohammed A. Quddus

B.Sc. Civil Eng., M. Eng. (Civil)

A thesis submitted as fulfilment of the requirements
for the degree of Doctor of Philosophy of the University of London
and for the Diploma of Membership of Imperial College London

Centre for Transport Studies
Department of Civil and Environmental Engineering
Imperial College London, United Kingdom
January 2006

Dedicated to my wife *Fatima* and my parents

ABSTRACT

The key aim of this research is to contribute to the development of a robust and reliable navigation system in order to support the positioning requirements of advanced transport telematics (ATT) services. This is achieved through the development of high integrity map matching algorithms.

In the last two decades, satellite navigation technology, especially the Global Positioning System (GPS), has established itself as a major positioning technology for land vehicle navigation. Deduced Reckoning (DR) sensors, which consist of an odometer and a gyroscope, are commonly used to bridge any gaps in GPS positioning. However, DR sensor positioning errors can grow rapidly if not controlled by another sensor or system such as GPS. Digital road maps are used for spatial reference of the vehicle location via a process known as map matching. Map matching algorithms use inputs generated from positioning technologies and supplement this with data from a high resolution digital road network map to provide an enhanced positioning output. Existing map matching algorithms have weaknesses which decrease their capability to support many ATT services. Three high integrity map matching algorithms are developed in this research. They are the improved topological, probabilistic, and fuzzy logic map matching algorithms. These algorithms are successfully implemented, tested and validated using real field test data. A reference (truth) vehicle trajectory, as determined by high accuracy GPS carrier phase positioning, is used to validate the algorithms. The integrity (level of confidence) of the algorithms is analysed by taking into account the uncertainty associated with the map-matched location and the error sources associated with the navigation system and the digital map. The effects of navigation systems and digital map quality on the performance of map matching algorithms are also investigated for suburban and urban road networks.

The results suggest that all three map matching algorithms developed in the course of this research have the potential to support the navigation function of a wide range of ATT services. However, of the three, the fuzzy logic map matching algorithm offers the highest performance, both in terms of link identification and location determination.

ACKNOWLEDGEMENTS

I would like to express my most sincere thanks and gratitude to my supervisors, Dr. Robert Noland and Dr. Washington Ochieng for their stimulating discussions, patient guidance, constructive comments, mathematical direction, and critical reviews of my research throughout the course of this research work. This thesis would not have been possible at all without their support and encouragement. Exceptional financial backing from Dr. R. Noland and Dr. W. Ochieng is also gratefully acknowledged.

Heartfelt thanks and appreciation are due to Mr. Robin North, Dr Shaojun Feng and Mr. Jahangeer Ashraf for their extensive help during field trials. I am also gratefully acknowledged the hard work of Mr. Robin North to proof read my thesis. Continual discussions with Dr. Shaojun Feng and Dr. Lin Zhao also greatly helped to renovate my navigation concepts.

Particular thanks to Professor Michael Bell, Mr. Richard Anderson, and Professor John Polak for providing sporadic but timely funding opportunities which helped to keep me in continuous employment with Imperial College London.

Special thanks are extended to my colleagues and friends at Imperial namely, Mr. Mahmud Ashraf, Mr. Steve Robinson, Mr. Jan-Dirk Schmoecker, Dr. Stephane Hess, Dr. Daniel Graham, Mrs. Jackie Sime, Mr. Rajesh Krishnan, Mr. Zia Wadud, Dr. Arnab Majumdar, Mr. Lyoong Oh, Mr. Moazzam Ishaque, Mr. Omar Bhatti, and Mr. Motalib Hossain for their enjoyable company and encouragement during the study period.

Many thanks are also due to all CTS (Centre for Transport Studies) members. It has been my great pleasure to work with so many scholars and talented people.

Mohammed Quddus
Centre for Transport Studies
Imperial College London

Table of Contents

List of Figures

List of Tables

CHAPTER 1

INTRODUCTION

1.1 Background

Telematics is the science of distributing, receiving, and storing information by means of telecommunication devices in conjunction with informatics systems. It is normally applied to pass information from one computer to another using a communication platform (either by wire or over the air) and hence permits access to any form of knowledge at a given location. This allows control, management, or service functions which can speed up the dissemination of information, save time, increase cooperation between individuals and groups, and enhance the quality of services. Since telematics is achieved through generic technologies, this can be applied to many different sectors, specifically transport, healthcare, distance learning, teleservices, emergency services, and libraries.

The application of telematics in the transport sector is increasingly seen as a new possibility for improving the performance of transport systems while maintaining the conditions imposed by environmental and safety goals (Nijkamp et al., 1996). Transport for London, for instance, is introducing GPS satellite technology to all 8000 London buses to provide bus arrival times to passengers at bus stops[1]. Due to the sophisticated telematics devices required for transport applications, these systems are collectively known as *Advanced Transport Telematics Systems* (ATTS).

[1] London Buses, Home Page: http://www.tfl.gov.uk/buses, Accessed July 2005.

The term *"Advanced Transport Telematics Systems (ATTS)"* is normally used in Europe, the equivalent term used in America and Japan is *"Intelligent Transportation Systems (ITS)"*. A few definitions of ITS are presented below:

ITS America (1992) - *"ITS is composed of a number of technologies, including information processing, communications, control, and electronics. Joining these technologies to our transportation system can save lives, save time, and save money"*.

National Research Council, NRC (2004) - *"ITS applies computers, information management, advanced electronics, and communications technology to reduce traffic congestion, enhance safety, save energy, and in other ways generally improve the performance of the nation's highways and transit"*.

Drane and Rizos (1998) - *"ITS is a worldwide movement to use advanced technology to make our surface transport systems more efficient, less congested, safer and less polluting"*.

Therefore, ATTS (or ITS) can be defined as the integrated application of advanced sensors, computers, electronics, navigation, and communication technologies to vehicles and roadways to increase safety, reduce congestion, enhance mobility, minimize environmental impact, increase energy efficiency, and promote economic productivity for a healthier economy. ATT offers an opportunity for revolutionary and integrated rethinking of urban and regional transport planning. Acknowledging the rapid change in travel behaviour patterns and information impacts, transport telematics seeks to facilitate faster, easier, better and safer multi-modal travel.

Major ATTS research and development programs are underway in the United States, Europe, and Japan (ITS America, 1992; Elliot and Darley, 1995). The details of potential applications of ATTS can be found in Nijkamp et al. (1996), McQueen and McQueen (1999), and Klein (2001). According to ITS America (1992), there are five major functional areas in ITS:

- Advanced Traffic Management Systems (ATMS)
- Advanced Traveller Information Systems (ATIS)

- Advanced Vehicle Control Systems (AVCS)
- Commercial Vehicle Operations (CVO)
- Advanced Public Transport Systems (APTS)

Advanced Traffic Management Systems (ATMS) make use of advanced surveillance, navigation, communication, and computer technology to monitor, analyse, and improve the performance of transport systems. The main elements of ATMS include dynamic traffic control systems, motorway ramp metering, incident management systems and congestion management.

Advanced Traveller Information Systems (ATIS) provide a range of information that aids motorists (private or public) to reach a desired destination. On-board navigation systems are the basic building block for ATIS. When integrated with the information from the ATMS, the ATIS can provide locations of incidents, weather and road conditions, optimal routes, lane restrictions, and other location based service (LBS) applications.

Advanced Vehicle Control Systems (AVCS) assist the driver's control of the vehicle to promote safer and more efficient travel. This is perhaps the most ambitious of the functional areas. In AVCS, traffic accidents can be avoided using intelligent cruise control and systems that warn the driver of an imminent collision.

Commercial Vehicle Operations (CVO) mainly involve the use of Automatic Vehicle Location (AVL) systems linked with computer-aided dispatch (CAD) systems to operate fleets of trucks, buses, vans, taxis, and emergency vehicles. Automatic Vehicle Identification (AVI) systems automate toll collection without stopping at gantry and hence improve traffic flow in the network.

Advanced Public Transport Systems (APTS) are the public transport information and control systems that provide passengers at bus stops with information on the arrival times of buses or trains. They also permit priority signals for buses at signalized junctions with the assistance from ATMS and ATIS.

Besides these functional areas, other ATTS groups have also emerged over time. Electronic payment systems (Chadwick, 1994; Elliott and Dailey, 1995; Ochieng et al., 1999), emergency management (such as notification and personal security, and vehicle

management), and information management are, for example, relatively new ATTS functional areas. It is important to stress that ATTS functional areas will increase over time as the user needs change and demands increase, or new and enhanced technologies emerge.

An examination of each of the functional areas described above indicates that a navigation system plays a key role in almost all functional areas. While a positioning system is never considered as a stand-alone component of an ATT service, it is generally integrated into a larger system which is much more complex, involving many different subsystems such as man-machine interface, sensors, computers, and communication (Drane and Rizos, 1998). Due to the enormous benefits that can be achieved by solving transport problems in urban areas, it is essential that the navigation system meets the specified requirements in an urban environment (Ochieng and Sauer, 2002). This is difficult given the characteristics of urban areas where physical restrictions are imposed due to tall buildings, urban canyons, narrow streets, and tunnels.

In general, two essential components used in the navigation module of an ATTS are: (1) a device to determine the geometric position of the vehicle, and (2) a Geographic Information System (GIS) based digital road map for spatial (physical) reference of the vehicle location. The most common geometric positioning devices used for land vehicle navigation are Deduced Reckoning (DR) motion sensors, ground-based (terrestrial) radio frequency, global navigation satellite systems such as the Global Positioning System (GPS), and integrated navigation systems such as the integration of GPS and DR.

DR is the process of estimating the position of a vehicle (or a moving object) with respect to a known position using information on heading, speed, time, and distance travelled by the vehicle. This method of navigation is primarily used in spacecraft, missiles, ships, aircraft, land vehicles, and more recently, mobile robots. A range of sensors is employed to determine the direction of the object (for example, gyroscopes, and compasses) and the distance travelled by the object (for example, odometers, and accelerometers). The quality of position solution using a DR method largely depends on the performance (i.e., cost) of the sensors.

For land vehicle applications, low-cost sensors are normally used in a DR configuration. The basic DR configuration, which is suitable for land vehicles, consists of a distance

sensor (usually the vehicle odometer to measure distance) and a gyroscope (to measure heading). A major problem with DR is that it determines vehicle location (i.e., coordinates) relative to an initial position. A small error in heading grows over time and results in a large error in position. This means that the absolute positioning error accumulates in proportion to the distance travelled. Therefore, frequent calibration of DR sensors is required using an external navigation system. For ease of reference the basic DR configuration will be referred to as DR in the rest of the thesis.

A relatively complex DR configuration is referred to as an inertial navigation system (INS). The INS provides a complete navigation solution that includes position, velocity, attitude (roll, pitch and heading), acceleration, and angular rate of the vehicle or platform being navigated. The principle of an INS is also based on a relative positioning technique which requires information on the initial position of the vehicle. Different inertial sensors are used to measure rotation rate and acceleration of the vehicle at regular intervals. An INS consists of an inertial measurement unit (IMU) and navigation processors. An IMU contains a group of sensors such as accelerometers (two or more, usually three) and gyroscopes (three or more, but usually three) that are rigidly mounted to a common base to keep the same relative orientations (Grewal et al., 2001). On-board navigation processors estimate the gravitational acceleration that is not measured by accelerometers. A double integration technique is then applied to the net acceleration to obtain an estimate of the position of the vehicle. Some of the common types of sensor errors include scale factor error which results from aging or from manufacturing tolerance and non-linearity which is present in most sensors to some extent. Due to these numerous errors in INS, the position, velocity and attitude information degrade over time (i.e., mean-squared navigation errors increase over time). The user equipment is usually expensive due to acquisition, operating and maintenance costs. Moreover, the power requirements of an INS, which shrinks along with size and weight, are still higher than those of GPS receivers. As a result, this type of navigation system is not appropriate for land vehicle navigation and is not considered any further in this study.

In terrestrial Radio Frequency (RF) systems, a radio tower broadcasts its location which may be received by a vehicle in the vicinity. The received signals are then used to determine the position of the vehicle. In this positioning system, the accuracy does not degrade with time or distance travelled as it does in DR. However, the usage of such a system is limited to areas that are within the coverage of the radio towers emitting the

broadcast signals. The use of such systems is also not commonly available to the general public. Moreover, the maintenance of such a system is also very costly.

GPS is an absolute positioning and time transfer system owned and operated jointly by the US Department of Defence (DoD) and Department of Transportation (DoT). Although GPS has been widely used as a positioning sensor in land vehicle navigation over the last ten years, it is affected by both systematic errors and random errors (Ochieng, 2004). The factors that contribute to positioning errors can be classified into different groups, namely (a) satellite related errors such as clock and orbital instability, (b) propagation related errors such as ionospheric refraction and tropospheric refraction, (c) receiver related errors such as multipath, clock bias and antenna phase centre variation, (d) GPS signal masking or blockage, and (e) satellite geometric contribution to position error. Due to these factors associated with GPS, the required navigation performance (RNP) for some ATT services cannot be achieved in areas where the radio signals are obstructed, such as urban canyons, streets with dense tree cover, and tunnels.

GPS data may be augmented with DR sensor data with the use of an Extended Kalman Filter (EKF) to achieve the required availability in some areas (Zhao et al., 2003). This is known as an integrated navigation system (GPS/DR). DR readings are calibrated when GPS is available. If the GPS receiver suffers from signal masking or the quality of the position solution is not good, the calibrated DR readings are then used to determine the position of the vehicle.

The digital road network map is the other important component of the navigation module assisting an ATTS. Since land vehicles primarily travel on known road networks, the road map is used as a spatial reference to locate them. This, for example, assists drivers to relate their observed positions obtained from the navigation system with a physical location in the real-world and hence can guide them along a pre-calculated route. However, the digital road map also contains errors arising mainly from the processes of creation and digitization of maps. The errors can be estimated using either the scale of the map or field experiments.

System and sensor complementarity, such as the integration of GPS, DR and digital map data can be used to enhance geometric positioning capability. A *map matching algorithm* can then be formulated to integrate the positioning data with the digital road network

data. Map matching not only enables the physical location of the vehicle to be identified but also improves the positioning accuracy if a good digital map is available. If the vehicle positions and the digital map are very accurate, the algorithm becomes very straightforward and simply snaps the positioning data to the nearest road. However, accurate positioning data and network data may not be available in the real world and hence map matching algorithms are essential. The research presented in this thesis is concerned with situations in which it is not possible, or desirable, to obtain such higher accuracy digital map and positioning information as to make a simple snapping algorithm feasible. Moreover, the simple snapping technique may give incorrect results in urban areas where the density of roads is high. Consequently, an efficient map matching algorithm is a required component of the navigation module designed to support ATTS.

The general purpose of a map matching algorithm is to identify the correct road segment on which the vehicle is travelling and to determine the vehicle location on that segment. The parameters used to select a precise road segment are mainly based on the proximity between the position fix and the road, the degree of correlation between the vehicle trajectory derived from the position fixes and the road centreline, and the topology of the road network. Orthogonal projection of the position fix onto the selected road segment is normally used to calculate the vehicle location on the segment.

The complexity of the map matching algorithms necessarily depends on the nature of the application and the availability of data inputs. Therefore, various difficulty levels are associated with map matching algorithms. For example, map matching algorithms for a fixed bus-route are very simple because the bus is travelling on a known route. In this case, the purpose of the algorithm is to locate the bus onto one of the road segments that builds up the bus route. In this way, the search domain to identify the correct road segment is significantly reduced. The most complex algorithm is the general map matching algorithm that does not assume any prior knowledge or any other information regarding the expected location of the vehicle.

The methodologies used in past research to develop map matching algorithms vary from a simple search technique (for example, Kim et al., 1996; Bernstein and Kornhauser, 1996; white et al., 2000; Greenfeld, 2002) to a highly mathematical technique (for example, Kim et al., 2000; Pyo et al., 2001; Najjar and Bonnifait, 2003; Yang et al., 2003). The generic limitations of the existing map matching algorithms are given below:

- The algorithms are unreliable, especially at junctions and in the vicinity of parallel roads.
- They are not suitable for urban road networks due to inaccurate results.
- There is no method to determine the accuracy offered by the algorithms.
- There is no discussion on the level of confidence (integrity) of the map-matched locations.
- No sensitivity analysis has been done to assess how the navigation sensors and the digital map quality affect the performance of map matching algorithms.
- The algorithms ignore the error sources associated with the navigation sensors and the digital maps.

As a result, existing map matching algorithms are not capable of satisfying the requirements of many ATT services[2]. Importance, therefore, should be given to the navigation requirements of the ATT services while developing a map matching algorithm. The requirement of positioning accuracy for an accident and emergency service, for instance, may be higher than that for a transit vehicle control and management service. Therefore, a more robust technique must be utilised to develop a map matching algorithm to support the navigation function of the accident and emergency service. Due to errors associated with the positioning data and the digital map data, there is always a level of uncertainty associated with map matching algorithms. Consequently, a quality indicator representing the level of confidence in map-matched location is essential for such applications.

The type of navigation system and the quality of the digital map may influence the performance of the map matching algorithms. In order to quantify such effects, testing and validation of a map matching algorithm are necessary, preferably using a number of different digital maps and a variety of navigation systems.

[2] Chapter 4 presents the details of existing map matching algorithms together with their limitations

1.2 Aims and Objectives

The overall aim of this research is to contribute to the realization of an integrated and reliable land-vehicle navigation system, by developing high *integrity* map matching algorithms, testing them in different road networks of varying complexity, and validating their accuracies and performances. Such a navigation system will find application in many ATT services including vehicle route guidance, automatic vehicle identification and monitoring, accident and emergency responses, public transport operations, and many more.

To achieve this aim, the following objectives are formulated. To:

- Investigate state-of-the-art navigation systems and their ability to support the navigation function of the ATT services requiring spatial and temporal location information.
- Demonstrate how a map matching algorithm becomes an essential component of the navigation module capable of satisfying the required navigation performance (RNP) of some ATT services.
- Perform a detailed literature review of the existing map matching algorithms and their limitations to support the navigation function of ATT services.
- Enhanced a number of map matching algorithms based on different techniques such as topological analysis of the road network, probabilistic principles, and fuzzy logic to overcome limitations of the existing map matching algorithms.
- Implement and validate the developed map matching algorithms using real-world field data.
- Develop a way to determine the *integrity* of map matching algorithms. "*Integrity"* refers to the development of a metric (0 to 100) representing the quality (level of confidence) of the map-matched locations based on the various error sources associated with navigation systems and digital maps.
- Investigate the effects of navigation systems and digital maps on the performance of map matching algorithms and compare the performance of the developed map matching algorithms with the current ones.

- Examine the implication of the enhanced map matching algorithms on the application domains and look into the impact of Galileo and EGNOS (European Geostationary Navigation Overlay Service) on the map matching algorithms.

1.3 Outline of the Thesis

This thesis is organised into ten chapters. Chapter one provides the background to the study, its aim and objectives, and the outline of the thesis.

In chapter two, a description of ATT services requiring a navigation system is presented. Some potential ATT services such as en-route guidance, fleet management, accident and emergency management, road user charging, public transport operations, traffic control and management, and on-board emissions monitoring systems are discussed to demonstrate that a navigation module is a core subsystem of those services. This chapter also investigates how a map matching algorithm becomes an essential component in the navigation module of ATTS. The required navigation performance (RNP) parameters (*accuracy, integrity, continuity*, and *availability*) are defined in the contexts of road vehicle navigation. This chapter ends with the presentation of RNP parameters for various ATT services.

Chapter three describes the different components (systems, sensors, and digital maps) of a navigation module intended to support the navigation function of an ATT service. This involves the discussion of various space-based radio navigation systems such as GPS and differential GPS, vehicle-based sensors such as deduced reckoning (DR), an integrated navigation system (GPS/DR), and a digital road network map. This chapter also demonstrates how an Extended Kalman Filter (EKF) is utilised for the integration of GPS and DR to achieve a continuous positioning solution in all environments. The inherent error sources associated with these positioning systems and digital maps are also illustrated. Finally, a formal definition of a *map matching algorithm* is given.

In chapter four, a review of the pertinent literature on map matching algorithms is presented. The existing literature on map matching algorithms is divided into three groups based on the methodologies used to develop them. They are the geometric, topological, and advanced map matching algorithms. The performance of these map matching algorithms is also discussed, and their limitations of the existing map matching

algorithms both in terms of link identification and location determination, are then presented. This chapter ends with the discussion of the motivation for this thesis.

Chapter five describes the development of a simple but improved map matching algorithm based on topological analysis of the road network. The basic characteristics of this algorithm are to formulate various weighting factors based on the proximity between the position fix and the road segment, the similarity between the heading derived from the navigation system and the direction of the road segment, and the location of the position fix relative to the road segment. Data on the historical trajectory of the vehicle is used to avoid sudden switching of mapped locations between unconnected road links. The algorithm takes into account the speed of the vehicle while using heading data from the navigation sensors. A step-by-step procedure for implementing the map matching algorithm is presented. The algorithm is then implemented and tested using real-world field data collected in London.

Chapter six illustrates the development of a probabilistic map matching algorithm. This algorithm takes all links as candidate links that fall within a confidence region around a position fix. This gives more than 99% probability that the actual vehicle position lies on one of the candidate links. A method for the derivation of the confidence region based on the uncertainty (the variance-covariance matrix) associated with the positioning system is presented. Two distinct processes are defined for the identification of the correct link in the developed algorithm: (1) the *matching process at a junction* (MPJ), and (2) the *subsequent matching process on a link* (SMPL). This chapter also discusses how the thresholds for the detection of minimum speed[3] and turning manoeuvres (left or right) at junctions are derived from the field experiments. An optimal estimation method is introduced to determine the vehicle location on the selected link. This estimation takes into account error sources associated with the network map data and the navigation system. A step-by-step procedure for implementing this map matching algorithm is presented. The developed algorithm is then tested in complex road networks, including roundabouts, using a digital map of scale 1:2500.

Chapter seven describes the development of a fuzzy logic map matching algorithm. The suitability of the fuzzy logic method to develop a map matching algorithm is discussed. A brief overview of fuzzy logic is then presented. A novel approach is developed for the

[3] The detection of the minimum speed is required to efficiently use vehicle heading data

identification of correct links consisting of two processes: (1) the *initial map-matching process* (IMP), and (2) the *subsequent map matching process* (SMP). Various knowledge-based IF-THEN rules are established comprising the speed of the vehicle, the heading and the historical trajectory of the vehicle, the connectivity and the orientation of road links, and the contribution of satellite geometry to horizontal errors. The physical location of the vehicle on a link is then estimated using an optimal estimation technique. A step-by-step procedure for implementing this map matching algorithm is presented. The last section of this chapter describes the implementation of the algorithm using real-world data and the presentation of results.

Chapter eight discusses the validity and integrity of map matching algorithms. First, a description of a generic validation technique for map matching algorithms is provided. The higher accuracy GPS carrier-phase observables are used in the validation methodology. The application of this validation technique to a map matching algorithm is then presented. The integrity (level of confidence) of a map matching algorithm is described. This includes the definition of integrity, the factors affecting the integrity of a map matching algorithm, and the derivation of a metric to quantify integrity. Three factors are considered in developing the integrity: (1) the uncertainty associated with the map-matched location, (2) the capability of the map matching algorithm to identify the correct link, and (3) the capability of the map matching algorithm to accurately estimate the vehicle location. A fuzzy logic technique is used to derive the metric (0 to 100) which represents the integrity of a map-matched location. The application of the metric to the developed map matching algorithms is discussed.

Chapter nine describes the process to evaluate the performance of the three map matching algorithms developed in this research. This involves assessing how the quality of digital maps and the types of navigation systems affect the performance of a map matching algorithm. The quantification of such effects is then discussed using each of the map matching algorithms with a choice of digital maps (map scale 1:50000, 1:2500, and 1:1250) and navigation systems (GPS and GPS/DR). Suburban and urban road networks are considered separately. The integrity method developed in Chapter 8 is fully evaluated in this chapter. This chapter then illustrates the performance of the developed map matching algorithms against the performance of the current commonly cited algorithms.

Chapter ten discusses conclusions and recommendations for further research. The thesis ends with a list of publications arising out of this research.

CHAPTER 2

ADVANCED TRANSPORT TELEMATICS (ATT) APPLICATIONS

2.1 Introduction

Chapter one demonstrated that positioning systems play a key role in all functional areas of Advanced Transport Telematics Systems (ATTS). This chapter gives an overview of different ATT applications and services. Various user groups and services are defined and ATT services requiring positioning and navigation capabilities are identified. A detailed discussion of the navigation module of some important ATTS is presented. The required navigation performance (RNP) parameters of *accuracy, integrity, continuity*, and *availability* are defined for some potential ATT services. This is essential in order to determine whether the navigation unit of a service has the capability to satisfy the associated RNP.

2.2 Advanced Transport Telematics Systems (ATTS) User Groups and Services

The navigation module of an ATTS is responsible for providing spatial and temporal information. For example, buses equipped with a navigation system can determine their locations and send the information back to a control centre enabling bus operators to predict the arrival of buses at bus stops and hence improve the service level of public transport systems. Table 2.1 shows the different user groups and services defined in a draft American National Plan (Chadwick, 1994).

Table 2.1: ATTS user groups and services

User Groups	Services
Travel and Traffic Management	Pre-trip travel information
	En-route driver information*
	Route guidance*
	Ride matching and reservation
	Traveller services information*
	Traffic control+
	Incident management*
	Travel demand management
	Emissions testing and mitigation
	On-board emissions monitoring (OEM)+
	Highway-rail intersection (HRI)
	Traffic data quality management
Public Transportation Management	En-route transit information*
	Operation automations*
	Personalized public transit
	Public travel security
Electronic Payment	Electronic payment systems+
Commercial Vehicle Operations	Commercial vehicle electronic clearance*
	Automated roadside safety inspection
	On-board safety and security monitoring+
	Commercial vehicle administrative processes*
	Fleet management*
	In-situ vehicle condition monitoring
Emergency Management	Emergency notification/personal Security*
	Emergency vehicle management*
	Disaster response and evacuation (DRE)
Advanced Vehicle Safety	Longitudinal collision avoidance+
	Lateral collision avoidance+
	Intersection collision avoidance+
	Vision enhancement for crash avoidance
	Safety readiness
	Automated highway systems
	Pre-crash restraint deployment
	Stolen vehicle recovery+

* Services that require navigation and positioning capabilities
+ Additional services which can be assisted by navigation and positioning technologies

Six user groups and 29 different services are defined. The services marked with an asterisk are those that require positioning and navigation capabilities. Out of 29 services, 11 services require a navigation module for spatial and temporal location information (Chadwick, 1994). Five additional ATT services have emerged over the last few years. These services are also included in Table 2.1 (in italics) making a total of 34 ATT services. However, this list of ATT services is by no means exhaustive. As the user needs will change and increase or new and improved technologies become available, the ATT services will increase.

With the rapid progress in the development of radio-navigation technology (such as GPS) in recent years, it is envisaged that most of the ATT services can benefit from navigation and positioning technologies. For example, the appropriate integration of GPS (carrier phase), wireless communications and 3D digital terrain models (DTM) can assist a vehicle proximity warning system and hence reduce collisions among vehicles. A total of 8 ATT services in Table 2.1 marked with a "+" are identified as the additional services (after Chadwick, 1994) that can be assisted by a navigation and positioning module.

2.3 Services Supported by the Navigation Modules

The navigation module of an ATTS should provide spatial and temporal vehicle location information in all environments. It normally consists of stand-alone GPS and digital map data. This section describes some important ATT services and looks into how the navigation modules of these ATTS help to achieve their overall objectives. Different types of navigation systems are also explored in order to see whether they are capable of providing the required positioning information.

2.3.1 Route Guidance

Route guidance is one of the most important ATT services. A number of studies have shown that route guidance helps in reducing traffic congestion and its associated environmental, social and financial costs, minimizing travel time, and conserving energy by making drivers more aware of the various options available to them in making a trip (Arnott et al., 1991, Abdel-Aty et al., 1991, Weymann wt al., 1995, and Liu et al., 2004). Two types of route guidance systems have emerged: (1) Pre-trip guidance, and (2) En-route guidance. Pre-trip guidance is given before the trip in a form of a printout which includes turns, road names, travel distances, junction names and landmarks. En-route

guidance, on the other hand, requires turn-by-turn driving instructions to a driver in real-time and hence it is much more useful.

En-route guidance gives directions to drivers in real-time to assist navigation. In some cases, en-route guidance may be used as the sole means of navigation by users unfamiliar with a particular area (e.g. commonly used in rental cars). In others, it may provide additional information for a user already familiar with an area, allowing them to choose the most appropriate route. En-route guidance can be broadly categorised as autonomous or dynamic (Sheridan, 2001). Autonomous systems work by positioning the vehicle and displaying its location on the road map stored in the vehicle. Once the user enters details of their origin and destination the system devises a route by optimising on a chosen criterion, e.g. shortest time or least cost. Directions are then provided to the driver by updating the vehicle position along the chosen route. Dynamic route guidance systems, on the other hand, provide the same basic level of service as autonomous systems but combine this with traffic conditions in an automated fashion. Users of the dynamic system may choose different levels of automation. Some may want to be informed of traffic information and then make their own route decisions whilst others may want to combine travel information with a guidance system to automatically change the route in response to new information. This may involve re-routing in response to known congestion or re-routing to allow the traveller to use services at specific locations, e.g. to find a hotel, restaurant or a particular point of interest.

Given knowledge of where the vehicle is, and the specification by the driver of the desired destination, en-route guidance information refers to navigation directions in a turn-by-turn format which form an efficient driving route. The information includes the name of the road on which the vehicle is currently travelling, distance to the next turn, the name of the road to turn onto, and the direction of the upcoming turn. These are then conveyed to the driver via visual and audio interfaces. Some of this information is shown in Figure 2.1. The integration of the vehicle position with digital road network maps provides the driver the majority of information essential for route guidance.

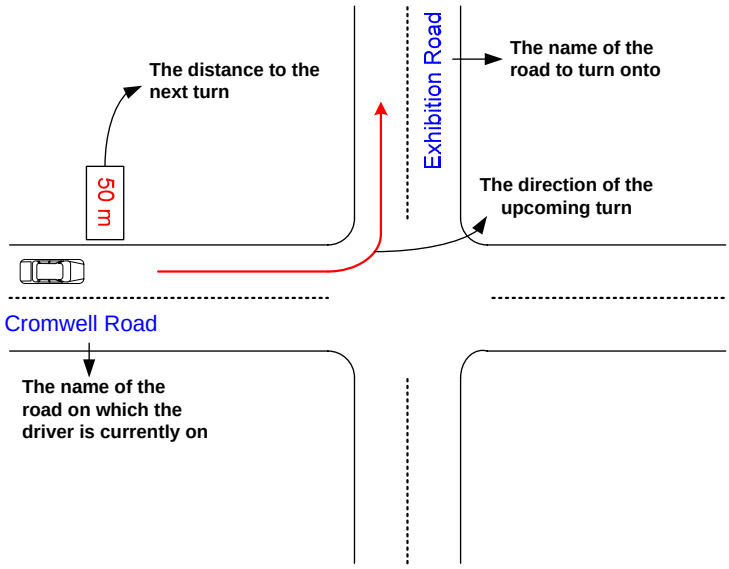

Figure 2.1: The essential information for route guidance

In order to acquire such essential information for route guidance, the vehicle needs to be equipped with a series of interconnected functional subsystems. Each of the subsystems consists of a group of software and hardware components. In general, the subsystems can be categorised into four major modules:

- *Intelligent navigation module:* determines the vehicle's temporal and geometric position in the road network at all times based on various sensor readings and a *map matching technique.*

- *Route guidance module:* determines the optimal routing between origin and destination or anywhere in between prior to or during a journey based on real-time updates on the state of the road network from the traffic management centre and locational data from the navigation module.

- *Driver support module* (man-machine interface): accepts driver inputs for direction generation and responds with audible or displayed directions at the right time.

- *Communication module:* keeps the on-board system in contact with a traffic management centre to stay appraised of current traffic conditions.

Figure 2.2 shows a simplified schematic diagram of a dynamic route guidance system. Among the four modules, the navigation module is of primary interest for current research. This module usually consists of a GPS receiver and a digital map. A CD-ROM

installed in the vehicle contains the digital map database and the other detailed information required for route guidance, such as turn restrictions, road classification (one-way or two way), and other points of interest.

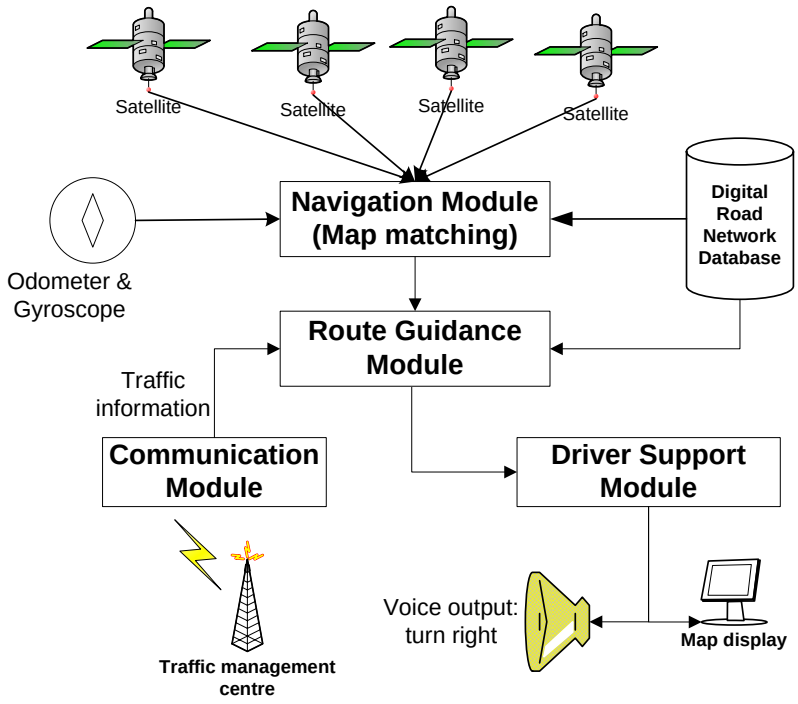

Figure 2.2: A simplified version of route guidance system

However, stand-alone GPS suffers signal masking in areas with heavily tree-lined roads, urban canyons, and wooded areas. GPS signal interference from wireless communications as well as reflections of this signal from buildings, large vehicles, and other reflective surface also make the utilisation of GPS very difficult. Therefore, to obtain navigation data continuously in all environments GPS data needs to be integrated with vehicle-based deduced reckoning (DR) motion sensors data. This is known as an integrated navigation system (GPS/DR). A basic DR configuration usually consists of the vehicle speed sensor (to measure vehicle displacement) and a gyroscope (to measure the rate of change of vehicle heading). This is fully described in the next chapter. A *map matching algorithm* can then be used to integrate the positional data with the digital map data in order to obtain second-by-second vehicle locations on the road network. Poor map matching can place the vehicle on the wrong road, confusing the drivers and making the route guidance ineffective. As a result, the performance of the route guidance largely depends on the performance of the map matching algorithm.

Implementation of the driver support module varies widely among vehicle types, however, in basic terms it is basically a collection of hardware and software that performs human-machine interface (HMI) to display the outputs of the route guidance module. The communication module keeps a continuous link between the vehicle (the route guidance module) and the traffic management centre. This is essential for route guidance analysis in order to obtain real-time traffic information so that an optimal route can be selected.

A fuller description of in-vehicle route guidance can be found in Foster (1989), Collier (1992), Kirson (1992), Jackson (1995), and Ruimin and Qixin (2003).

2.3.2 Fleet Management

Fleet management systems are one of the foremost ATT applications. Fleet Management refers to the management of a fleet of vehicles in an organised manner using certain tools such as computer software, communication systems, and vehicle location technologies to improve operational efficiency and effectiveness. A good fleet management system provides a wide variety of services (such as quicker dispatch, vehicle security, digital messaging, dynamic routing and monitoring driver compliance) designed to help companies manage their vehicle fleets. Examples of fleet operators are:

- Haulage Companies
- Couriers/Parcel Delivery Services
- Taxi services
- Secure Transport Services
- Municipalities (local and national authorities, e.g. local councils, NHS)

A typical fleet management system has three subsystems: (1) in-vehicle subsystem, (2) communication subsystem, and (3) dispatch centre subsystem (Figure 2.3).

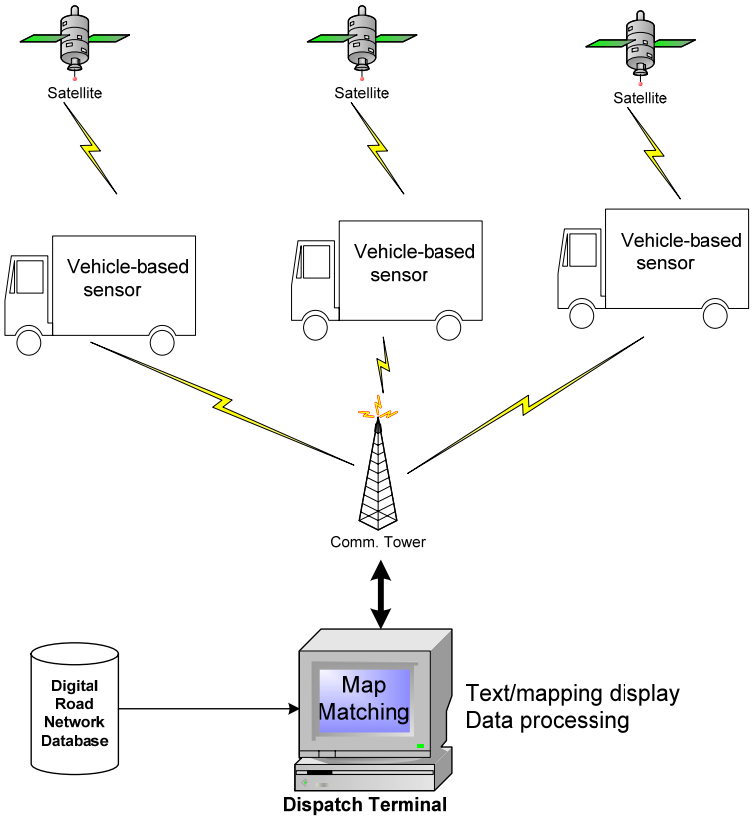

Figure 2.3: A simplified fleet management system

The in-vehicle subsystem is responsible for computing vehicle location and status determination and distributing this information to the dispatch terminal. This subsystem also receives messages from the dispatch centre. Real-time positions of the vehicles must be continuously computed at all times. The positioning data (easting, northing, speed, and heading) is then sent to the dispatch terminal to obtain physical locations (i.e., addresses) and road related information. The speed and heading data are used to deduce whether the vehicle is stationary or moving and the direction of travel. Accurate positioning of the vehicle helps to determine whether the vehicle is on a freeway, on a parallel service road, or in a cul-de-sac. All of these parameters contribute to the automatic status determination of each vehicle, hence, putting the fleet under full control. The type of technology required for the vehicle position and location computation largely depends on the fleet management requirements. Stand-alone GPS gives an accuracy of 10-30m (2σ) and this may be satisfactory for some applications in suburban areas. However, this accuracy cannot be achieved in urban areas where the GPS coverage is impaired.

Moreover, there are many applications in the security fleet domain which require accuracy in the 5 to 30 m (2σ) range (McLellan et al., 1992). The reason for this high

positional accuracy is that locating the vehicle on the incorrect road and thus selecting the wrong vehicle to be dispatched may not be acceptable for such a critical application. Therefore, the navigation module should include an integrated navigation system (GPS/DR) as discussed in the previous section. A suitable *map matching algorithm* within the dispatch terminal is then used to reconcile GPS/DR data with digital map data. The vehicles then do not need to be equipped with a CD-ROM containing the digital road database as the map matching algorithm is performed within the dispatch terminal provided a position display is not required in the vehicle. The dispatch centre subsystem is also responsible for the determination of which vehicles should be monitored, the selection of the type of road network map that should be displayed, the storage of incoming data from the vehicle fleets (i.e., location, speed, heading, time) for the purpose of post analysis and display. The communication subsystem which links a fleet of vehicles with the dispatch terminal can be selected from a range of communication systems.

2.3.3 Accident and Emergency Management

One of the most important factors in saving lives resulting from road accidents is a timely response from emergency medical services. Emergency Notification Systems ("*mayday*") have been developed in the US to reduce the time between when the accident occurs and when medical services are provided. The detection of road accidents, however, is normally left to non-automatic systems (emergency calls). An accident may be detected by a CCTV (closed-circuit television) camera only if the area is under the coverage of a video-surveillance system. However, this is not the case for most of the road networks. Satellite-based radio navigation technology can be critical to the location of sites of accidents. The integration of different vehicle-based sensors, GPS, digital road network maps, and mobile communications can facilitate a safety-of-life (SOL) accident notification system. The system may have three components: (1) accident sensing, (2) accident location (i.e., coordinates), and (3) communication. Sensing should be automatic and may be based on airbag deployment, rapid vehicle deceleration, or chassis deformation. Once the accident has occurred, additional in-vehicle sensors may be used to determine:

- Number of vehicle occupants
- Direction of the vehicle before the accident

- Presence of fire
- Use of seatbelts and/or deployment of airbags
- The number of rollovers

This information helps emergency service personnel to assess the seriousness of the accident. After detecting the accident, it is important for the emergency service provider to know the exact location of the vehicle. Stand-alone GPS technology or vehicle-based DR motion sensors may not be suitable for such a SOL critical application. However, the integration of GPS data with DR motion sensors data and digital road network data with the assistance of a robust *map matching algorithm* has the potential to precisely identify the location of an accident even in high built-up urban areas, tunnels, and wooded areas with a high positioning accuracy (5-10 m, 2σ). A wireless communication system (e.g., GSM, GPRS, WLAN, or a combination of them), transmits the information about the accident and its location from the crashed vehicle to the control centre (i.e., emergency services agencies). The control centre can then quickly decide to send emergency vehicles (police, fire service, and ambulance) depending on the seriousness of the accident, the type of road (rural or urban), the number of vehicles involved and, the additional information from the driver or passengers about the injury. The usefulness of this system is apparent in some circumstances, for example, accidents during night-time in low visibility.

In addition to emergency medical aid to vehicle occupants in the event of a traffic accident, the system has other potential applications as well. For instance, the control centre can send an immediate emergency communication to the traffic management centre in the event of a road accident. The traffic management centre can then notify surrounding traffic about the exact location of traffic congestion following the accident using on-road variable message signs (VMS). This also assists nearby traffic to divert to appropriate roads.

2.3.4 Road User Charging

Traffic congestion is one of the key problems in all major cities. This is due to an inequality between network capacity and travel demand as the number of vehicles using a network within a given period of time increases, the functionality of the network decreases (Mazzoleni, 2001). Consequently, traffic flow decreases, travel time and fuel

consumption increases and travel cost to motorists increases. This also imposes incremental costs to non-motorists in the form of increased emissions and reduced mobility for pedestrians and cyclists. Efforts to reduce traffic congestion primarily focus on the expansion of road network capacity and establish a set of traffic control strategies aimed at reallocating traffic across network links and shifting the time patterns of travel demand (Mohring, 1999). However, recent empirical studies of induced travel effects have established that behavioural reactions to network capacity expansion will lead to an increase in total travel (Hansen and Huang, 1997; Noland, 2001; Noland and Cowart, 2000).

Road user charging (i.e., tolling) is an alternative option in order to enforce individual users to internalize the external cost of their travel decisions on other drivers and hence reduce congestion (Vickrey, 1969). The challenge is to make vehicle data available to the infrastructure provider. The traditional philosophy is that users are charged according to the distance travelled on certain roads (distance-based charging) or for using a particular road (link-based charging) or for driving within a particular area (area-based charging). In terms of charges, two types of charging have emerged: (1) fixed charges (e.g., London congestion charging), and (2) variable charges (e.g., electronic road pricing in Singapore). The variable charges could be a function of time of day, type of road, level of congestion, engine size, energy consumption, speed, acceleration, and vehicle exhaust emissions, for example.

The methods to collect the charges (either variable or fixed) are normally known as electronic tolling, electronic road pricing, and road user charging which are collectively termed as Electronic Fee Collection, EFC, (Catling, 2000). This has been based on the concept of either labour-intensive collection of EFC using various electronic cards (i.e. pre-paid magnetic strip cards) or automatic short-range communication between an in-vehicle unit and road-side equipment using Dedicated Short-Range Communication (DSRC). Electronic road pricing (ERP) in Singapore (introduced in 1998), for instance, uses a DSRC system for EFC. This allows motorists to pay road tolls without stopping at the gantries. The latest development of EFC uses a system which has the knowledge of the user position and, hence, can offer more advanced services. The benefits associated with this system include the removal of costly road-side equipment, the improvement of emergency assistance to motorists, and real-time detailed traffic information to motorists (He et al., 2001).

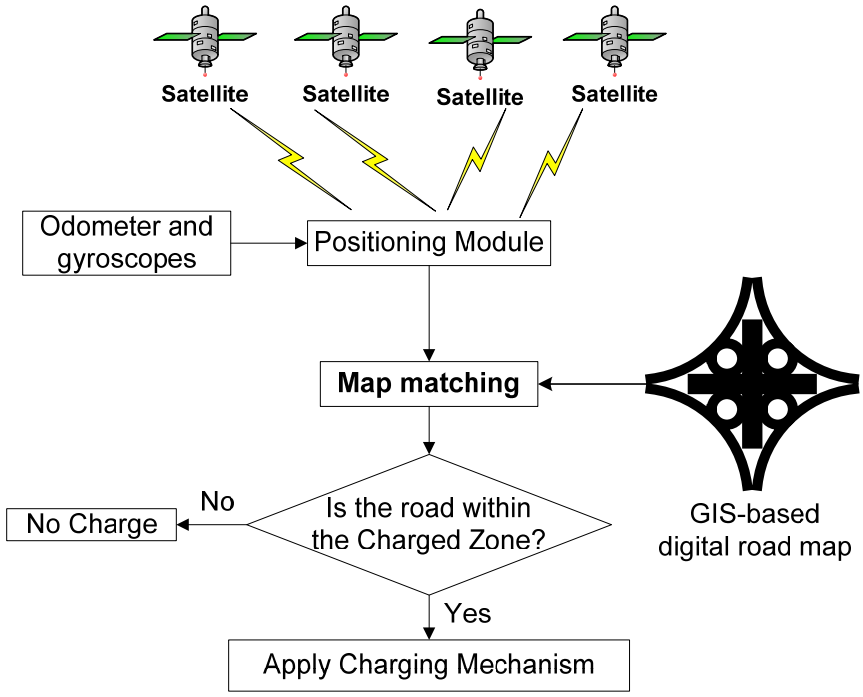

Figure 2.4: A block diagram of a GPS-based EFC system

Global Navigation Satellite System (GNSS) such as GPS is the key tool for this new EFC. However, GPS-based EFC may not be suitable in urban areas. The solution to this problem could be the use of GPS/DR as a navigation module. Another important element of this new EFC system is Geographic Information Systems (GIS)-based digital road maps which verify whether the vehicle uses a toll road. This can be achieved by an efficient *map matching algorithm*. A simple version of a GPS-based EFC system is shown in Figure 2.4.

2.3.5 Public Transport Operations

An Automatic Vehicle Location (AVL) system tracks the location of buses in a road network in real-time and reports the information back to a host (master control centre) via a communication infrastructure. Systems based on AVL are being used extensively by public transport providers. DoT (1998) reported that there were at least 58 AVL systems in operation in US. Over the last few years, AVL system usage has increased by more than 200 percent and many more AVL systems are being planned (DoT, 1998).

The advantages of AVL systems are numerous (Greenfeld, 2000). When AVL systems are integrated with CAD (computer aided dispatch) software, dispatchers can take corrective action to service deviations and pinpoint vehicle location during emergencies.

Furthermore, AVL systems can provide real-time data to traveller information systems. When AVL systems are integrated with traffic signal control systems, the real-time vehicle location information provides input to traffic signal pre-emption algorithms which determines whether a bus should be given priority at signalised junctions (Figure 2.5). Driver and passengers also benefit because the silent alarm feature of AVL systems increases driver and passenger safety.

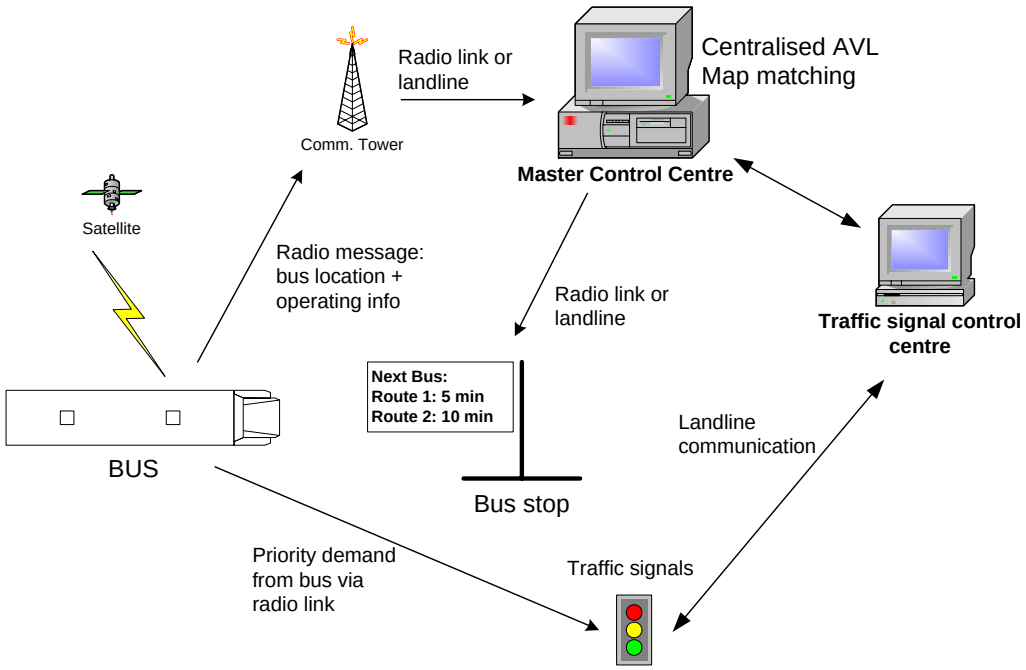

Figure 2.5: GPS-based public transport operation

Using AVL systems, real-time schedule information (i.e. expected time of arrival) can be provided to passengers at bus stops with digital displays (Figure 2.5). This relies on tracking the current location of the bus on the designated bus route and then estimating the time it will take to arrive at further downstream bus stops along the bus route. The estimated travel times can be fixed based on historical speed data or may be dynamically updated to take account of the current traffic situations. Real-time status information makes it easier to integrate buses with other modes of public transport, e.g. trains. Passengers can make more informed decisions based on likely journey times if they are using multiple modes of transport or have multiple route choice options.

Most current AVL systems monitor the position of buses with terrestrial infrastructure consisting of roadside beacons, road-based sensors, and microwave sensors. Transport for London (TfL) has found that this approach is prohibitively expensive, especially if

deployed across the whole of the Greater London area. Substantial infrastructure is required to provide power and communications, which are vulnerable to accidental damage, vandalism, and environmentally induced deterioration. Consequently, the maintenance costs of such infrastructure are prohibitively quite high (TfL, 2004).

If satellite-based radio navigation technology such as GPS is installed on each bus this could enhance the flexibility of the system and make it more cost-effective (Sheridan, 2001). For example, the majority of Southampton's Buses are now fitted with GPS and GPRS equipment to provide bus arrival information on electronic signs at bus stops (Southampton ROMANSE[4]). In an urban area an AVL system supported by the stand-alone GPS may have location tracking problems. Since buses usually travel on the pre-defined routes, GPS data can be integrated with the bus odometer data in order to obtain continuous bus position information. However, an enhanced *map matching technique* needs to be employed to identify a road segment and bus location on this segment. London Buses is introducing a GPS-based AVL technology (the integration of GPS, DR, and map matching) on all 8000 London buses to provide bus arrival times to passengers at bus stops[5].

2.3.6 Traffic Control and Management

The measurement of traffic flow is one of the most challenging tasks in transport. The main sensor technologies used for monitoring traffic flow are CCTV cameras, inductive loop detectors, microwave vehicle detection systems, infrared detectors, gantry and ramp metering sensors. Nevertheless each of these technologies experiences shortcomings such as high equipment costs, high installation or maintenance costs, especially if deployed widely enough to provide control for a large urban area. Substantial infrastructure is then required to provide power and communications, which are again vulnerable to accidental damage, vandalism and environmentally induced deterioration.

Floating car data has become a viable alternative to extensive ground infrastructure in recent years mainly because of developments in positioning and communications

[4] Southampton ROMANSE (ROad MANagement System for Europe), Home Page: http://southampton.romanse.org.uk/, Accessed June 2005.

[5] London Buses, Home Page: http://www.tfl.gov.uk/buses, Accessed July 2005.

technology. GNSS technology can now provide accurate vehicle positions at relatively low cost. GPS equipped floating cars can provide a significant aid to traffic control management, because each car can then record and transmit its position, direction and speed to the traffic management and control centre in real-time. Data from a sufficient number of floating cars, can give accurate and wide area information on traffic flow (Farman et al., 2003). The combined usage of GPS data from floating cars and terrestrial sensor data also has the potential to aid an accurate and continuous measurement of traffic congestion. However, the success of a satellite-based system depends on its performance in urban areas where the need for information is greatest. As discussed, satellite-based positioning systems are least effective in dense urban areas due to signal blockage and reflection. One solution to this problem is to integrate GPS with different vehicle-based sensors and a digital road map using a *map matching method*.

Based on this traffic data the road network can be controlled through a variety of methods. Actions based on the analysis of the data may be implemented automatically based on existing control algorithms. In other cases it could require manual intervention to make dynamic adjustments, or the analysis of traffic data may contribute to longer-term network design.

For instance, the main function of an urban traffic control system is to co-ordinate adjacent traffic signals in urban areas to optimise traffic flow. The most widely used urban traffic control system in the UK is SCOOT (Split Cycle Offset Optimisation Technique) which has proved to be an efficient tool for managing traffic on signalised road networks, and is now used in over 170 towns and cities in the UK and overseas (DETR, 1999). Systems such as SCOOT are able to automatically adjust signal timings in response to traffic conditions. Other systems may rely on using historic data to improve fixed signal timings. An urban traffic control system may also include additional features such as emergency green wave routes which provide a rolling sequence of green signals on successive junctions along a predefined route to provide emergency vehicles with maximum priority. Variable message signs (VMS) can be used to provide information on parking spaces, possible areas of congestion or diversion details. They may simply provide information, e.g. ‘delay expected at a location L’, or may give guidance, e.g. ‘take route A if you are going to destination D’.

2.3.7 On-board Emissions Monitoring

Environmental problems associated with transport are a serious concern among transport planners and policy makers. One of the key characteristics of these problems is that they arise from the interaction of human behavioural systems (i.e., driver characteristics) and physical systems. For instance, vehicle fuel consumption and exhaust emissions largely depend on the vehicle operating and driver behaviour patterns (Holmen and Niemeier, 1998; Ericsson, 2001, Nam et al., 2003). Thus, to improve our understanding of environmental and health problems associated with vehicle emissions it is necessary to integrate data on both travel and traffic behaviour with environmental data (Ochieng et al., 2003b). An on-board emissions monitoring system is such a system which can measure spatio-temporal vehicle exhaust emissions as a result of variation in vehicle performance, driver behaviour, and road and traffic characteristics (Frey et al., 2001; North et al., 2004).

Ochieng et al. (2003b) developed a low-cost on-board monitoring system, the Vehicle Performance and Emissions Monitoring System (VPEMS). The high level functional architecture of VPEMS is shown in Figure 2.6. As can be seen, VPEMS has two main components: the Mobile Unit (MU) and the Master Control Centre.

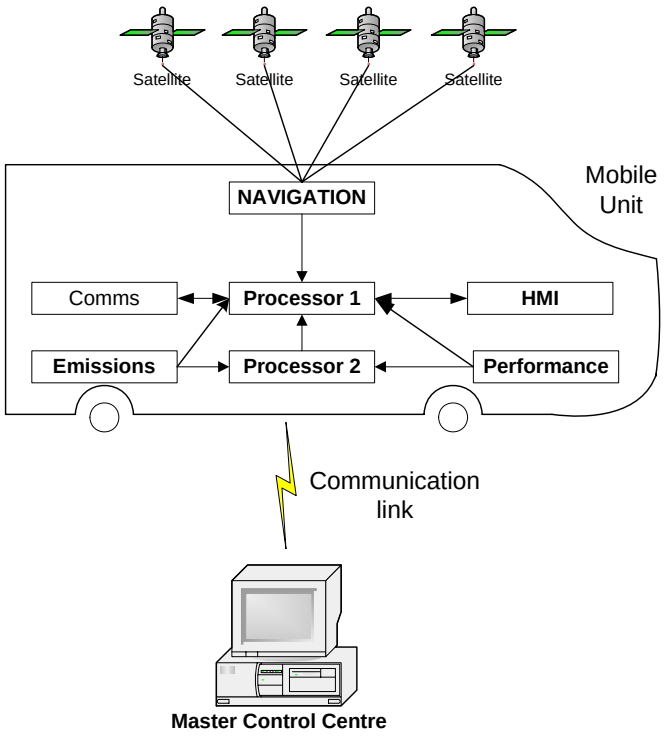

Figure 2.6: VPEMS high level functional architecture

The MU is installed on the vehicle to capture real-time second-by-second spatio-temporally referenced vehicle/driver performance, travel and vehicle exhaust emissions data. Data captured by the MU is then transmitted to the master control centre via Global System for Mobile (GSM) technology for storage, analysis and display. The navigation function of VPEMS is responsible for the derivation of all spatial, temporal, and derivative data on the vehicle including 3D position, time, speed and acceleration. It is currently supported by a GPS receiver with optional deduced reckoning (DR) augmentation.

In order to investigate the variation of vehicle emissions at different types of roadways (i.e., motorways, urban arterials) and for different locations along a roadway (e.g., junctions, roundabouts, road segments), the positioning data from the VPEMS navigation module needs to be integrated with the digital road network data. This also permits link-based emissions distribution data to be collected. This can be achieved by a *map matching algorithm*. The next generation of the VPEMS navigation system could therefore be supported by a GPS receiver integrated with DR sensors and map data utilising a *map matching algorithm*.

2.4 Vehicle Navigation and Positioning Systems Developed in Industry

According to Krakiwsky (1993), the first vehicle navigation and positioning system built by industry was in 1975. The number of such systems reached 18 in 1989 and 31 in 1992. Krakiwsky (1993) also provides an overview of automatic vehicle location systems developed by industry worldwide. As can be seen in Figure 2.7, there were over 130 such systems built worldwide where USA and Japan are leaders in developing the systems. Canada, Germany and UK formed the second leading countries to build vehicle location and navigation systems. The positioning technologies used in land vehicle navigation systems have undergone a major evaluation over the last few years. Several positioning techniques are being used in land navigation systems worldwide. These are GPS, DR, microwave-based tag and beacon technology, terrestrial radio frequency (RF), and map matching.

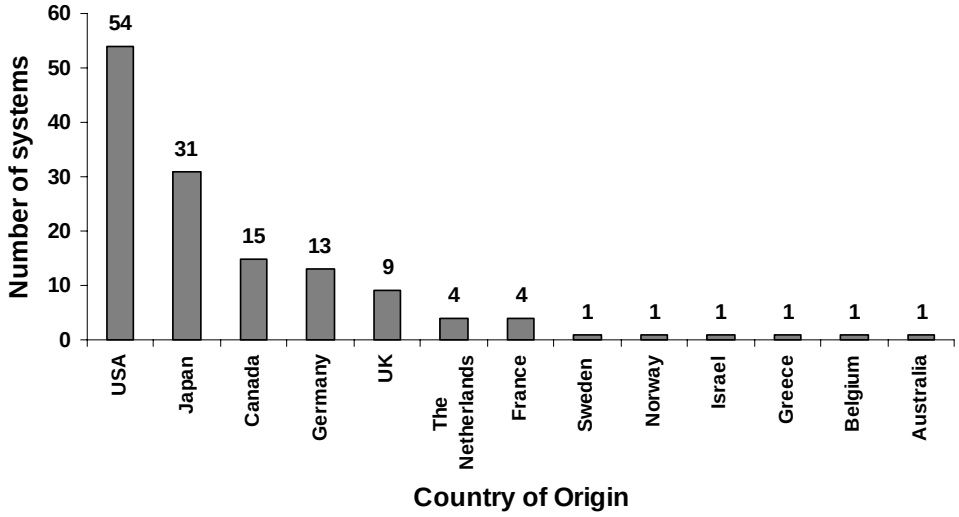

Figure 2.7: AVL systems by country of origin (source: Krakiwsky, 1993)

The initial intention of industry to develop GNSS enabled devices was to support a range of fleet tracking services (e.g., trucks and emergency fleets). This has changed dramatically over the years. The use of GNSS-based devices in automatic vehicle location (AVL), in-car navigation, and other location based services (LBS) has been risen sharply over the last few years. According to the US DoT, there were more than 420 million cars and 130 million trucks in the world that made use of GPS technology in 2003. Most of the leading car manufacturers have developed a GNSS-based in-car navigation system. Examples include BMW's BMW-Assist system, Mercedes's Teleaid system and Honda's Internavi. The OnStar[6] GPS-based land navigation system developed by General Motors (GM) supports over 4 million vehicles. The OmniTRACS System[7] developed by Qualcomm Corp. is a pioneer for fleet tracking with over 500,000 trucks and other fleet vehicles tracked in North America. Telematics Research Group[8] (TRG) estimated that there will be over 40 million GNSS-enabled automobiles in the US alone.

A range of vehicle navigation systems built by industry are shown in Table 2.2, identifying the name of the manufacturer, the product, and the associated features of the system. Information on each product was obtained from the internet and the academic publications. It is noticeable that the navigation module of many systems is normally

[6] http://www.onstar.com
[7] http://www.qualcomm.com
[8] http://www.telematicsresearch.com

supported by a GPS receiver together with a road map. It has not been possible to determine whether the systems used any map matching algorithm. Therefore, the horizontal positioning accuracy offered by these systems can not be identified. But this also largely depends on the quality of the road map data. The positioning module of the NavTrax system jointly developed by the Pulsearch Navigation Systems and the University of Calgary-Canada is supported by an integrated DGPS/DR and a simple *map matching* algorithm (McLellan et al., 1992). However, the performance of the system has not been reported in the publication domain.

Table 2.2: Real-time vehicle positioning devices developed in industry

Manufacturer	Product and Year	Characteristics	Shortcomings
Germin	Germin Quest v7[9] (2005)	• mainly used for car navigation/route guidance • the navigation module is supported by a combination of GPS and road map data • 2D accuracy: 10-20m (2σ) • DGPS (WAAS) enabled (3-5 m, 2σ) • acquisition time: 2 mins (autolocate) 15 sec (warm) 45 sec (cold)	• not suitable for urban areas • no *map matching* algorithm • no statistics on the performance of the navigation module in terms of road segment identifications • no statistics on integrity and availability
Pulsearch Navigation Systems and University of Calgary, Canada	NavTrax (1992)	• an automatic vehicle location and navigation system claimed to be suitable for fleet management systems • the navigation module is supported by an integrated navigation system (GPS and DR) and a simple *map matching algorithm* • DGPS enabled	• no statistics on the performance of the navigation module in terms of road segment identification • 2D accuracy not reported • no statistics on integrity and availability

[9] http://www.globalpositioningsystems.co.uk/garmin-quest-v7-eu-via-free-upgrade-description.html

ETAK and Bosch	Travelpilot[10] (1991)	• primarily used in fleet management (trucks) • the navigation module is supported by a DR and map data using a simple *map matching* algorithm • coverage: US and Europe	• 2D accuracy has not been reported • no use of GNSS • no statistics on integrity and availability
Navman	Navman iCN650[11] (2005)	• basically designed for in-car navigation and guidance • the navigation module includes a GPS receiver (SiRF) and a road map • horizontal positioning accuracy: 5 m (95%) under in suitable condition • DGPS (WAAS/EGNOS/MSAS) enabled (3-5m, 2σ) • acquisition time: 8 sec (hot) 38 sec (warm) 45 sec (cold) • Coverage: 16 Western European countries (3D map view)	• not suitable for urban area • no *map matching* algorithm • no statistics on the performance of the navigation module in terms of road segment identification • no statistics on integrity and availability
TomTom	TomTom GO 500[12] (2005)	• designed for in-car navigation and guidance • on-demand traffic information, weather reports, and speed camera location • facilities to avoid toll roads and congestion charge zones • the navigation module consists of a GPS receiver and road map data • horizontal positioning accuracy: typical GPS accuracy • coverage: Great Britain	• not suitable for urban areas • no *map matching* algorithm • no statistics on the performance of the navigation module in terms of road segment identifications • no statistics on integrity and availability

[10] Buxton et al. (1991)
[11] http://www.globalpositioningsystems.co.uk/navman-icn650-description.html
[12] http://www.globalpositioningsystems.co.uk/tomtom-go-500-description.html

Mio	Mio 269[13] (2005)	• claimed to be suitable for in-car navigation and guidance • on-demand traveller information • the navigation module is supported by a GPS receiver (SiRF Star III) and road map data • horizontal positioning accuracy: typical GPS accuracy • coverage: Europe	• not suitable for urban areas • no *map matching* algorithm • no statistics on the performance of the navigation module in terms of road segment identifications • no statistics on integrity and availability
Teydo	FleetOnline™[14] (2005)	• an asset tracking service • the navigation module is supported by a GPS receiver • horizontal positioning accuracy: 6 m (3σ) • acquisition time: 24 sec (hot) 38 sec (warm) 90 sec (cold)	• reported 2D accuracy is quite high. However, it is unlikely that a typical GPS receiver can able to deliver such a high accuracy in an urban area • no statistics on integrity and availability
Microsoft	AutoRoute 2005[15] (2005)	• suitable for various location based services (LBS) e.g., hotels and restaurants • the navigation module is supported by a GPS device and road map data • horizontal positioning accuracy: typical GPS accuracy • Coverage: 140000 restaurants, 60000 hotels, 4000 golf courses in Europe	• not be suitable for LBS applications in urban areas. • no statistics on integrity and availability

It is worthwhile to note that it is not possible to verify the performance of these existing navigation systems reported in Table 2.2. This is due to the fact that the methods for deriving the accuracy statistics are not in the publication domain either due to a lack of full appreciation of performance scheme or due to commercial sensitivities. The fourth

[13] http://www.globalpositioningsystems.co.uk/mio-268-and-eu-with-uk-and-ireland-on-sd-description.html
[14] http://www.teydo.com/teydo/uk/en/
[15] http://www.pugh.co.uk/Products/microsoft/autoroute-2005.htm

column in Table 2.2 gives some of the limitations determined in this research. Although many such real-time vehicle location and positioning systems are available, there are a number of credible reasons to conclude that they will not fully support ATT services presented in Table 2.1. This is because these systems are incapable of satisfying the required navigation performance (RNP[16]) of ATTS described below.

2.5 Required Navigation Performance (RNP)

The concept of Required Navigation Performance (RNP) was first introduced by the International Civil Aviation Organization (ICAO) in 1983 to provide the specification of airspace based on demonstrated levels of navigation performance and certain functional capabilities, rather than a required set of navigation sensors or equipments. RNP extends the capabilities of modern airplane navigation systems by providing real-time estimates of navigation uncertainty, assurance of performance through its containment concepts, and features that ensure the repeatability and predictability of airplane navigation. There are four parameters used to define RNP - *accuracy, continuity, integrity and availability*. Although RNP parameters have their origin in aviation, the concept of RNP has been extended to land and marine transport modes (Ochieng and Sauer, 2002). These parameters are defined below (ICAO, 1997; Ochieng et al., 2003a):

- *Accuracy* is defined as the nearness of a measurement to the standard or true value i.e., a highly accurate navigation system will provide measurements very close to the standard, true or known values. A rigorous statement of accuracy includes statistical measures of uncertainty and variation. Accuracy is generally represented by standard deviation of errors (difference between measurements on the map and the true value). The true values of map attributes or labels can be obtained from an independent source of higher accuracy measurement such as GPS carrier phase observables (under certain conditions), higher resolution satellite imaginary, aerial photography, or a ground visit. Accuracy should not be confused with precision. Precision is the degree to which several measurements from the same medium agree with each other. It is an indicator of the scatter in the data. The less the scatter, the higher the precision.

[16] This is fully described in section 2.4.1

- *Integrity* relates to the level of trust that can be placed in the correctness of the information supplied by the navigation system. It is the ability of a navigation system to give timely and valid warnings to users when the system should not be used for navigation or positioning for the intended period of operation (POP). This suggests that the navigation system must deliver a warning (usually known as an alarm) of any malfunction (given that an alarm limit is exceeded) to users within a given period of time (time-to-alarm) and with a given probability. Integrity risk is the probability of an undetected failure that results in the Total System Error (TSE) exceeding the Containment Alarm Limit.

- *Continuity* is defined as the capability of the navigation system to perform its function without non-scheduled interruptions during an intended period of operation. More specifically, continuity is the probability that the system will be available for the duration of an operation, presuming that the system was available at the beginning of the operation. The probability that the navigation system will be interrupted and not provide guidance information for the intended period of operation is known as continuity risk. This risk measures the potential system unreliability.

- *Availability* is defined as the percentage of time over a specified time interval that the service is available for use, taking into account all outages, whatever their origins. The service can be termed as available if all the accuracy, integrity and continuity requirements are fulfilled.

Other desirable requirements include the navigation sampling rate (i.e., the frequency of update), time-to-first-fix (TTFF) which is the receiver warm-up time[17], the timing accuracy, the speed and heading accuracy, and the maximum outage time (i.e., the maximum acceptable level of outage without compromising on service availability.

[17] Receiver warm-up time can be defined as the period between the beginning of GPS signal acquisition and the availability of first acceptable position fix. This is often usually high if the receiver is not used for a long time (cold-start).

2.4.1 RNP for ATT

As can be seen in Table 2.1, many ATT services require positioning data. Therefore, the next step is to define the subsequent RNP which should be satisfied to make sure that the services are deliverable. The RNP for civil aviation is well documented (for example, see Table 1 in Ochieng et al., 2003a). However, the RNP for surface transport applications is not well defined and is usually categorised in terms of applications (i.e., highway, transit, and rail applications). The Federal Radionavigation Plan, FRP, (2001) reports that the US Department of Transportation's modal administrations, as well as state and local governments and private industry, are currently working on Intelligent Transportation Systems (ITS) and aim to clarify and verify user navigation requirements. The RNP for surface transport in Europe is also still to be consolidated and agreed (Ochieng and Flament, 1996). However, preliminary studies have identified the RNP for some potential services as shown in Table 2.3 (Chadwick, 1994, Ochieng et al., 1999, and FRP, 2001)

Table 2.3: The RNP for some ATT applications and services

Applications & services	Accuracy (m, 2σ)	Availability (%)	Integrity (sec)
Navigation and route guidance	5-20	99.7	1-15
Automatic vehicle location (generic)	10-30	99.7	1-15
Emergency location	5-10	99.7	1-5
Public safety	10	99.7	1-15
Accident management	30	99.7	1-15
Collision avoidance	1	99.7	1-15
Rail position location	10-30	99.9	1-5
Automatic announcement of bus stops	5-10	99.7	1-15
Transit vehicle control and command	30-50	99.7	1-15

It should be noted that the RNP parameters in Table 2.3 are far from complete, as requirements for the use of positioning systems in ATT services continue to evolve. As more user services emerge, even higher requirements will be essential, especially in urban areas where there are potential economic, social and environmental benefits in solving urban transport problems. For this reason, a positioning system capable of delivering higher accuracy will be required in urban areas compared to open space. Therefore, a stand-alone GPS may not be able to satisfy the RNP parameter specification for the corresponding service in some areas. However, the integration of GPS, DR, and digital map data has the potential to support the navigation module of ATTS.

Although the availability of integrity parameters in surface transport may not be as critical as in aviation, this is still important as it provides a level of confidence in the total service and hence increases user acceptance and safety and will help to more effectively realise the potential benefits of ATT services (Ochieng and Sauer, 2002).

2.6 Summary

This chapter presented an overview of Advanced Transport Telematics (ATT) services. It was shown that positioning systems play a key role in all functional areas of ATTS. A number of specific services were identified in which a positioning system must be included as a core requirement for the services. This chapter also discussed some of the ATT services and examined the suitability of various navigation systems for the navigation modules of those services. More specifically, the necessity of a map matching algorithm to integrate various navigation sensors and map data was discussed. The RNP parameters for various surface transport systems were presented. This is essential in order to see whether a navigation module has the capability to satisfy the RNP for a particular service.

CHAPTER 3

LAND VEHICLE POSITIONING AND NAVIGATION

3.1 Introduction

Global Navigation Satellite Systems (GNSS), such as GPS, and digital road maps are used to obtain positioning information required for some advanced transport telematics (ATT) services. However, GPS often requires a level of augmentation with other navigation sensors such as Deduced Reckoning (DR) motion sensors, in order to achieve the required navigation performance (RNP) in some areas where signal reception is poor such as urban canyons, streets with dense tree cover, and tunnels. One of the common solutions is to integrate GPS with DR by employing a Kalman Filter (Zhao et al., 2003). Integrated navigation systems also rely on various types of sensors. However, even with very good sensor calibration and sensor fusion technologies, inaccuracies in the positioning systems are often inevitable. There are also errors associated with spatial road network data. Therefore, map matching algorithms are usually employed to reconcile inaccurate locational data with inaccurate digital road network data.

This chapter describes various systems and sensors used for land vehicle positioning and navigation. This includes GPS, DR, differential GPS, and integrated GPS/DR. An extended Kalman Filter (EKF) algorithm used to integrate GPS and DR is described. Various error sources associated with these systems are then discussed. This chapter also looks into the uncertainty associated with the digital road network map. This comprises errors in map creation and digitisation. Finally, the map matching concept is briefly described. Subsequent chapters will describe the current and new algorithms in detail.

3.2 Systems and Sensors

Space-based satellite systems and vehicle-based motion sensors are normally utilised to acquire the positioning information that is essential for some ATT services. This includes the use of global navigation satellite systems (GNSS) such as GPS, the utilisation of a basic DR configuration which includes a vehicle speed sensor, magnetometer or low-cost rate gyro, and the integration of GPS with DR. Other newer technologies such as Ultra Wide Band (UWB), Bluetooth, and INS based on low-cost, high-performance, smaller-sized MEMS (Micro-Electro-Mechanical Systems) sensors can also be employed to aid in positioning and navigation of land vehicles. For example, Bluetooth, which is a short-range wireless communications technology, may be used with a proximity method to locate the moving object. Since the location of the Bluetooth access point (AP) is known, when a mobile object comes within range of the AP (typically less than 10m from it), the location of the object can be assumed to be somewhere within the Bluetooth cell (Rizos, 2005). This section introduces commonly used space-based navigation systems and vehicle-based DR sensors, and their integration, rather than new technologies which are still being developed and validated.

3.2.1 Global Navigation Satellite Systems (GNSS)

A global navigation satellite system (GNSS) is a network of satellites that transmit high frequency radio signals containing time and ranging data that can be received by a user's receiver, enabling the user to identify antenna location anywhere around the globe: on land, at sea, and in the air. The US Global Positioning System (GPS), the Russian GLObalnaya NAvigatsionnaya Sputnikovaya Sistema (GLONASS) and the upcoming European Galileo system are examples of GNSS.

The US GPS is in operation with a constellation of 29 Block II/IIA/IIR satellites at the time of writing[18] and is constantly being upgraded with the replacement of the Block II/IIA satellites by the Block IIR/IIF satellites to meet higher standards of reliability (Seeber, 2003). Because of the huge potential market for satellite navigation services, the competition expected from the Galileo system, and the technological developments in security related areas, the US government has introduced various initiatives to enhance

[18] US Naval Observatory Home page: ftp://tycho.usno.navy.mil/pub/gps/gpsb2.txt

the performance of the GPS system (Sauer, 2004). This is known as the GPS modernisation program which is aimed at achieving improvements to satellite design, addition of new user signals, the initiatives for the accuracy improvement, and the improvements to the control systems. The modified Block IIR-M satellites, for instance, will have a civil signal, designated L2C, on L2, and another civil signal, L5, on a third frequency at 1176.45 MHz (McDonald, 1999; Fontana et al., 2001). The next Block III satellites (GPS III) are in design stages (Seeber, 2003).

The constellation of the second GNSS, the GLONASS, reached Full Operational Capability (FOC) in mid 1996 but due to severe financial and technical problems, the constellation could not be maintained at the FOC level over the years (Sauer, 2004). At the time of writing the number of operational satellites has dropped down to twelve.[19]

The third GNSS, Galileo, is the European based radio-navigation system. It is currently being developed in Europe, with a constellation of 30 satellites, by the European Space Agency (ESA) to specifically provide the higher standard of integrity and reliability required to ensure the safety of life (SOL) during transport by air, land, and sea. It is projected to eventually be co-functional with the US GPS constellation.

GPS and GLONASS are known as the first generation (1G) GNSS, modernised GPS is known as the 1.5G GNSS, and Galileo and GPS III are known as the 2G GNSS (Seeber, 2003).

The US 1G GNSS (GPS) is of primary interest to this research as it is the only comprehensive system currently in operation. It is therefore described below.

3.2.1.1 NAVSTAR GPS

The NAVigation System with Timing And Ranging (NAVSTAR) Global Positioning System (GPS) is a satellite-based radio-navigation, positioning, and time-transfer system. It is designed, financed, and deployed by the US Department of Defense (US DoD) and operated jointly by the US DoD and the Department of Transportation (US DoT). Civilian access to GPS is guaranteed through an agreement between the DoD and US

[19] Source: Russian Federation Ministry of Defence; http://www.glonass-center.ru

DoT. It is recognised as the major space based navigation system with the primary purpose of enhancing the effectiveness of US and allied military forces (DoD, 2001). The system achieved FOC in 1995 with a constellation of 24 active satellites (28 in March 2000) approximately uniformly dispersed around six circular orbits. The orbits are nongeostationary and approximately 20,200 km altitude above the Earth's surface with orbital periods of one-half of a sidereal day (≈11.967h).

Three or more GPS satellites are always visible from most points on the Earth's surface, which is one of the design criteria of GPS. The original objectives of GPS were the instantaneous determination of position and velocity (i.e., navigation), and the precise coordination of time (i.e., time transfer). The potential for using GPS for various applications including transport, communications and the environment continue to be demonstrated worldwide. GPS provides 24-hour, all-weather 3D positioning and timing all over the world, with a predicted horizontal accuracy of 22m (95%) (US DoD, 2001). For a detailed description of the various aspects of GPS, the reader is referred to US DoD (1995), Kaplan (1996), Parkinson et al. (1996), Tsui (2000), US DoD (2001), Hoffmann-Wellenholf et al. (2001), and Leick (2004). However, a very brief overview of GPS is presented below.

The GPS baseline system is comprised of three main segments: the space segment, the control segment, and the user segment. These are defined below (Parkinson et al., 1996; Drane and Rizos, 1998; Seeber, 2003):

- **Space Segment:** This segment consists of the active satellite constellation. The basic functions of the satellites are to receive and store data transmitted by the control segment, to maintain accurate time by means of several onboard atomic frequency standards, and to transmit information and signals to users on one or both L-band frequencies.

- **Control Segment:** This segment includes facilities required for satellite health monitoring, telemetry, tracking, command and control, navigation message computations and up-linking.

- **User Segment:** This segment comprises the entire range of applications equipment and computational methods that are available to the users.

The signal that leaves a GPS satellite antenna is a combination of three components: the two L-band carrier waves (L1 and L2), the ranging codes modulated on the carrier waves (C/A code and P-code), and the Navigation Message. The GPS signals are highly directional and hence are easily susceptible to being blocked or reflected by solid objects (buildings and trees) and water surfaces. The two ranging codes are the C/A (the "clear/access" or "coarse/acquisition") code and the P (the "private" or "precise") code. The current GPS signal characteristics are presented in Table 3.1.

Table 3.1: The current GPS signal characteristics

Items	Characteristics	Comments
Carrier waves	• L1:1575.42MHz, wavelength~19cm • L2:1227.6MHz, wavelength~24cm	• L1 is modulated by both the C/A and P(Y) codes • L2 modulated by the P(Y) code only
C/A-code	• 1023 bit pseudorandom noise (PRN) code • Chipping rate: 1.023MHz, chip length ≈ 300m, transmitted on L1 • Repeats every 1 milliseconds	• Civil Access • C/A is not encrypted • Different PRN for each satellite
P(Y)-code	• Chipping rate: 10.23MHz, chip length ≈ 30m • Repeats every 267 days • Transmitted on L1 and L2	• Restricted to military use • Require specially designed receiver devices • Y refers to an encrypted version of P-code
Navigation Message	• A bit of stream of ones and zeros (1 and 0) with a data rate of 50 Hz transmitted on L1 • Message is divided into frames (25), each frame has 1500 bits=30s • Repeats every 20 repetitions of C/A code	Transmits data on ephemeris, satellite clock, ionospheric parameters and satellite health etc.

The GPS offers two positioning services: (1) the Precise Positioning Service (PPS), and (2) the Standard Positioning Service (SPS). The GPS PPS is mainly available to military and other authorised users of the United States and its allies equipped with special types of PPS receivers (US DoD, 2001). Since this study is only concerned with civil applications, PPS is not considered any further. The GPS SPS was a positioning and timing service provided on the GPS L1 signal for civilian use. The SPS is initially designed to provide a less accurate positioning capability than PPS through the use of a method known as selective availability (SA). With the removal of the effects of selective availability (SA) in May 2000, the GPS SPS positioning accuracy has improved.

Point positioning in the SPS is based on the principle of time of arrival (TOA) ranging. A GPS L1 signal transmitted from each satellite contains the ephemeris data (within the Navigation Message) from which the user's GPS receiver can estimate the satellite position and satellite clock bias relative to GPS system time. Each satellite transmits a signal at a certain time T_s in the satellite time frame. The receiver then receives the signal at a later time T_r in the receiver time frame. If the satellite and receiver clocks are fully synchronised and if all signal propagation delays are ignored, the time difference between the transmission and reception would be equal to the signal travel time. Since satellite and receiver clocks are two different devices with different performance parameters, they are not synchronised. Therefore, the distance measured is called the *pseudorange* (PR_r^s) between the satellite *s* and the receiver *r*. This is given as (Seeber, 2003):

$$PR_r^S = R_r^S + cdt_r - cdt_S + I_r^S + T_r^S + \delta_{r,orbit}^S + \delta_{r,multipath}^S + \varepsilon \qquad \textbf{(3.1)}$$

where

PR_r^s	is the measured range between the satellite *s* and the receiver *r* (*m*)
R_r^s	is the topocentric distance between the satellite *s* and the receiver *r* (*m*)
c	is the speed of light in vacuum (*m/s*)
dt_s	satellite clock error (*s*)
dt_r	receiver clock error (*s*)
I_r^s	range delay due to ionospheric refraction (*m*)
T_r^s	range delay due to tropospheric refraction (*m*)
$\delta_{r,orbit}^s$	satellite orbit error (*m*)
$\delta_{r,multipath}^s$	multipath error (*m*)
ε	observation noise (*m*)

The Navigation Message allows a computation of the satellite position (x_s, y_s, z_s) and the satellite clock bias (dt_s). If the effects of ionospheric, tropospheric, satellite orbit, and multipath error on the pseudorange are ignored, then only four unknowns remain in equation (3.1), the 3-D receiver position (x_r, y_r, z_r) and the receiver clock bias (dt_r). The pseudorange measurements between the receiver (*r*) and four satellites are then

sufficient to estimate the receiver position and the receiver clock bias. They can be given by:

$$\begin{aligned} PR_r^1 &= \sqrt{(x_1 - x_r)^2 + (y_1 - y_r)^2 + (z_1 - z_r)^2} + cdt_r - cdt_1 + \varepsilon_r^1 \\ PR_r^2 &= \sqrt{(x_2 - x_r)^2 + (y_2 - y_r)^2 + (z_2 - z_r)^2} + cdt_r - cdt_2 + \varepsilon_r^2 \\ PR_r^3 &= \sqrt{(x_3 - x_r)^2 + (y_3 - y_r)^2 + (z_{31} - z_r)^2} + cdt_r - cdt_3 + \varepsilon_r^3 \\ PR_r^4 &= \sqrt{(x_4 - x_r)^2 + (y_4 - y_r)^2 + (z_4 - z_r)^2} + cdt_r - cdt_4 + \varepsilon_4^4 \end{aligned} \quad \textbf{(3.2)}$$

where $PR_r^1, PR_r^2, PR_r^3, PR_r^4$ are the pseudoranges from the receiver to the four satellites (*s1*, *s2*, *s3*, and *s4*).

As these are nonlinear simultaneous equations, it is difficult to solve for the four unknowns in equation (3.2). One common technique to estimate the unknowns is to linearise them. When more than four satellites are available from the user point-of-view, another approach to solve the problem is to use all the satellites. Adding more pseudorange observations provides redundancy to the solution. For instance, if eight satellites are simultaneously observed, eight equations can be derived with only four unknowns. The receiver position is then determined using the theory of least-squares, and a variance-covariance matrix is generated for the receiver position and the clock offset. According to Kaplan (1996), equation (3.2) takes the following form after linearization and taking partial derivatives of the pseudoranges:

$$\begin{pmatrix} \Delta PR_r^1 \\ \Delta PR_r^2 \\ \Delta PR_r^3 \\ \vdots \\ \Delta PR_r^m \end{pmatrix} = \begin{pmatrix} \frac{\partial PR^1}{\partial x_r} & \frac{\partial PR^1}{\partial y_r} & \frac{\partial PR^1}{\partial z_r} & \frac{\partial PR^1}{\partial t} \\ \frac{\partial PR^2}{\partial x_r} & \frac{\partial PR^2}{\partial y_r} & \frac{\partial PR^2}{\partial z_r} & \frac{\partial PR^2}{\partial t} \\ \frac{\partial PR^3}{\partial x_r} & \frac{\partial PR^3}{\partial y_r} & \frac{\partial PR^3}{\partial z_r} & \frac{\partial PR^3}{\partial t} \\ \vdots & \vdots & \vdots & \vdots \\ \frac{\partial PR^m}{\partial x_r} & \frac{\partial PR^m}{\partial y_r} & \frac{\partial PR^m}{\partial z_r} & \frac{\partial PR^m}{\partial t} \end{pmatrix} \begin{pmatrix} \Delta x_r \\ \Delta y_r \\ \Delta z_r \\ \Delta dt_r \end{pmatrix} + \begin{pmatrix} \varepsilon_r^1 \\ \varepsilon_r^2 \\ \varepsilon_r^3 \\ \vdots \\ \varepsilon_r^m \end{pmatrix} \quad \textbf{(3.3)}$$

where ΔPR is the difference between the observed and the computed pseudoranges, *m* is the total number of satellites, $\Delta \boldsymbol{x}$ is the unknown to be estimated. Equation (3.3) can be written in vector-matrix form as:

$$\boldsymbol{\rho} = \mathbf{A}\mathbf{x} + \boldsymbol{\varepsilon} \tag{3.4}$$

where $\boldsymbol{\rho}$ is the vector of residual observations (i.e., $\Delta \boldsymbol{PR}$) , $\boldsymbol{A}$ is known as the design matrix which is a function of the direction to each of the satellites as observed from the receiver, and ε is the error term.

To solve equation (3.4), one can use Least Squares Estimation (LSE) which gives:

$$\hat{\mathbf{x}} = \left(\mathbf{A}^{\mathrm{T}}\mathbf{A}\right)^{-1}\mathbf{A}^{\mathrm{T}}\boldsymbol{\rho} \tag{3.5}$$

The variance-covariance matrix (*vcv*) associated with the errors in the computed position and the clock bias is just a scalar multiple of the "cofactor matrix" $\boldsymbol{P}$. This is defined as:

$$vcv = \sigma^2_{UERE}\boldsymbol{P} = \sigma^2_{UERE}\left(\mathbf{A}^{\mathrm{T}}\mathbf{A}\right)^{-1} \tag{3.6}$$

$$= \sigma^2_{UERE}\begin{pmatrix} A_{11} & A_{12} & A_{13} & A_{14} \\ A_{21} & A_{22} & A_{23} & A_{24} \\ A_{31} & A_{32} & A_{33} & A_{34} \\ A_{41} & A_{42} & A_{43} & A_{44} \end{pmatrix}$$

$$vcv = \begin{pmatrix} \sigma_x^2 & \sigma_{xy} & \sigma_{xz} & \sigma_{xdt_r} \\ \sigma_{yx} & \sigma_y^2 & \sigma_{yz} & \sigma_{ydt_r} \\ \sigma_{zx} & \sigma_{zy} & \sigma_z^2 & \sigma_{zdt_r} \\ \sigma_{dt_r x} & \sigma_{dt_r y} & \sigma_{dt_r z} & \sigma^2_{dt_r} \end{pmatrix} \tag{3.7}$$

where, σ^2_{UERE} is the variance of the observed ranges (i.e., user equivalent range error, UERE), **A** is the design matrix containing the partial derivatives of the observations with respect to the unknown parameters, $\boldsymbol{P}$ is the cofactor matrix which is a function of the satellite-receiver geometry at the time of the observations. The cofactor matrix can therefore be used to evaluate the relative strength of the observing geometry, and to quantify how the measurement errors can be translated to the expected errors in the

position estimates. An error ellipse around a position fix (2-D in *xy* plane) can then be derived using σ_x^2, σ_y^2, and σ_{xy}.

The geometrical position of the user's receiver with respect to the satellites being tracked plays a considerable role in the position solution error (Zhao, 1997). This geometry can be expressed in terms of various dilution of precision (DOP) parameters to characterise its contribution to the positioning error. DOP parameters in GPS are defined as the ratio of the square root of diagonal elements of the *vcv* matrix and σ_{UERE} which is given by:

$$GDOP = \frac{\sqrt{\sigma_x^2 + \sigma_y^2 + \sigma_z^2 + \sigma_{dt_r}^2}}{\sigma_{UERE}} \tag{3.8}$$

where *GDOP* is a scalar and dimensionless quantity termed as the geometric dilution of precision

GDOP can also be computed as the square root of the trace of the cofactor matrix ***P*** which can be given by

$$GDOP = \sqrt{A_{11} + A_{22} + A_{33} + A_{44}} \tag{3.9}$$

The relationship between the error in position solution (σ_{pos}), the range error (σ_{UERE}) and GDOP can then be expressed as:

$$\sigma_{pos} = GDOP * \sigma_{UERE} \tag{3.10}$$

Since UERE is not known exactly, σ_{pos} is only the approximation of the GPS position solution error is taken to be equal to the *GDOP* multiplied by the pseudorange error factor. In general, the more satellites that can be observed and used in the final solution, the better the results. *GDOP* is a measure of the geometrical strength of satellites with respect to the user position. According to equation (3.10), the smaller the *GDOP,* the more accurate the position. Therefore, *GDOP* can also be used to select a subset of four satellites, which provides the best *GDOP*, and hence the best position solution. Satellites

that spread around the horizon provide the best horizontal position, but the weakest vertical elevation.

Several other DOP parameters are also used to characterize the accuracy of various components of the position and time solutions. These are position dilution of precision (*PDOP*), horizontal dilution of precision (*HDOP*), vertical dilution of precision (*VDOP*) and time dilution of precision (*TDOP*). All of these DOPs are a function of geometry of the current satellites visible above the receiver's mask angle[20]. In other words, the positions of the satellites relative to the user determine the DOP value. The *PDOP* , for instance, is a measure of the accuracy in 3-D position for a constant σ_{UERE} and can be defined as:

$$PDOP = \frac{\sqrt{\sigma_x^2 + \sigma_y^2 + \sigma_z^2}}{\sigma_{UERE}} \tag{3.11}$$

The *PDOP* represents an indication of positioning accuracy at an instant in time rather than for the whole session. The higher the *PDOP*, the poorer the solution for a particular instant in time. When using pseudorange techniques, *PDOP* values in the range of 4 to 5 are considered very good, while *PDOP* values grater than 10 are considered very poor (US DoD, 2001). Poor geometry can be the result of satellites being in the same plane, orbiting near each other, or at similar elevations.

The *HDOP* is a measurement of the accuracy in 2-D horizontal position for a constant σ_{UERE} which is defined as:

$$HDOP = \frac{\sqrt{\sigma_x^2 + \sigma_y^2}}{\sigma_{UERE}} \tag{3.12}$$

A value of *HDOP* of less than 3 normally reflects a good position solution (2-D) for that instant in time (US DoD, 2001). If an observed *HDOP* for a position fix is 2 and the estimated user equivalent range error (UERE) is 4.0 (95%), then the estimated horizontal

[20] The minimum acceptable satellite elevation above the horizon to avoid blockage of line-of-sight

positioning accuracy is 8.0 (95%). Since the UERE and HDOP are changeable over a short period of time, there is little practical use in estimating a horizontal positioning accuracy in this manner. Positioning accuracy can be estimated by calculating statistical differences between observations from GPS and some known reference points. A more detailed description of DOP and issues related can be found in Spilker (1996).

Error Budget of GPS observables

Figure 3.1 shows various error sources associated with GPS positioning. There are two main components of error budget for a GPS observation that determines the accuracy of a GPS position solution: (1) geometric dilution of precision (GDOP), (2) user equivalent range error (UERE).

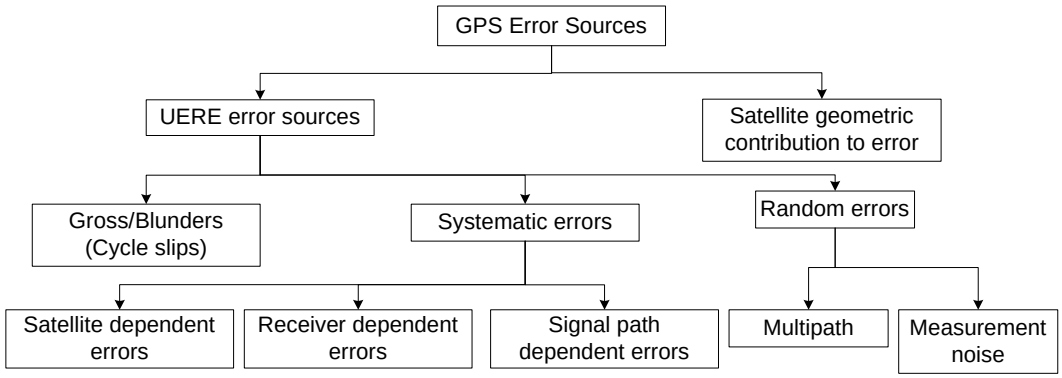

Figure 3.1: GPS error sources

The GDOP is already described above and therefore, is not considered any further in this section. However, there are numerous error sources which influence the UERE. The statistical sum of all systematic errors or biases contributing to the measurement error is referred to as range bias. The SPS SIS (signal in space) global average horizontal error is 13 m (95%) and the worst site positioning domain accuracy (SIS only) is 36 m (95%) (US DoD, 2001). Sandhoo et al. (2000) estimate the typical SPS SIS UERE (m, 1σ) for various GPS error sources after switching off selective availability (S/A) as shown in Table 3.2. Details on SIS URE errors can also be found in Parkinson et al. (1996), Hotchkiss (1999) and Farrell and Barth (1999).

Table 3.2:The order of range error associated with GPS error sources

Major error sources	**UERE (m, 1σ)**
Satellite orbit and clock offset	2.3
Ionospheric error	7.0
Tropospheric error	0.2
Receiver measurement error	0.6
Multipath	1.5
Total pseudorange error budget	7.5
GPS Stand-alone horizontal accuracy (2σ) for HDOP=1.5	**22.5 (=2*7.5*1.5)**

The observed GPS range, without the removal of biases, is referred to as a biased range or the pseudorange. The main contributors to the GPS range error that also contribute to overall GPS position error are ephemeris error, satellite clock and hardware inaccuracies, tropospheric and ionospheric refraction, receiver noise, and multipath effects. For a detailed analysis of these error sources, the reader is referred to US DoD (2001), Seeber (2003), and Leick (2004). A very brief overview of some of the major error sources is presented below.

Ephemeris errors:

The satellite ephemeris bias is the discrepancy between the true position (and velocity) of a satellite and its known value. Ephemeris errors are satellite dependent and very difficult to completely correct and compensate because there are many forces acting on the predicted orbit (US DoD, 2001). The direct measurement of all forces acting on a satellite orbit is difficult and hence it is nearly impossible to accurately account or compensate for all error sources when modelling the orbit of a satellite. The details of ephemeris errors are well documented in Montenbruck and Gill (2000), Leick (2004), Hoffmann-Wellenhof et al. (1997), and Seeber (2003).

Satellite clock errors:

Each satellite carries two caesium (Cs) and two rubidium (Rb) atomic clocks with a fundamental frequency of 10.23 MHz. As discussed in the interface control document (ICD-GPS-200C, 2000), the GPS Control Segment maintains GPS system time to within

1 microsecond of UTC (USNO[21]) except for leap seconds. The GPS Master Control Station in Colorado Springs, USA continuously runs a Kalman Filter that estimates the satellite clock behaviour as a second order polynomial. The corresponding coefficients are transmitted to the user receiver via the Navigation Message. They are usually referred to as offset (s), drift (s/s), and drift-rate (s/s^2) (US DoD, 2001). What is available to users is actually a *prediction* of the clock behaviour for some time into the future (24 hours or more ahead). As the random deviations of even caesium and rubidium oscillators are not predictable, such deterministic models of satellite clock error are accurate to about 20 nanoseconds, or 6m in equivalent range, depending upon the time since the last Navigation Message update (Drane and Rizos, 1998). The range error due to satellite orbit and clock offset is 2.3 m (1σ) (Table 3.2).

Ionospheric refraction:

The ionosphere is the region of Earth's atmosphere extending from about 50 to 1000 km above the earth's surface. The charged particles (free electrons) in the ionosphere influence the propagation of microwave signals as they pass through the layer. The largest effect is on the speed of the signal, and hence the ionosphere primarily affects the measured range. For GPS frequencies, the resulting range error can vary from less than 1 m to more than 100 m (Klobuchar, 1991, 1996). The ionosphere is a dispersive medium and the propagation delay in this layer depends on the electron content along the signal path and on the frequency used. In general, the higher the frequency the less the impact of the ionosphere on the propagation of microwave signals. Since L1 and L2 signals experience different propagation delays in the ionosphere, a dual frequency receiver can reduce the effect of the ionospheric refraction on the range error (Seeber, 2003). Overall, however, this is estimated to be the largest component at 7.0m (Table 3.2).

Tropospheric refraction:

The troposphere is the lower part of the Earth's atmosphere extending from the surface to about 50km. It is an electronically neutral (non-ionised) atmospheric layer containing most of the mass of the neutral atmosphere and practically all of the water vapour. Tropospheric delay is a function of the satellite elevation angle and the altitude of the receiver, and is dependent on the atmospheric pressure, temperature, and water vapour

[21] United Sates Naval Observatory, Home Page: http://www.usno.navy.mil

pressure (Brunner and Welsch, 1993). The range error due to the effect of tropospheric propagation is estimated at 0.2m (SPS, SIS, 1σ) (Table 3.2).

Multipath:

The carrier wave propagates along a straight line. Due to reflecting surfaces near the GPS receiver, a satellite-emitted signal after arrives at the receiver via more than one path, hence distorting the C/A-code and P-code modulations, and the carrier phase observations (Leick, 2004). This phenomenon is known as multipath (Figure 3.2). Multipath is one of the major error sources in GPS positioning. It should be noted that multipath is frequency dependent. As a result, carrier phases are less affected than code ranges (Lachapelle, 1990). The range error associated with the carrier phase multipath is generally restricted to 5 cm compared to 3m for the C/A-code and 30cm for the P-code (Raquet, 1998). The estimated SPS SIS URE error due to the effect of multipath is 1.5m (1σ) (see Table 3.2).

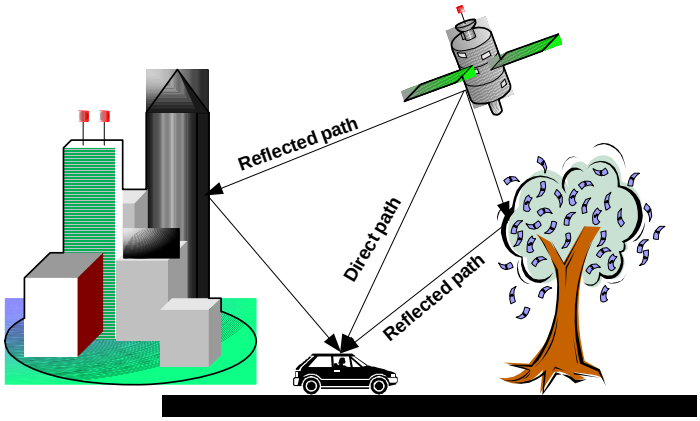

Figure 3.2: Multipath effect

3.2.1.2 Differential GPS

In order to eliminate or minimise some of the errors that affect GPS and to thereby obtain higher accuracies, GPS can be used in a relative or differential positioning mode known as differential GPS (DGPS). The technique involves estimating the errors in the pseudoranges for all satellites in view observed at a given time and at a given point which is usually referred to as the reference station (RS). The time-varying correction data is derived when simultaneous observations from the same satellites are made between the

RS receiver at a known location and the rover receiver at an unknown location. These differential observations form a differential baseline vector between the RS and the rover receiver as shown in Figure 3.3. Errors in the satellite position and atmospheric delay estimates are highly correlated at both receivers. The relatively accurate pseudorange correction ($PR_r^s - R_r^s$) is then possible to compute at the RS receiver. This is because the true range (R_r^s) from the RS to the satellite can be determined from the RS's coordinates and the broadcast satellite coordinates. These differential corrections are then passed by radio link to the remote, or roving receiver which is capable of applying these individual pseudorange corrections to each satellite used in the navigation solution.

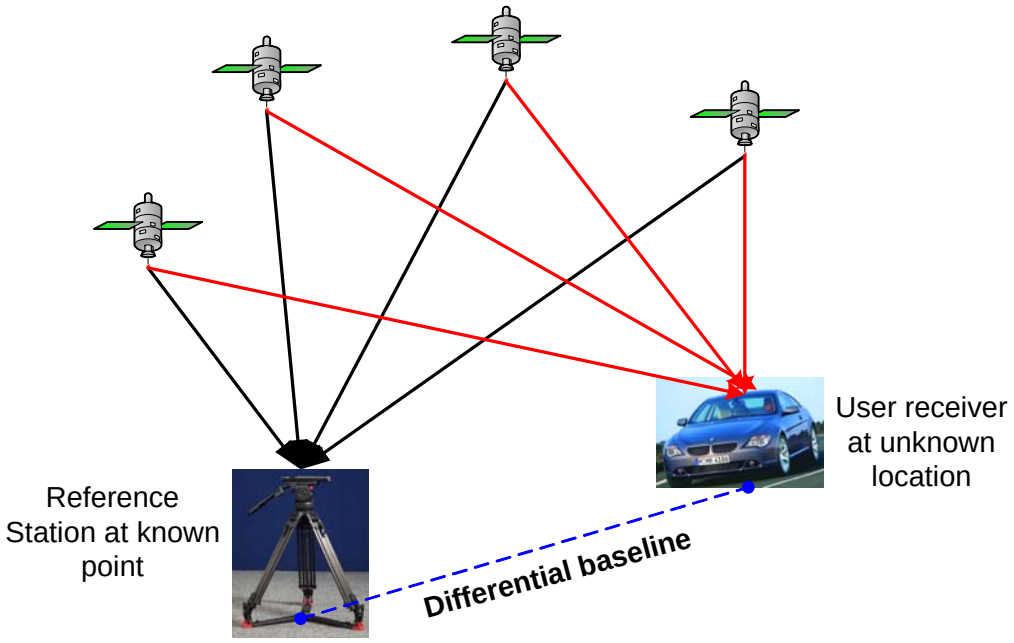

Figure 3.3: Differential (Relative) GPS positioning

Differential positioning only removes common-mode errors, those errors common to both the reference and remote receivers (multipath or receiver noise are not included). Other uncommon errors are reduced when receivers are close together (baseline length less than 30 km). Two types of differential techniques have emerged: (1) Differential code GPS (using C/A or P-code), and (2) Differential carrier GPS (required to track carrier phases both at a RS and rover at the same time). Position accuracies of 1-10 meters are possible with differential code GPS based on C/A code SPS signals. Centimetre relative positioning is possible with differential phase GPS if integer ambiguity can be resolved successfully. This procedure is fully described in Chapter 8. Because of the spatial constraints in urban areas resulting in both geometric and measurement precision

problems, it is unlikely that differential position would perform better (in terms of coverage) than the stand-alone GPS navigation (Ochieng et al., 2003c).

3.2.2 Deduced Reckoning (DR) Motion Sensors

Vehicle navigation using deduced reckoning (DR) motion sensors is based on the integration of an estimated or measured displacement vector. Usually, it is composed of two or more sensors that measure the heading and displacement (speed) of a vehicle. In general, a gyro system is used to measure the rate of change of heading and the vehicle odometer is used to measure displacement and speed. By combining these two measurements, the vehicle track from its starting point can be determined. A variety of gyroscopes have materialized in recent years, e.g. mechanical, optic, electrostatic and the relatively new micro-electro-mechanical system (MEMS) technology sensors, with variations in accuracy, stability and cost. The odometer uses the wheel rotation sensor to measure wheel revolutions. The wheel revolutions are then transformed into the distance travelled, normally based on an assumed constant wheel circumference. Using time between two consecutive observations, the speed or velocity of the vehicle can also be determined. A major problem with DR is that it determines vehicle location (i.e. coordinates) relative to a reference point. This means that the absolute positioning error accumulates proportionally with the distance travelled.

Piezoelectric vibrating type gyroscopes based on MEMS technology are attractive due to their low cost but exhibit relatively weak performance. Errors associated with these devices include gyro bias drift, gyro scale factor error, installation misalignment, temperature, vibration and electro-mechanical properties of the operational environment. The geomagnetic field sensor is also subject to errors introduced by magnetic variation and magnetic interference. The most significant of these are the bias drift and scale factor error.

The bias drift can be explained by the existence of an output (rate of change of heading) with no corresponding input (e.g. a causal factor such as vehicle turning). The drift depends on the type of gyroscope (i.e. the manufacturing process and quality) and can be as much as *10 degrees/second* (Zhao et al., 2003). It is usually an unknown random constant and affects the measurements cumulatively, irrespective of whether the vehicle is moving or not.

The scale factor error is caused by calibration errors and electro-mechanical properties of the operational environment. Unlike the bias drift, the scale factor error affects the measurements only when the vehicle makes a turn. Although the scale factor error varies with time, the change should not be significant over a short period of time. Hence, the scale factor error can be modelled as a random constant disturbed by white noise with a low covariance (Zhao et al., 2003).

Factors affecting the odometer output accuracy are the scale factor error, status of the road and pulse truncation. The most significant error is the scale factor error which represents the difference between the true scale coefficient and the calibrated one, is the most significant as it affects the distance measurement whenever the vehicle is moving. It is caused by calibration error, tyre wear and tear, tyre pressure variation and vehicle speed. Although the scale factor will vary during a period of travel, the change should not be significant over a short time.

Due to the character of these errors, the horizontal positioning error of DR could be controlled by an external calibration or augmentation with other positioning devices such as GPS.

3.2.3 Integrated Navigation Systems

In order to achieve the RNP in some areas where the satellite coverage may be restricted, GPS can be augmented with DR with the use of a Kalman Filter (KF) to form an integrated navigation system (GPS/DR). The KF is a set of mathematical equations that provides an efficient computational solution for the combination of different types of noisy data. More precisely, it is a linear minimum mean-square error (MMSE) filtering process for combining noisy sensor outputs (i.e., GPS receivers, gyroscopes, odometers) to estimate the state of a system (i.e., position, velocity, heading, acceleration of a vehicle) with uncertain dynamics (i.e., unpredictable disturbances of the host vehicle or unpredictable changes in the sensor parameters). The application of a KF to nonlinear systems is known as the Extended Kalman Filter (EKF). An EKF algorithm can be used to estimate the optimal result of system states by integrating GPS and DR. A fuller description of this EKF algorithm can be found at Zhao et al (2003). A brief overview is presented below.

State Equation

The vehicle dynamic model can be established as a set of state equations. The following states are considered by Zhao et al. (2003):

$$\mathbf{x} = [e \quad n \quad v_v \quad H_v \quad a \quad \omega \quad \delta S \quad \delta K \quad \varepsilon_G]^T \tag{3.13}$$

where,

x = state vector

e = terrestrial easting position, in *metres (m)*

n = terrestrial northing position, in *metres (m)*

v_v = forward velocity of the vehicle, in *m/s*, with forward being positive

H_v = heading of the vehicle, in *radian*, with north being zero and clockwise being positive

a = the acceleration of the vehicle, in m/s^2

ω = the rate of the heading, in *rad/s*

δS = the odometer scale factor error, in *m/pulse*

δK = the rate gyro scale factor error, in *milivolt/rad/s*

ε_G = the bias drift of the rate gyro, in *rad/s*

The dynamic equations relating these states can be written as:

$$\left.\begin{aligned}
\dot{e} &= v_v \cdot \sin H_v + w_1 \\
\dot{n} &= v_v \cdot \cos H_v + w_2 \\
\dot{v}_v &= a + w_3 \\
\dot{H}_v &= \omega + w_4 \\
\dot{a} &= w_5 \\
\dot{\omega} &= -\beta_\omega \omega + w_6 \\
\delta\dot{S} &= w_7 \\
\delta\dot{K} &= w_8 \\
\dot{\varepsilon}_G &= -\beta_g \varepsilon_G + w_9
\end{aligned}\right\} \tag{3.14}$$

where w_k (k =1 to 9) are the dynamic noise, β_w, β_g are the skew correlation times (i.e. inverse of correlation times). It can be seen that this is a non-linear set of equations as both the equations for $\dot{e}$ and $\dot{n}$ are non-linear.

These equations can be rewritten in matrix form as:

$$\mathbf{x}_k = \mathbf{\Phi}_{k-1}\mathbf{x}_{k-1} + w_k \qquad w_k \sim N(0, Q_{w,k}) \tag{3.15}$$

where $\mathbf{x}_k$ is the state vector, $\mathbf{\Phi}_{k-1}$ is the state transition matrix which relates the state at time step *k-1* to time step *k*, w_k models the uncertainty of the state with $w_k \sim N(0, Q_{w,k})$ where $Q_{w,k}$ is the state noise covariance matrix.

Measurement Equations

From the GPS receiver, the information on position (φ_{GPS}, λ_{GPS}), speed (v_{GPS}) and heading (H_{GPS}) of the vehicles can be derived. From the odometer and rate gyroscope, the pulses (ΔN_{odo}) during a time interval Δt, representing the displacement travelled, and direct current (DC) voltage output (V_{RG}), representing the heading-rate of the vehicle, can be acquired. So the measurement state vector is defined as (Zhao et al., 2003):

$$z = [\,\lambda_{GPS} \quad \varphi_{GPS} \quad v_{GPS} \quad H_{GPS} \quad \Delta N_{odo} \quad V_{RG}\,]^T \tag{3.16}$$

And the measurement equations are defined as:

$$\left.\begin{aligned}
&\lambda_{GPS} = e/R \cdot \cos\varphi_{GPS} + v_2 \\
&\varphi_{GPS} = n/R + v_1 \\
&v_{GPS} = v_v + v_3 \\
&H_{GPS} = H_v + v_4 \\
&S \cdot \Delta N_{odo} = 1/2 \cdot a \cdot \Delta t^2 + v_v \cdot \Delta t - \delta S \cdot \Delta N_{odo} + v_5 \\
&V_{RG} = (K + \delta K)(\omega + \varepsilon_G) + v_6
\end{aligned}\right\} \tag{3.17}$$

where v_k (k=1 to 6) are the observation noise, *S* and *K* are the nominal scale factors for the odometer and gyroscope respectively; Δt is the interval time; *R* is the radius of the earth. It can be seen that the measurement equations are also non-linear because of the last measurement equation.

These equations can be rewritten in matrix form as:

$$\mathbf{z}_k = \mathbf{H}_k \mathbf{x}_k + v_k \qquad v_k \sim N(0, R_{v,k}) \tag{3.18}$$

where $\mathbf{z}_k$ is the measurement vector, $\mathbf{H}_k$ is the measurement matrix relating state to measurement, v_k models the noise in the measurement with $v_k \sim N(0, R_{v,k})$ where $R_{v,k}$ is the measurement noise covariance matrix.

Kalman Filter Design

Having identified the state equation and the measurement equation, an EKF algorithm is designed. Due to the non-linear properties of both the system dynamic equations and measurement equations, linearization is required. The state transition and observation matrices are derived as follows (Gelb, 1979):

$$\mathbf{\Phi}_{k-1} = \begin{bmatrix} 1 & 0 & \sin H_v \cdot \Delta t & v_v \cdot \cos H_v \cdot \Delta t & 0 & 0 & 0 & 0 & 0 \\ 0 & 1 & \cos H_v \cdot \Delta t & -v_v \cdot \sin H_v \cdot \Delta t & 0 & 0 & 0 & 0 & 0 \\ 0 & 0 & 1 & 0 & \Delta t & 0 & 0 & 0 & 0 \\ 0 & 0 & 0 & 1 & 0 & \Delta t & 0 & 0 & 0 \\ 0 & 0 & 0 & 0 & 1 & 0 & 0 & 0 & 0 \\ 0 & 0 & 0 & 0 & 0 & 1-\beta_\omega \cdot \Delta t & 0 & 0 & 0 \\ 0 & 0 & 0 & 0 & 0 & 0 & 1 & 0 & 0 \\ 0 & 0 & 0 & 0 & 0 & 0 & 0 & 1 & 0 \\ 0 & 0 & 0 & 0 & 0 & 0 & 0 & 0 & 1-\beta_g \cdot \Delta t \end{bmatrix} \tag{3.19}$$

$$\mathbf{H}_k = \begin{bmatrix} 1/R\cos(\varphi_{GPS}) & 0 & 0 & 0 & 0 & 0 & 0 & 0 & 0 \\ 0 & 1/R & 0 & 0 & 0 & 0 & 0 & 0 & 0 \\ 0 & 0 & 1 & 0 & 0 & 0 & 0 & 0 & 0 \\ 0 & 0 & 0 & 1 & 0 & 0 & 0 & 0 & 0 \\ 0 & 0 & \Delta t & 0 & \Delta t^2/2 & 0 & -N_{odo} & 0 & 0 \\ 0 & 0 & 0 & 0 & 0 & K+\delta K & 0 & \omega+\varepsilon_G & K+\delta K \end{bmatrix} \tag{3.20}$$

State vector prediction:

$$\hat{\mathbf{x}}_k^- = \mathbf{\Phi}_{k-1} \hat{\mathbf{x}}_{k-1} \tag{3.21}$$

Variance-covariance matrix prediction:

$$\mathbf{P}_k^- = \Phi_{k-1}\mathbf{P}_{k-1}\Phi_{k-1}^T + \mathbf{Q}_{k-1} \quad \textbf{(3.22)}$$

Kalman gain matrix computation:

$$\mathbf{K}_k = \mathbf{P}_k^-\mathbf{H}_k^T(\mathbf{H}_k\mathbf{P}_k^-\mathbf{H}_k^T + \mathbf{R}_k)^{-1} \quad \textbf{(3.23)}$$

Update state estimate using measurement:

$$\hat{\mathbf{x}}_k = \hat{\mathbf{x}}_k^- + \mathbf{K}_k(\mathbf{z}_k - \mathbf{H_k}\hat{\mathbf{x}}_k^-) \quad \textbf{(3.24)}$$

Variance-covariance matrix update:

$$\mathbf{P}_k = (\mathbf{I} - \mathbf{K}_k\mathbf{H}_k)\hat{\mathbf{P}}_k^- \quad \textbf{(3.25)}$$

The complete process of the EKF is shown in Figure 3.4.

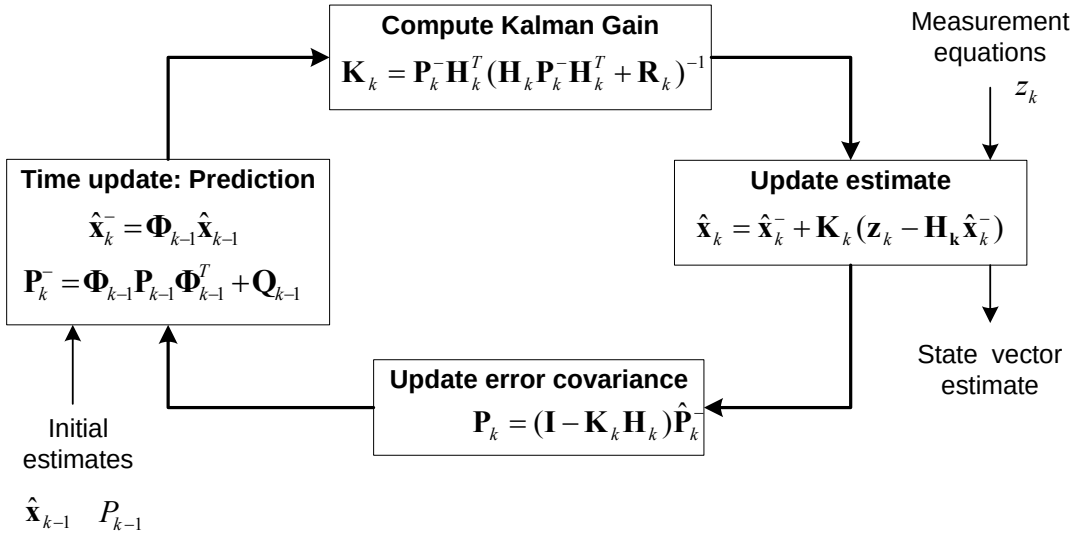

Figure 3.4: A complete picture of the operation of the Kalman Filter

3.3 Digital Road Network Maps

The road network map database is a vital component for any transport telematics services requiring spatial and temporal positioning information (Scott and Drane, 1994). The road map is a graphical representation of the important spatial information that a driver needs to negotiate during a trip especially to a new location, and hence it serves as the interface between the driver and the navigation technology being used. A compact, informative road map is only the end product of a long and complex map creation process whose principles and procedures have been advanced over centuries (Drane and Rizos, 1998). This section discusses some issues related to digital map quality.

3.3.1 Errors in Map Creation

The creation of a road network map involves a series of decisions on how features of the earth will be represented in an electronic map. Every such decision introduces a potential error in the final map. According to the National Research Council, NRC (2002), the steps in the process include: map scale, level of generalization, projection, datum, and coordinate system.

Map scale can be defined as the ratio of distance on a map over the corresponding distance on the ground, represented as 1:M where M is the scale denominator. Map scale is an issue because as scale becomes larger the amount of detail that can be presented in a map is also increased. The ability to measure the length of linear features on the ground (road centreline), the position of point features (junctions and roundabouts), and the areas of polygons with a high level of accuracy are also increased. Map scales are usually divided into three categories, namely large, medium and small. A large-scale map extends over the range 1:1 to 1:24,000. A typical large-scale map is a UK road network map (Land-line.Plus) at a scale of 1:1250. Medium-scale maps range from 1:24,000 to 1:100,000. Anything smaller than 1:100,000 are considered small scale. Maps for ATT applications should have a larger scale within urban areas compared to rural areas due to the typically higher density of road network features. The benefits that can be achieved in urban areas by solving transport problems will also therefore require a high positioning accuracy.

Whenever the surface of the earth is represented on a map, the features on the earth are generalized to some degree (NRC, 2002). For example, roads are represented as a single

"centreline" and curvatures are represented as piecewise linear lines (for a gentle curve) or as a polyline (for a sharp curve). This generalisation reduces the accuracy of the representation of the features on the ground and can introduce significant bias.

Map projection is a technique for presenting data from a curved surface on a flat surface e.g., computer screen, sheet of paper etc. There are many methods for map projection. The most common one is the Universal Transverse Mercator (UTM) projection. Changing a map projection implies simultaneously changing the relationships of area, shape, and direction on a map. Each of these factors can introduce error into the representation of a point, line, and area on a map.

The fourth choice that may introduce further error in the map is the selection of horizontal and vertical datum. A datum is defined as a reference of a quantity for calculation of other quantities (Czemiak and Reilly, 1998). For a relatively small-scale map, a datum can have a serious effect on the placement of GPS positions onto a GIS base map (NRC, 2002).

The other potential error source is the coordinate system used. Most GPS receivers give positioning data in the WGS84[22] (i.e., Latitude and Longitude) coordinate system. However, the users normally exploit their local coordinate systems. For example, the UK road network data is in the British Grid coordinate system (i.e., Easting and Northing). Therefore, transformation, conversion and projection are essential to bring both systems to the same coordinate system. The process may also introduce error (NRC, 2002).

3.3.2 Errors in Digitisation

Digitisation of a road map typically involves recording the spatial road data (point, line, and polygon) along with their associated labels and attributes digitally into a GIS environment. As discussed, there are numerous errors associated with a paper map that will be automatically transmitted to the digital map format. Moreover, the digitising process (entering spatial data using a digitising tablet and puck) has its own inherent error that most likely will increase the error of the digital map. The Census Bureau found that a misalignment of the digitising puck by 0.05 in. from a line on the paper map changed a point's position by 416 ft on the new digital map during the digitisation of the US

[22] WGS 84 is the 1984 revision of the World Geodetic System used for global datum system for horizontal datum.

Geological Survey (USGS) paper topographic maps of source scale 1:1,000,000 (NRC, 2002). This type of error is common when digitising a paper map. Moreover, a variation in a room's temperature and humidity may shrink or expand the unstable base to which the paper map is attached, and hence introduce error.

3.3.3 Digital Map Quality

Digital map data is usually based on a single-line-road-network representing the centreline of the road. Road attributes such as width, number of lanes, turn restrictions at junctions, and roadway classification (e.g., one-way or two-way road) normally do not exist in the map data. Therefore, the accuracy and uncertainty of digital road network data is a critical issue if the data is used for land vehicle navigation. One must be aware of the following concerns regarding the quality of road network data:

- The features (e.g., roundabouts, junctions, medians, curves) of the real-world that have been omitted or simplified in the road map. This is usually known as topological error.
- The accuracy of the classification (e.g., junction or roundabout) of those features
- Data currency i.e., how currently the map was created
- The displacement of a map feature (e.g., road centreline, specific junction) from its actual location in the road. This is generally known as geometric error.

Both geometric and topological errors of map data may introduce significant horizontal errors in land vehicle positioning and navigation. While the geometric error can be corrected with suitable hardware, software and algorithms, the topological error cannot be easily corrected (Goodwin and Lau, 1993). The accuracy (2D) of a digital map is defined as the closeness of a measurement or estimate to a true value. A rigorous statement of accuracy includes statistical measures of uncertainty and variation. Accuracy is generally represented by the standard deviation of errors (difference between measurements on the map and the true value). The true values of map attributes or labels can be obtained from an independent source of higher accuracy measurement such as GPS carrier phase observables, higher resolution satellite imagery, aerial photography, or a ground visit. If

e^1, e^2, ……..,e^n represent a series of differences between measurements on a map and their true values, the accuracy of this map is given by σ^2_{map}, where

$$\sigma^2_{map} = \frac{\sum_{i=1}^{n}(e^i - \mu)^2}{n} \qquad \textbf{(3.26)}$$

in which $\mu = \frac{\sum_{i=1}^{n} e^i}{n}$ and n is the number of measurements.

There are also empirical methods available to estimate map accuracy. For instance, the University of Texas at Austin-Department of Geography (UTADG) developed a method to compute map accuracy from knowledge of the errors introduced by different sources. This method calculates an estimate of overall accuracy by summing the squares of specified components of the map and taking the square root of the sum. For example, assuming the scale of a map is 1:2500, the estimated error due to the source document is 2.5 m (1mm*2500), map registration is 1.25m (0.5mm*2500) and digitising is 0.5m (0.2mm*2500), the total error of a map of scale 1:2500 is 2.84m. Following this methodology, the total estimated error of the map scale 1:25000 is 28.39m.

The UK Road network data supplied by Navigation Technologies (NavTech) has a map scale of 1:2500. Therefore, the maximum horizontal error is estimated to be 2.84 m (using UTADG method described above). Figure 3.5 shows the graphical comparison of this digital road map (road centreline) with another digital road map (map scale 1:50000) obtained from the UK Ordnance Survey (UKOS). The true vehicle positions obtained from higher accuracy GPS carrier phase observables are denoted by the dot symbols. The NavTech map data and the true vehicle positions data agree reasonably well and suggest that the section of the road map is a roundabout. However, the UKOS map data indicate that the section of the map is a five-legged junction. If UKOS map data is used in vehicle navigation, the horizontal positioning error may be increased significantly.

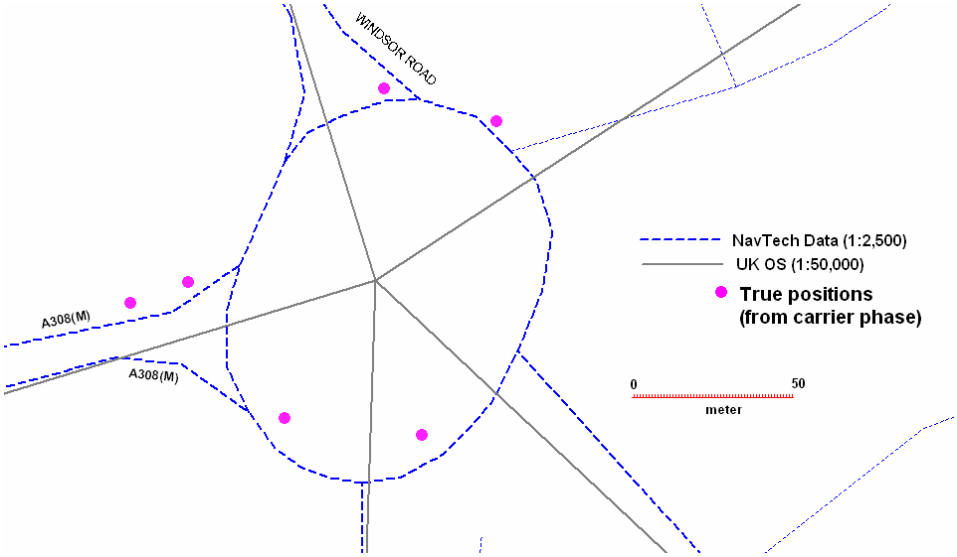

Figure 3.5: A graphical comparison of road network data from two different sources

3.4 Map Matching

The state-of-the-art navigation systems usually rely on a combination of various types of sensors. Even with very good sensor calibration and sensor fusion technologies, inaccuracies are inevitable. Moreover, there is also imprecision associated with the GIS-based digital road map due to errors in map creation and digitisation. As a result of such inaccuracies in the positioning systems and a flawed GIS digital base map, actual vehicle positions do not match with the spatial road map although the vehicle is known to be restricted on the road network. This phenomenon is known as spatial mismatch. The spatial mismatch is often more severe at junctions, roundabouts, complicated flyovers and built-up urban areas with complex route structure environments. Moreover, it is also difficult to achieve the required navigation performance (RNP) in such areas.

However, an algorithm can be formulated by taking into account the historical trajectory of the vehicle and topological information of the road network (e.g., connectivity and orientation of links) to precisely identify the correct link on which the vehicle is travelling. Furthermore, an estimation of the vehicle location on the link can also be determined taking into consideration all error sources associated with the navigation system and digital map database. This is referred to as a map matching algorithm.

Suppose a vehicle, equipped with a GPS receiver, is travelling along a finite system of streets, $\overline{N}$ (Figure 3.6a). The system $\overline{N}$ is not exactly known (see White et al., 2000 ,

and Greenfeld, 2002 for details). Applying various mapping techniques, a network representation N (Figure 3.6b) of $\overline{N}$ can be formed where N consists of a set of curves in $\boldsymbol{R^2}$, each of which is called an arc. Each arc ***A***, which is a single line representation of the road centreline, can be completely described by a fixed series of points $A^0, A^1, ..., A^{nA}$, each of which is also in $\boldsymbol{R^2}$. Those points are divided into *nodes* and *shape points*. The endpoints (i.e., A^0 and A^{nA}) of the arc ***A*** are normally referred to as *nodes* while the other points (i.e., A^1, A^2, ... A^{nA-1}) are referred to as *shape points*.

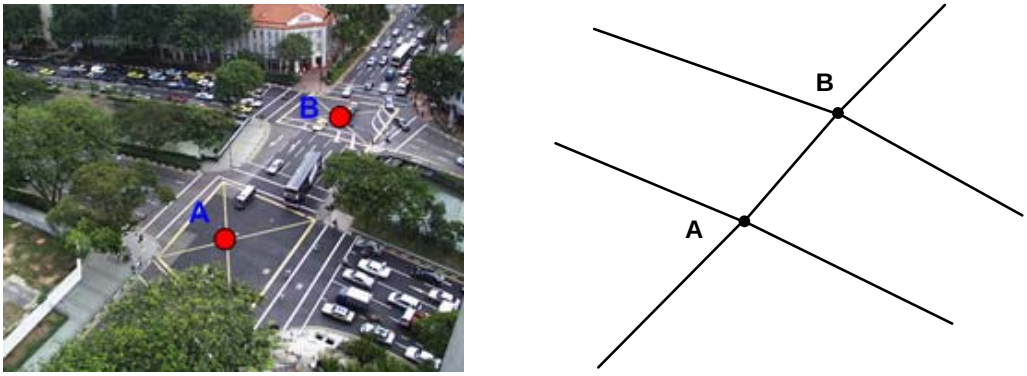

(a) (b)

Figure 3.6: (a) an actual street system, $\overline{N}$, and (b) its network representation, N

Navigation data is obtained from GPS via an on-board receiver as the vehicle is travelling on an arc, ***A***. Suppose that the vehicle position is represented by P^t at a given time t where the actual position of the vehicle at that time is $\overline{P}^t$. Now the task is to identify an arc ***A*** in ***N*** that contains $\overline{P}^t$ such that P^t may be correctly displayed. Since the vehicle is constrained to be on ***A***, the next step is to determine the location of $\overline{P}^t$ (i.e., easting and northing) on the street relative to the end points of the arc. This concept is known as map matching.

The purpose of map matching is to integrate the positioning data with the spatial road network data, to identify the actual link on which the vehicle is travelling, and to determine the vehicle location on that link. Assume that P represents the position fix obtained from the navigation system when the actual location of the vehicle is at Q (Figure 3.7a). P deviates from the road centreline due to error in the map and the navigation data. A map matching algorithm identifies the correct link (AB) for the position fix P and snaps back the position fix onto the link AB ((Figure 3.7b).

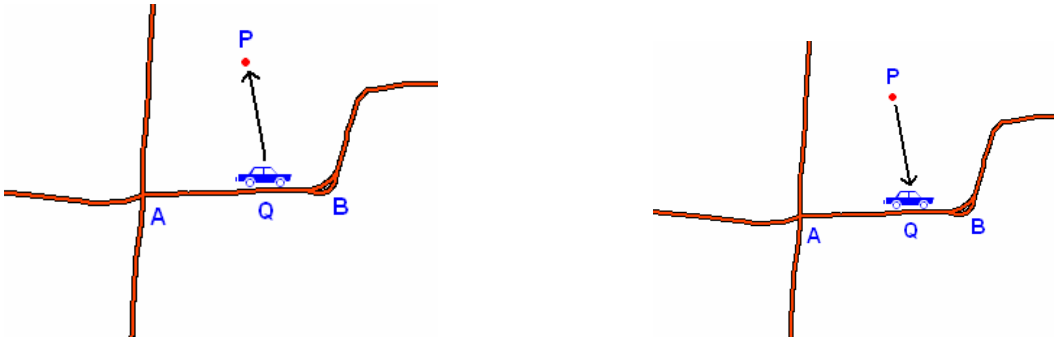

(a) *(b)*

Figure 3.7: Map matching concept

Topological features on the road network include both nodes and links. Curved roads are normally represented as polylines and straight roads are represented as lines in a digital map. In other words, arcs (roads) without *shape points* are referred to as lines and arcs with *shape points* are referred to as polylines. Each polyline consists of a series of lines depending on the number of *shape points* within the arc. Each arc is assumed to be piece-wise linear.

For simplicity, each *shape point* is assumed to be a node. Each line and node is associated with a set of identifying attributes. The attributes of the node are the *x*-coordinate and *y*-coordinate that identify the spatial position of the node (Figure 3.8a). A node with the same *x*-coordinate and *y*-coordinate has the same identification number. The attributes of each line (i.e., link) are determined from the nodes within the line (i.e., start node and end node) as in Figure 3.8b. Therefore, connectivity information among links at a junction can be derived from these two geographic data files and can then be used as an important input to the map matching algorithm.

Node ID	Easting	Northing
1	525841	178856
2	525488	178626
3	525463	178656
4	525432	178703
5	525498	178617
6	525399	178772
7	525933	178863
8	525320	178917

(a)

Link ID	Start_node	End_node
1	1	7
2	2	3
3	3	4
4	4	6
5	5	2
6	6	13
7	7	10
8	8	167

(b)

Figure 3.8: Numerical format of (a) node, and (b) link data

However, the spatial digital road network data obtained from the vendors may not be utilised straightforwardly as an input to map matching algorithms, as it normally does not contain the connectivity information of links (i.e., start and end node of links). Moreover, polylines have to be disaggregated into lines using nodes and shape points. *Link* and *node* data in numerical format are also necessary and they can be extracted from the digital map. A flow chart for the procedure is shown in Figure 3.9 for a digital map data obtained from the Digimap[23] service.

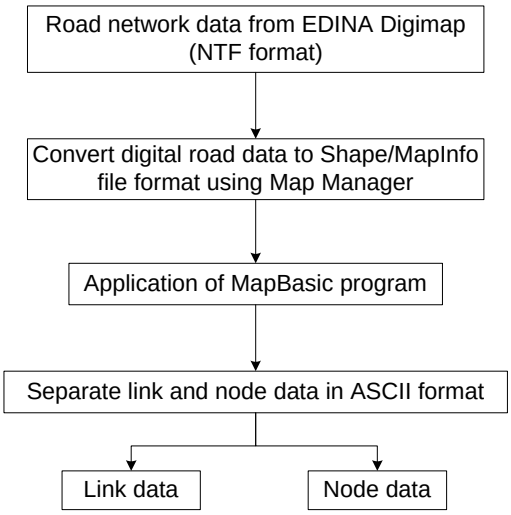

Figure 3.9: Procedure to extract link and node data in ASCII format from a digital map

Figure 3.10(a) represents a portion of a digital map from Digimap consisting of a simple overlay of the road network. The attribute table associated with the map data does not have node coordinates and link connectivity information. Using the procedure outlined in Figure 3.9, node and link information in numerical format can easily be extracted. Figure 3.10(b) shows the same portion of the digital map including the node identification number which is very important for link connectivity information.

[23] Digimap is an EDINA (Edinburgh Data and INformation Access) service that delivers maps and map data of Great Britain to UK tertiary education

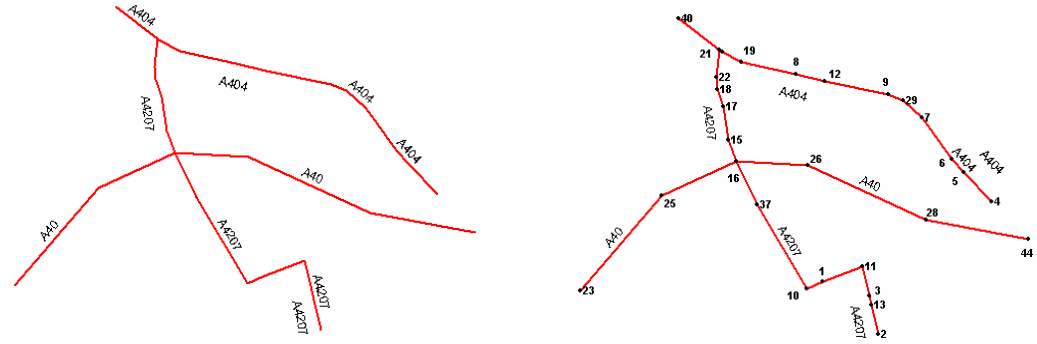

Figure 3.10: A portion of a digital map from EDINA Digimap (a) overlay of road network without nodal information, (b) with nodal information

3.5 Summary

This chapter discussed the state-of-the-art of navigation systems used for land vehicles. It was described that stand-alone GPS was not sufficient to provide the required coverage in urban areas. This was because GPS suffers both the systematic errors and random noise. Errors include satellite related errors such as clock bias and orbital errors, propagation related errors such as ionospheric refraction, tropospheric refraction and multipath, and receiver related errors such as clock bias. The errors associated with a low-cost DR sensor were then presented. These include the scale factors for the odometer and the gyro, and the bias drift of the gyro. The integration of a low-cost DR sensor and GPS was proposed as a means to increase the coverage of GPS in urban areas employing an EKF algorithm, a brief overview of which was presented.

This chapter also discussed the importance of the road network map database to aid land vehicle positioning and navigation. Two major error sources associated with the map data were the error in map creation and error in map digitisation. Due to the error sources both in the navigation systems and the digital map data, it was suggested that a map matching algorithm should employed for accurate locational information on the vehicle travelling on the road network. However, in many cases this requires that the standard digital road network data be further processed to provide the link connectivity information. An example of this was then presented.

The next chapter will review existing map matching algorithms and their limitations and will go on to discuss in detail the motivation of this research.

CHAPTER 4

REVIEW OF EXISTING MAP MATCHING ALGORITHMS

4.1 Introduction

As discussed in Chapter 3, the purpose of a map matching algorithm is twofold: (1) to identify the correct link among the candidate links and (2) to determine vehicle location on that link. Scott (1994) acknowledges that correct link identification is a key component of any map-aided estimator such as a map matching algorithm. Most existing map matching algorithms address the problem of link identification. This is because the performance derived from the map matching algorithm can be misleading if the vehicle location is projected to an incorrect link. It is also equally important to accurately estimate the vehicle location on the selected link to obtain the high accuracy positioning required for some ATT services as discussed in Chapter 2 (section 2.4.1). However, there are limitations in existing algorithms both in the identification of correct links and in the determination of vehicle locations.

This chapter presents a general review of existing map matching algorithms. First, an overview of the algorithms is presented by classifying them into three groups: geometric, topological, and advanced map matching algorithms. The corresponding performance of each is then described. This is followed by a description of these limitations in terms of link identification, vehicle location determination, validation and integrity (level of confidence). In light of these limitations, the motivation of this thesis is then defined.

4.2 Literature Review

Map matching algorithms are often used to determine the location of a vehicle on a road. Most of the formulated algorithms utilise navigation data from GPS or GPS/DR and road network data from a digital map. One of the common assumptions found in the literature for implementing map matching is that the vehicle is essentially constrained to a finite network of roads. While this assumption is valid for most vehicles under most operating conditions, problems may be encountered for off-roadway situations such as car parks or on private land. Most of the studies also report that the digital map used for map matching should be a high scale in order to generate the position outputs without an error (e.g., Zhao, 1997).

Zhao (1997) provides a good overview of the basic theory behind the map matching process. He suggests the use of a number of techniques in a map matching process e.g., (a) a semi-deterministic approach, (b) a probabilistic approach, (c) a fuzzy-logic-based approach, and (d) a pattern recognition process.

The semi-deterministic algorithm is similar to the algorithm proposed by French (1989). The basic requirement of this algorithm is that an initial vehicle location (i.e., initial coordinates) and a direction of travel must be known in advance. Various conditional tests are then performed to determine whether the vehicle is travelling on the known road network. However, Zhao (1997) does not unambiguously discuss what types of parameters can be included in the conditional tests.

The probabilistic algorithm requires the definition of an elliptical or rectangular confidence region around a position fix obtained from a navigation sensor. This technique was first introduced by Honey et al. (1989) in order to match position from a DR sensor to a map. Zhao (1997) discusses this technique in the case of GPS and suggests that the error region can be derived from the error variances associated with the GPS position solution. The error region is then superimposed on the road network to identify a road segment on which the vehicle is travelling. If an error region contains a number of segments, then the evaluation of candidate segments are carried out using heading, connectivity, and closeness criteria. While such criteria are conceptually beneficial, Zhao (1997) does not go into the details of their implementation. Indeed, there are many other

parameters e.g., speed of the vehicle, distance to the downstream junction, etc. that can be used to improve further the map matching process.

Zhao (1997) also suggests the use of a qualitative decision making process to identify the correct road segments among the candidate segments. An example here is a fuzzy-logic process. He derives eight rules for the case in which the position solution is achieved from a DR sensor. The rules are a combination of those suggested by Huang et al. (1991) and Kao and Huang (1994). Significant efforts and experimental tests are essential to derive knowledge-based fuzzy rules in the case where the navigation solution can be obtained from GPS or integrated GPS/DR.

Zhao (1997) states that map matching is basically a pattern recognition process and therefore, concludes that many pattern recognition processes can be used. One of the main candidates is a neural network. However, this has not been fully described in Zhao's book. Most of the map matching algorithms described in the following section are based on the theories outlined in Zhao (1997) with enhancements proposed by other researchers including Greenfeld (2002), White et al. (2000), Taylor el al. (2001), etc.

Procedures for map matching vary from those using simple search techniques (Kim et al., 1996), to those using more complex mathematical techniques such as a Kalman Filter (Kim et al., 2000). Approaches for map matching algorithms found in the literature can be categorised into three groups: geometric, topological and advanced. The following sections briefly describe these algorithms.

4.2.1. Geometric Analysis

A geometric map matching algorithm makes use of the geometric information of the digital road network by considering only the shape of the links (Greenfeld, 2002). It does not consider the way links are connected to each other.

The most commonly used geometric map matching algorithm is a simple search algorithm. In this approach, each of the positioning fixes matches to the closest 'node' or 'shape point' of a road segment. This is known as point-to-point matching (Bernstein and Kornhauser, 1996). A number of data structures and algorithms exist in the literature to

select the closest node or shape point of a road segment from a given point (e.g., Bentley and Maurer, 1980; Fuchs et al., 1980).

This approach is both easy to implement and very fast. However, it is very sensitive to the way in which the network was digitised and hence has many problems in practice. That is, other things being equal, arcs with more shape points are more likely to be properly matched. In a straight arc with two end nodes, all positioning points above the arc match only with the end nodes of the arc. Figure 4.1 illustrates a point-to-point map matching approach.

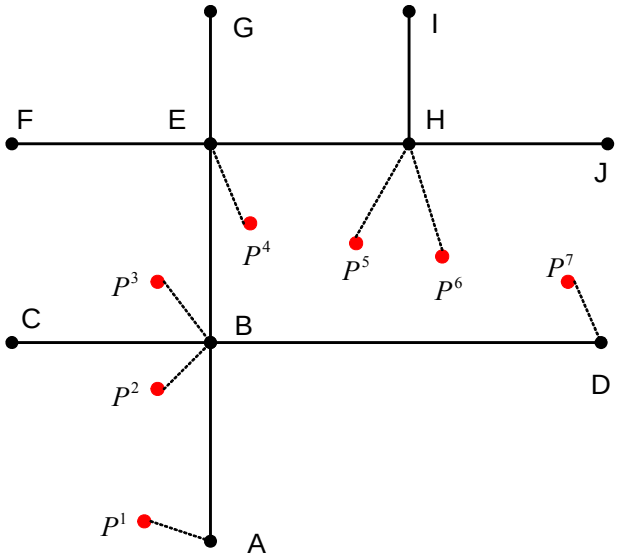

Figure 4.1: Point-to-point map matching approach

In this example, the position fixes from the navigation system are indicated by P^1 to P^7 when the vehicle travels on a road network consisting of ten nodes (A to J). The actual links on which the vehicle is travelling during this period are AB and BD. However, the results from the point-to-point map matching show that the vehicle travels on AB, then BE, EH and finally BD. This is incorrect.

Another geometric map matching approach is point-to-curve matching (Bernstein and Kornhauser, 1998, White et al., 2000). In this approach, the position fix obtained from the navigation system is matched onto the closest curve in the network. Each of the curves comprises line segments which are piecewise linear. Distance is calculated from the position fix to each of the line segments. The line segment which gives the smallest distance is selected as the one on which the vehicle is apparently travelling. Although this

approach gives better results than point-to-point matching, it does have several shortcomings that make it inappropriate in practice. For example, it gives very unstable results in urban networks due to the high road density. Moreover, the closest link may not always be the correct link. Figure 4.2 shows the results of the point-to-curve map matching algorithm for the same road network configuration shown in Figure 4.2. It can be seen that the algorithm selects AB, BE and BD as the correct links when the vehicle actually travels on AB and then BD. There is, however, an improvement in this approach compared to the point-to-point map matching algorithm.

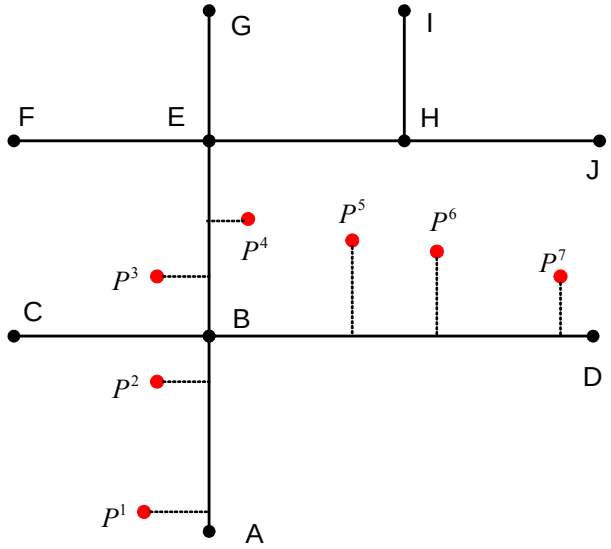

Figure 4.2: Point-to-curve map matching approach

The other geometric approach is to compare the vehicle's trajectory against known roads. This is also known as curve-to-curve matching (Bernstein and Kornhauser, 1996; White et al., 2000; Phuyal, 2002). This approach firstly identifies the candidate nodes using point-to-point matching. Then, given a candidate node, it constructs piecewise linear curves from the set of paths that originates from that node. Secondly, it constructs piecewise linear curves using the vehicle's trajectory i.e., the positioning points, and determines the distance between this curve and the curve corresponding to the road network. The road arc which is closest to the curve formed from positioning points is taken as the one on which the vehicle is apparently travelling. This approach is quite sensitive to outliers and depends on point-to-point matching, sometimes giving unexpected results.

Bernstein and Kornhauser (1996) describe several algorithms (or parts of algorithms) for matching an estimated position to a network representation of the street system. Two things are apparent from their study. First, it is clear that this is a complex and fairly difficult task. Point-to-point and point-to-curve matching are unlikely to work very well, especially when there are errors in the position and/or errors in the network representation. Hence, more complicated algorithms must often be used. Second, though a number of different algorithms can be used, it seems clear that it is both important to perform some kind of curve-to-curve matching and to incorporate topological information in the algorithm. Bernstein and Kornhauser conclude that the more attention that is given to the topological information, the better the algorithm performs.

White et al. (2000) describe several algorithms (or parts of algorithms) for matching an estimated position to a network representation of the street system and attempt to evaluate four of them. Since most route changes occur at intersections, their study suggests that particular attention needs to be paid to the problems that arise at intersections. The discussion focuses on urban routes since most algorithms appear to work well on highways. However, they recommend that the algorithms need to be evaluated on a wider array of routes, especially in urban areas. The limited number and variety of routes considered in their study preclude more general conclusions from being made.

An enhancement of the point-to-curve map matching algorithm is proposed by Srinivasan et al. (2003). Their study recommends the execution of double checks (a bearing check and a turning check) before mapping the position fix onto the closest road segment. *A bearing check* is performed between the instantaneous vehicle heading obtained from GPS and the bearing of the road segment. *A turning check* is introduced to make sure that the heading difference between two consecutive position fixes from GPS agreed reasonably well with the turn calculated from the topology of the road network. They state that the enhanced point-to-curve algorithm improves the correct link identification. Although their method uses vehicle heading from stand-alone GPS, the effect of vehicle speed on heading is ignored. It is well known that the vehicle heading is inaccurate at low speeds (Taylor et al., 2001; Ochieng et al., 2004). Moreover, this method is highly sensitive to outliers.

Bouju et al. (2002) examine two map matching approaches: (1) point-to-curve, and (2) point-to-curve with the aid of vehicle direction. Their study finds that the first approach is the simplest and fastest. However, it introduces significant horizontal errors especially

near junctions or in parallel street scenarios where the nearest link is not always the actual link. This approach normally gives good results when applied to a map with a smaller scale. The second approach is almost similar to the first one but it takes into account the direction of the vehicle. If the difference between vehicle direction and link direction exceeds a pre-defined threshold, then a shift is applied to correct the position. Some modifications are suggested to improve the performance of the algorithms: (a) the use of historical information on the vehicle position, (b) the application of topological analysis of the road network, (c) the use of speed information obtained from GPS, and (4) the use of road design parameters such as turn restrictions and roadway classification.

Taylor et al. (2001) propose a novel method of map matching using GPS, height aiding from the digital road map and virtual differential GPS (VDGPS) corrections, referred to as the *road reduction filter (RRF)* algorithm. Due to the use of height aiding, they report that one less satellite is required for the computation of the vehicle position (i.e., height aiding removes one of the unknown parameters) using GPS. The initial matching process of this algorithm is based on the geometric curve-to-curve matching proposed by White et al. (2000) which is quite sensitive to outliers. The proposed algorithm does not consider link connectivity information which could improve its performance. As previously mentioned, it is also well known that the vehicle heading from GPS is not accurate if the vehicle speed is low. This has not been considered in this algorithm. Although the proposed algorithm is based on the bearing of the vehicle, there was no indication how to deal with the situation when the vehicle is stopped on a road segment for a few seconds. Moreover, the orthogonal projected location of the GPS fixes on the arc is used to determine the vehicle positions. However, Greenfeld (2002) found that the orthogonal projection of the position fixes on an arc is often different from the actual location of the vehicle on the arc. The algorithm is also not appropriate for urban areas.

4.2.2. Topological Analysis

In GIS, *Topology* refers to the relationship between entities (points, lines, and polygons). The relationship can be defined as adjacency (in the case of polygons), connectivity (in the case of lines), or containment (in the case of points in polygons). *Topology* should not be confused with *topography*. *Topography* refers to surface slope (i.e., ridges, valleys). Therefore, a map matching algorithm which makes use of the geometry of the links as

well as the connectivity and contiguity of the links is known as a topological map matching algorithm (Greenfeld, 2002, Chen et al., 2003, and Meng et al., 2003).

Greenfeld (2002) reviews several approaches for solving the map matching problem and proposes a weighted topological algorithm. This is based on a topological analysis of a road network and uses only coordinate information on observed positions of the user. It does not consider any heading or speed information determined from GPS. The map matching process is composed of two sub-algorithms: (1) InitialMapping, and (2) Map. The purpose of the 'InitialMapping' sub-algorithm is to find an initial match. The procedure is to select the closest node from the position fix and to determine all the links which are connected to this node. When the next position fix is available, the proposed method maps the position fix onto one of the selected links. This sub-algorithm is applied to the following circumstances: (a) when the first position fix is received from GPS, (b) when the distance between the two consecutive fixes exceeds a pre-selected distance tolerance, and (c) when the 'Map' sub-algorithm is not capable of fixing a position fix. Based on the initial match, the 'Map' sub-algorithm performs subsequent topological analysis using a weighting scheme. The weighting scheme is based on the perpendicular distance of the position fix from the link (proximity), the degree of parallelism between the GPS line[24] and the link (orientation), and the intersecting angle (intersection). The total weighting score for a particular link is given by

$$W = W_D + W_{AZ} + W_I \tag{4.1}$$

where,

W - the total score

W_D - the weight for proximity

W_{AZ} – the weight for similarity

W_I – the weight for an intersection, if it exists

The intersecting angle is the angle between a GPS line and the road link. Following the identification of the correct link using one of the sub-algorithms discussed above, Greenfeld then determines the vehicle location on the link by an orthogonal projection.

[24] A line formed between two consecutive position fixes

This method is very sensitive to outliers as these can lead to the determined vehicle heading to be inaccurate. The other deficiency of this algorithm is not to take into account the vehicle speed as GPS position fixes are scattered randomly when the speed is less than 3.0m/sec (Taylor et al., 2001 and Ochieng et al., 2004). Another issue is that the weighting score for the intersecting angle turns out to be zero when the vehicle travels along a link as there is usually no intersection between the GPS line and the link. The intersecting angle, however, gives a score at junctions but sometimes assigns a wrong link as shown in Figure 4.3. Assume that the vehicle is travelling along the route A-C and the position fixes during this period are denoted by P^1, P^2, P^3, and P^4. The algorithm selects the link AB for the position fixes P^1 and P^2 which is correct.

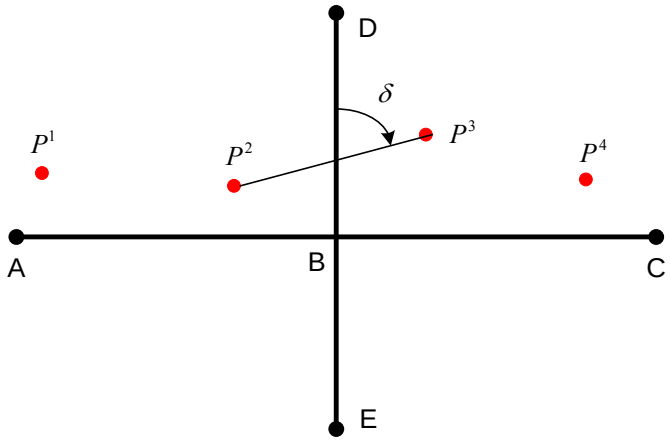

Figure 4.3: The higher score assigned to an incorrect link

However, the algorithm identifies BD as the correct link for the fix P^3 although the actual position of the vehicle during this epoch is on BC. This is because the weighting score from the intersecting angle (δ) gives BD a positive score. Moreover, P^3 is much closer to BD compared to BC. Greenfeld suggests that additional research is required to verify the performance of the algorithm to make an accurate position determination on a given road segment. Quddus et al. (2003) also test this algorithm for a relatively sparse road network and conclude that the algorithm sometimes identifies incorrect road segments (also see Chapter 5 for a typical geometric configuration).

Meng et al. (2003) also use a topological analysis of the road network to develop a simplified map matching algorithm. This algorithm is based on the correlation between the trajectory of the vehicle and the topological features of the road (road turn, road curvature, and road connection). A number of conditional tests are applied to eliminate

road segments that do not fulfil some pre-defined thresholds. The thresholds are obtained from the statistical analysis of field-test data. The algorithm is implemented using the navigation data from GPS/DR and digital map data including information on the turn restrictions at junctions which can substantially improve the performance of the map matching algorithms. The algorithm does not work well at some junctions where the bearings of the connecting roads are not significantly different. In these circumstances, the algorithm switches to a post-processing mode to identify the correct link, making it unsuitable for real-time applications. However, a qualitative decision making process based on the speed of the vehicle, the direction of the vehicle from a turn-rate gyro, the distance travelled by the vehicle, the quality of the digital map, and the errors associated with the navigation sensors might be utilised to correctly identify the correct link in real-time applications for such circumstances.

Li and Fu (2003) develop an improved map matching algorithm also based on topological analysis of the road network. Similar to the Greenfeld algorithm (Greenfeld, 2002), this method also derives vehicle heading from the line formed by two consecutive position fixes in order to examine the similarity between the vehicle direction and the link direction. There are three main stages in the algorithm: (1) searching mode, (2) normal running mode and (3) turning mode. In searching mode, the point-to-curve approach is used to select the correct link. The vehicle position fixes should then continue to match on the previously identified link until the vehicle makes a turn. This is known as normal running mode. In turning mode, the algorithm goes back to the searching mode and identifies the new link. The inherent problems associated with the point-to-curve matching approach make this algorithm less effective in urban areas. Moreover, the criteria to detect a turning manoeuvre are unclear from the study presented.

4.2.3. Advanced Map Matching Algorithms

Advanced map matching algorithms are referred to as those algorithms that use more refined concepts such as a Kalmam Filter (e.g., Krakiwsky et al., 1988; Tanaka et al., 1990; Jo et al., 1996, Kim et al., 2000), Dempster-Shafer's theory (also known as Belief Theory) (e.g., Najjar and Bonnifait, 2003; Yang et al., 2003), a fuzzy logic model (e.g., Zhao, 1997; Kim et al., 1998, Kim and Kim 2001, Syed and Cannon, 2004), or the application of Bayesian interference (Pyo et al., 2001). Most of these algorithms are briefly described below.

Kim et al. (2000) develop an integrated navigation system consisting of GPS, DR, and a map matching technique for ATT applications. Their study implies that several ATT services require 2-D horizontal positioning accuracy of 5 to 10m (95%) for the driver's safety. They try to achieve such a high accuracy of positioning by the efficient use of digital road maps. First, a simple point-to-curve matching approach is used to identify the correct link. Then the orthogonal projected location of the position fix onto the link is used to obtain an initial vehicle location. Due to the projection, the cross-track error is reduced significantly. However, the along-track error remains a key issue. A Kalman Filter is then designed to re-estimate the vehicle position with the objective of minimising the along-track error. Their results suggest that the along-track error associated with the initial vehicle position is 22.8m (95%). This is reduced to 10.6m (95%) after re-estimating the vehicle position using the Kalman Filter. Vehicle positions estimated by DGPS (accuracy higher than 5m) are used as a reference to calculate these error statistics. As stated earlier, the point-to-curve method is not sufficient to select the correct link especially in dense urban road networks. If the identification of the link is incorrect, then the inputs to the Kalman Filter will also be inaccurate which may lead to further positioning errors. The method can be improved using a more efficient technique for the selection of the correct link taking into account the heading and speed of the vehicle as well as a topological analysis of the road network.

Yang et al. (2003) develop an improved map matching algorithm based on Dempster-Shafer's (D-S) theory of evidence using rule based logical inference systems. The inputs to the algorithm (i.e., vehicle positions from GPS) are smoothed with a Kalman Filter (KF). The distance between a GPS position fix and the surrounding road segments is obtained using the point-to-curve matching concept. Weights are then given to segments based on the calculated distances. For example, if the distance is between 15m and 20m, then the weight is 0.7, and if the distance is between 5m and 10m then the weight is 0.9. D-S's theory of evidence is then applied to obtain the correct segment. Their results suggest that the algorithm identifies 96% of the road segments correctly (based on 1075 position fixes). However, this may not always be the case in urban areas, as the point-to-curve method does not fully consider the topology of the road network.

Najjar and Bonnifait (2003) develop a novel road-matching algorithm to support a real-time car navigation system. The study first describes the integration of DGPS with ABS (Anti-Lock Braking) sensors for continuous positioning information. The vehicle,

therefore, does not need to be equipped with any additional extra sensors such as a gyroscope. Their map matching method is based on several criteria using Belief Theory. The criteria are the proximity criterion (based on the distance between the position fix and the link) and the heading criterion (based on the difference between the heading of the vehicle and the direction of the candidate segment). Based on each criterion, a degree of Belief (*yes, perhaps, no*) is assigned to each link. These criteria are then combined using Demspter-Shafer's rule. If a link is associated with a large Belief to the *yes* hypothesis from both criteria, then it is selected as the correct link. For example, if the proximity criterion assigns a link with a large mass to the *yes* hypothesis (i.e., $m_p(yes)=0.8$) and the heading criterion also gives the same link a large mass to the *yes* hypothesis (i.e., $m_h(yes)=0.9$), then the link can be selected as the correct link. The method however can give inaccurate results in parallel streets, as it does not consider the topology of the road network. The algorithm did not take into account the errors associated with the navigation sensors and the digital map data. Therefore, the location of the vehicle estimated by the algorithm will not be robust as it will be adversely affected by these errors. Moreover, their study fails to validate their map matching algorithm in order to evaluate its performance in terms of correct link identification and horizontal accuracy determination.

Kim and Kim (2001) develop a novel adaptive-fuzzy network-based *C*-measure to find the exact road on which a car travels. The basic idea of this algorithm is to identify a link based on a *C*-measure (a measurement for the total weighting score given to a link). The *C*-measure has a recursive form and normally depends on several factors: (a) the distance between the filtered position obtained from the navigation filter and its orthogonal position on the road, (b) the shape of the road, and (c) the *C*-measure at the previous epoch. A threshold value for *C* is obtained using an adaptive neuro-fuzzy inference system. The link associated with the maximum C is taken as the correct link if the *C* is greater than the pre-defined threshold. Following the identification of the correct link, an orthogonal projection of the position fix onto the link is then used to estimate the vehicle location. Their result suggests that the maximum horizontal error in an urban area is 15m although there is no indication how the actual vehicle positions (reference) are determined to compute such an error statistic, especially in an urban environment. The errors associated with the navigation sensors (GPS/DR) and the digital maps are not considered, although they are available. The inputs to the fuzzy inference system used to

determine the threshold for the *C*-measure are therefore likely to be insufficient in the case of complex road networks.

Syed and Cannon (2004) also describe a map matching algorithm based on a fuzzy logic model. The algorithm consists of two sub-algorithms: (1) first fix mode, and (2) tracking mode. In the first sub-algorithm, a fuzzy inference system (FIS) is used to identify the correct link for the initial position fix. The characteristic of this FIS is to select a set of links which are within 50m of the GPS/DR position fix. A link is then identified based on the direction of the vehicle relative to the direction of the links and the heading change from the gyroscope. The location of the vehicle is then determined by an orthogonal projection of the position fix onto that link. Following the identification of the first link and the location of the vehicle on it, the algorithm then goes into the second sub-algorithm. Another FIS is used to see whether the subsequent position fixes can be matched to the link identified in the first fix mode. The inputs are proximity, orientation and distance travelled by the vehicle along the link. If there is any outlier in the GPS/DR outputs or a turn is detected, then the algorithm goes back to the first fix mode. The algorithm normally takes about 30 seconds in order to complete the first fix mode. This is too long for some services like en-route guidance where the vehicle can travel through a few junctions within this period. In urban areas, the algorithm may have to use the first fix mode frequently and then each time there is a delay to identify the first correct link. Their map matching algorithm also does not take into account the error sources associated with the navigation sensors and the digital maps and hence the determination of vehicle location is not robust.

Fu et al. (2004) propose a hybrid map matching algorithm by analysing the geometry of the road network. A fuzzy logic model is used to identify the correct link among the candidate links. Two inputs used in the FIS are: (1) the minimum distance between the position fix and the link, and (2) the difference between the vehicle direction and the link direction. The fuzzy subsets associated with the first input are *very small* (<20m), *small* (20m-40m), *medium* (40m-60m), *large* (60m-80m), and *very large* (>80m). The fuzzy subsets associated with the second input are *very small* ($<5^0$), *small* (15^0- 30^0), *medium* (30^0- 45^0), *large* (45^0- 60^0), and *very large* ($>60^0$). The single output of their fuzzy inference system is the possibility of matching the position fix to a link. This simple fuzzy logic model is sensitive to measurement noise. Moreover, the vehicle heading obtained from GPS is inaccurate at low speed. This has not been taken into account. As

the algorithm selects a link for each position fix with no reference to historical trajectory, there is a high possibility of selecting a wrong link, especially at junctions.

Xu et al. (2002) propose a new map matching method based on turn restriction information at junctions stored in a map database. The integration of GPS and DR are achieved using a Kalman Filter (KF). Their map matching method comprises several steps: (a) initialisation, (b) the estimation of the vehicle position between junctions, (c) the estimation of the vehicle position near a junction when no turn is detected, and (d) the estimation of the vehicle position near a junction when a turn is detected. However, no indication is given on how to accurately obtain an initial vehicle location on a link. If the initialisation is wrong, then the subsequent process will also be wrong. This method may provide inaccurate results at diverging junctions where the directions of the candidate links do not vary markedly. The errors associated with the navigation sensors and the quality of the digital map are again not taken into account. Therefore, a robust technique is required to estimate the vehicle location on the links. Furthermore, the study also does not report the performance of the algorithm.

Pyo et al. (2001) develop a map matching algorithm using the Multiple Hypothesis Technique (MHT). The MHT was first introduced by Reid (1979) to track manoeuvring targets in an uncertainty environment. The MHT, which uses measurements from a validation region, is re-formulated as a single target problem to develop the map matching method. Pseudo-measurements are generated for all links within the validation region as defined using the error ellipse derived from the navigation sensors (GPS/DR). Pseudo-measurements (position and heading) are defined as the projected points of the GPS/DR positions on the links. The topological analysis of the road network (connectivity, orientation, and road design parameters) together with the pseudo-measurements is used to derive a set of hypotheses and their probabilities for each GPS/DR sensor output. When a probability of a hypothesis becomes smaller than a pre-defined threshold, then the hypothesis is deleted. Again, when the ratio of a probability of a hypothesis to the largest probability becomes smaller than another pre-defined threshold, then the hypothesis is also pruned. The map matching is only applied to the valid hypotheses and then a Kalman Filter is executed to estimate the bias (between the map-matched location and GPS/DR sensor output).

The main disadvantage of this map matching algorithm is not to introduce a method for an initial map matching as the performance of the subsequent matching largely depends on the initial matching. Their results suggest that the map matching process cannot be applied to 4%, 11%, and 13% of the cases when implemented in high road density areas, 2-lane roads, and 4-lane roads respectively. This is counterintuitive given that one is likely to obtain more position fixes in 4-lane roads (wider) in an open space, compared to narrow roads in a high road density area. The reason for such an uncharacteristic result may be because the error ellipse does not include a link (road centreline) with large road width as shown Figure 4.4.

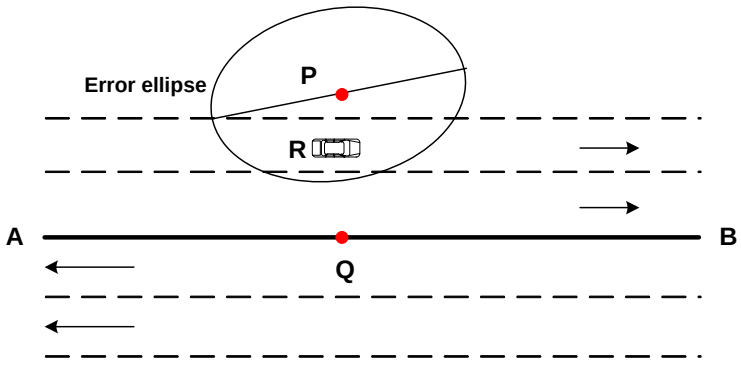

Figure 4.4: The error ellipse and the 4-lane road

In Figure 4.4, P represents the vehicle position fix from GPS/DR when the vehicle travels along the second lane of a 4-lane road. The line AB indicates the centreline of the road. It is noticeable that the error ellipse is able to include the actual position (R) of the vehicle. However, due to the wider road (4-lane road) the ellipse does not contain the centreline (AB) of the road and hence the proposed map matching algorithm cannot match the position fix, P, to a link. A larger error ellipse may be required in such cases as suggested by Zhao (1997). Even the map matching process selects the link (AB) as the correct link, the distance (PQ) is usually large for a wider road which may introduce more bias when using the Kalman Filter and lead to another link being deemed more "correct".

4.2.4. Performance of Existing Map Matching Algorithms

Most of the existing studies do not assess the performance of the developed map matching algorithms. However, a few studies report the performance measures that are shown in Table 4.1. The navigation sensors used in the algorithms, the test environments, the percentage of correct link identification, and the 2-D horizontal accuracy are shown in

columns two, three, four, and five respectively. The most used navigation sensors are either GPS or GPS/DR. The percentage of correct link detection ranges between 86 (White et al., 2000) to 93 (Syed and Cannon, 2004). The 2-D horizontal positioning accuracy ranges between 15m to 10.6m (100%). It is very surprising that none of the studies states the scale of the digital map used to estimate performance given the large impact that this can have on map matching performance.

Table 4.1:The performance of some existing map matching algorithms

Authors and year of publication	Navigation sensors	Test Environments	Correct Link Identification (%)	Horizontal Accuracy (m)
Kim et al. (2000)	GPS	Suburban	-	10.6 (100%)
Kim and Kim (2001)	GPS/DR	Urban and suburban	-	15m (100%)
White et al. (2000)	GPS	Suburban	85.8	-
Pyo et al. (2001)	GPS/DR	Urban and suburban	88.8	-
Taylor et al. (2001)	GPS + Height	Suburban	-	11.6 (95%)
Bouju et al. (2002)	GPS	Suburban	91.7	-
Yang et al. (2003)	GPS	Suburban	96	-
Syed and Cannon (2004)	GPS/DR	Urban and suburban	92.8	-

4.3 Limitations of Existing Map Matching Algorithms

The literature review presented in this chapter suggests that existing map matching algorithms are not capable of satisfying the RNP parameters of some important ATT services. This section discusses the limitations of existing map matching methods, in terms of link identification, location determination, validation, and integrity.

4.3.1. Identification of Links

One of the important tasks of map matching algorithms is to select the correct link among the candidate links since an incorrect selection can lead to a sequence of wrong selections (Scott, 1994; Syed and Cannon, 2004). Accurate link identification is critical especially in dense urban areas where the average distance between roads is very small. Consequently,

one should reduce the possibility of error by taking into account all available data from the navigation sensors and the digital map. If the navigation data is obtained from GPS, then the heading and speed information can be attained as a by-product of the positioning solution[25]. The heading and speed of the vehicle can play a vital role in selecting the correct link, especially at junctions where the speed of the vehicle is comparatively low. It should be noted that vehicle heading measurements from GPS tend to be unstable at low speed (Taylor et al., 2001; Ochieng et al., 2004). However, this is improved when heading is measured with DR gyro sensor. None of the existing algorithms take into account speed information when using heading from GPS observables during the identification of a correct link.

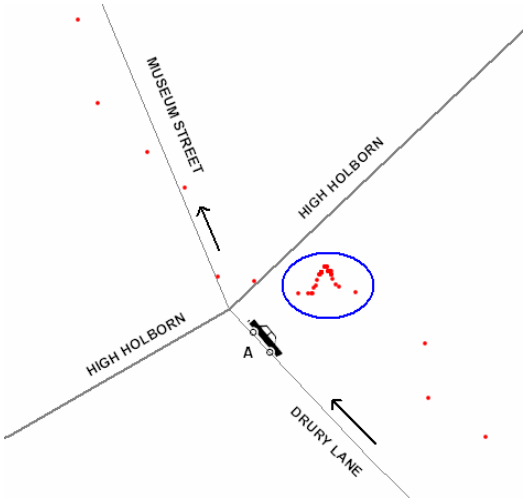

(a)

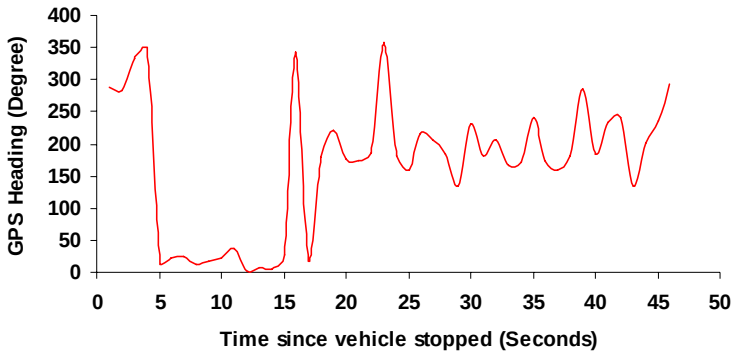

(b)

Figure 4.5: The vehicle heading from GPS when the vehicle speed is zero

[25] Most use the Doppler frequency shift of the radio signals to determine velocity

Figure 4.5 illustrates the problem. The red dots represent the vehicle position solutions from GPS (Figure 4.5a). The position fixes within an ellipse specify those that result when the vehicle is stationary on the Drury Lane at A for 46 seconds in response to a traffic signal at the junction. During this period, the vehicle heading is unsteady and varies from 2 to 350 degrees (Figure 4.5b).

Some of the advanced map matching algorithms utilise a circular confidence region (with a fixed radius) around a position fix to select the candidate links for matching at junctions. Syed and Cannon (2004), for instance, use a circle of 50m radius for all epochs. These fixed confidence regions sometimes may contain unexpected links which have similar characteristics to the actual link, especially in urban areas where the road density is relatively high. It may also not contain any links at all as shown in Figure 4.4. The error regions, therefore, should be dynamically determined. One way to estimate error ellipses is to use the variance-covariance matrix associated with the GPS (or GPS/DR) position solutions and the errors associated with the digital map data. Some of the advanced map matching algorithms use dynamic confidence regions albeit calculated based on the navigation sensor errors only (Najjar and Bonnifait, 2003; Pyo et al., 2001). Such confidence regions do not always contain the centreline of the road network, especially when the road width is large. One way to deal with this problem is to account for the bias introduced by using the road centreline alone to represent the roadway.

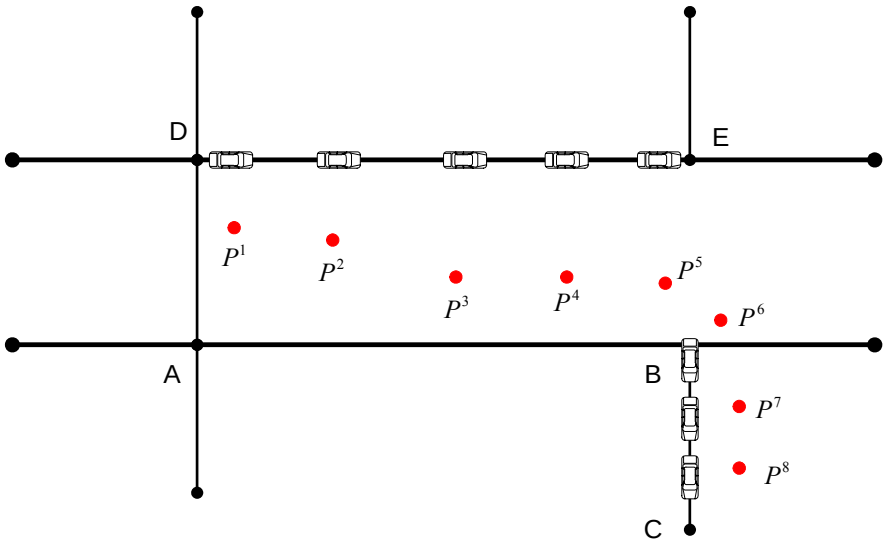

Figure 4.6: Incorrect match using a single epoch for initial matching

Most of the existing map matching algorithms use a single epoch with limited inputs (proximity and similarity in orientation) for the initial map matching process. Since the topological analysis of a road network, especially 'link connectivity' is not available during the first epoch, the initial match resulting from a single epoch may be incorrect. This is explained in Figure 4.6. Assume that a vehicle travels from junction A to junction C. The vehicle position fixes from the navigation system are denoted by P^1 to P^8. Two strong candidate links for the first epoch (P^1) are AB and DE. An initial map matching process (using a single epoch) identifies DE as the correct link because P^1 is closer to DE than AB and the directions of these candidate links are the same. The subsequent position fixes (P^2 to P^5) must also be matched onto DE since the vehicle direction from the navigation sensors is more likely to be similar to the direction of DE. This type of mismatch can be avoided if a few first good position fixes (4 to 5 epochs) are considered in the initial matching process. If the initial matching process identifies the same link for these position fixes, then the link can be chosen as a first correct link. This can give increased confidence in the initial matching process and hence the subsequent matching process will be more accurate.

In the subsequent matching process, most of the existing map matching algorithms use the difference between the vehicle heading from the navigation sensors and the current link heading from the map data. If the difference exceeds the pre-defined thresholds, then the algorithm searches for a new link based on topological analysis of the road network. The performance depends on the determination of the thresholds. Most of the studies choose the thresholds arbitrarily. Field tests may be used to establish the thresholds. This is, however, not always sufficient.

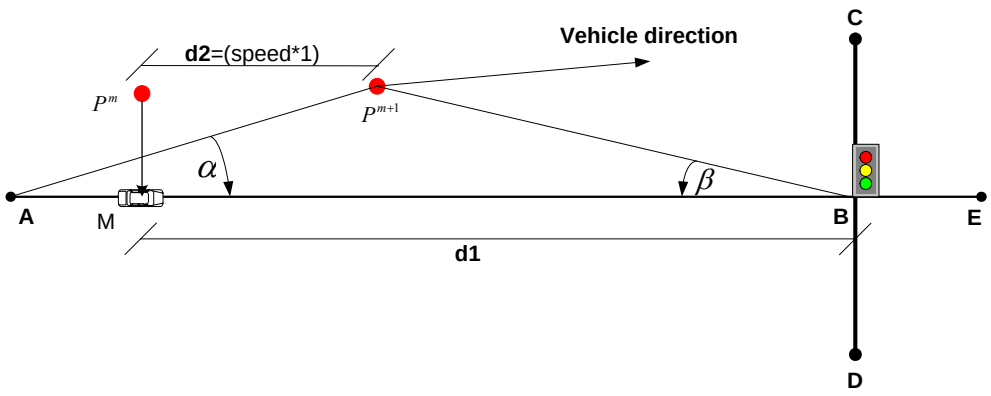

Figure 4.7: Parameters to increase the performance of the subsequent matching process

If a high level of performance is desired, other available information as shown in Figure 4.7 should be considered. If the task is to identify the correct link for the position fix P^{m+1} (given that the position fix P^m maps at M on AB is correct), the available parameters are the distance to the downstream junction (*d1*), the location of the position fix relative to the current link (α and β), the distance travelled on the current link calculated from the speed of the vehicle (*d2*), the gyro rate reading (if available), and the quality of the position fixes[26]. Road design parameters such as turn restrictions at junctions, roadway classification (one-way or two-way roads), and underpasses information can also significantly improve the performance of the map matching algorithm. However, these are not readily available in most of the road network databases, as discussed in Chapter 3.

4.3.2. Determination of Vehicle Location on the Selected Link

In many ATT applications and services, it is important to know where the vehicle is not only in terms of the link on which it is travelling, but also where the vehicle is on the link itself. Therefore, map matching algorithms normally need to place the vehicle on the road. This is also essential for real-time display of the vehicle on a map without error. The determination of the vehicle location on the link is a rather challenging task, especially considering the errors associated with both the digital map and navigation sensors. Most existing map matching algorithms apply a simple perpendicular projection of the position fixes onto the selected links, and ignore the numerous errors associated with the positioning sensors and the spatial road network data.

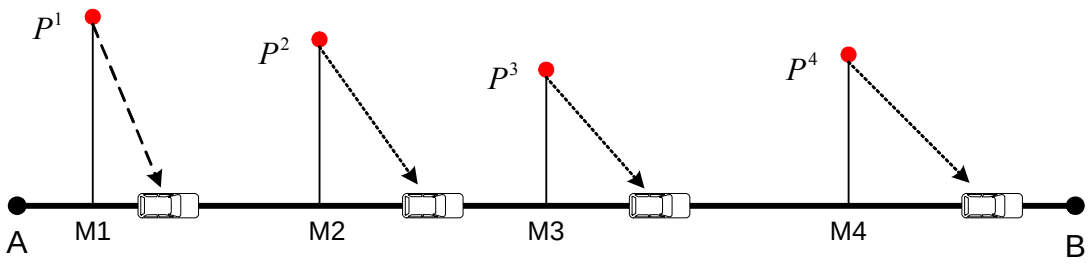

Figure 4.8: Actual vs Perpendicular projected location of the vehicle on the map

In Figure 4.8, the points P^1 to P^4 represent the positioning fixes when a vehicle travels on the link AB. The arrows in this figure indicate the actual locations of the vehicle on the link whereas M1, M2, M3, and M4 represent the orthogonal projected locations on the

[26] This may be evaluated from HDOP and signal-to-noise ratio

link. Clearly, there are significant differences between the actual and projected locations. This is due to a combination of the various error sources associated with the positioning sensors and map data. The following factors need to be considered if high positioning accuracy is desired:

- Uncertainty in map data (especially variance in link direction)
- Variances in the easting and northing components of the position fix
- Uncertainty in vehicle speed obtained from the navigation sensors
- Uncertainty in vehicle heading obtained from the navigation sensors

A robust method needs to be employed to combine all these error sources.

4.3.3. Validation and Integrity (Level of Confidence)

Validation of a map matching algorithm is essential to derive any statistics on its performance in terms of correct link identification and vehicle location determination. A precise vehicle reference (true) trajectory is required in order to assess the performance. Existing map matching algorithms do not provide a meaningful validation technique. Although some of the studies report the accuracy of the algorithms, it was unclear from these studies how the accuracy was calculated. Kim et al. (2000) uses code-based DGPS to obtain true vehicle positions. However, the performance of DGPS is strongly affected by signal multipath, among other factors, and varies according to the surrounding environments. The typical accuracy of DGPS is on the order of 0.5m to 5m (95%) (US DoA, 2003). Consequently, the vehicle positions obtained from DGPS may not be suitable to derive the reference trajectory of the vehicle.

The integrity of a map matching algorithm directly reflects the level of confidence that can be placed in the map-matched position. None of the existing studies discuss the integrity issue in the context of a map matching algorithm. Integrity measures can be used to detect a failure mode in the map matching process. The identification of detection can be utilised to provide a timely warning to the driver that the position solution should not be used for navigation or positioning, and to aid recovery from the failure mode.

4.4 Summary of Motivation for the Research

It has been shown that the most existing map matching algorithms have limitations in terms of the identification of correct links and the determination of accurate vehicle location on the links. These algorithms are consequently not appropriate for some important ATT applications such as accident and emergency management, en-route guidance, and public transport operations in which high accuracy positioning information is essential.

Map matching algorithms can be developed to overcome the limitations of the existing algorithms discussed earlier in this chapter. The following factors are readily available and they must be considered in developing an improved map matching algorithm:

- Topology and quality of the road network
- Proximity between the vehicle position fix and the road link
- Similarity between the vehicle heading and the direction of the road link
- Gyro-rate reading (if DR is available)
- Vehicle speed at the current epoch (from GPS or GPS/DR)
- Quality of the position fixes (HDOP, signal-to-noise ratio)
- Location of the position fix relative to the current link
- Distance to the downstream junction
- Historical navigation information of the vehicle (link ID, vehicle location, vehicle heading and speed)
- The variance-covariance matrix associated with the position fix obtained from the navigation sensors (GPS or GPS/DR)
- Error sources associated with the digital map data

The developed map matching algorithms should be implemented and tested using a number of road networks from both urban and suburban areas.

A validation technique can then be developed to assess the performance of the map matching algorithms. This may be based on the reference trajectory obtained from high precision (cm-level accuracy) GPS carrier phase observables. The effects of navigation sensors and digital map quality on the performance of the map matching algorithms can also be investigated. For this purpose, the navigation data will be collected from GPS and

GPS/DR and the digital map data will be collected from maps of scales 1:1250, 1:2500, and 1:50000. The performance of the developed map matching algorithms will then be estimated for all combinations of inputs.

Integrity measures representing the level of confidence of the map-matched positions can also be developed based on the uncertainty associated with the map-matched location, the vehicle heading, and the link direction. The rationale of integrity can be described using an independent dataset from GPS carrier phase observables.

Finally, the performance of the developed map matching algorithms can be compared with the performance of existing map matching algorithms.

4.5 Summary

This chapter reviewed the literature on existing map matching algorithms. Based on the methodologies used in the map matching techniques, these algorithms were classified into three major groups: (1) geometric, (2) topological, and (3) advanced. A brief description of these algorithms along with their performance was also presented. The limitations of these algorithms were discussed in detail. It was found that the existing map matching algorithms are not suitable for some ATT services such as navigation and route guidance, emergency location. The motivation of this thesis was then described. This may be summarised as developing high integrity map matching algorithms suitable for ATT applications.

CHAPTER 5

AN IMPROVED TOPOLOGICAL MAP MATCHING ALGORITHM

5.1. Introduction

This chapter describes the development of an enhanced map matching algorithm based on various similarity criteria between the road network geometry and derived navigation data. The aim is to use fewer inputs and to make the algorithm as simple and as fast as possible. The basic characteristic of the algorithm presented in this chapter is the use of navigation data from either GPS or an integrated GPS/DR system including position, speed, and heading. Data on the historical trajectory of the vehicle (i.e., data on earlier map-matched positions) is used to avoid sudden switching of mapped locations between unconnected road links. The topological aspects of the road network such as link connectivity and shape points (representing link curvature) are used to improve the performance of the algorithm. Heading and speed data from the positioning sensors are also employed which lead to further improvements in the performance of the algorithm, especially at junctions. The details of the algorithm are described below by first describing and defining the data inputs, followed by a description of the map matching process, and a procedure for identifying data outliers. The developed algorithm is tested using positioning data from an integrated GPS/DR system and road map data from a digital map of scale 1:1250.

5.2. Definition of Data Inputs

The inputs to the algorithm are the navigation data and the topological features of the digital map data. The navigation data include position (easting and northing), speed, heading, and associated error variances. They are the outputs of either GPS or GPS/DR

systems. The topological data include two geographic data files (GDFs): (1) node data including shape points, and (2) link data. The node GDFs consist of node or shape point identifications (IDs) and the corresponding coordinates. The link GDFs consists of link (IDs), from node IDs, to node IDs, link length, and link direction.

5.3. Map Matching Process

The map matching process is shown diagrammatically in Figure 5.1. The three data sources used as inputs to the map matching algorithm are link, node, and positioning data. The process is initiated with nodal matching to identify the correct link (among all the links connected to the node closest to the position fix provided by the navigation sensor) and the determination of the physical location of the vehicle on that link. The next step is to execute some conditional tests based on information from the previous map-matched position to confirm whether the next position fix can be matched to the link identified at the previous step. This is followed by the determination of the physical location on the link. It is vital to carry out the first step carefully and reliably, as there could potentially be many candidate links.

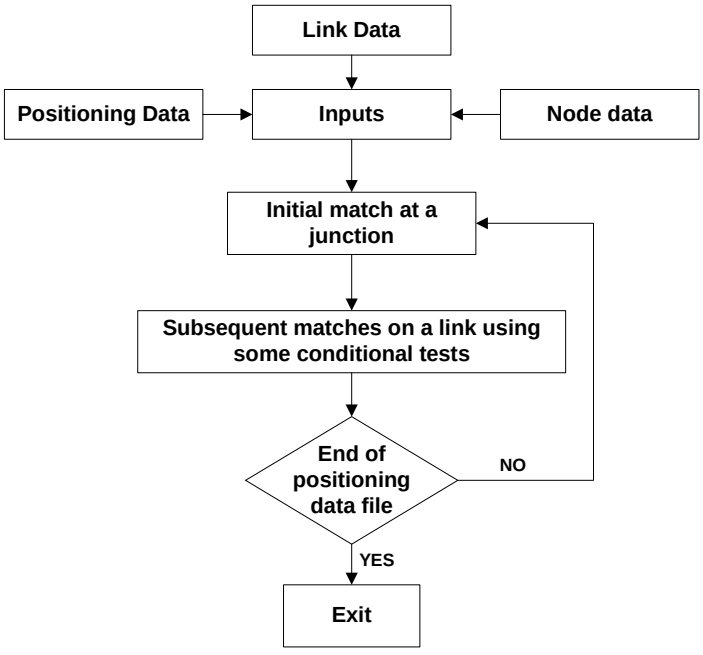

Figure 5.1: Diagrammatic representation of the map-matching algorithm

5.3.1. Identification of the Correct Link

The most difficult part of any map matching algorithm is to select the correct link from among the candidate links (White et al., 2000, Greenfeld, 2002, and Quddus et al., 2003). This will usually occur at junctions in a network. Based on the various similarity criteria between the derived position fixes and the road attributes, a weighting system can be used to select the correct link as proposed by Greenfeld (2002). The criteria used in the Greenfeld algorithm are the similarity in orientation (i.e., the degree of parallelism between the line formed by two consecutive GPS points and the street network arc), the proximity of the position fix to the link, and the size of the intersecting angle between the GPS derived line and the link. The weighting scheme evaluates several candidate links for the correct match by computing a likelihood score based on these criteria. Greenfeld (2002) suggests that similarity in orientation is more important than proximity, but this can be adjusted by altering the weights assigned to each criterion.

The same similarity criteria are used in the algorithm developed here. To improve the performance of the algorithm, however, the weighting scheme is enhanced by introducing additional criteria and other parameters including vehicle speed, the position of the vehicle relative to candidate links, and heading information directly from the GPS data string or the integrated GPS/DR system. Different weighting factors are used to control for the importance of each of these criteria in determining the best map matching procedure. Each weighting scheme is described in turn in the following sections.

5.3.1.1. Weighting for heading

Suppose that a map matching algorithm places a vehicle's position fixes P^1, P^2 and P^3 on link AB and that the vehicle is approaching junction B (Figure 5.2). Now the task is to identify the next correct link for the position fix P^4 using the navigation data associated with this position fix and the attributes of the links connected to junction B.

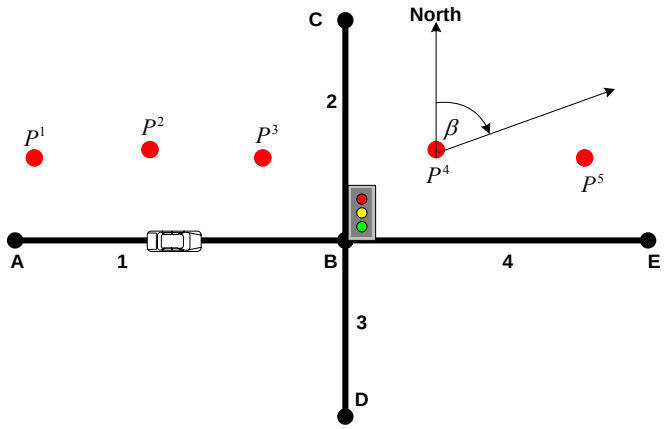

Figure 5.2: Similarity in vehicle heading and bearing of the link

Since the last known location of the vehicle is on link AB, the candidate links for the position fix P^4 are BC, BE and BD assuming that the vehicle does not make a U-turn at junction B. If a U-turn is identified, then link BA also needs to be considered as a candidate link. To select the correct link among these candidate links, a weighting scheme based on vehicle heading relative to link heading can be applied.

The angle β, provided by either GPS or GPS/DR, represents the heading of the vehicle at point P^4 measured relative to a northerly direction for the line between P^3 and P^4. This angle gives a good indicator of the probable direction of the vehicle at this point. The heading of each candidate link denoted as β', is then determined from the link GDFs (in this case, 90˚ for link BE, 0˚ for link BC, and 180˚ for link BD). The difference between the GPS or GPS/DR derived heading (β) and the spatially derived heading (β'), denoted as $\Delta\beta$, is used to formulate the weighting scheme for heading as:

$$WS_H = A_H \cos(\Delta\beta') \qquad \textbf{(5.1)}$$

where,

$$\Delta\beta = \beta - \beta'$$

$$\Delta\beta' = \Delta\beta \;\; if \; -180^0 \le \Delta\beta \le 180^0$$

$$\Delta\beta' = 360^0 - \Delta\beta \;\; if \; \Delta\beta > 180^0$$

$$\Delta\beta' = 360^0 + \Delta\beta \;\; if \; \Delta\beta < -180^0$$

and, WS_H is the weighting score for vehicle heading relative to link heading, A_H (>0) is the weighting parameter for WS_H and its value can be obtained from equation (5.6), described in section 5.3.1.4.

The lower the value of $\Delta\beta'$, the higher the possibility that the candidate link is the correct link, i.e., as the value of $\Delta\beta'$ increases the value of WS_H decreases, as defined by the use of the *cosine* function. Moreover, the *cosine* function allows negative weights if $\Delta\beta'$ is greater than 90^0.

5.3.1.2. Weighting for proximity

The weighting for proximity is based on the shortest (or the perpendicular) distance from the position fix to the link.

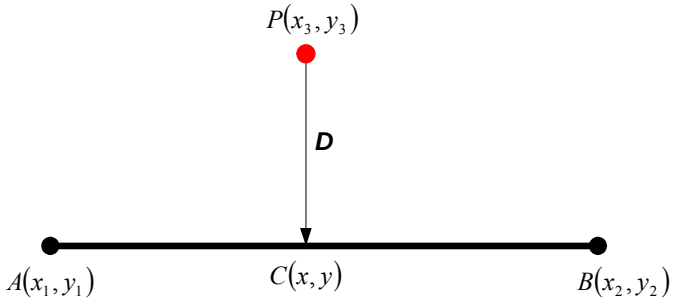

Figure 5.3: Perpendicular distance

Suppose that $P(x_3, y_3)$ is the position fix and AB is a link (see Figure 5.3), then the perpendicular distance from this point to the link is,

$$D = \frac{x_3(y_1 - y_2) - y_3(x_1 - x_2) + (x_1 y_2 - x_2 y_1)}{\sqrt{(x_1 - x_2)^2 + (y_1 - y_2)^2}} \qquad \textbf{(5.2)}$$

It is reasonable to assume that if D decreases then, proximity between the fix and the link increases; therefore the weighting score for perpendicular distance is defined as,

$$WS_{PD} = A_{PD}\omega \qquad \textbf{(5.3)}$$

where,

WS_{PD} is the weighting score for the perpendicular distance (D), A_{PD} (>0) is the weighting parameter for WS_{PD} and its value can be obtained from (5.6), ω is a scale factor that varies between 0 and 1 depending on D . This is defined as:

$$\omega = 1 \text{ if } D < 5 \text{ m}$$
$$\omega = 1.0 - 0.01D \text{ if } 5 \le D \le 100$$
$$\omega = -1 \text{ if } D > 100$$

The first condition satisfies that WS_{PD} is constant when D is less than 5m. The second condition implies that WS_{PD} decreases if D increases. The third condition confirms that WS_{PD} is negative if D is greater than 100m. The smaller the perpendicular distance the higher the score, i.e., if the point P is close to the link AB, then there is a greater possibility that the link is the correct link.

5.3.1.3. Weighting for relative position

$P(x_i, y_i)$ is a position fix obtained from a navigation system (Figure 5.4) and BP represents the distance between the closest node (i.e., B) and the position fix, P. The terms $\alpha_1, \alpha_2, \alpha_3$ and α_4 in Figure 5.4 are the smallest angles between BP and the links AB, BC, BD, and BE respectively. They usually are sufficient to define the location of this fix (P) relative to these links.

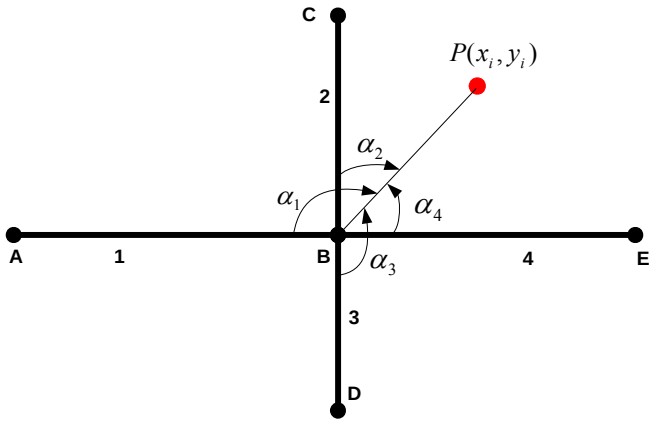

Figure 5.4: Location of a position fix relative to the link

Since the good candidate links for this position fix (*P*) are more likely to be either link BC or link BE, one would expect that the weighting score should be higher for these links than the other links, i.e., the smaller the angle (α) the higher the probability that this is the correct link. This may not be the case in high density road networks, especially in an urban canyon where the effect of multipath is severe and the position fix contains a larger horizontal error.

The weighting score can be given by

$$WS_{RP} = A_{RP}\cos(\alpha_i) \tag{5.4}$$

where,

WS_{RP} is the weighting score for the location of the vehicle relative to the link, A_{RP} (>0) is the weighting parameter for WS_{RP} and its value can be obtained from equation (5.6).

5.3.1.4. Total weighting scores (TWS)

The total weighting score can then be obtained by summing up the individual scores. Therefore, the total weighting score (*TWS*) is defined as follows:

$$TWS = A_H\cos(\Delta\beta') + A_{PD}\omega + A_{RP}\cos(\alpha) \tag{5.5}$$

The values of $\cos(\Delta\beta')$, ω, and $\cos(\alpha)$ in equation (5.5) vary between -1 and 1 depending on the measurements of $\Delta\beta'$, *D*, and α. Therefore, the value of *TWS* can be carefully controlled by selecting different values of the weighting parameters A_H, A_{PD}, and A_{RP}. The *TWS* is then used to calculate the total weight assigned to a candidate link. The link which provides the highest *TWS* is taken as the correct link for that positioning fix. The following formulation is proposed to select the value of the weighting parameters:

$$\left.\begin{aligned} A_H &= aA_{PD} \\ A_{RP} &= bA_{PD} \end{aligned}\right\} \tag{5.6}$$

where a and b are the *non-negative weighting factors* which give the strength of the relationship between A_H, A_{RP}, and A_{PD}. The magnitude of a and b depends on the a priori knowledge of the statistical performance of the sensors and the quality of the digital road network. An experiment can be conducted with real data collected on a representative built-up environment to investigate the relative importance of different weights which provide an optimal map matching result. The upper bound of a and b can be set to 4 to obtain a comparable magnitude of different weighting scores. After fixing the value of a and b, any positive value of A_{PD} should provide correct results. Since A_{PD} represents the weighting parameter for the perpendicular distance, D, for ease of reference, it can be taken as the average horizontal error of GPS SPS (SIS only) which is 13m (2σ).

An experiment was conducted with 1800 epochs of positioning data collected in Central London (see section 5.6 below for the details on data collection) to determine the value of a and b. The feasible values of a and b are shown in Table 5.1. For each combination of a and b, the corresponding error of the map matching algorithm in identifying the correct links[27] is estimated. The navigation data is obtained from GPS/DR and the digital map data is obtained from a map of scale 1:2500. The value of the weighting parameter A_{PD} is taken as 10.

The map matching error is usually large when both a and b are less than 1, and b is greater than a. This suggests that the weighting score for heading (WS_H) should be given more importance than for the relative position (WS_{RP}) and that the weighting score for the relative position (WS_{RP}) should be given more importance than the weighting score for proximity (WS_{PD}). This may be particularly important if positioning data is obtained from the integrated GPS/DR system where the heading information is quite accurate. This leads to the condition of $a > b > 1$. The lowest map matching error is found when a =3 and b =2. A similar empirical analysis is also conducted when the navigation data is obtained from stand-alone GPS. The minimum map matching error is found when a =2.5 and b =2. These values are used in the subsequent analysis.

[27] Since the test vehicle was travelling on a known route, the correct links can be identified.

Table 5.1: An empirical analysis to derive the value of a and b

a	*b*	Error in map matching (%)	*a*	*b*	Error in map matching (%)
0.5	0.5	44.9	0.5	2.5	55.6
1.0	0.5	54.6	1.0	2.5	50.6
1.5	0.5	48.2	1.5	2.5	38.0
2.0	0.5	44.5	2.0	2.5	39.2
2.5	0.5	39.9	2.5	2.5	33.6
3.0	0.5	40.2	3.0	2.5	17.5
3.5	0.5	44.6	3.5	2.5	13.6
4.0	0.5	48.6	4.0	3.0	15.0
0.5	1.0	49.6	0.5	3.0	61.2
1.0	1.0	33.6	1.0	3.0	55.3
1.5	1.0	38.6	1.5	3.0	42.3
2.0	1.0	35.8	2.0	3.0	38.1
2.5	1.0	34.8	2.5	3.0	39.2
3.0	1.0	33.1	3.0	3.0	33.6
3.5	1.0	30.2	3.5	3.0	17.5
4.0	1.0	28.6	4.0	3.0	15.0
0.5	1.5	48.7	0.5	3.5	62.5
1.0	1.5	52.6	1.0	3.5	51.2
1.5	1.5	33.6	1.5	3.5	42.8
2.0	1.5	15.0	2.0	3.5	38.0
2.5	1.5	15.2	2.5	3.5	38.1
3.0	1.5	16.2	3.0	3.5	36.0
3.5	1.5	20.5	3.5	3.5	33.6
4.0	1.5	21.0	4.0	3.5	18.3
0.5	2.0	48.5	0.5	3.5	64.5
1.0	2.0	50.2	1.0	3.5	50.6
1.5	2.0	39.2	1.5	4.0	42.8
2.0	2.0	33.6	2.0	4.0	42.3
2.5	2.0	15.0	2.5	4.0	38.0
3.0	**2.0**	**11.5**	3.0	4.0	39.2
3.5	2.0	16.1	3.5	4.0	36.0
4.0	2.0	16.2	4.0	4.0	33.6

5.3.1.5. Typical geometric configuration

The weighting scheme is tested using a geometric configuration that could potentially give an incorrect match. Figure 5.5 displays a simple geometric configuration with data for a vehicle moving from A to E where the position fixes are denoted by P^1, P^2, P^3, P^4, and P^5. Therefore, the actual links for these fixes would be either AB or BE. As can be seen, the position fix (P^3) is very close to link BC. In this case it is plausible that the path followed by the vehicle is from link AB to BC.

The values along the arrow symbols indicate the vehicle-heading at each position fix. The identification of the correct link for the points P^1 and P^2 using the weighting scheme is very straightforward and it is determined as the link AB. The next step is to identify a link

for the point P^3 which is almost on the link BC. One could assume that the weighting scheme gives the link BC the highest *TWS* for this fix.

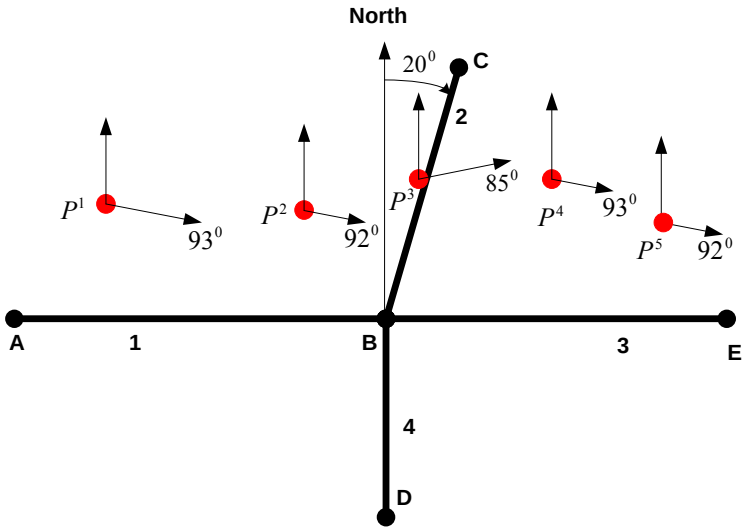

Figure 5.5: A specific geometric configuration with observed position fixes

Using the parameters values, for example, $a = 3, A_{PD} = 10, b = 2$, the weighting scores are derived for each link. Table 5.2 shows that link BE has the highest *TWS* confirming a good performance of the map matching method developed here.

Table 5.2: Calculation of TWS for the point P^3 using developed algorithm

Link	Parameters	*TWS*
AB	$\Delta\beta_1' = 5^0, D_1 = 20, \alpha_1 = 110^0$	31.05
BC	$\Delta\beta_2' = 65^0, D_2 = 1, \alpha_2 = 0^0$	42.57
BE	$\Delta\beta_3' = 50^0, D_3 = 20, \alpha_3 = 70^0$	**44.73**
BD	$\Delta\beta_4' = 95^0, D_4 = 4, \alpha_4 = 160^0$	-11.80

The weighting scheme described in Greenfeld (2002) is also applied to the above configuration (Figure 5.5) in order to examine whether the Greenfeld algorithm can identify the correct link. He defined the total weighting score (W) as:

$$W = C_{AZ}.\cos^{n_{AZ}}(\Delta AZ) + (C_D - a.D^{n_D}) + C_I.\cos^{n_I}(\Delta AZ) \qquad \textbf{(5.7)}$$

and the values of the parameters in (5.7) taken by Greenfeld (2002) as:

$C_{AZ} = 10, n_{AZ} = 5, C_D = 10, a = 0.1, n_D = 1.2, C_I = 10$ and $n_{AZ} = 10$.

The results are shown in Table 5.3, where ΔAZ represents the heading difference between the line created through P^2 and P^3 and each candidate link, D is the distance between P^3 and each candidate link, C_I is the weighting score for intersection between the line (created through P^2 and P^3) and each candidate link. C_I =1 if an intersection exists, 0 otherwise. We are interested in column 3 which is the total weighting score for each link. The highest weighting score is given to the link BC with an indeterminate selection between links AB and BE. This shows that the Greenfeld algorithm fails to select the correct link for the above network configuration. This is mainly due to the incorrect measurement of the vehicle heading at the point P^3 and the higher weighting score given to the proximity.

Table 5.3: Calculation of W for the point P^3 using Greenfeld's algorithm

Link	Parameters	W
AB	$\Delta AZ = 30^0$, D_1=20	11.23 ($C_I \approx 0$)
BC	$\Delta AZ = 40^0$, $D_2 = 1$	**13.23**
BE	$\Delta AZ = 30^0$, D_3=20	11.23 ($C_I \approx 0$)
BD	$\Delta AZ = 120^0, D_4 = 4$	9.15 ($C_I \approx 0$)

5.3.2. Estimation of Vehicle Location

If it is assumed that the above method identifies the correct link AB for the position fix, P^s (easting, e_S and northing, n_S), as shown in Figure 5.6. The next step is to estimate the vehicle location (i.e., coordinates) on the link.

This is achieved by an orthogonal projection of the position fix (P^S) onto the link (AB). If x_1 and y_1 represent easting and northing components of node A, and x_2 and y_2 represent easting and northing components of node B, then the projected easting (e_{mm}) and northing (n_{mm}) on the link can be regarded as the map-matched location on the link AB. This is obtained as follows:

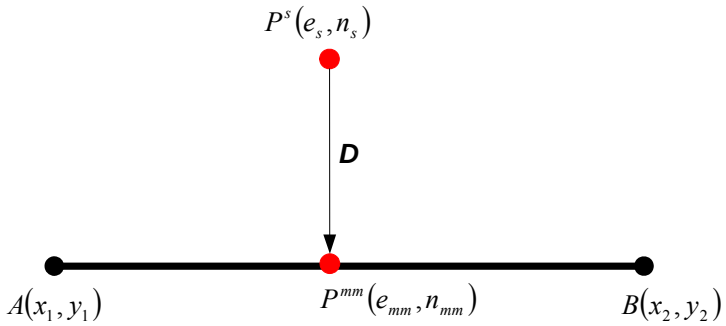

Figure 5.6: Estimation of vehicle location on the selected road link

$$\left.\begin{aligned} e_{mm} &= \frac{(x_2 - x_1)[e_S(x_2 - x_1) + n_S(y_2 - y_1)] + (y_2 - y_1)(x_1 y_2 - x_2 y_1)}{(x_2 - x_1)^2 + (y_2 - y_1)^2} \\ n_{mm} &= \frac{(y_2 - y_1)[e_S(x_2 - x_1) + n_S(y_2 - y_1)] - (x_2 - x_1)(x_1 y_2 - x_2 y_1)}{(x_2 - x_1)^2 + (y_2 - y_1)^2} \end{aligned}\right\} \quad \textbf{(5.8)}$$

5.3.3. Examining whether the Vehicle is still on the Current Link

After determining the vehicle location on the correct link for the first position fix, the algorithm will then examine whether subsequent position fixes can also be matched to the same link. Therefore, three conditions have been introduced to test this criterion. They are:

- The difference between the heading of the two consecutive positioning lines (i.e., the line between $P(x_i, y_i)$ and $P(x_{i+1}, y_{i+1})$, and the line between $P(x_{i+1}, y_{i+1})$ and $P(x_{i+2}, y_{i+2})$) is greater than 45^0
- The difference between the heading obtained from the two consecutive positioning fixes is greater than 45^0
- The alpha (α) is greater than 90^0

If any of the above conditions are true, then the algorithm assumes that the vehicle is at a junction and hence a re-initialisation process is required. Otherwise, the vehicle is still on the previous link and the new location is calculated using equation (5.8).

5.4. Outlier Identification

If the map matching algorithm makes use of positioning data from stand-alone GPS, then there is a possibility of the presence of outliers in the derived position fixes. With the integrated GPS/DR system, a significant number of outliers may be eliminated. However, there is still the possibility of obtaining some outliers or spikes especially in urban areas due to the effect of signal multipath. This could happen at a node or equally at any other place due to errors associated with the navigation sensors and the digital map. The position fix P^4 in Figure 5.7, is considered as an outlier if $\Delta\delta > 45^0$ (i.e., if there is a sudden change in two consecutive GPS/DR line headings). This outlier may cause matching errors especially if $\Delta\delta$ is large and P^4 is much closer to DE. To avoid such matching errors an outlier is finalised only after the next few position fixes (3 to 4) have been observed and analysed. A detailed description on filtering outliers can also be found in Greenfeld (2002). However, this treatment of outliers cannot be applied to a real-time ATT service that requires second-by-second positioning information.

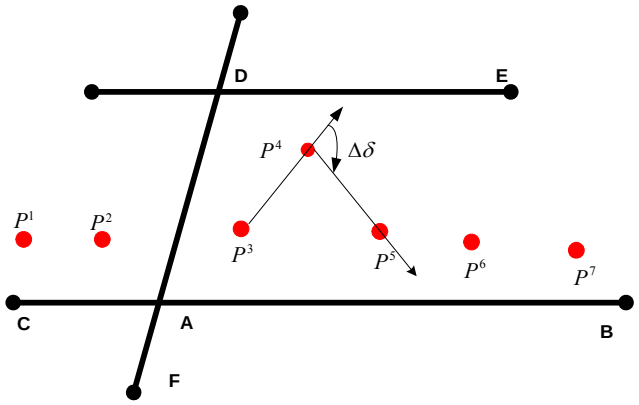

Figure 5.7: Outlier treatment

5.5. Algorithm Step by Step

The algorithm uses the following steps to assign the vehicle to the correct links and to determine its locations on those links.

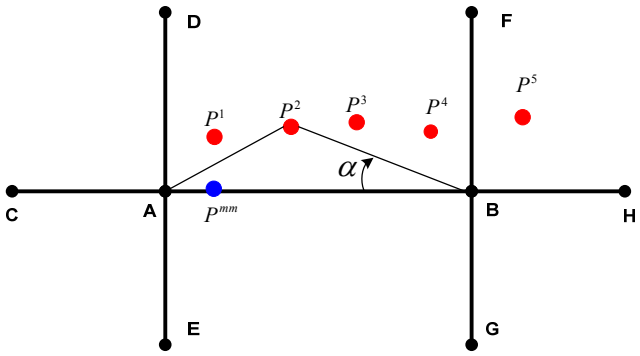

Figure 5.8: Map matching process

1. Read street network geographic data files (both node and link). Calculate length and heading for each link and store them in the link data file.
2. Find the closest node (i.e., **A**) from an observed position fix (***P*^{1}** for initial matching) as shown in Figure 5.8.
3. Select all the links as candidate links (AC, AB, AD, and AE) that are connected to the closest node (A).
4. Using the weighting formula as shown in equation 5.5, select the correct link (say AB) for the position fix ***P*^{1}**.
5. Determine the vehicle location (say P^{mm}) on the correct link (AB) using equation (5.8)
6. Go to the next position fix, ***P*^{2}**. Calculate $\Delta\beta'$ and α from the navigation data associated with the fix and the geometry of the link AB. If $\Delta\beta'>45^0$, then it is assumed that the vehicle has already made a turning manoeuvre (left or right) and If $\alpha>90^0$, then it is also assumed that the vehicle has already crossed a junction. If any of these above conditions is true, the algorithm goes back to the step-2 and re-initialises the matching process. Otherwise, this position fix (***P*^{2}**) is mapped on the same link (i.e., AB) using step 5.

5.6. Data Collection and Algorithm Testing

Comprehensive field tests are required to collect the positioning data from various road environments. This is necessary because the performance of a map matching algorithm is likely to depend on road network characteristics. A vehicle was equipped with a *GPSi-*

AVL[28] navigation platform (115x113x45 mm) consisting of a 12-channel single frequency (L1) high sensitivity GPS receiver (for C/A code-ranging), a low-cost rate gyroscope and the interfaces required to connect to the vehicle speed sensor (odometer) and the reversing light. The rate gyro and the vehicle odometer support the basic DR configuration. The positioning and speed accuracies of the GPS receiver are 25 m CEP (Circular Error Probable) and 0.1m/s respectively. The heading drift of the rate gyro is 3 deg/hr. In the *GPSi-AVL* unit, although the gyro scale factor does not need to be determined, the odometer scale factor needs to be determined relatively frequently. This is because the wheel diameter may change over time due to tyre wear and tear. The route in London was chosen carefully to have a good mix of important spatial urban characteristics including open spaces, urban canyons, tall buildings, tunnels, bridges, and potential sources of electromagnetic interference. Navigation data was obtained from a series of comprehensive field tests in London between 2002 and 2005. The total duration of field campaigns was about 20 hrs. The line in red indicates the test routes covered (Figure 5.9).

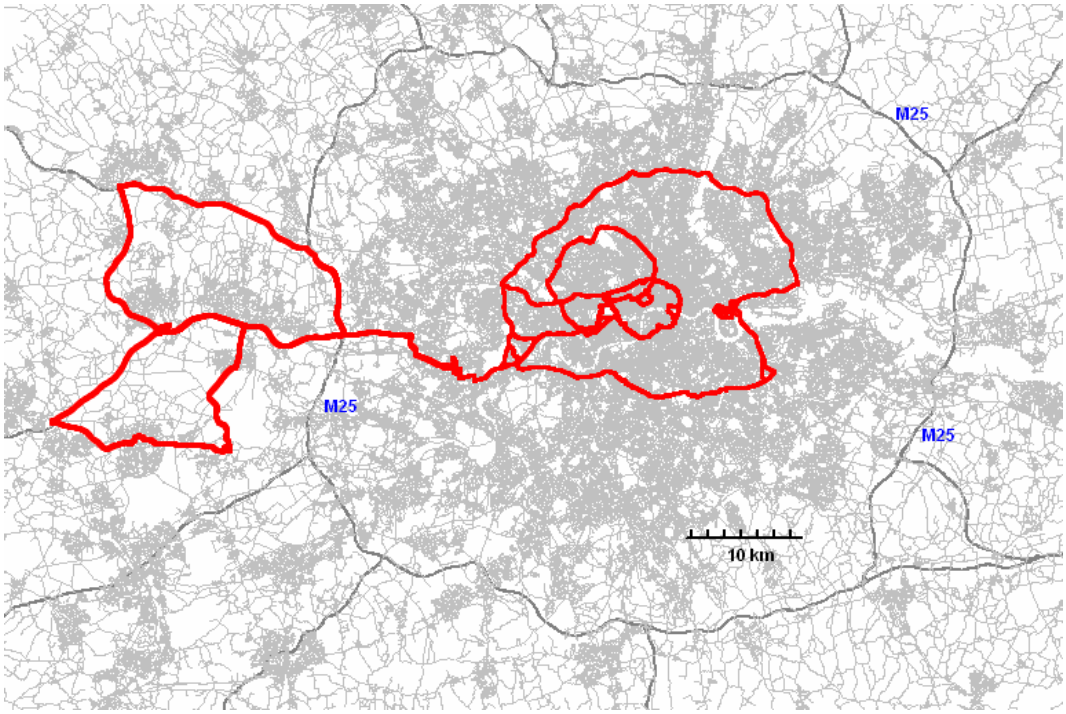

Figure 5.9: The test routes from all field campaigns

[28] Manufactured by Neve Technologies, Home page: http://www.neveits.com

The basic outputs of the GPS receiver are positioning data (longitude and latitude), speed, heading, satellite availability, and HDOP at one second intervals. The odometer gives the distance travelled by the vehicle per second and the rate gyro provides the rate of change of heading per second.

Odometer and rate gyro (the basic DR) readings are calibrated when GPS is available using the EKF algorithm described in Chapter 3 (section 3.2.3). If the GPS receiver suffers signal mask or the horizontal dilution of precision (HDOP) is greater than a pre-defined threshold, which is an indication that navigation satellite geometry is not good enough to get a high accuracy position, the calibrated DR readings are used to measure the state of the vehicle. In urban canyons where the HDOP may indicate a good value (less then 5), the error associated with the position solutions can be hundreds of metres due to the effect of multipath. In order to take into account such an effect, the signal-to-noise ratio can also be employed. The signal-to-noise ratio (C/N_O) is a measurable value of the signal strength. This parameter is a receiver, antenna and satellite dependent quantity and it varies with the receiving environment, the atmospheric conditions and the satellite elevation (Wang and Yang, 2004). The *GPSi-AVL* unit used in this study does not give C/N_O as an output but provides a quality indicator that directly reflects the level of confidence in the solution. This indicator is termed as Horizontal Figure Of Merit (HFOM). A small HFOM (usually less than 5) indicates that the solution is of good quality. If the HDOP was greater than 5, or the number of visible satellite was less than 4, or if the HDOP was less than 5 but the HFOM was also greater than 5, then the calibrated DR readings are used to measure the state of the vehicle.

The positioning data (easting and northing), speed, heading, and the error variances were then available from two navigation systems: stand-alone GPS and integrated navigation system (GPS/DR) employing an EKF algorithm. In order to assess the level of coverage (*ability to obtain a position fix*) offered by GPS and the integrated system, the position fixing data was overlaid onto a high-resolution digital road network base map at a scale of 1:2500. The statistics generated from the field data showed that GPS coverage[29] was obtained for 96% of the mission duration, while that of the integrated system was 100%. The longest period of GPS outage was found to be 100s.

[29] GPS coverage is defined as the percentage of time when the number of visible satellites is at least 4 and the HDOP is less than 5.

The accuracy (*position fixing with a desired level of accuracy*) assessment was carried out by comparing both GPS positions and the EKF algorithm results with the digital map at a scale of 1:2500. The analysis was carried out in defined accuracy bands of 5*m*, 10*m*, 20*m*, 30*m*, 40*m* and 50*m* with respect to the centreline of the road. It was found that GPS and the integrated system have similar actual fix density, where more than 65% fixes are within 5*m* of accuracy and almost 100% are within 60*m*. It is therefore clear that the integrated (GPS/DR) system performs better than stand-alone GPS in providing continuous positioning with an accuracy of better than 60m largely due to improved level of coverage.

In order to carry out a more detailed analysis, some typical parts of the test route have been looked at in greater detail. Figure 5.10 shows the vehicle travelling inside the Blackwall tunnel where there was a GPS outage for a period of 100*s*. It was found that 49% of the fixes were within 10*m* of the centreline of the road and 100% of the fixes were within 30*m*. This is a measure of the performance of the basic DR unit working on its own but using calibration factors derived when the GPS position fixing capability was available.

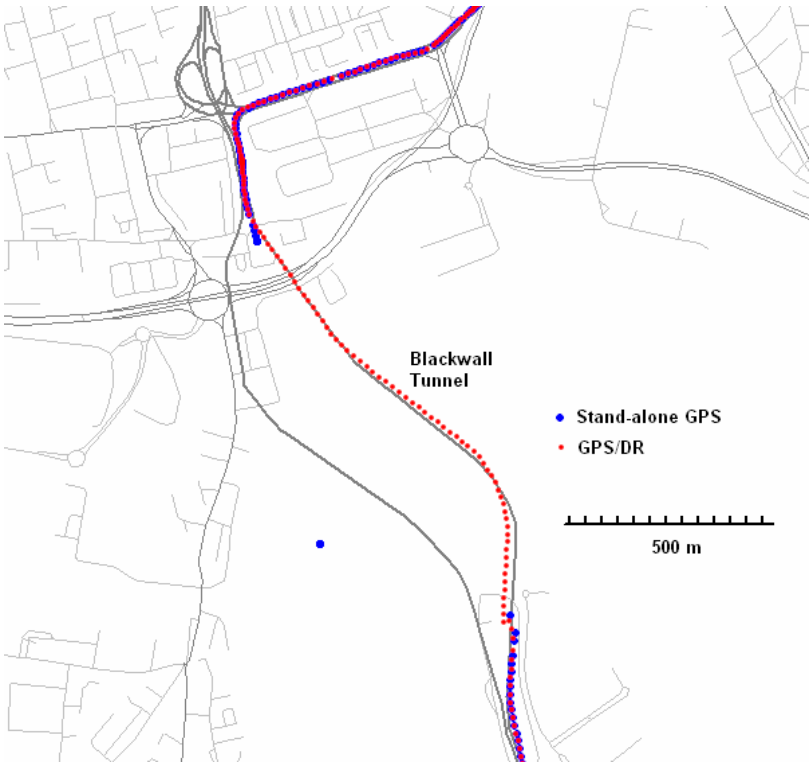

Figure 5.10:Travelling inside the Blackwall Tunnel

The positioning results from the output of the integrated (GPS/DR) system, based on the EKF algorithm, are shown in Figure 5.11 and Figure 5.12 for a part of the experimental route in the Central London road network. Each of the dots represents the vehicle position. Note that in most cases the points deviated from the actual route taken due to positioning errors (despite 100% of all position fixes being within 50m of the road centreline). The spatial network data used as a reference had a map scale of 1:2500, and was obtained from the UK Ordinance Survey (UKOS). The arrow symbols in the figures show the path followed by the vehicle on the network.

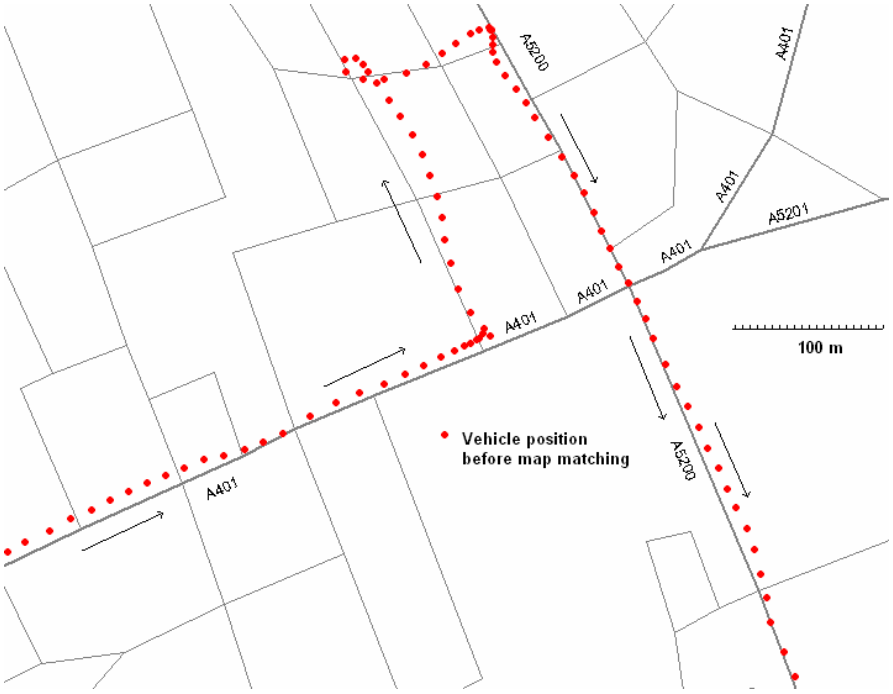

Figure 5.11: Position fixes from the raw output of the GPS/DR EKF algorithm

As already mentioned, the purpose of the map matching algorithm developed here is twofold, firstly to match each of the vehicle positions to a link (road segment), and secondly to determine the vehicle location on that link.

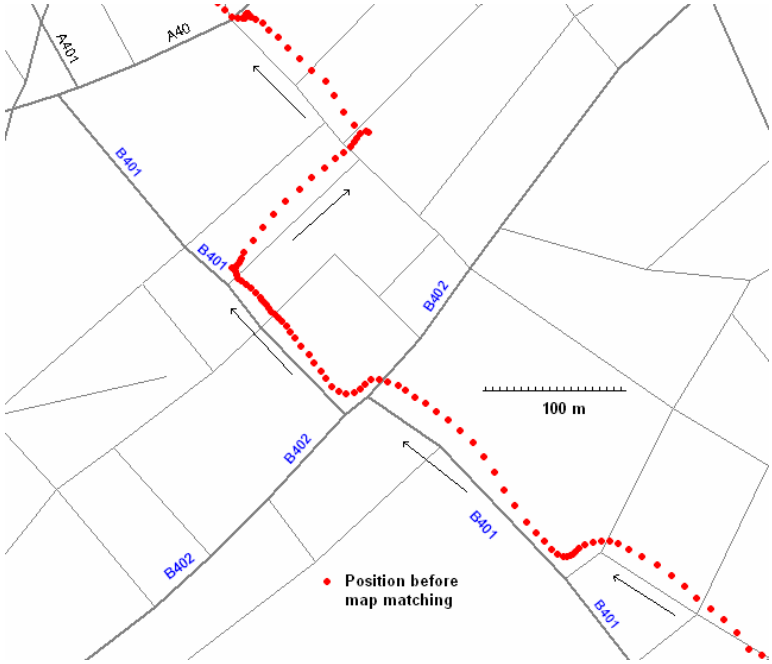

Figure 5.12: Position fixes from the raw output of the GPS/DR EKF algorithm

Figure 5.13 and Figure 5.14 show the results of the topological map matching algorithm for the sample routes shown in Figure 5.11 and Figure 5.12 respectively. Equation (5.5) was used to select the actual link among a number of candidate links.

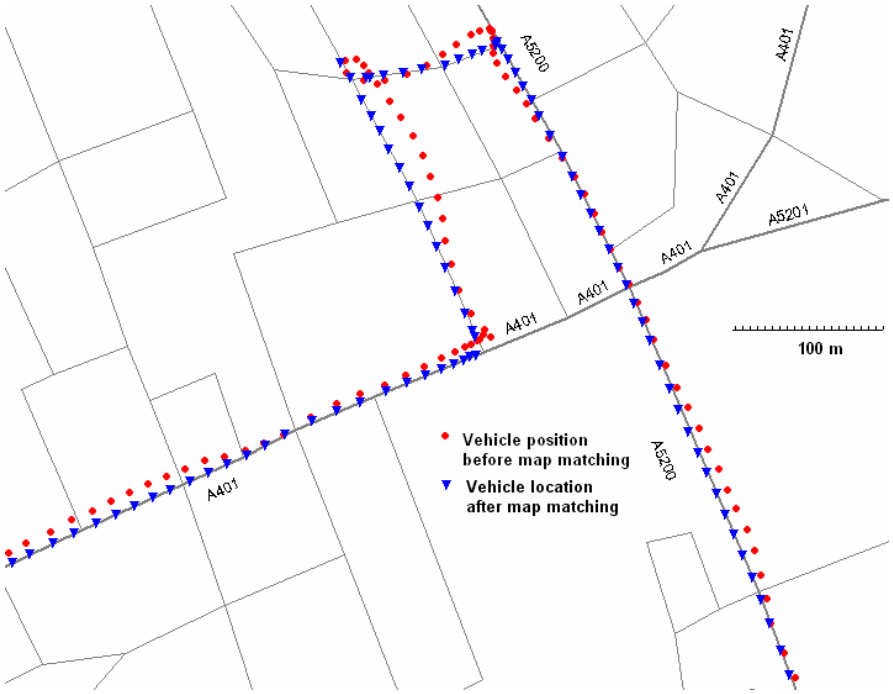

Figure 5.13: Map matching results for Figure 5.11

The values of the weighting factors *a* and *b* are taken as 3 and 2 respectively whereas the value of the weighting parameter A_{PD} is taken as 10. Therefore, the corresponding values of weighting parameters A_H and A_{RP} are 30 and 20 respectively (see equation 5.6).

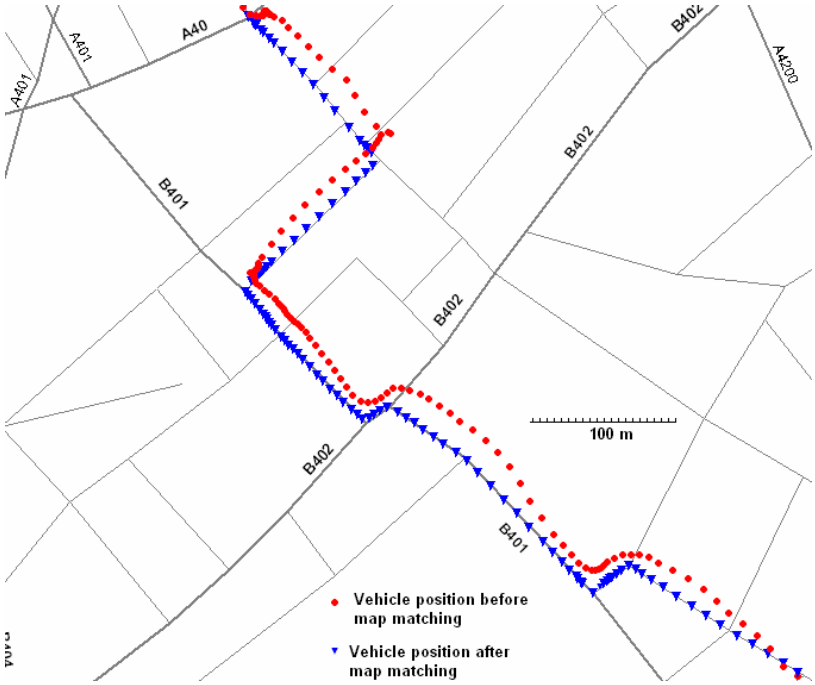

Figure 5.14: Map matching results for Figure 5.12

However, any positive value for A_P (with *a* =3 and *b* =2) was found to provide the same results. Equation (5.8) was then used to determine the location of the vehicle on the selected link. The results suggest a very good agreement between the vehicle trajectory derived from the map-matched positions and the actual path taken by the vehicle. Chapter 8 presents the validation and integrity measure of the map matching algorithms and Chapter 9 describes the results of this new map matching algorithm for different road networks in greater detail.

5.7. Summary

The first improved map matching algorithm, based on a topological analysis of the road network, was presented in this chapter. Starting with a description of data inputs, both the identification of the correct link and the determination of the vehicle location on that link were described. To determine the correct link among the candidate links, the algorithm

used historical information on vehicle trajectory, topology of the road network, and heading and speed information from the positioning sensors. The performance of the algorithm was evaluated against the performance of a widely cited map matching algorithm developed by Greenfeld (2002) for a typical road network configuration. The results showed that there is an improvement in the developed algorithm in terms of link identification. Chapter 9 gives the detailed results on the performance of the Greenfeld algorithm and the new algorithm developed in this chapter in terms of link identification and location determination.

In order to make the algorithm as simple as possible, the orthogonal projection of the position fixes onto the links was used to estimate the vehicle locations. A step-by-step procedure to implement the developed map matching algorithm was also presented. The algorithm was tested using the positioning data from the integrated GPS/DR and high resolution road network data from a map of scale 1:2500. The vehicle trajectory derived from the map-matched locations agreed reasonably with the actual path taken by the vehicle.

The algorithm was also applied to other road networks with varying complexity such as dense urban roads, complex roundabouts, merging and diverging sections of motorways (see Chapter 9 for details). Although the performance of the algorithm was found to be superior compared with other existing algorithms, it is not always reliable in more complex road networks with high resolution digital maps[30]. For example, this algorithm is quite sensitive to the outliers in dense urban roads where the distance between roads is less than 100m. One of the important assumptions of this approach is that the vehicle is always on the known road network. This is not necessarily true as the vehicle could be off the road network (e.g., car park, petrol station etc.). Therefore, a more reliable algorithm which can deal with the off-road conditions needs to be developed to make this approach appropriate for all types of road networks. Moreover, a robust technique is required to estimate the vehicle location. Therefore, further developments of map matching algorithms based on probabilistic theory and qualitative decision-making processes will be presented in the next chapters. The performance of the three map matching algorithms developed in this study is eventually compared in Chapter 9.

[30] This is fully explained in Chapter 9

CHAPTER 6

A PROBABILISTIC MAP MATCHING ALGORITHM

6.1 Introduction

This chapter describes the development of a probabilistic map matching algorithm. As discussed in the previous chapter, a topological map matching algorithm starts with nodal matching to identify the correct link among the links connected to the node closest to the position fix. This approach may not always be suitable for complex urban road networks with high resolution digital maps, especially when the positioning data contains outliers. Instead of using the links connected to the closest node, the map matching algorithm developed in this chapter takes all links as candidate links that fall within an error ellipse around a position fix. The dimensions of the error ellipse are chosen based on the error variance-covariance matrix associated with GPS or GPS/DR. The size of the error ellipse normally depends on the probability (95% or 99%) that the ellipse contains a true link. This should help to mitigate the problem associated with outliers in the positioning data.

Most existing map matching algorithms, including the topological map matching algorithm developed in the previous chapter, use an orthogonal projection from the position fix to the link to estimate the vehicle location on a link. Because of network mapping and GPS positioning error, this may not be a robust estimation of vehicle location as explained by Greenfeld (2002). In order to improve the determination of vehicle location, an optimal estimation method is introduced in the algorithm developed in this chapter. This estimation takes into account error sources associated with the network map data and the navigation system.

The details of the developed algorithm are explained below by first describing the enhancement of the proposed probabilistic map matching algorithm compared to existing probabilistic approach. This is followed by the description of inputs required to

implement the algorithm. Then methods for the identification of the correct links and the determination of the vehicle location on those links are presented. The developed algorithm is then tested in complex road networks including roundabouts using a digital map of scale 1:2500.

6.2 Enhancement over Existing Probabilistic Algorithms

As discussed in Chapter 4 (section 4.2), the probabilistic approach to a map matching algorithm was first introduced by Honey et al. (1989) for the case of a navigation solution obtained from a DR sensor. Zhao (1997) extended this concept for the case of a navigation solution obtained from GPS. Other studies which used a probabilistic approach or a part of this approach are, for example, Kim et al. (2000) and Pyo et al. (2000). Enhancements to the probabilistic algorithm in this research are the following.

- In the probabilistic method discussed in this chapter, the elliptical error region is only constructed when the vehicle travels through a junction (in contrast to constructing it for each position fix as suggested by Zhao (1997)) and there is no need to create the error region when the vehicle travels along a link. This makes the algorithm faster as there are a number of processes involved in the creation of the error region and hence the identification of the correct link. The proposed method is more reliable as the construction of an error region in each epoch may lead to incorrect link identification.

- A number of criteria are developed based on empirical studies to detect a turning manoeuvre of the vehicle at a junction. This helps to effectively identify the switching of the vehicle from one link to another. This has not been done rigorously in previous research.

- The enhanced probabilistic algorithm developed in this thesis takes into account the inaccuracy of the heading from a navigation sensor when the vehicle travels at low speeds. This effectively assists the algorithm to correctly match the position fixes at low speed, especially in urban areas where there are frequent stops e.g., traffic lights.

- The significant contribution to the enhancement of the probabilistic algorithm developed in this chapter lies in the development of an optimal estimation for the determination of vehicle location on a link. This optimal estimation technique takes into account various error sources associated with the navigation sensor and the digital map quality.

6.3 Map Matching Process

The capability to identify the physical location of a vehicle on a link is a key requirement in many ATT applications as described in Chapter 2. In order to achieve the RNP, system and sensor complementarity, such as in the case of the integration of GPS, DR, and digital map data (Figure 6.1) could be used to enhance geometric positioning capability. This is achieved by the map matching process developed below.

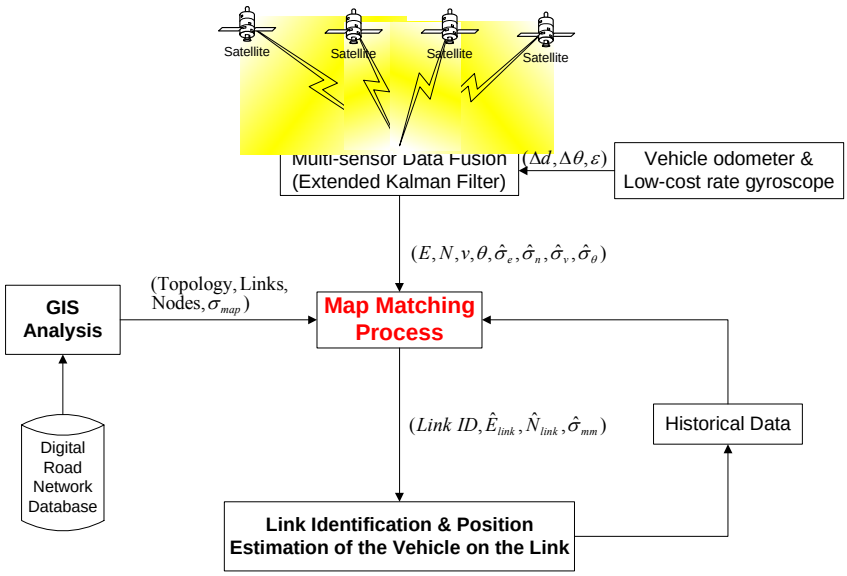

Figure 6.1: A schematic diagram of the developed map matching process

The map matching algorithm takes positioning data as inputs either from stand-alone GPS or integrated GPS/DR. In the case of a GPS/DR system, the integration is achieved via an Extended Kalman Filter (EKF) algorithm fully described in Zhao et al. (2003). The EKF algorithm takes inputs from the GPS and DR (the gyro-rate reading ($\Delta\theta$), the odometer reading (Δd) and the errors associated with them (ε_θ and ε_d). The outputs of positioning data are easting coordinate (E), northing coordinate (N), vehicle speed (v), heading (θ), and the error variances associated with them (i.e., $\hat{\sigma}_e, \hat{\sigma}_n, \hat{\sigma}_v, \hat{\sigma}_h$

respectively). The map matching algorithm takes inputs from the positioning system and the digital map data (e.g., topology, links, nodes, and the error variance of map data, σ_{map}). The outputs of the matching process are the correct link ID, the location of the vehicle (i.e., easting coordinate, $\hat{E}_{link}$ and northing coordinate, $\hat{N}_{link}$) on that link and the uncertainty associated with the position solution ($\hat{\sigma}_{mm}$). This map matching process not only enables the physical location of the vehicle to be identified but also improves the positioning capability if a good digital map is available.

6.3.1 Identification of the Correct Link

As previously mentioned, the most complex element of any map matching algorithm is to identify the actual link from among the candidate links (Greenfeld, 2002; Quddus et al. 2003, White et al., 2000). For this probabilistic algorithm, two distinct processes are defined for the identification of the correct link, namely (a) the *map-matching process at a junction* (MPJ) and (b) the *subsequent map-matching process on a link* (SMPL). The function of the MPJ is to identify the correct link at a junction. Since the vehicle is expected to travel on this initial road segment for a few seconds, a number of subsequent position fixes are expected to be matched to this road segment. Therefore, after successfully identifying the correct link for an initial GPS or GPS/DR fix, the SMPJ starts matching the subsequent position fixes. In the SMPJ, the fixes are matched to the same road segment identified in the MPJ given that specified criteria (as explained in section 6.3.1.2 below) are fulfilled. Otherwise, the algorithm goes back to the MPJ for the identification of a new road segment for the last non-matched position fix. Both of these processes are explained below.

6.3.1.1 Map-matching process at a junction (MPJ)

The MPJ selects a road segment for the initial position fix at a junction. If an initial match is incorrect, then the subsequent matching will also be incorrect. Therefore, a robust method is required for the MPJ. The key characteristic of the MPJ is the use of an elliptical confidence region around a position fix based on error models associated with GPS or GPS/DR. Road segments that are within the confidence region are taken as the candidate segments. This is achieved by first identifying all nodes that are within the confidence region. Road segments that are originated from (or destinated to) these nodes are selected as candidate links. If the confidence region does not contain any segments,

then it is assumed that the vehicle is off the known road segments. In such a situation, the derived GPS or GPS/DR positions are used as the final locations of the vehicle. In a situation where the confidence region contains one or more candidate segments, a connectivity test or a filtering process is carried out based on the difference in heading between the candidate link and the derived vehicle heading to determine the more appropriate candidate road segments. If there is only one such candidate segment, then the final selection process is very straightforward. However, in the case of there being more than one candidate segment, the link connectivity, vehicle heading relative to the candidate segments, closeness to the candidate segments, and the historical information on vehicle location are used to select the most appropriate segment. In every application of the MPJ, the algorithm selects a new road segment. The process is summarized in the flow chart in Figure 6.2.

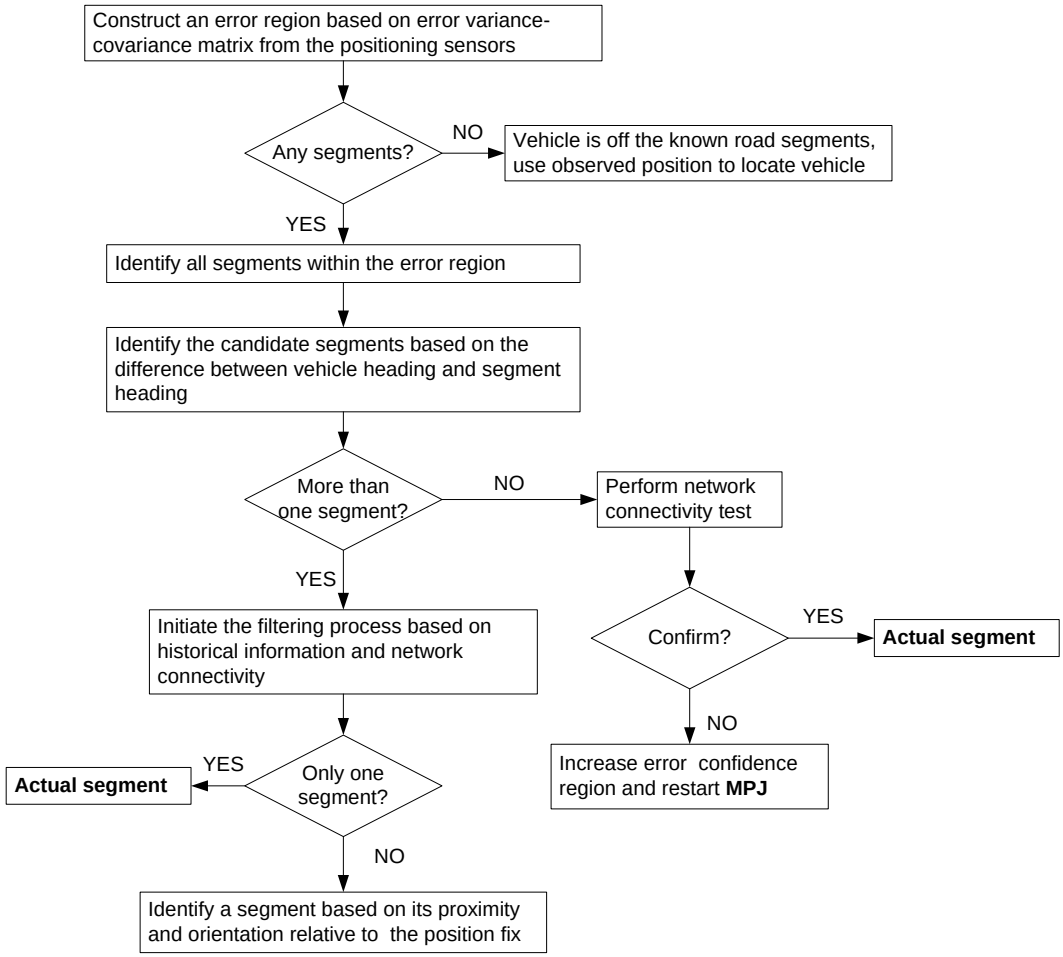

Figure 6.2: The identification of the actual segment in the initial matching process

One of the main tasks in the MPJ is to derive an error ellipse around a position fix. This is explained below.

Derivation of error ellipse

In a one-dimensional (1-D) variable such as distance, weight, angle etc., the standard deviation and the variance are normally used to specify the precision of measurements. In the case of a linear accuracy measure, one standard deviation (i.e, 1σ) would correspond to a 68.27% *confidence interval.* This means that the standard deviation of this sample defines the interval on either side of the mean (or correct) quantity that contains 68.27% of all the results. 31.73% of the results will therefore be outside this range. The probability of the result being in the interval of two standard deviations (2σ) on either side of the mean is 95.45%. In general, the 95% confidence level is taken as the measure of adequate accuracy, and this corresponds to 1.96 standard deviations. The probability corresponding to 3σ is 99.73%, which is inclusive of almost all results. This concept can be extended to two dimensions, so that areas can be constructed corresponding to distinct error probabilities such as 50%, 95%, etc. In two-dimensional (2-D) problems, such as the horizontal position of a point, an error ellipse around the point may be used to determine the precision of its measurements (Anderson and Mikhail, 1998). The orientation of the ellipse (β) as shown in Figure 6.3a largely depends on the correlation between *x* (easting) and *y* (northing) coordinates. If they are uncorrelated, then the semi-major and semi-minor axes of the ellipse will be parallel to *x* and *y* respectively. The error ellipse becomes a circle if the two coordinates (easting and northing) have equal precision.

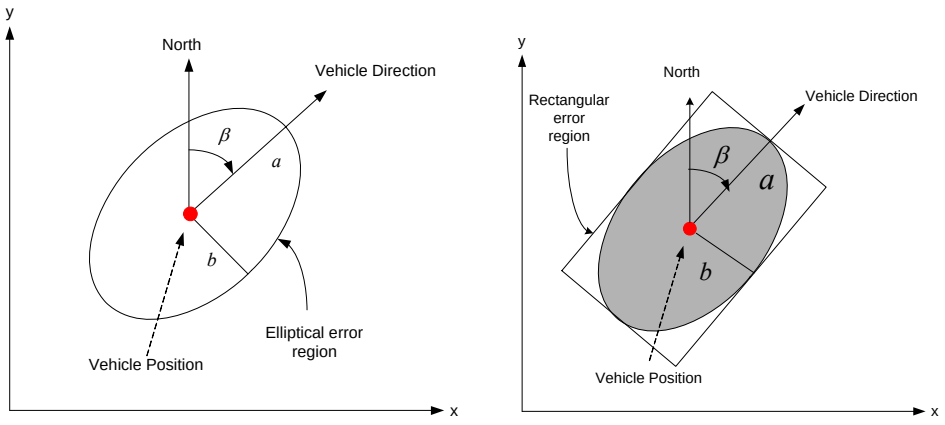

(a) ***(b)***

Figure 6.3: Error ellipse and rectangle around a position fix

Consider the general case where the variance-covariance matrix for a position fix is given by:

$$A = \begin{bmatrix} \sigma_x^2 & \sigma_{xy} \\ \sigma_{yx} & \sigma_y^2 \end{bmatrix} \quad \textbf{(6.1)}$$

where σ_x^2 and σ_y^2 are the positional error variances (easting and northing directions respectively) from the positioning system, σ_{xy} is the covariance

The semi-major (*a*) and the semi-major (*b*) axes of the corresponding ellipse can be calculated as follows:

The characteristic polynomial for A is given by

$$D(\lambda) = \det(A - \lambda \mathrm{I}) = \begin{bmatrix} \sigma_x^2 & \sigma_{xy} \\ \sigma_{yx} & \sigma_y^2 \end{bmatrix} - \lambda \begin{bmatrix} 1 & 0 \\ 0 & 1 \end{bmatrix} = 0 \quad \textbf{(6.2)}$$

which gives

$$(\sigma_x^2 - \lambda)(\sigma_y^2 - \lambda) - \sigma_{xy}^2 = 0 \quad \textbf{(6.3)}$$

The eigenvalues of a square matrix *A* are the roots of the characteristic equation of *A*. The roots are:

$$\lambda = \frac{(\sigma_x^2 + \sigma_y^2)^2 \pm \sqrt{(\sigma_x^2 + \sigma_y^2)^2 - 4(\sigma_x^2 \sigma_y^2 - \sigma_{xy}^2)}}{2} \quad \textbf{(6.4)}$$

The square roots of these two eigenvalues are the semi-major (a) and semi-minor (b) axes of the standard error ellipse. They are given by

$$a = \sqrt{1/2(\sigma_x{}^2 + \sigma_y{}^2 + \sqrt{(\sigma_x{}^2 - \sigma_y{}^2)^2 + 4\sigma_{xy}{}^2})} \quad \textbf{(6.5)}$$

$$b = \sqrt{1/2(\sigma_x{}^2 + \sigma_y{}^2 - \sqrt{(\sigma_x{}^2 - \sigma_y{}^2)^2 + 4\sigma_{xy}{}^2})} \quad \textbf{(6.6)}$$

The angle β can be determined by

$$\beta = \pi / 2 - 1/2 \arctan(\frac{2\sigma_{xy}}{\sigma_x^{\ 2} - \sigma_y^{\ 2}}) \quad \textbf{(6.7)}$$

Equations (6.5) and (6.6) need to be multiplied by an expansion factor ($\hat{\sigma}_0$) to compensate for the error associated with GPS due to orbital instability, atmospheric propagation, multipath, and receiver noise. Assuming that the distribution of the measurement errors is a standard normal distribution, the standard error ellipse (when $\hat{\sigma}_0$=1) corresponds to a 39% confidence region. To obtain a 99% confidence level, the value of the expansion factor should be taken as 3.03 (Zhao, 1997).

In addition to the positioning sensor errors, there are also uncertainties associated with the digital road network data which could include errors due to plotting, errors in the original sources, measurement errors and processing mistakes. Hence, it is necessary to multiply the derived error region by another expansion factor to get a higher confidence level (Zhao, 1997). For simplicity, an error rectangular can be used in place of the error ellipse as shown in Figure 6.3b. The semi-major and semi-minor axes of the error ellipse (*a* and *b*) are taken as the larger and smaller sides of the error rectangle respectively. Since the centres of the error ellipse and the error rectangle are the same and the area of the error rectangle is bigger than the area of the error ellipse, the road segments within the error ellipse should be included among the segments within the error rectangle.

6.3.1.2 Subsequent map-matching process on a link (SMPL)

The SMPL is used to match subsequent position fixes to the previously selected road segment, which is identified using the MPJ. Several factors need to be considered including the speed of the vehicle, whether there is a turning manoeuvre, or a manoeuvre through a junction. The speed of the vehicle needs to be taken into account since GPS or GPS/DR derived headings are not sufficiently accurate when the speed is low. Equally, the detection of a turning manoeuvre or a manoeuvre through a junction is a good indication that the vehicle is no longer located on the original segment. If the vehicle speed is lower than the threshold for the minimum speed and there is no indication of any manoeuvring through a junction by the vehicle, the SMPL process continues. In such cases, the vehicle heading needs to be re-calculated to be equal to the heading of the road segment obtained from the map database. The new calculated vehicle heading is used to

identify any turning manoeuvre for the next position fix. Field tests are necessary to determine a threshold for the minimum speed and this is explained in the next section.

In case of speeds higher than the threshold minimum speed, the SMPL also continues if there is neither a turning manoeuvre nor a junction crossing. The criterion to determine a turning manoeuvre is also explained in detail in the next section with some field test results. The decisive factor to determine whether the vehicle crosses any junction (in the case of manoeuvres through a junction) can be determined from the relative position of the current GPS or GPS/DR fix compared to the previously selected road segment. The complete flow chart for the identification of the link on which a vehicle is travelling is presented in Figure 6.4.

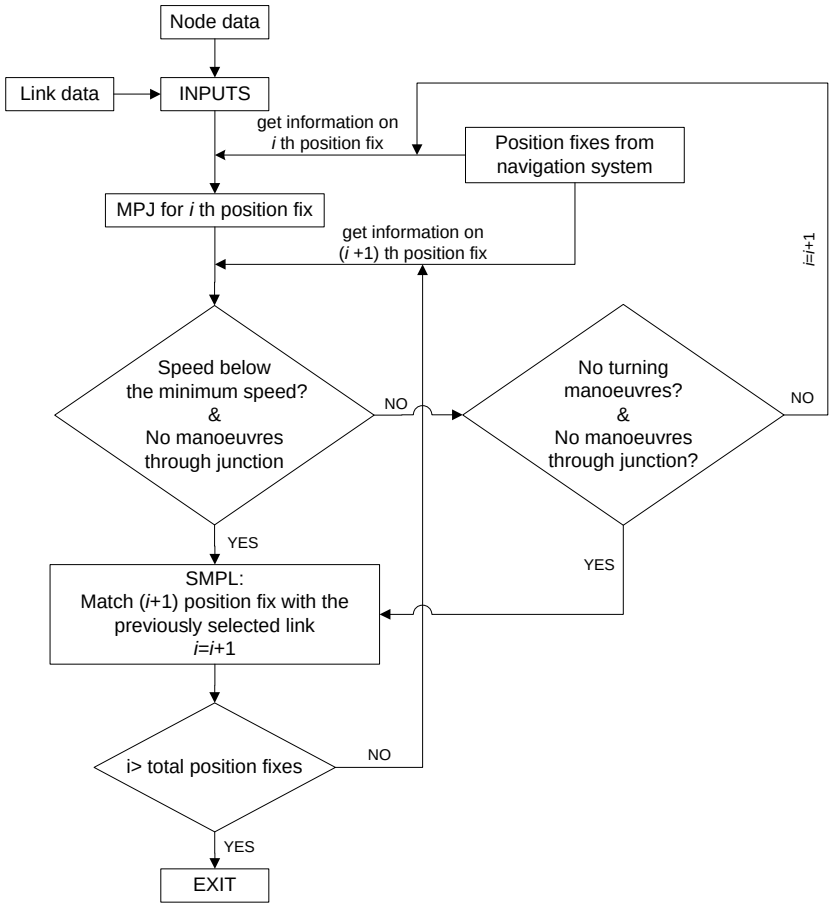

Figure 6.4: Flow chart for true road segment identification

Detection of a turning manoeuvre and the minimum speed

The map matching algorithm makes use of the vehicle heading to identify whether there is a turning manoeuvre at a junction. A turning manoeuvre is an indication that the vehicle may have switched road segments. Therefore, the algorithm searches for a new road segment (using the MPJ) if a turning manoeuvre is confirmed. However, at low speed the error associated with vehicle heading is usually unacceptably high. Hence, it is essential to determine the speed below which the map matching algorithm should *not* rely on vehicle heading (either from GPS or integrated GPS/DR).

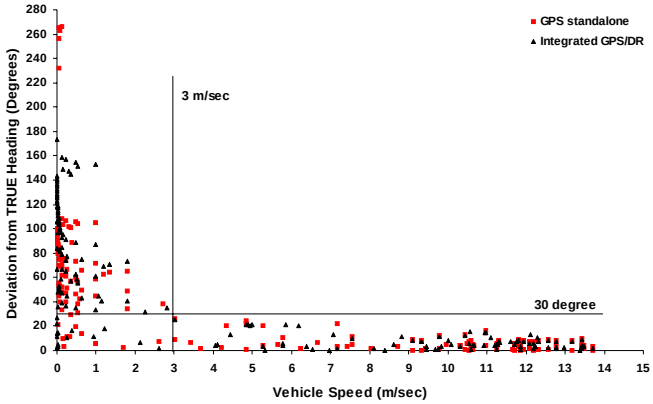

Figure 6.5: The absolute deviation of vehicle heading vs speed

A field test was carried out to determine the minimum speed at which GPS or GPS/DR derived vehicle headings are not reliable. The test vehicle was driven on known road segments. Since the vehicle travelled on known road segments, the actual vehicle headings were calculated from the digital map database of map scale 1:2500. The absolute deviation of vehicle heading was obtained from the difference between the calculated actual heading and the observed/estimated GPS or GPS/DR heading. The deviation of heading was then plotted against the corresponding vehicle speed (see Figure 6.5) for both GPS and GPS/DR system. For this case the difference in heading was always less than 30 degrees when the vehicle speed exceeded 3 m/sec (i.e., 10.8 km/hr) for both the GPS and the GPS/DR system i.e., the vehicle headings derived from the GPS and the road segment heading on which the vehicle is travelling is correlated when the vehicle speed is above 10.8 km/hr. Taylor et al. (2001) report that the correlation is low when the vehicle is travelling at 8 km/hr or below. The satellite geometry can be considered to have been good since HDOP was always less than 2.0. Therefore, the

algorithm can rely on the vehicle heading information, if the vehicle speed is greater than 3 m/sec. Hence the minimum speed threshold is set to 3m/sec (i.e., 10.8 km/hr). It is worthwhile to note that the threshold for the minimum speed may vary according to the type of GPS receiver and its error characteristics.

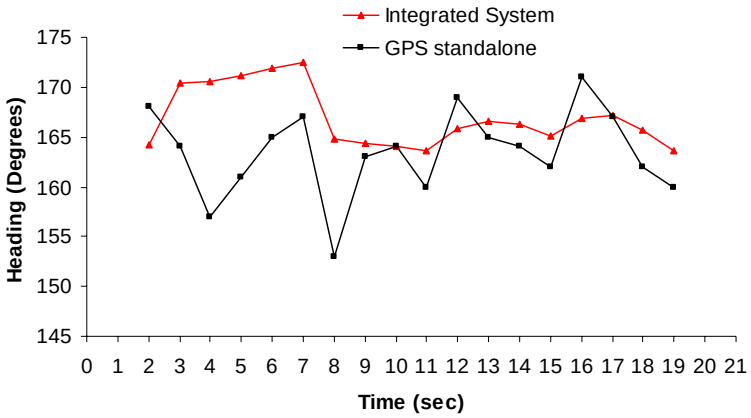

Figure 6.6: Characteristics of GPS and GPS/DR headings when the vehicle is travelling on a straight road.

In order to determine the threshold for the vehicle heading that could be used for detecting a turning manoeuvre, it is also necessary to know how the vehicle heading varies on a straight road segment. To determine this, another field test was carried out on a straight road segment. The vehicle was intentionally driven with a number of overtaking manoeuvres to examine the effects on heading changes. Figure 6.6 shows the change in vehicle headings on a typical straight road when the speed is greater than 3 m/sec. In all cases, HDOP was less than 2.0. The maximum difference between observed vehicle headings was 20 degrees for GPS and 15 for GPS/DR. The reason for such a large difference in heading on a straight road is due to the overtaking manoeuvres. However, neither an increasing nor decreasing trend was observed for the heading.

Another field test was carried out to examine the change in vehicle headings during a turning manoeuvre at junction. This test was also useful for determining the time needed to complete a turning manoeuvre. Figure 6.7 shows the changes in observed vehicle heading during a right turning (British-style i.e., left-turn elsewhere) manoeuvre of a vehicle at a four-legged junction when the vehicle speed is above the minimum speed and HDOP is less than 2.0. Clearly, there is a trend (in this case an increasing trend) of heading during the turning manoeuvre. The time to complete a right- or left-turning

manoeuvre usually depends on speed and the size of the junction. In this case, the time to complete a right-turning manoeuvre was 4 sec.

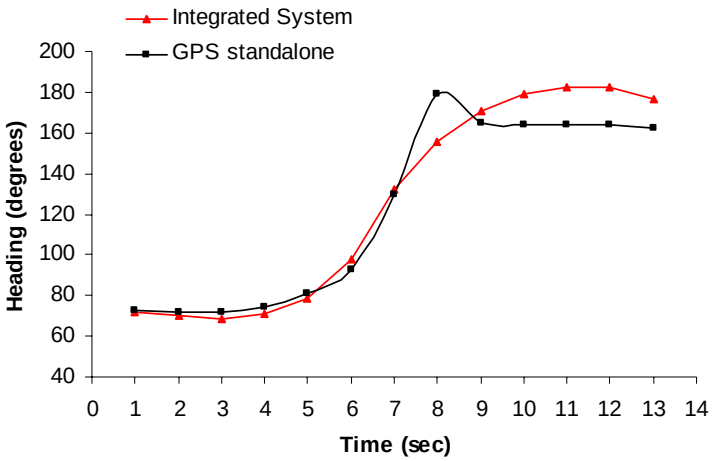

Figure 6.7: Characteristics of GPS and GPS/DR headings during a right turning manoeuvre of a vehicle at junction

Based on the test results above, the following conditions satisfy a turning manoeuvre (left, right or U-turn) of a vehicle at a junction.

- Increasing or decreasing trend in heading for about 2 to 5 sec
- Absolute difference in heading between the current and the last fix (assumed as α) is more than 30 degrees (for both GPS and GPS/DR)
- Absolute difference in heading between the current and the second to last fix (assumed as β) is more than 35 degrees (for both GPS and GPS/DR)

6.3.2 Determination of the Physical Location of the Vehicle on the Link

Assuming that the correct link has been identified as per the MPJ and/or SMPL, the physical location of the vehicle on the link can be determined in two ways using the available data. One way is to use map data and vehicle speed from the positioning sensors and the other is to adopt the perpendicular projection of a GPS or GPS/DR fix onto the link. Since both methods are associated with errors, an optimal estimation procedure may be used to determine the final location of the vehicle on the road segment.

The direction of the selected road segment and the vehicle speed (v) from the navigation sensors can be used to calculate the vehicle position on a link. Suppose P^t and P^{t+1} represent the vehicle position on a link at time t and $t+1$ respectively (Figure 6.8). The initial easting and northing coordinates of the vehicle at point P^t are known and may be obtained from stand-alone GPS. From the bearing of the link (i.e., θ) and speed of the vehicle at P^{t+1}, the increment in easting and northing coordinates can be obtained as follows:

$$\left.\begin{aligned} \Delta E_i &= (v*1)\sin\theta \\ \Delta N_i &= (v*1)\cos\theta \end{aligned}\right\} \qquad \textbf{(6.8)}$$

Therefore, the position of the vehicle at point P^{t+1} can be calculated as follows:

$$\left.\begin{aligned} E_{i+1} &= E_i + \Delta E_i \\ N_{i+1} &= N_i + \Delta N_i \end{aligned}\right\} \qquad \textbf{(6.9)}$$

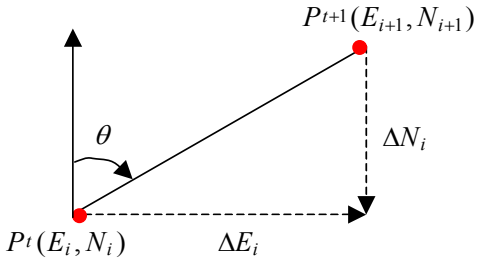

Figure 6.8: Determination of vehicle position from map data and vehicle speed

The other method for determining vehicle position is from the navigation sensor as shown in Figure 6.9. Suppose the navigation unit (GPS or GPS/DR) locates the vehicle at point P^s with easting coordinate, E_s and northing coordinate, N_s . The projected easting (e_{gps}) and northing (n_{gps}) coordinates on the link AB can be obtained as follows:

$$\left.\begin{aligned} e_{gps} &= \frac{(x_2-x_1)[E_s(x_2-x_1)+N_s(y_2-y_1)]+(y_2-y_1)(x_1y_2-x_2y_1)}{(x_2-x_1)^2+(y_2-y_1)^2} \\ n_{gps} &= \frac{(y_2-y_1)[E_s(x_2-x_1)+N_s(y_2-y_1)]-(x_2-x_1)(x_1y_2-x_2y_1)}{(x_2-x_1)^2+(y_2-y_1)^2} \end{aligned}\right\} \qquad \textbf{(6.10)}$$

In Figure 6.9, AB is a link on which a vehicle equipped with a navigation unit travels. P^{gps} (e_{gps}, n_{gps}) indicates the vehicle position obtained from the orthogonal projection of P^S on the link AB. P^{map} (e_{map}, n_{map}) represents the vehicle position obtained from the digital base map and speed from the navigation system. Both measurements have random and unbiased measurement errors. The optimal estimation of the vehicle position, which can be termed as the map-matched location, P^{mm} (e, n), is derived from these two measurement methods as follows:

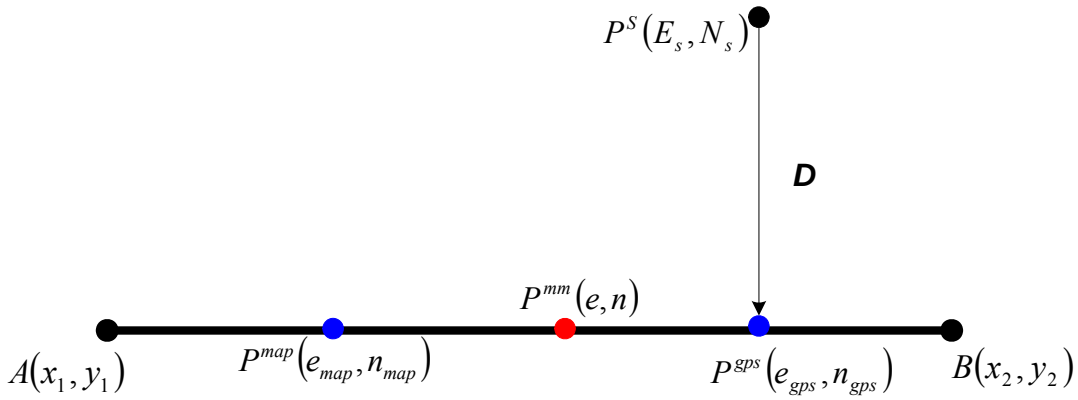

Figure 6.9: Optimal estimate of vehicle position on the link

The easting coordinates from two methods are denoted by e_{map} and e_{gps} respectively. They can be described by the following equations

$$e_{map} = e + \omega_{map,e} \tag{6.11}$$

$$e_{gps} = e + \omega_{gps,e} \tag{6.12}$$

where e is the true estimate of the easting coordinate, $\omega_{map,e}$ is the easting component of the error associated with the digital map and speed, $\omega_{gps,e}$ the error associated with the easting component of the position fix where $E(\omega_{map,e}\omega_{gps,e}) = \rho\sigma_{map,e}\sigma_{gps,e}$ in which ρ is the correlation coefficient between error terms and $\sigma_{map,e}$ and $\sigma_{gps,e}$ are the standard deviation of $\omega_{map,e}$ and $\omega_{gps,e}$ respectively.

Since there is no more information available about the estimate of e, the optimal estimate is simply the linear function of the measurements in the form

$$\hat{e} = k_1 e_{map} + k_2 e_{gps} \tag{6.13}$$

where k_1 and k_2 still need to be specified and are independent of e. The estimation error is denoted by

$$\tilde{e} = \hat{e} - e \tag{6.14}$$

The criterion of the optimality is to minimize the mean square of $\tilde{e}$. Moreover, the estimate needs to be unbiased since k_1 and k_2 are independent of the value of e. This is true when

$$E[\tilde{e}] = E\left[k_1(e + \omega_{map,e}) + k_2(e + \omega_{gps,e}) - e\right] = 0 \tag{6.15}$$

By applying, $E[\omega_{map,e}] = E[\omega_{gps,e}] = 0$ and $E[e] = e$, equation (6.15) becomes

$$k_1 e + 0 + k_2 e + 0 - e = 0, \qquad \text{i.e.,}$$

$$k_1 = 1 - k_2 \tag{6.16}$$

The mean square error is given by

$$\begin{aligned} E[\tilde{e}^2] &= E\left[((k_1(e + \omega_{map,e}) + (1 - k_1)(e + \omega_{gps,e})) - e)^2\right] \\ &= E\left[(k_1\omega_{map,e} + (1 - k_1)\omega_{gps,e})^2\right] \\ &= E\left[k_1^2\omega_{map,e}^2 + (1 - k_1)^2\omega_{gps,e}^2 + 2k_1(1 - k_1)\omega_{map,e}\omega_{gps,e}\right] \\ &= k_1^2 E[\omega_{map,e}^2] + (1 - k_1)^2 E[\omega_{gps,e}^2] + 2k_1(1 - k_1)E[\omega_{map,e}\omega_{gps,e}] \\ &= k_1^2\sigma_{map,e}^2 + (1 - k_1)^2\sigma_{gps,e}^2 + 2k_1(1 - k_1)\rho\omega_{map,e}\sigma_{gps,e} \end{aligned} \tag{6.17}$$

Differentiating equation (6.17) with respect to k_1 and setting the result to zero yields

$$\frac{\partial E\left[\tilde{e}^2\right]}{\partial k_1} = 2k_1\sigma_{map,e}^2 - 2(1-k_1)\sigma_{gps,e}^2 + 2\rho\omega_{map,e}\sigma_{gps,e} - 4k_1\rho\omega_{map,e}\sigma_{gps,e} = 0 \text{, i.e.,}$$

$$k_1 = \frac{\sigma_{gps,e}^2 - \rho\omega_{map,e}\sigma_{gps,e}}{\sigma_{map,e}^2 + \sigma_{gps,e}^2 - 2\rho\omega_{map,e}\sigma_{gps,e}} \quad \textbf{(6.18)}$$

From equation (6.16), it can easily be shown that

$$k_2 = \frac{\sigma_{map,e}^2 - \rho\omega_{map,e}\sigma_{gps,e}}{\sigma_{map,e}^2 + \sigma_{gps,e}^2 - 2\rho\omega_{map,e}\sigma_{gps,e}} \quad \textbf{(6.19)}$$

The optimal estimation of the easting coordinate is therefore (from equation (6.13)),

$$\hat{e} = \left(\frac{\sigma_{gps,e}^2 - \rho\omega_{map,e}\sigma_{gps,e}}{\sigma_{map,e}^2 + \sigma_{gps,e}^2 - 2\rho\omega_{map,e}\sigma_{gps,e}}\right)e_{map} + \left(\frac{\sigma_{map,e}^2 - \rho\omega_{map,e}\sigma_{gps,e}}{\sigma_{map,e}^2 + \sigma_{gps,e}^2 - 2\rho\omega_{map,e}\sigma_{gps,e}}\right)e_{gps} \quad \textbf{(6.20)}$$

and hence equation (6.17) becomes

$$E\left[\tilde{e}^2\right] = \frac{\sigma_{map,e}^2\sigma_{gps,e}^2(1-\rho^2)}{\sigma_{map,e}^2 + \sigma_{gps,e}^2 - 2\rho\omega_{map,e}\sigma_{gps,e}} \quad \textbf{(6.21)}$$

where $\sigma^2 = E\left[\tilde{e}^2\right]$ is the variance of the error term $\tilde{e}$. Equation (6.21) can be rewritten as

$$\sigma_e^2 = \frac{\sigma_{map,e}^2\sigma_{gps,e}^2(1-\rho^2)}{\sigma_{map,e}^2 + \sigma_{gps,e}^2 - 2\rho\omega_{map,e}\sigma_{gps,e}} \quad \textbf{(6.22)}$$

Similar to equation (6.20), the optimal estimation of the northing coordinate can be determined from

$$\hat{n} = \left(\frac{\sigma_{gps,n}^2 - \rho\sigma_{map,n}\sigma_{gps,n}}{\sigma_{map,n}^2 + \sigma_{gps,n}^2 - 2\rho\sigma_{map,n}\sigma_{gps,n}}\right)n_{map} + \left(\frac{\sigma_{map,n}^2 - \rho\sigma_{map,n}\sigma_{gps,n}}{\sigma_{map,n}^2 + \sigma_{gps,n}^2 - 2\rho\sigma_{map,n}\sigma_{gps,n}}\right)n_{gps} \quad \textbf{(6.23)}$$

where $\sigma_{gps,n}$ is the standard deviation of the error associated with the northing component of the position fix, n_{gps} is the measurement of northing from the navigation sensor.

Similar to equation (6.22) the variance is given by

$$\sigma_n^2 = \frac{\sigma_{map,n}^2\sigma_{gps,n}^2(1-\rho^2)}{\sigma_{map,n}^2 + \sigma_{gps,n}^2 - 2\rho\sigma_{map,n}\sigma_{gps,n}} \quad \textbf{(6.24)}$$

6.3.2.1 Calculation of error variances

The error variances $\sigma_{gps,e}^2$ and $\sigma_{gps,n}^2$ can be directly obtained from the variance-covariance matrix associated with the navigation sensor (i.e., GPS or GPS/DR). This is fully discussed in Chapter 3. However, the derivation of error variances $\sigma_{map,e}^2$ and $\sigma_{map,n}^2$ is given below:

According to equation (6.8), the increment in easting and northing of the position fix is given by

$$\Delta E_i = v\sin\theta \quad \textbf{(6.25)}$$

$$\Delta N_i = v\cos\theta \quad \textbf{(6.26)}$$

The uncertainty associated with equation (6.25) is

$$d(\Delta E_{i+1}) = \sin\theta dv + v\cos\theta d\theta$$

Therefore, the standard deviation of the error component $\omega_{map,e}$ is

$$\sigma_{map,e} = \sqrt{(\sin\theta\Delta v)^2 + (v\cos\theta\Delta\theta)^2} \quad \textbf{(6.27)}$$

where Δv is the uncertainty associated with the vehicle speed obtained from the positional variance-covariance matrix and $\Delta\theta$ is the uncertainty (in radians) associated with the link heading obtained from road map data.

Similar to equation (6.27), the standard deviation of the error component $\omega_{map,n}$ can be obtained from

$$\sigma_{map,n} = \sqrt{(\cos\theta\Delta v)^2 + (-v\sin\theta\Delta\theta)^2} \quad \textbf{(6.28)}$$

A special case

Assume that there is no correlation between the error terms from two measurement techniques i.e., $E[\omega_{map,e}\omega_{gps,e}] = 0$ and $\rho = 0$ then equation (6.18) and (6.19) become

$$k_1 = \frac{\sigma^2_{map,e}}{\sigma^2_{map,e} + \sigma^2_{gps,e}} \quad \text{and} \quad k_2 = \frac{\sigma^2_{map,e}}{\sigma^2_{map,e} + \sigma^2_{gps,e}}$$

The optimal estimation is therefore obtained from (6.20) and (6.23) as

$$\hat{e} = \left(\frac{\sigma^2_{map,e}}{\sigma^2_{map,e} + \sigma^2_{gps,e}}\right)e_{gps} + \left(\frac{\sigma^2_{gps,e}}{\sigma^2_{map,e} + \sigma^2_{gps,e}}\right)e_{map} \quad \textbf{(6.29)}$$

$$\hat{n} = \left(\frac{\sigma^2_{map,n}}{\sigma^2_{map,n} + \sigma^2_{gps,n}}\right)n_{gps} + \left(\frac{\sigma^2_{gps,n}}{\sigma^2_{map,n} + \sigma^2_{gps,n}}\right)n_{map} \quad \textbf{(6.30)}$$

the error variance for the easting component can now expressed as (from equation 4.22)

$$\sigma^2_e = \frac{\sigma^2_{map,e}\sigma^2_{gps,e}}{\sigma^2_{map,e} + \sigma^2_{gps,e}}$$

Alternatively,

$$\frac{1}{\sigma_e^2} = \frac{1}{\sigma_{map,e}^2} + \frac{1}{\sigma_{gps,e}^2} \tag{6.31}$$

It is noticeable from equation (6.31) that the error variance, σ_e^2, is less than either $\sigma_{map,e}^2$ or $\sigma_{gps,e}^2$ which is to say that the uncertainty in estimating the vehicle position is decreased by combining the two types of measurement methods.

Some observations

(a) If $\sigma_{map,e} = \sigma_{gps,e}$ i.e., the error variances from the two measurement methods are the same, then the optimal estimation is the average value of the two measurements i.e.,

$$\hat{e} = \frac{e_{map} + e_{gps}}{2}$$

(b) If $\sigma_{map,e}$=0 then, then the optimal estimation is equal to the measurement of first method i.e., $\hat{e} = e_{map}$

(c) If $\sigma_{gps,e} = 0$ then, the optimal estimation is equal to the measurement of second method i.e., $\hat{e} = e_{gps}$

(d) If $\sigma_{map,e} > \sigma_{gps,e}$ then, $\hat{e}$ dictates 'weighting' e_{gps} more heavily than e_{map} (see equation (6.29)).

6.4 Algorithm Step-by-Step

There are two basic procedures in the probabilistic map matching algorithm. The first is the matching process at a junction (MPJ) and the second is the subsequent matching process on a link (SMPL) as explained in the previous sections.

MPJ:

The MPJ is a function of search space, proximity of the position fix to the link, orientation of the fix relative to the link, the topology (connectivity) of the map, and the historical trajectory of the vehicle. This MPJ procedure involves the following steps:

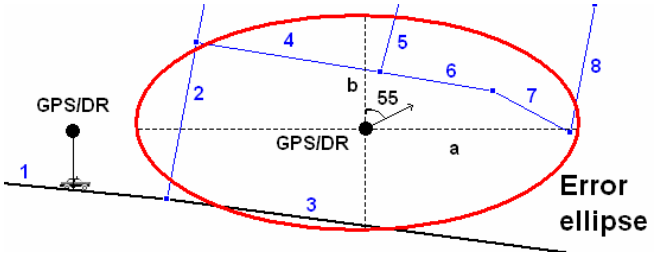

Figure 6.10: Matching process at a junction

- Define a search space from the quality of the position fix (i.e., an error ellipse)
- Identify all the road segments within the search space as shown in Figure 6.10 (e.g., 2, 3, 4, 5, 6, 7, 8)
- Select candidate links by comparing vehicle and link headings. If the difference is less than 45^0 then the link is considered as a candidate link (e.g., the candidate links are 2, 3, 4, 5, 6, and 7 for this case)
- Use historical data and link connectivity for further filtering. Since the vehicle's previous location is on link-1, the next vehicle location should be either on link-2 or link-3. If the vehicle's previous location is not known (in the case of initial matching), the algorithm goes to the next step to select the correct link
- Select the final link based on proximity and orientation of the position fix relative to the links. This gives link-3 as the final link.
- The vehicle location on link-3 is then estimated using equations 6.24 and 6.25.

SMPL:

The SMPL is a function of heading difference between vehicle (derived from GPS or GPS/DR) and link (derived from map data), distance-to-junction (D), speed and gyro rate (if available). In this procedure, the position fixes are matched to the previously identified link if the following criteria are fulfilled:

- No turning manoeuvres (detected according to the conditions given in section 6.3.1.2)

- Distance-to-junction (D) is greater than 10 m
- Gyro-rate reading is less than 15^0

The location of the vehicle is then estimated using equations (6.29) and (6.30).

6.5 Algorithm Testing

The probabilistic map matching algorithm developed in this chapter was tested using the real data described in Chapter 5 (section 5.6). The positioning data (easting and northing coordinates), speed, and heading were available from two positioning systems: stand-alone GPS and an integrated navigation system (GPS/DR) employing an EKF algorithm. This means that the map matching algorithm can be tested with locational data from either GPS or the integrated GPS/DR system and digital spatial road network data from any large scale map. Here, the map matching algorithm is tested using the navigation data from GPS/DR and the digital map data from a map of scale 1:2500 supplied by *Saturn Technologies Limited*.

The algorithm is tested for two scenarios with different network characteristics and with different traffic manoeuvres. These are: a complex urban road network where the typical distance between roads is very small (Figure 6.11), and travelling through a roundabout (Figure 6.12). Each of the black round dots in these figures represents the vehicle position before map matching. The arrow symbols in the figures show the path followed by the vehicle on the network.

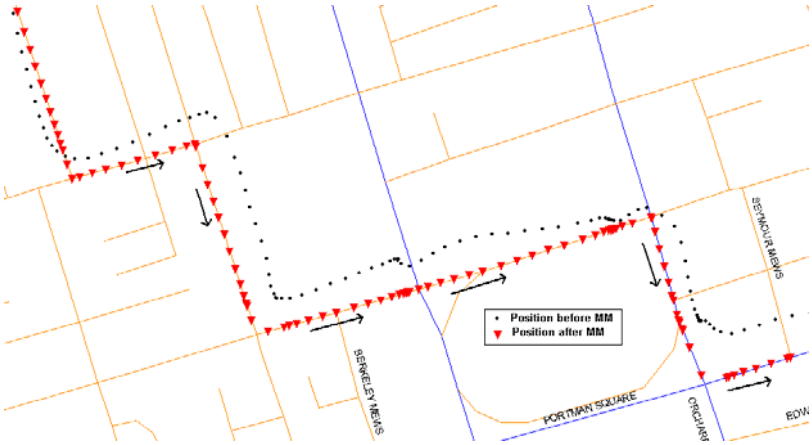

(Presentation map scale 1 cm : 20 m)

Figure 6.11: Map matching results on complex urban road network

The semi-major axis (i.e., a) and the semi-minor axis (i.e., b) of the error ellipse (see equations 6.5 and 6.6) are between 20m to 50m and 15m to 46m respectively whenever MPJ is required. The rectangular confidence region constructed from the major and minor axes of the error ellipse always contains one or more road segments. This is an indication that the vehicle was not travelling off the road segments included on the digital map. The threshold value for the minimum speed is taken as 3m/sec, α is taken as 30^0, and β is taken as 35^0. These values are used to detect any manoeuvres at junctions.

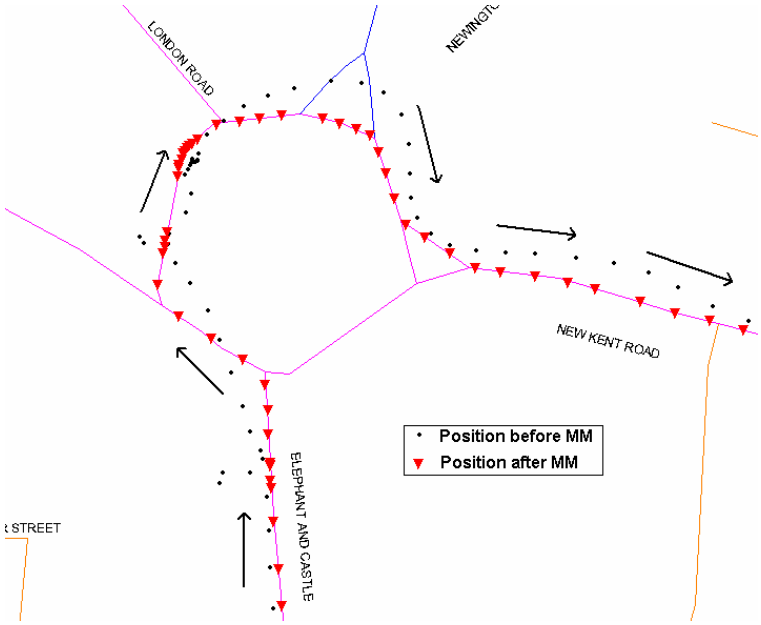

(Presentation map Scale: 1cm: 24m)

Figure 6.12: Map matching results at roundabout

Each of the triangular symbols on the road segments represents the vehicle position after map matching. As can be seen, there is a very good agreement between the map-matched locations and the position fixes from GPS/DR. The position of the vehicle on a selected road segment was estimated using two positioning methods (estimation using map data with the vehicle speed information from the positioning unit and the other is from the orthogonal projection of the GPS/DR fix on the road segment). The optimal positions were estimated from equations (6.29) and (6.30) for the easting and northing coordinates respectively. Chapter 9 quantifies the performance of this new map matching algorithm in terms of accuracy and integrity.

6.6 Problems Associated with the Matching Process at Junction (MPJ)

As discussed in section 6.3.1.1, the purpose of the MPJ process is to select road segments that fall within an error ellipse. This is obtained by first selecting all nodes (i.e., road junctions) that are within the error ellipse. The segments that are originated from (or are destined to) these nodes are considered as candidate segments. Although the MPJ process normally identifies the correct segment near a junction, there maybe some circumstances in which the MPJ need to start on a road segment which is further from the junctions. The error ellipse then does not contain any junctions (see Figure 6.13). Consequently, the MPJ process developed in section 6.3.1.1 would identifies no road segments and would assumes that the vehicle is off the known-road-network. This is incorrect as the vehicle can be on link-AB (for example) in the case of Figure 6.13. This type of scenario can occur if the map matching process needs to be re-initialised between the middle of two junctions (i.e., motorway) and if there is no historical information available.

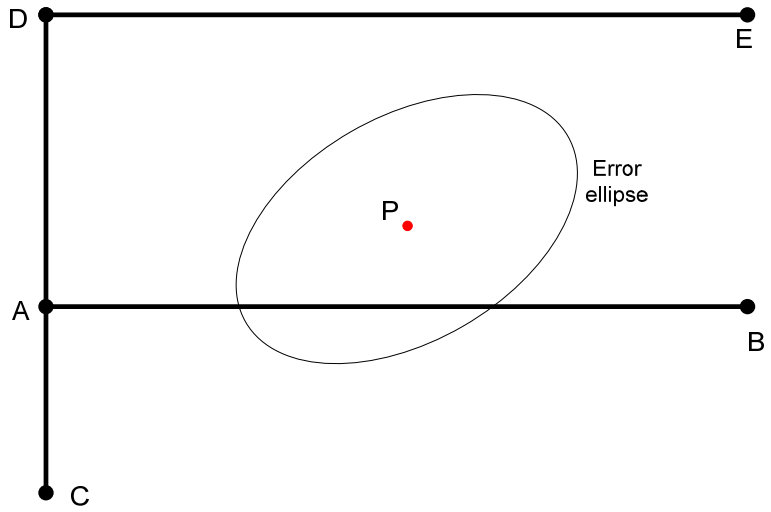

Figure 6.13: No nodes within an error ellipse

This type of ambiguity can be resolved by using the alternative method discussed below. An error circle with a radius equal to the semi-major axis of the error ellipse can be used. This gives an assurance that the error circle selects all segments that would have been selected by the error ellipse. Moreover, the error circle is relatively easy to formulate compared to an error ellipse. A straight line representing the road segment can then be formed using the coordinates of the starting node and end node. This is a one-off offline process that could be performed for all road segments within the spatial digital map data. Therefore, the problem of identifying road segments within an error ellipse then

transforms to the problem of identifying whether a line intersects a circle or not. This is known as a circle-line intersection problem. This is fully described below.

The scenarios that need to be investigated to see whether a line (i.e., a road segment) is within a circle (i.e., an error circle) are shown in Figures 6.14 – 6.19. In these figures, a road segment is represented by AB and a circle is represented by a radius of r and the centre at point (h, k).

- Figure 6.14: no intersection between them
- Figure 6.15: the line (AB) intersects (but not physically) the circle at a single imaginary point, Q (α, β). In this case, AB is known as a tangent line, and the point, Q, is known as a virtual intersection point.
- Figure 6.16: the line (AB) physically intersects a circle at a single real point, Q (α, β) (in this case, the line is also known as a tangent line)
- Figure 6.17: the line (AB) intersects (but not physically) a circle at two imaginary points, P (α_1, β_1) and Q (α_2, β_2).
- Figure 6.18: the line (AB) intersects a circle at two points of which one is a real point, P (α_1, β_1) and the other is an imaginary point, Q (α_2, β_2).
- Figure 6.19: the line (AB) physically intersects a circle at two real points, P (α_1, β_1) and Q (α_2, β_2)

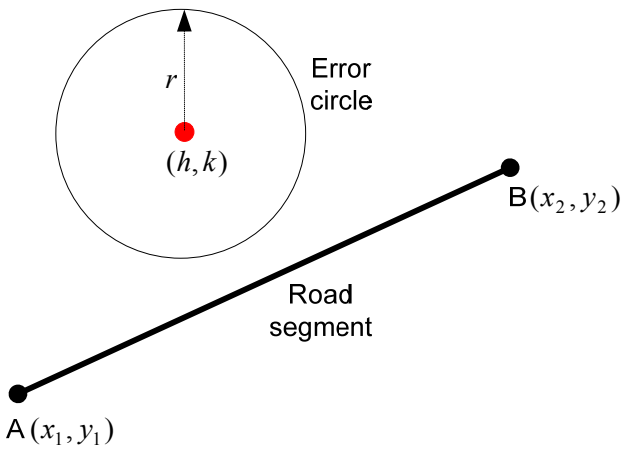

Figure 6.14 : No intersection between an error circle and a road segment

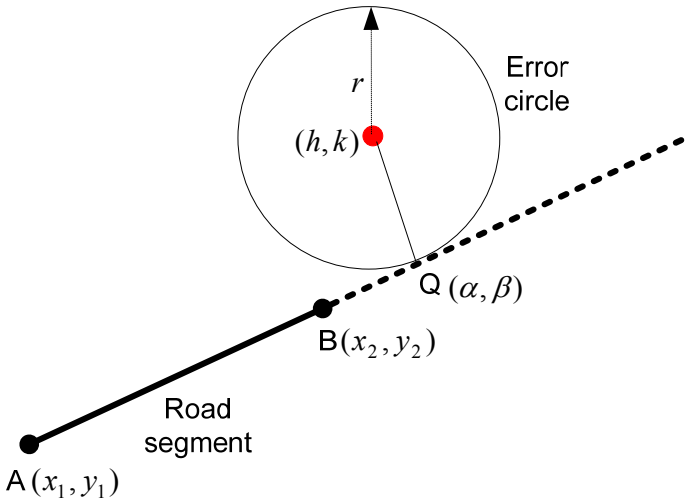

Figure 6.15: A road segment intersects an error circle in a single point but not physically

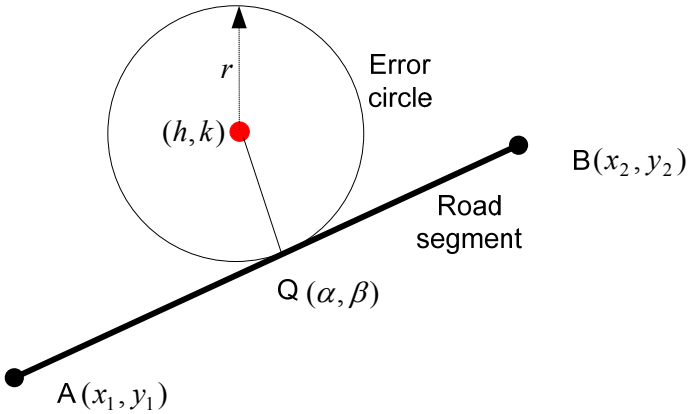

Figure 6.16: A road segment intersects an error circle in a single point physically

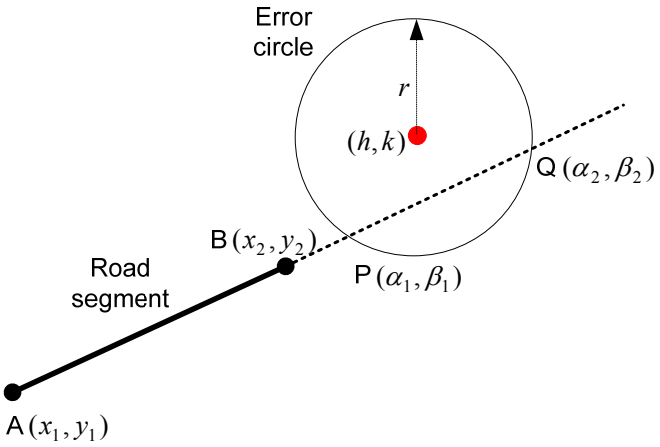

Figure 6.17: A road segment intersects an error circle but not physically

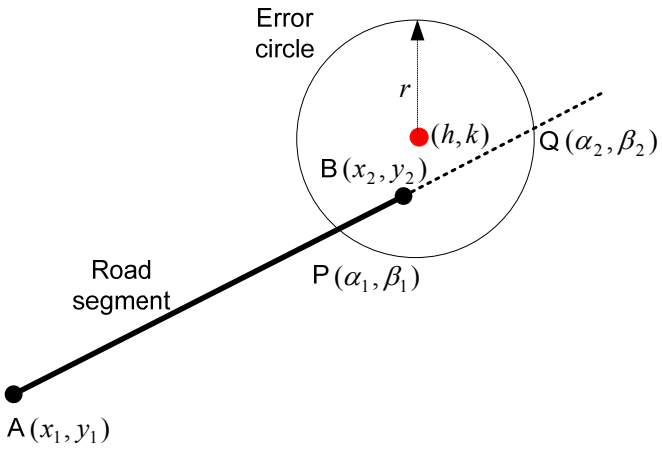

Figure 6.18: A line intersects a circle in two points of which one is a real point and the other is an imaginary point

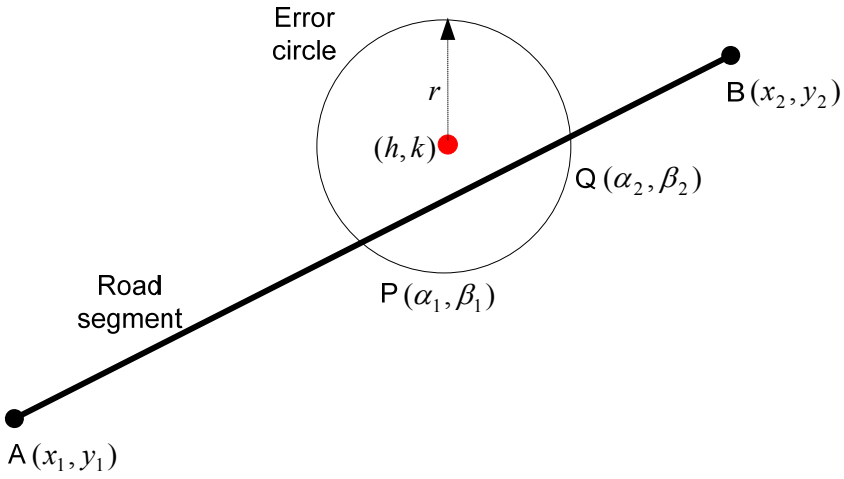

Figure 6.19: A road segment intersects an error circle physically

The scenarios represented by Figures 6.16, 6.18, and 6.19 suggest that the road segment (AB) is within the error circle. However, the mathematical criteria to see whether the line (AB) intersects the circle of radius *r* need to be established and is therefore given below:

If the difference in the easting coordinates between two nodes A (x_1, y_1) and B (x_2, y_2) is Δx and the difference in the northing coordinates between two nodes A and B is Δy then

$$\Delta x = x_1 - x_2 \qquad \textbf{(6.32)}$$

$$\Delta y = y_1 - y_2 \qquad \textbf{(6.33)}$$

The equation of the circle of radius r and centre (h, k) is:

$$(x-h)^2 + (y-k)^2 = r^2 \tag{6.34}$$

The equation of the line passing through point A (x_1, y_1) and B (x_2, y_2) is:

$$y = mx + c \tag{6.35}$$

where

$$m = \frac{\Delta y}{\Delta x} \qquad \text{and} \qquad c = \frac{x_1 y_2 - y_1 x_2}{\Delta x}$$

The points of intersection between equations (6.34) and (6.35) can be expressed as:

$$\alpha = \frac{m^2 k + h - mc}{1 + m^2} \pm \frac{\sqrt{r^2 - g^2}}{\sqrt{1 + m^2}} \tag{6.36}$$

$$\beta = \frac{m^2 k + mh + c}{1 + m^2} \pm \frac{m\sqrt{r^2 - g^2}}{\sqrt{1 + m^2}} \tag{6.37}$$

where

$$g = \left(\frac{(k - mh - c)}{\sqrt{1 + m^2}} \right)$$

The expression $(r^2 - g^2)$ in equation (6.36) or (6.37) can be used to see whether the line intersects the circle.

- If $(r^2 - g^2)<0$ then there is no intersection between the line and the circle
- If $(r^2 - g^2)=0$ then the line is a tangent to the circle intersecting it at a single point
- If $(r^2 - g^2)>0$ then the line intersects the circle at two points

We are interested in the last two conditions where the road segment can be considered as a candidate segment. However, the road segment (i.e., the line) does not always intersect the circle in real points (see Figure 6.15 and 6.17). If any of the following conditions are true then it can be said that the segment physically intersects the circle:

- $|x_1| \le \alpha \le |x_2|$ or $|x_2| \le \alpha \le |x_1|$
- $|y_1| \le \alpha \le |y_2|$ or $|y_2| \le \alpha \le |y_1|$

This procedure can effectively eliminate the problem of omitting a road segment that is actually within a confidence region. Because of the increased number of tests that need to be performed in this method of identifying a road segment, there is a possibility that the run-time of the algorithm may increase. A future research project requires to investigate this issue.

6.7 Summary

A probabilistic map matching algorithm was presented in this chapter. Probabilistic approaches were applied for the identification of the correct road segment and the estimation of the vehicle location. The innovative feature of the algorithm was that an error ellipse derived from the quality of the position fix was used to select the candidate links. The topology of the map, the orientation of the position fix relative to the link, the proximity of the fix to the link, the connectivity of the links at a junction and the historical trajectory of the vehicle were then used to identify the correct link for a particular position fix. An optimal estimation method which took into account errors associated with the positioning system and the digital road network was introduced to locate the vehicle on a link. A step-by-step procedure was also presented to demonstrate how to implement the algorithm. The algorithm was then tested in two complex urban road networks including a 5-legged roundabout. Initial results showed good agreement between the vehicle trajectory obtained from the map-matched locations and the actual route taken by the vehicle. Further experiments on the algorithms are presented in Chapter 9. This chapter also discussed the limitation associated with the MPJ process and then developed a method to deal with such a limitation.

In high road density areas, it may be that there may be many road patterns matching the trajectory of the vehicle reported by the positioning system at any given moment (see

Figure 6.10). Consequently, it may be difficult to precisely identify the road on which the vehicle is travelling. To a certain extent, the map matching algorithm may suggest that the vehicle is "more likely" to be on certain roads, and "less likely" to be on other roads. Therefore, techniques for dealing with qualitative terms such as likeliness are essential in the map matching algorithm for the identification of the correct link. The next chapter describes a map matching process based on a qualitative decision making process such as fuzzy logic.

CHAPTER 7

A FUZZY LOGIC MAP MATCHING ALGORITHM

7.1 Introduction

In dense urban areas, the vehicle trajectory directly derived from the positioning system is often quite different from the actual route due to inherent problems associated with GPS in urban canyons as well as imperfections of the map database generated during digitization. Therefore, the error ellipse, derived from the uncertainty of the position solution, is relatively large and normally contains a high number of links. This may create difficulties in the map matching process with respect to determining the link on which a vehicle is travelling. In such a case, a map matching algorithm may suggest that the vehicle is more likely to be on a link and less likely to be on the others. This type of ambiguity needs to be resolved if a relatively accurate positioning is desired. Therefore, a method suitable for dealing with a qualitative term such as likeliness is necessary in map matching algorithms for the selection of the correct link among candidate links.

Fuzzy logic is one technique that is an effective way to deal with qualitative terms, linguistic vagueness, and human intervention (Zhao, 1997). In fuzzy logic, linguistic terms with vague concepts can be expressed mathematically by making use of fuzzy sets. A set of rules representing expert knowledge and experience is used to draw inferences through an approximate reasoning process. In a map matching process, identification of the correct link on which the vehicle is travelling is a qualitative decision-making process involving a degree of ambiguity.

The inputs to the proposed algorithm come either from GPS or GPS/DR. The basic characteristics of this approach to map matching are to build various knowledge-based IF-THEN rules comprising the speed of the vehicle, the heading and the historical trajectory of the vehicle, the connectivity and the orientation of road links, and the

contribution of satellite geometry to horizontal errors. The physical location of the vehicle on a link is then estimated using the optimal estimation technique discussed in Chapter 6 (section 6.3.2).

This chapter is organised as follows. Firstly a brief overview of fuzzy logic theory is provided. This is followed by a detailed description of the proposed fuzzy logic-based map matching algorithm. The last section briefly describes the implementation and testing of the algorithm using real-world data.

7.2 Enhancement over Existing Fuzzy Logic Based Algorithms

Fuzzy logic based map matching algorithms have been developed by a number of researchers (e.g., Zhao, 1997; Kim et al., 1998, Syed and Cannon, 2004) over the last few years. The generic limitations of these algorithms can be found in Chapter 4. Only a summary of the relevant limitations are mentioned here. These include: (a) ignoring most of the available inputs to the fuzzy logic model, (b) overlooking the connectivity among road links and the historical trajectory of the vehicle, which can enhance the performance of map matching algorithms, (c) ignoring the error sources associated with the spatial road network and the navigation sensor, and (d) failing to validate the map matching algorithms to assess their performance. This research builds on existing fuzzy logic-based map matching algorithms to develop an improved algorithm that takes account of these limitations, specifically:

- a number of new input variables (at no extra cost) are included in the proposed fuzzy logic map matching algorithm. These are: (1) the speed of the vehicle, (2) the connectivity among road links, (3) the quality of position solution e.g., HDOP, and (4) the position of a fix relative to a candidate link. These inputs are incorporated into the rules in order to improve the performance of the algorithm.

- the membership functions are optimised using a true input/output data obtained from a high accuracy GPS carrier phase observations.

- three sets of knowledge-based fuzzy rules are formulated when the navigation solution comes from either stand-alone GPS or GPS/DR. The first set (six rules)

is for an initial map-matching process (IMP), the second set (thirteen rules) is for subsequent map-matching on a link (SMP-Link), and the third set (four additional rules) is for subsequent map-matching at a junction (SMP-Junction). It is worthwhile to note that Zhao (1997) develops a total of eight rules in the case of a navigation solution obtained from a DR sensor. These particular rules do not represent completely the stand-alone GPS or the integrated GPS/DR scenarios.

- an optimal estimation technique which takes into account error sources associated with the navigation sensors and the digital map data is used to determine the location of the vehicle on a link.

7.3 Overview of Fuzzy Logic Theory

Fuzzy logic is a superset of conventional (Boolean) logic that has been extended to handle the concept of partial truth i.e., truth values between "completely true" and "completely false". It was introduced in the 1960's by Zadeh (1965). Zadeh worked in the field of control engineering and his intention in introducing the fuzzy theory was to deal with problems involving knowledge expressed in vague, linguistic terms. To represent the shades of meaning of linguistic terms (e.g., the speed of the vehicle is low, the distance to the downstream junction is long, etc), the concept of grades of membership or the concept of possibility values of membership was introduced in fuzzy logic. A comprehensive review of fuzzy logic theory can be found in Zadeh (1965, 1973, 1989), Mamdani and Assilian (1975), and Sugeno (1985). A brief overview is presented below.

Consider a simple knowledge-based fuzzy rule-"If the speed of the vehicle is high and the travel time is low then the traffic congestion on the link is low". The input variables of this rule are the speed of the vehicle and the travel time and the input fuzzy subsets are high and low respectively. The output variable is the traffic congestion and the output fuzzy subset is low. Since fuzzy subsets describe vague concepts, the truth of any proposition (i.e., the speed of the vehicle is high) in fuzzy logic becomes a matter of degree. This is achieved by the fuzzification of the input variable using a membership function (MF) described below. A MF is a curve that defines how each point in the input space (e.g., a speed range in the above example) is mapped to a membership value between 0 and 1.

One of the challenging issues in fuzzy logic is to define the shape of the MF. Different types of MFs are used. Examples are triangular, trapezoidal, Z-shaped, S-shaped, gaussian, generalised bell, and sigmoidal, etc. The shape of a MF is usually determined empirically based on the linguistic statements associated with the inputs. After the fuzzification of all inputs, fuzzy knowledge-based IF-THEN rules are formulated. The output of each rule is also a fuzzy set which is achieved by either a min (minimum) method (the minimum of all degree of membership values associated with inputs) or a prod (product) method (the product of all degree of membership values associated with inputs) (Mamdani and Assillian, 1975). The output fuzzy sets of each rule are then combined into a single fuzzy set using the aggregation method. Three methods are used for the aggregation method: (1) max (maximum), (2) probor (Probabilistic OR), (3) sum (Mamdani and Assillian, 1975). The last step is called the defuzzification process. The input to this process is a fuzzy set obtained from the output of the aggregation method. The output of the defuzzification process is a single number (crisp). Several methods are available for the defuzzification process, e.g., centroid, the largest of maximum, the smallest of maximum, bisector, and weighted average, etc (MathWorks, 2000).

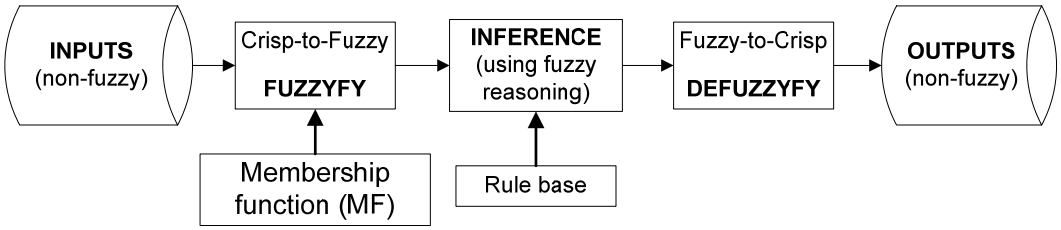

Figure 7.1: Fuzzy inference system (FIS)

Figure 7.1 shows a fuzzy inference system (FIS) which is the process of formulating the mapping from a given input to an output using fuzzy logic. The mapping provides a basis from which a decision can be made. There are two main types of FIS: (1) Mamdani-type (Mamdani and Assillian, 1975) and (2) Sugeno-type (Sugeno, 1985).

7.3.1. Mamdani's Fuzzy Inference System

Figure 7.1 shows a Mamdani FIS where the output inference is also expected to be a fuzzy set. The following six steps can be used to compute the system output from a set of given inputs.

- Determine a set of state input variables and knowledge-based fuzzy rules
- Fuzzify the inputs using the input membership functions
- Combine the fuzzified inputs according to fuzzy rules to establish a rule strength
- Determine the consequence of each rule by combining the rule strength and the output membership function
- Combine the consequences to get an output distribution, and
- Defuzzify the output distribution if a crisp output is needed.

The Mamdani FIS can be illustrated with the following example. Consider a three-legged junction as shown in Figure 7.2. Assume that P represents a vehicle position obtained from an in-vehicle navigation sensor when the vehicle travels through the junction. The task is to identify the correct link among the candidate links (DA, AB or AC) on which the vehicle is actually travelling. The direction of the vehicle at P obtained from the navigation sensor is θ.

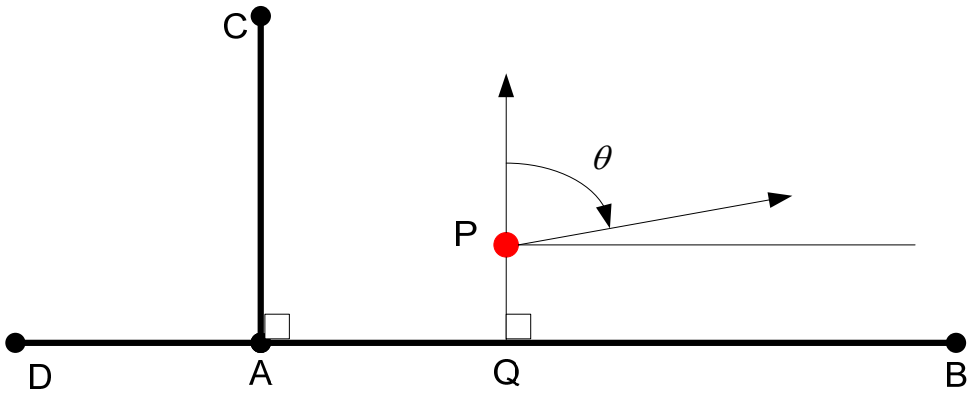

Figure 7.2: A three-legged junction with a vehicle position from a navigation sensor

PQ denotes a perpendicular distance from P to link AB. The distance, PQ, and the angular difference, $\Delta\varphi = \left|90^0 - \theta\right|$, are the two primary determining factors as to whether P is matched onto link AB. Link AB would be the desired link if PQ is short and $\Delta\varphi$ is small. Knowledge-based IF-THEN rules can be formed based on these two inputs, for example:

- If PQ is short and $\Delta\varphi$ is small then the possibility of matching P on link AB is high
- If PQ is long and $\Delta\varphi$ is large then the possibility of matching P on link AB is low

where, *short (or long) and small (or large)* are linguistic values defined by fuzzy subsets on the ranges PQ and $\Delta\varphi$ respectively. The *if* part of the first rule "If PQ is short and $\Delta\varphi$ is small" is called the *antecedent* or *premise*, while the *then*-part of the rule "The possibility of matching P on link AB is high" is called the *consequent* or *conclusion*. There are five steps involved in the FIS (MathWorks, 2000). These are explained below for the case of the above example:

Step 1: Fuzzification of inputs and outputs

The first step is to fuzzify the input and output variables using MFs. There are two inputs in this example: (1) perpendicular distance, PQ, (2) angular difference, $\Delta\varphi$. The fuzzy subsets associated with PQ are short and long. One has to be familiarised with the basic understanding of the linguistic statement when developing MFs. For example, the knowledge of range, mean, and variance of PQ is desirable if one has to define the membership function associated with the input PQ. Now, the difficulty is how to define that PQ is "*short*" or "*long*". As discussed in Chapter 3, the average horizontal error of GPS SPS (SIS only) is 13m (2σ). Therefore, a value close to this horizontal error can be used as a reference when developing MFs for PQ. For instance, the statement "*PQ is short"* is true (i.e., $\mu_{PQ}=1$) if PQ is less than or equal to10m. The statement is partially true (i.e., $0<\mu_{PQ}<1$) if PQ is greater than 10m and less than or equal to 20m. The statement is false (i.e., $\mu_{PQ}=0$) if PQ is greater than 20m. The membership value of the MF (μ_{PQ}) for the antecedent "*PQ is short*" can then be defined as:

$$\mu_{PQ}=\begin{cases}1 & \text{if PQ}\le 10\text{m}\\ 2-0.1*PQ & \text{if PQ}>10\text{m and PQ}\le 20\text{m}\\ 0 & \text{if PQ}>20\text{m}\end{cases} \qquad \textbf{(7.1)}$$

And the membership value of the MF (μ_{PQ}) for the antecedent "*PQ is long"* can be defined as:

$$\mu_{PQ} = \begin{cases} 0 & \text{if PQ} \le 10\text{m} \\ 0.1 * PQ - 1 & \text{if PQ} > 10\text{m and PQ} \le 20\text{m} \\ 1 & \text{if PQ} > 20\text{m} \end{cases} \quad \textbf{(7.2)}$$

The MFs for PQ is shown in Figure 7.3. The fuzzy subsets associated with $\Delta\varphi$ are small and large. $\Delta\varphi$ is fuzzified using the following equations:

The membership value of the MF for $\Delta\varphi$ *is small*:

$$\mu_{\Delta\varphi} = \begin{cases} 1 & \text{if } \Delta\varphi \le 10^0 \\ 2 - 0.1 * \Delta\varphi & \text{if } \Delta\varphi > 10^0 \text{ and } \Delta\varphi \le 20^0 \\ 0 & \text{if } \Delta\varphi > 20^0 \end{cases} \quad \textbf{(7.3)}$$

The membership value of the MF for $\Delta\varphi$ *is large*:

$$\mu_{\Delta\varphi} = \begin{cases} 0 & \text{if } \Delta\varphi \le 15^0 \\ 0.1 * \Delta\varphi - 1.5 & \text{if } \Delta\varphi > 15^0 \text{ and } \Delta\varphi \le 25^0 \\ 1 & \text{if } \Delta\varphi > 25^0 \end{cases} \quad \textbf{(7.4)}$$

The MFs for $\Delta\varphi$ is shown in Figure 7.3. The single output variable is the possibility of matching the position fix, P, on link AB and the fuzzy subsets are low, average, and high. A quality indicator between 1 to 100 can be used to represent the possibility of matching the fix on link. A high quality indicator indicates a high possibility. This variable is fuzzified using triangular MFs (Figure 7.3).

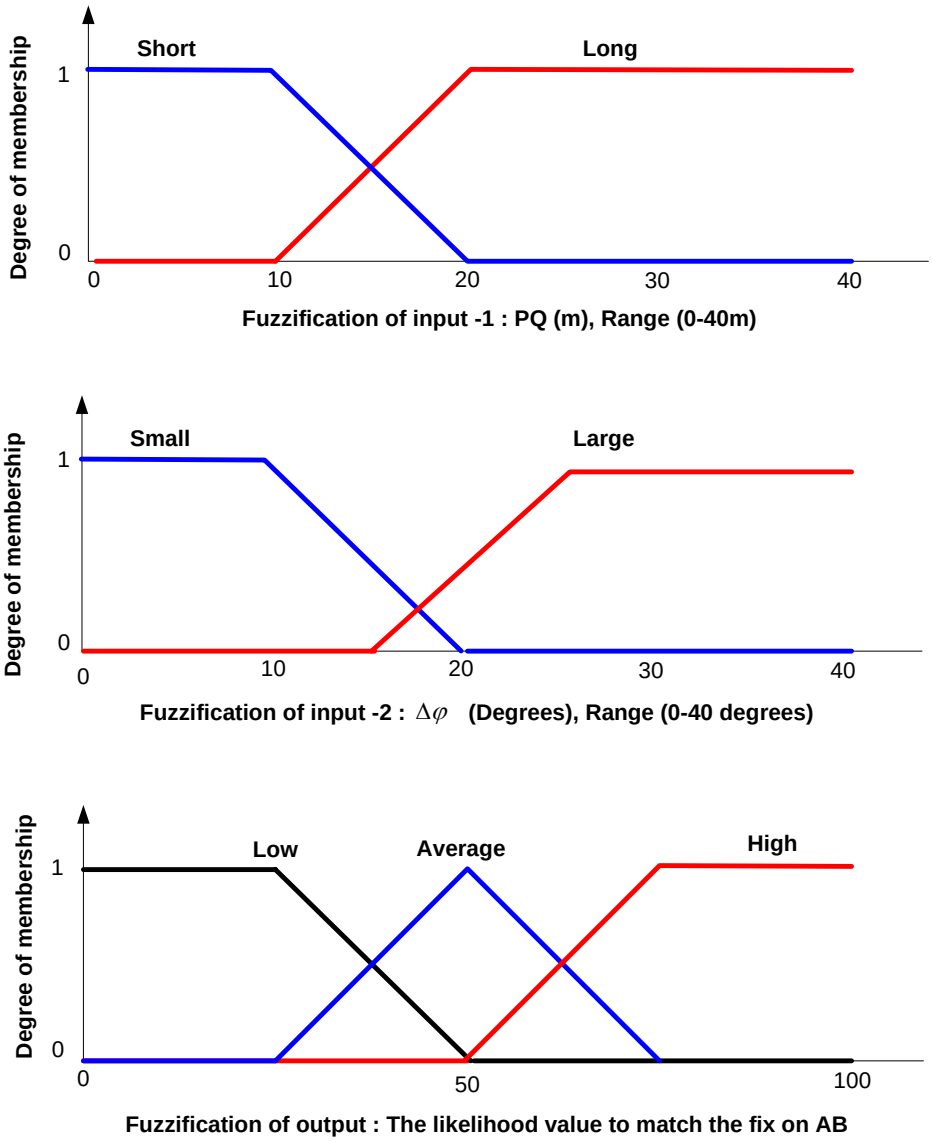

Figure 7.3: Fuzzification of inputs and output

Step 2: Application of fuzzy operators

Once the inputs have been fuzzified, the degree to which each part of the antecedent has been satisfied for each rule is known. If the antecedent of a given rule has more than one part, the fuzzy operator is applied to obtain one number that represents the result of the antecedent for that rule, known as *rule strength*. This number is then applied to the output function. Two types of fuzzy operators are normally used: (1) AND, and (2) OR. Two popular AND methods are: *min* (minimum) and *prod* (product). Two widely-used OR

methods are: *max* (maximum), and the probabilistic OR method[31]. In addition to these methods, one can create one's own methods for AND and OR.

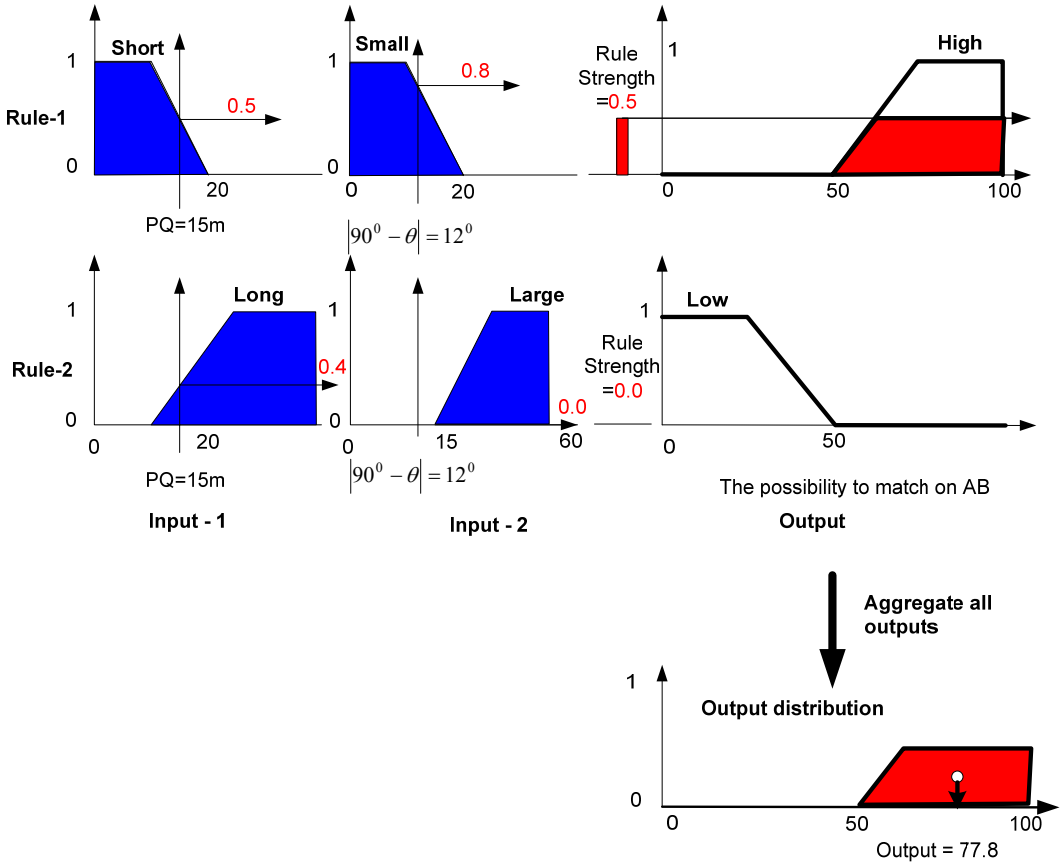

Figure 7.4: Mamdani's Fuzzy Inference System (FIS)

In this example, the fuzzy membership values of two antecedents from the first rule are 0.5 if PQ=15m and 0.5 if $\Delta\varphi = 15^0$. By applying the *min* method for the AND operator, the rule strength becomes 0.5 (Figure 7.4). The fuzzy membership values of two antecedents from the second rule are 0.4 and 0. Using the same *min* method, the rule strength is therefore 0.

Step 3: Application of the implication method

Before applying the implication method, the rule's weight should be taken into account. Every rule has a *weight* which is a number between 0 and 1. The number given by the

[31] The probabilistic OR method uses the technique of the algebraic sum

antecedent is then multiplied by the weight to obtain the final rule strength. The weight is normally taken as 1so that each rule has the same weight.

A consequent, which is a fuzzy set represented by a membership function of the output variable, is then reshaped using a number obtained from the rule strength of each rule. The number is 0.5 for the first rule and 0 for the second rule (Figure 7.4). Two methods are used: (1) *min* (minimum), which truncates the output fuzzy set, and *prod* (product), which scales the output fuzzy set. In this example, the *min* method is used and the result is shown in Figure 7.4.

Step 4: Aggregation of all outputs

The rules need to be combined in order to make a decision using all outputs from the implication method. This is known as the aggregation method. The input to this aggregation process is the list of truncated output areas returned by the implication process for each rule. The output of the aggregation process is an aggregate output fuzzy set. In this example, the inputs to the aggregation method are a trapezoid indicated by the red background and 0 (Figure 7.4).

Step 5: Defuzzification

The input for the defuzzification process is a fuzzy set and the output is a single crisp number. The most popular defuzzification method is the centroid calculation, which returns the center of area under the aggregate output fuzzy set. For this example, the output is 77.8 (Figure 7.4)

7.3.2. Sugeno's Fuzzy Inference System

Sugeno's FIS is quite similar to Mamdani's FIS. The basic difference is that the crisp output consequence is not computed by clipping an output membership function based on the rule strength as in Mamdani's FIS. In fact, there is no membership function for an output variable in Sugeno's FIS. Instead, the output is a crisp number called a singleton, computed by multiplying the output of each rule by a constant and then adding up the results. A generic rule for Sugeno's FIS is as follows:

If x is A and y is B then Z=f(x,y)

where $z=f(x,y)$ is either a first order polynomial (known as a '1st-order Sugeno fuzzy model') or a constant (known as a 'zero-order Sugeno fuzzy model'). Figure 7.5 illustrates a zero-order Sugeno's FIS with the same inputs and rules used in the previous example. Two constants are taken for the outputs (Z): high (Z_1) = 100 and low (Z_2) =25. The rules can be written as:

- If PQ is short and $\Delta\varphi$ is small then the possibility of matching P on link AB is high ($Z1$=100).
- If PQ is long and $\Delta\varphi$ is large then t the possibility of matching P on link AB is low ($Z1$=25).

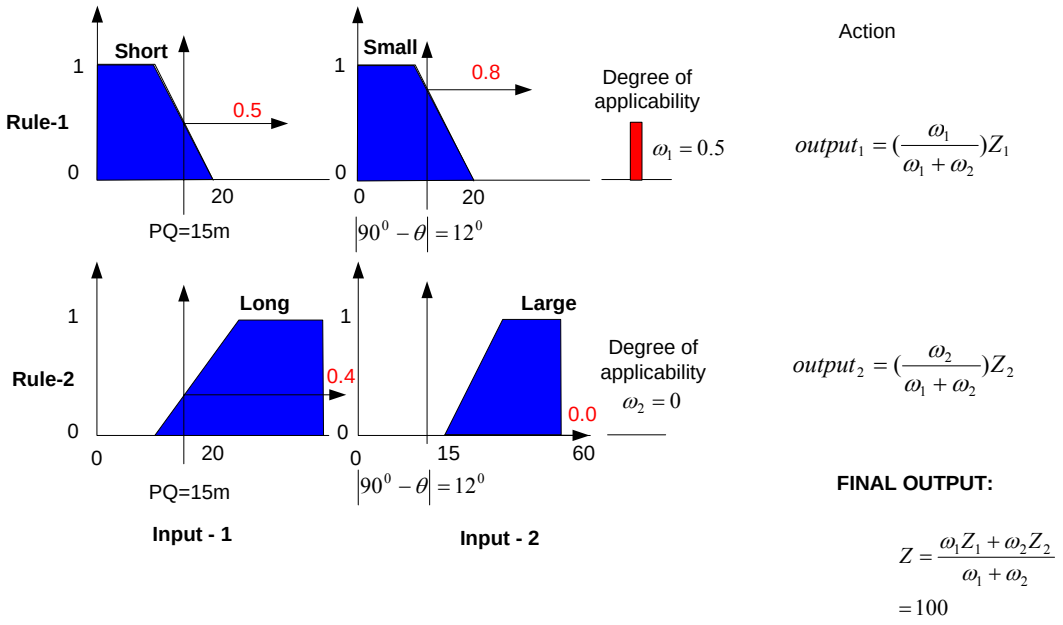

Figure 7.5: Sugeno's Fuzzy Inference System (FIS)

Rule strength in this FIS is referred to as the "degree of applicability" and the output is referred to as the "action" as shown in Figure 7.5. As can be seen, there is no output distribution, only a "resulting action" which is the weighted average of the rule strengths (degree of applicability) and the outputs (actions). The final output value is 100. This FIS usually needs a smaller number of rules as the output is already a linear function of the inputs rather than a fuzzy set (Abraham, 2001). Furthermore, the empirically chosen $f(x,y)$ can be optimized by a set of input/output data using the fuzzy logic toolbox of Matlab

(MathWorks, 2000). The Sugeno FIS is used in the further analysis presented in this chapter.

7.4. Map Matching Process

The fuzzy logic based map matching algorithm developed in this chapter has two stages: (1) the identification of the correct link and (2) the determination of the vehicle location on the selected link. These are explained below.

7.4.1. Identification of the Correct Link

Once again, identification of the actual link from among the candidates is the most challenging part of this algorithm. Therefore, a novel approach consisting of two distinct processes was developed for the identification of the correct link. The processes are: (1) the *initial map-matching process* (IMP) and (2) the *subsequent map-matching process* (SMP). Both of these processes are described below.

7.4.1.1. Initial map-matching process (IMP)

The selection of an initial link for the assignment of the initial position fix is known as the initial map-matching process (IMP). If an initial matching is incorrect then the subsequent matching will also be incorrect. Therefore, a sophisticated method is employed for the IMP. The IMP approach used in this research is a function of: the GPS receiver's time-to-first-fix (TTFF), the search space based on the error ellipse derived from the error variances (as explained in Chapter 6), the perpendicular distance from a position fix to the link, the bearing of the link, and the direction of the vehicle. A few first good position fixes on a link are used to identify the first link. This gives a level of confidence that the IMP is robust.

The IMP begins just after the initialisation of the GPS receiver which may take a minute or two after switching it on depending on its surrounding environments. The basic characteristic of the IMP is the use of an elliptical or rectangular confidence region around a position fix based on error models associated with GPS/DR. Road links that are within the confidence region are taken as the candidate links. If the confidence region does not contain any link, then it is assumed that the vehicle is off the known road links.

In such a situation, the measured GPS/DR position is used as the final location of the vehicle. In a situation where the confidence region contains only one segment, then the final selection process is very straightforward. In the case of more than one link, a fuzzy inference system (FIS) can be used to identify the correct link from among the candidate links.

The most important variables available during the IMP are the heading error (HE), which is defined as the absolute difference between the direction of the vehicle and the direction of the link, and the perpendicular distance (PD) from the position fix to the link. These two variables could be used as potential inputs to the FIS. However, the quality of the direction of vehicle data largely depends on the speed of the vehicle (Ochieng et al., 2004, and Taylor et al., 1999). Therefore, the speed of the vehicle could be used as an additional input to the FIS. The contribution of satellite geometry to the positioning error as determined by the horizontal dilution of precision (HDOP) could also be used as a quality indicator of the position fix.

Therefore, the state input variables of this FIS are: (1) the speed of the vehicle, *v* (m/sec), (2) the heading error, HE (degrees), (3) the perpendicular distance, PD (m), and (4) the HDOP. The speed of the vehicle can be obtained from GPS/DR and the fuzzy subsets associated with this variable are *zero*, *low* and *high*. The direction of the link is obtained from the spatial road network data and the direction of the vehicle is obtained from the GPS/DR. The fuzzy subsets related to the heading error are *small* and *large*. The PD is calculated as the minimum Euclidian distance between the position fix and the link. The fuzzy subsets associated with this variable are *low* and *high*. The HDOP could also be obtained from the GPS/DR and the fuzzy subsets are *good* and *bad*. The four system state input variables are fuzzified as shown in Figure 7.6. Z-shaped and S-shaped MFs are chosen in the fuzzification process. The single output of this FIS is the likelihood of matching the position fix to a link (denoted as *L1*). A zero-order Sugeno fuzzy model is considered which takes three constants for the output, *L1* e.g., *low (Z1)* = 10, *average(Z2)* = 50 and *high (Z3)* =100.

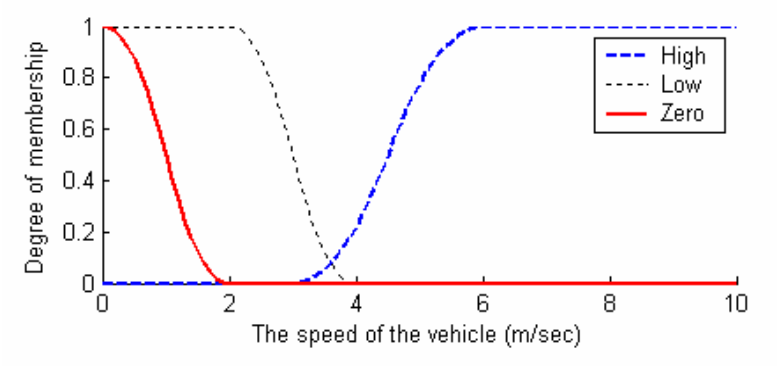

(a)

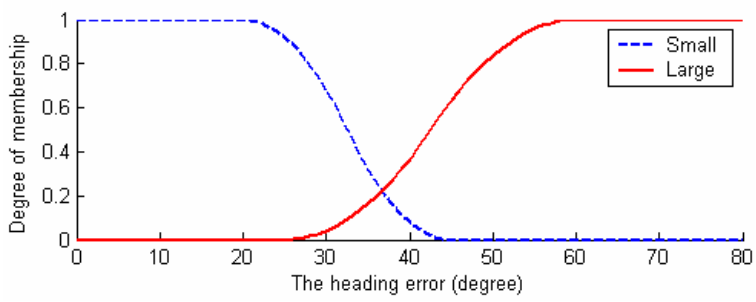

(b)

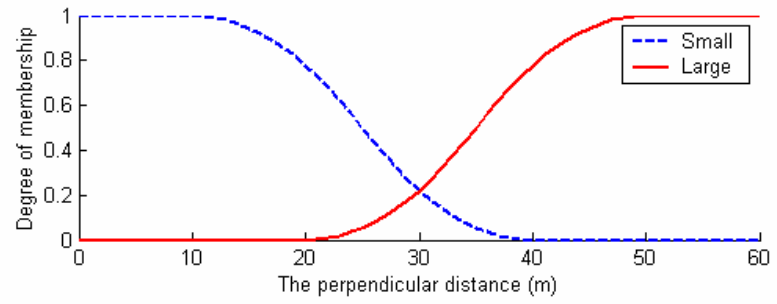

(c)

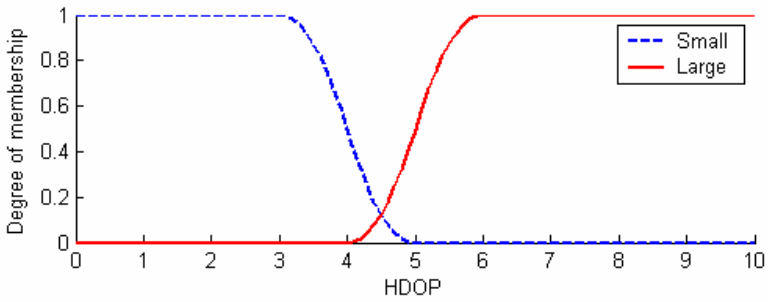

(d)

Figure 7.6: The fuzzification of (a) the speed of the vehicle, (b) the heading error, (c) the perpendicular distance, and (d) HDOP

The next step is to formulate the fuzzy rules which relate to each of the system state variables. The following six rules comprising the fuzzy knowledge are applied to this FIS. The weight of each rule is shown within the brackets at the end of each rule. Initially, a unit weight for each rule is considered.

- *If (v is high) and (HE is small) then (L1 is average) (1)*
- *If (v is high) and (HE is large) then (L1 is low) (1)*
- *If (HDOP is good) and (PD is short) then (L1 is average) (1)*
- *If (HDOP is good) and (PD is long) then (L1 is low) (1)*
- *If (HE is small) and (PD is short) then (L1 is high) (1)*
- *If (HE is large) and (PD is long) then (L1 is low) (1)*

The *min* (*minimum*) method is used to derive the "degree of applicability" (ω_i) of each fuzzy rule. The weighted average method, as shown in Figure 7.5, is used to obtain a crisp output. This crisp output is the likelihood associated with a link. The FIS is applied to all links within the confidence region. The link which gives the highest likelihood is taken as the correct link among the candidate links.

The above FIS is used to identify a link on which the vehicle is travelling. Since only a few inputs are available during the IMP, the link identified by the FIS for the first position fix may not be the actual link. Therefore, the IMP is performed for a few first good position fixes. If the FIS identifies the same link for those position fixes, then the link is chosen as a first correct link as illustrated in Figure 7.7.

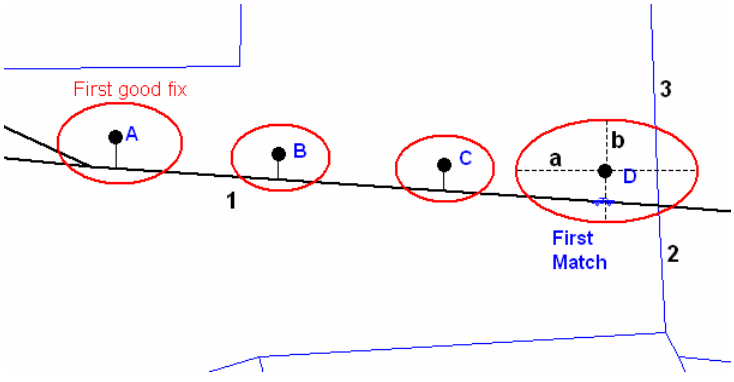

Figure 7.7: Example of initial map-matching process (IMP)

Suppose that the first good position fix from the GPS/DR is denoted by the point A (Figure 7.7). The FIS identifies link 1 as the correct link for this position fix. The FIS then identifies link 1 as the correct link for the subsequent position fixes B, C, and D. Therefore, it can be said with some confidence that the correct link for the position fix, D, is link 1.

7.4.1.2. The subsequent map-matching process (SMP)

After successfully implementing the IMP, the subsequent map-matching process (SMP) is used. The basic function of SMP is to match the position fixes following an initial match. Two types of SMPs are proposed: (1) SMP along a link (SMP-1) and (2) SMP at a junction (SMP-2). The purpose of SMP-1 is to match the subsequent position fixes to the link identified by IMP unless the vehicle is either about to cross or has already crossed a junction. The purpose of SMP-2 is to identify a new link among the candidate links at a junction for the last non-matched position fix. After identifying a new link using the SMP-2, the SMP-1 restarts to match the subsequent position fixes to the new link. Both of these processes are explained below.

SMP along a link (SMP-1)

In SMP-1 a Sugeno FIS is used to see whether the subsequent position fixes may be matched to the previously selected link. The SMP-1 is a function of the direction of the vehicle (θ), the gyro-rate reading ($\Delta\theta$), the distance along the link from the last matched position fix to the downstream junction ($d1$), and the speed of the vehicle (v).

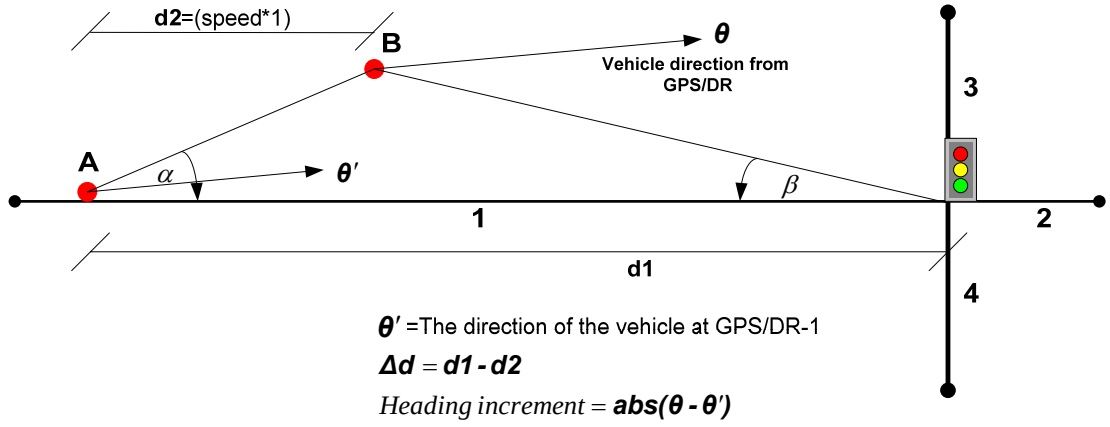

Figure 7.8: SMP along a link

Figure 7.8 shows the state variables of the vehicle travelling on a link. Point A represents the last matched vehicle position on link 1 which was identified by IMP (or SMP-2). Therefore, the task of SMP-1 is to select the correct link for the subsequent position fix, B. The term *d1* refers to the distance from the last matched vehicle position to the downstream junction and *d2* refers to the distance travelled by the vehicle within the last second which can be calculated from vehicle speed at B. The difference between these two distances i.e., $\Delta d = (d1\text{-}d2)$ can be used to see whether the vehicle crosses a junction. For example, if the Δd is negative, then it is most likely that the vehicle has already crossed the junction. The α and β define the location of the position fix, B, relative to link 1. If both of these angles are less than 90^0, then it is more likely that the vehicle has not crossed the junction. The angles θ and θ' indicate the directions of the vehicle at B and A respectively. The absolute difference between these two angles i.e., $abs(\theta - \theta')$ gives a heading increment (*HI*) at B for the last epoch. The lower the heading increment the higher is the possibility that the vehicle is still on link 1. If the *HI* is close to zero, then it is very likely that there has been left or right turn. In addition, the gyro-rate reading at B, which is the rate of change of heading for the last epoch, can also be used to see whether there has been a left or right turn in progress.

Therefore, the fuzzy variables of this FIS are: (1) the speed of the vehicle, *v* (m/sec) (2) the heading increment (*HI*) (degree) (3) the gyro-rate reading, $\Delta\theta$ (deg/sec) (4) the Δd (m) (5) the value of α (degree) (6) the value of β (degree), and (7) the HDOP. The single output of this FIS is denoted as *L2* and is the possibility of matching the current point (in this example case, B) on the previously identified link (in this example case, link 1) denoted by *L2*. The fuzzification of the state input variables are shown in Figure 7.9. *Z*-shaped, *S*-shaped and *gauss* MFs (for the 180^0 heading increment) are used in the fuzzification process. A zero-order Sugeno fuzzy model is considered which takes three constants for the output *L2* e.g., *low(Z1)* = 10, *average(Z2)* = 50 and *high(Z3)* =100.

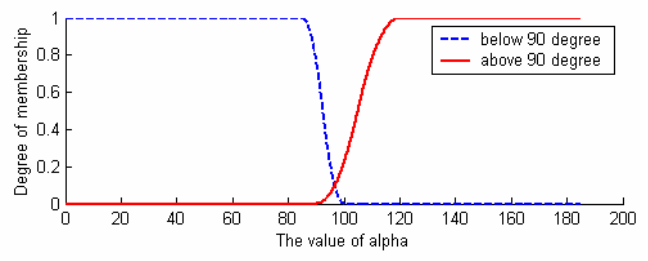

(a)

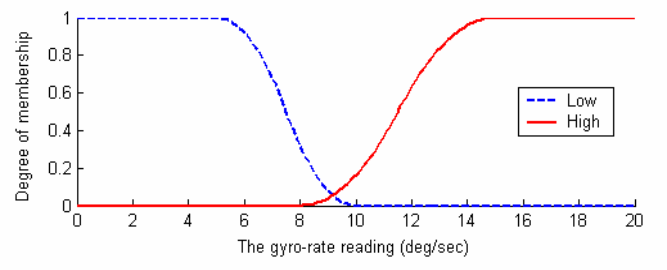

(b)

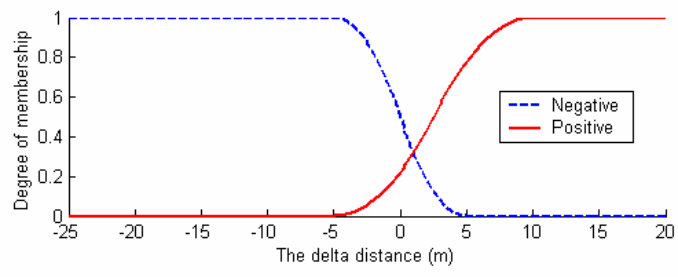

(c)

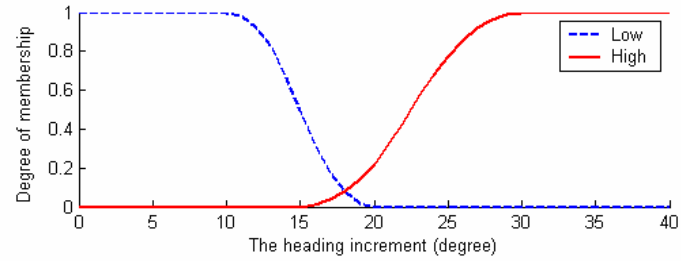

(d)

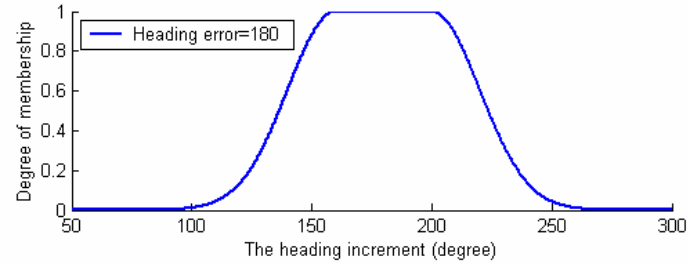

(e)

Figure 7.9: The MFs for (a) the α or β, (b) the gyro-rate reading, (c) the Δd, (d) the heading increment, and (e) a 180 degree heading increment

The following rules are applied to this FIS:

- *If ($\Delta\theta$ is small) and (α is below 90^0) and (β is below 90^0) then (L2 is high) (1)*
- *If ($\Delta\theta$ is small) and (Δd is positive) and (α is above 90^0) then (L2 is low) (1)*
- *If ($\Delta\theta$ is small) and (Δd is positive) and (β is above 90^0) then (L2 is low) (1)*
- *If (HI is small) and (α is below 90^0) and (β is below 90^0) then (L2 is high) (1)*
- *If (HI is small) and (Δd is positive) and (α is above 90^0) then (L2 is low) (1)*
- *If (HI is small) and (Δd is positive) and (β is above 90^0) then (L2 is low) (1)*
- *If ($\Delta\theta$ is high) and (α is below 90^0) and (β is below 90^0) then (L2 is low) (1)*
- *If (HI is large) and (α is below 90^0) and (β is below 90^0) then (L2 is low) (1)*
- *If (HDOP is good) and (v is zero) then (L2 is high) (1)*
- *If (HDOP is good) and (Δd is negative) then (L2 is average) (1)*
- *If (HDOP is good) and (Δd is positive) then (L2 is low) (1)*
- *If (v is high) and (HI is small) then (L2 is average) (1)*
- *If (HDOP is good) and (v is high) and (HI is 180^0) and ($\Delta\theta$ is high) then (L2 is high) (1)*

A threshold output value can be used to determine whether the position fix should match with the previously selected link. The threshold value can be derived empirically by applying the FIS to a given (true) input/output dataset.

SMP at a junction (SMP-2)

The SMP-2 begins when the vehicle is either about to cross or has just crossed a junction. A new link is determined among the candidate links using the same FIS described in IMP. However, two more input variables are available at this moment. These are the link connectivity and the distance error as shown in Figure 7.10.

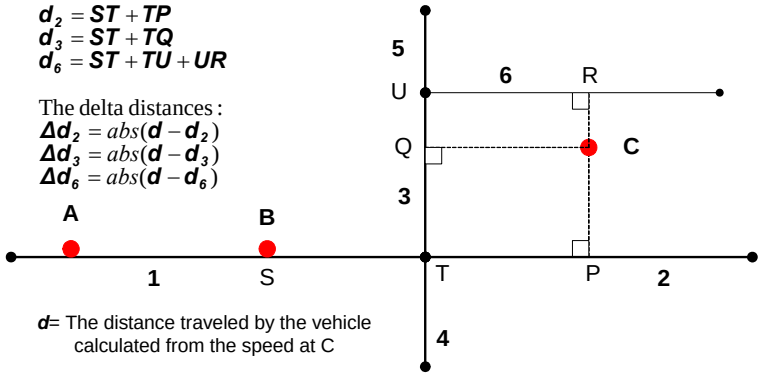

Figure 7.10: SMP at a junction

Suppose that the vehicle is travelling on link 1. The last map-matched position on that link is S. The task of SMP-2 is to select a new link for the position fix, C, as the vehicle has already crossed the junction. The candidate links for this position fix are 2, 3 and 6. Since the location of the vehicle at the previous epoch is on link 1, link connectivity helps to identify the correct link. For example, there is no direct connection between links 1 and 6. Therefore, it is unlikely that the vehicle is on link 6 for the position fix C. The term d refers to the distance travelled by the vehicle within the last second which can be calculated from the speed of the vehicle at C. The d_2, d_3, and d_6 represent the shortest paths travelled by the vehicle if the vehicle is on links 2, 3 and 6 respectively. The difference between d and d_2 (or d_3 or d_6) is the distance error associated with each link as shown in Figure 7.10. The distance error is an input to the FIS. For example, the link which gives the lowest distance error is a strong candidate for the correct link. The two additional state input variables are fuzzified as shown in Figure 7.11. The output variable of this FIS is the likelihood of matching to a link (*L3*). A zero-order Sugeno fuzzy model is again considered which takes three constants for the output *L3,* e.g., *low (Z1)* = 10, *average (Z2)* = 50 and *high (Z3)* =100.

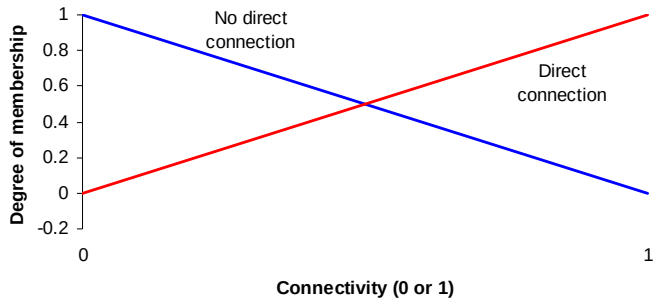

(a)

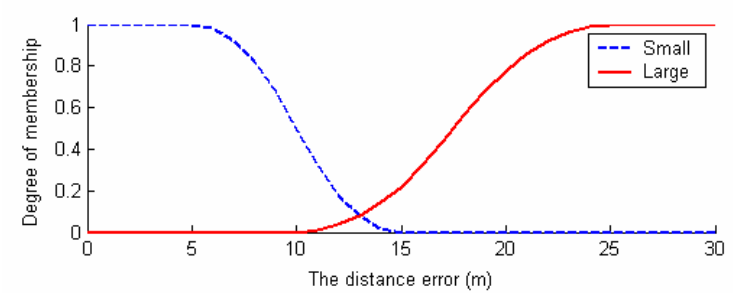

(b)

Figure 7.11: The MFs for (a) the link connectivity, and (b) the delta distance

Ten rules are used for this FIS. The first six rules are the same as presented in the FIS of IMP. The rest of the rules are given below.

- *If (The connectivity with the previous link is low) then (The L3 is low) (1)*
- *If (The connectivity with the previous link is high) then (The L3 is high) (1)*
- *If (The distance error is low) then (The L3 is high) (1)*
- *If (The distance error is high) then (The L3 is low) (1)*

The FIS is applied to all links within the error region and the link which gives the highest likelihood value is taken as the correct link.

7.4.1.3. Optimising fuzzy membership functions

The basic structure of the FIS described in the IMP and the SMP is a model that maps input characteristics to input MFs, input MFs to rules, rules to a set of output characteristics, output characteristics to output MFs, and finally output MFs to a single-valued (crisp) output or a decision associated with the output. However, the fuzzy MFs

used in all the FIS described are fixed and chosen empirically based on the interpretation of the characteristics of the variables in the model. The MFs can be optimized using a true input/output data set. The fuzzy logic toolbox of Matlab (MathWorks, 2000) has facilities which can easily optimize fuzzy MFs using an Adaptive Neuro Fuzzy Inference System (ANFIS).

The toolbox function, ANFIS, constructs an FIS using a given input/output data set whose membership function parameters are tuned (i.e., adjusted). The technique used to do this is very simple. ANFIS uses either a back-propagation algorithm alone or in combination with a Least-Squares type of method. This allows FIS to learn from the data it is modelling. The limitations of ANFIS identified by MathWorks (2000) are:

- Only supports Sugeno FIS
- Only supports first or zero order Sugeno-type systems (linear or constant output membership functions)
- Single output
- Unit weight for each rule

A detailed description of this method can be found in MathWorks (2000).

7.4.2. Determination of the Vehicle Location on the Selected Link

The location of the vehicle on a link is estimated using the optimal estimation technique described in Chapter 6 (section 6.2.2) in which the optimal easting ($\hat{e}$) and northing ($\hat{n}$) coordinates for a particular epoch are expressed as

$$\hat{e} = \left(\frac{\sigma^2_{gps,e}}{\sigma^2_{map} + \sigma^2_{gps,e}}\right) e_{map} + \left(\frac{\sigma^2_{map}}{\sigma^2_{map} + \sigma^2_{gps,e}}\right) e_{gps} \qquad \textbf{(7.5)}$$

$$\hat{n} = \left(\frac{\sigma^2_{gps,n}}{\sigma^2_{map} + \sigma^2_{gps,n}}\right) n_{map} + \left(\frac{\sigma^2_{map}}{\sigma^2_{map} + \sigma^2_{gps,n}}\right) n_{gps} \qquad \textbf{(7.6)}$$

where σ^2_{map} is the error covariance associated with map data, $\sigma^2_{gps,e}$ and $\sigma^2_{gps,n}$ are the easting and northing components of the error covariance associated with the navigation sensor. The error variance associated with $\hat{e}$ can now be expressed as

$$\frac{1}{\sigma^2_{mm,e}} = \frac{1}{\sigma^2_{map}} + \frac{1}{\sigma^2_{gps,e}} \quad \textbf{(7.7)}$$

where $\sigma^2_{mm,e}$ is the error variance associated with optimal estimation of $\hat{e}$.

7.4.3. Algorithm Step-by-Step

The two basic steps of this map matching algorithm are the initial map-matching process (IMP) and the subsequent map-matching process (SMP). The SMP has two stages: (1) SMP along a link and (2) SMP at a junction. Following the SMP, the position on the selected link is estimated using an optimal estimation technique described in Chapter 6 (section 6.2.2).

7.4.3.1. Steps involved in IMP

The most important part of the fuzzy logic map matching algorithm is the IMP. This is achieved by the following steps:

- Search for a good position fix after the receiver has acquired an initial position. This will normally take from a few seconds to 100 seconds depending on the surrounding environment, especially when the vehicle starts travelling from a cold-start of the receiver.
- Obtain the necessary inputs (such as an error ellipse, HDOP, the speed of the vehicle, the direction of the vehicle, the azimuth of the link, and the perpendicular distance from the position fix to the link) to implement a fuzzy inference system.
- Fuzzify input variables using their MFs. The single output variable is the likelihood (*low, average, and high*) associated with each link.
- Formulate fuzzy knowledge-based IF-THEN rules.
- Use Sugeno's FIS as described in section 7.3.2.
- Optimize all MFs based on a true input/output data set using the Fuzzy Logic toolbox of Matlab (MathWorks, 2000)

- Identify a link which gives the highest likelihood. This is considered as the correct link for the position fix.
- Continue steps 2 to 5 for the next few position fixes. If the algorithm selects the same link for these subsequent position fixes, then it is assumed to be the first correct link for these position fixes as shown in Figure 7.7. In order to achieve such a circumstance, the vehicle must travel on a link for a few seconds. Although the algorithm may then take a few seconds to obtain the first match, this gives a good level of confidence that the IMP is robust.
- Use a perpendicular projection from the position fix to the selected link to locate the vehicle on the link. It should be noted that the equations (7.5) and (7.6) cannot be used to locate the vehicle during IMP as the initial location of the vehicle is unknown.

7.4.3.2. Steps involved in SMP

The performance of the SMP largely depends on the performance of the IMP. The SMP has two stages: (1) SMP along a link and (2) SMP at a junction.

SMP along a link (SMP-1):

This describes how to match the subsequent position fixes just after IMP or SMP at a junction. The steps associated with this approach are:

- Acquire the essential inputs (as discussed in section 7.4.1.2) to implement a Sugeno FIS.
- Fuzzify all inputs using their *MF*s. The single output of this FIS (*L2*) is the possibility of matching the current position fix on the previously identified link.
- Formulate fuzzy knowledge-based IF-THEN rules.
- Use a Sugeno FIS as described in section 7.3.2.
- Optimize all *MF*s based on a true input/output data set using the Fuzzy Logic toolbox of Matlab (MathWorks, 2000).
- Derive a threshold value for *L2*. This can be achieved from the same true input/output data set used in the previous step. If the value of *L2* is higher than the specified threshold, then the position fix can be matched to the formerly

identified link. Otherwise, the algorithm assumes that the vehicle is near to a junction and SMP at a junction (SMP-2) needs to be applied.

SMP at a junction (SMP-2):

The purpose of this procedure is to identify the correct link when the vehicle travels through a junction. The following steps are involved:

- Attain the required input variables (as described in section 7.4.1.2) to implement a Sugeno FIS.
- Fuzzify input variables using their *MF*s. The single output variable is the likelihood (*L3*) associated with each link.
- Formulate fuzzy knowledge-based IF-THEN rules.
- Use a Sugeno FIS as described in section 7.3.2.
- Optimize all *MF*s based on a true input/output data set using the Fuzzy Logic toolbox of Matlab (MathWorks, 2000).
- Identify a link which gives the highest *L3*. This is considered as the new correct link for the position fix.

7.5. Algorithm Testing

The fuzzy logic map matching algorithm developed in this chapter was tested using the real data described in Chapter 5 (section 5.6). The algorithm was tested using the navigation data from GPS/DR and the digital map data from a map of scale 1:2500. The test was conducted for various scenarios with different network characteristics and with different traffic manoeuvres. Only a complex roundabout with a diverging motorway (Figure 7.12) and a complex urban road network (Figure 7.13) are shown here as an example. Chapter 9 describes the results for all other road networks. Each of the blue round dots in the Figure 7.12 and 7.13 represents the vehicle position before map matching. The arrow symbols in the figures show the path followed by the vehicle on the network. Each of the triangular symbols on the road segments represents the vehicle position after map matching.

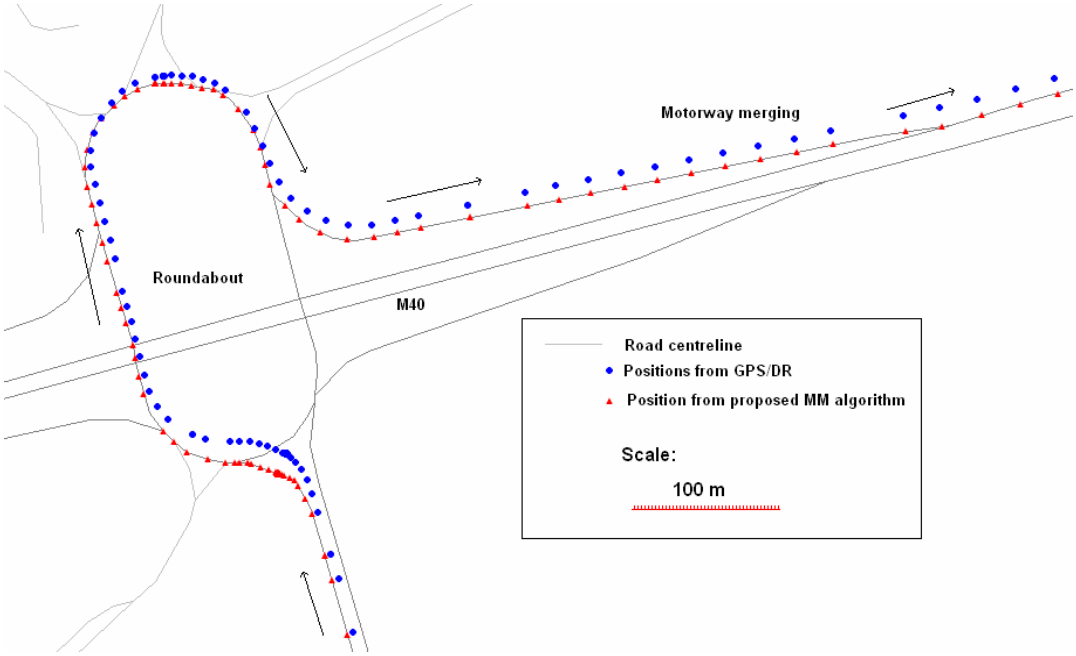

Figure 7.12: Map matching results for a part of test network which includes a roundabout and a motorway merging

A threshold value of 60 for the likelihood L2 (the output of FIS in SMP-1) was found to be adequate to identify whether the vehicle position should match with the previously selected road segment. This threshold value was empirically determined from a true input/output dataset. The MFs of all input variables was also trained and modified with the same input/output dataset using the fuzzy logic toolbox of Matlab (MathWorks, 2000). The position of the vehicle on a selected road segment was estimated using equations (7.1) and (7.2).

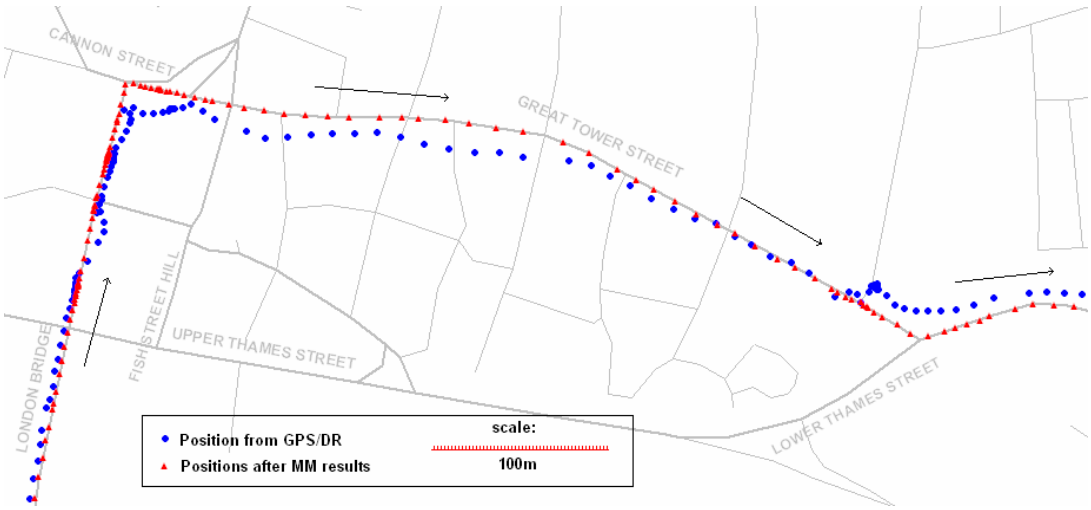

Figure 7.13: Map matching results for a part of test route in dense urban streets

The results showed that the fuzzy logic-based map matching algorithm identified 4570 links correctly out of 4605 total links. A fuller description of the results in terms of link identification and location determination can be found in Chapter 9.

7.6. Summary

A fuzzy logic map matching algorithm was presented in this chapter. The factors considered to build various knowledge-based IF-THEN rules were the speed, heading and historical trajectory of the vehicle, the connectivity and the orientation of the links and the satellite geometric contribution to the positioning error (HDOP). A zero-order Sugeno-type FIS was used to develop the algorithm. The membership functions were trained and modified by Matlab's ANFIS using a given input/output dataset. A discussion on how to effectively implement the developed algorithm was presented in section 7.4.3. The algorithm was then tested in two different road networks with varying complexity. These included complex roundabouts, merging or diverging sections of a motorway and complex road networks. The inputs to the map matching algorithm were taken from an integrated navigation system (GPS/DR) in order to attain vehicle location data continuously.

The next chapter will describe the validity and integrity of the map matching algorithms developed in this research.

CHAPTER 8

VALIDITY AND INTEGRITY

8.1 Introduction

Three different map matching algorithms are developed and tested in the preceding chapters. They are the topological map matching algorithm (Chapter 5), the probabilistic map matching algorithm (Chapter 6), and the fuzzy logic map matching algorithm (Chapter 7). Due to errors associated with the positioning data and the digital map data as (described in Chapter 3), there is always a level of uncertainty associated with map matching algorithms. Therefore, it is essential to measure the quality (level of confidence) of map matching and detect anomalies in map-matched locations. This can be achieved by calculating the "*integrity"*, which represents the level of trust that can be placed in the information provided by the map matching algorithm for each position. Moreover, it is also necessary to evaluate the overall accuracy of map matching algorithms in order to estimate their performance. This can be attained by "*validity"* which is concerned with how well the map matching algorithms measure what they are intended to measure. "*Validity"* here refers to overall algorithm performance characterisation; while *"integrity"* will clearly be required for each position fix in real-time. This chapter describes both the *"validity"* and *"integrity"* of map matching algorithms.

This chapter is organised as follows. First, a description of the validity of a map matching algorithm is provided. This is followed by a description of the basic principles of high precision positioning using the carrier-phase observable from GPS. After that, the proposed generic validation methodology for map matching algorithms is presented, followed by the application of the validation technique to a map matching algorithm. The following section describes the integrity of a map matching algorithm including the definition of integrity, the factors affecting the integrity of a map matching algorithm, and

the derivation of a metric to quantify integrity. This is followed by the application of the metric to the new map matching algorithms.

8.2 Validation of Map Matching Algorithms

A "reliable" method should give consistent results in different applications. Consistency, however, says nothing about being right or wrong (Kelly, 1996). The "rightness" or "truth value" of measurements is an issue of validity. Validity is always subject to human judgment as it asks the question, "Does this algorithm (or device or method) measure what it is said (or claimed) to measure?" (Westmeyer, 1981). According to Joppe (2000), "*Validity determines whether the system truly measures that which it was intended to measure or how truthful the research results are. In other words, does the research instrument allow you to hit "the bull's eye" of your research object? Researchers generally determine validity by asking a series of questions, and will often look for the answers in the research of others".*

A map matching algorithm needs to be validated in order to derive any statistics on its performance. For instance, it could be concluded that map-matched locations of a vehicle determined from the map matching algorithms are within 8m (2D, 95%) of the true positions. To derive such a result, the outputs of a map matching algorithm must be compared with a higher accuracy reference (truth) of the vehicle trajectory. Therefore, in this research algorithm validation is based on using a higher accuracy reference (truth) of the vehicle trajectory as determined with the high precision carrier-phase observables from GPS. The validation results of all three map matching algorithms developed in this research are presented in Chapter 9 in more detail.

8.2.1 High Precision Positioning

The basic GPS observations used for positioning are pseudoranges from the code measurements (C/A code and P code) and carrier phases (L1 and L2). The P-code is used to support the Precise Positioning Service (PPS) (2σ, 10-20 m) and the C/A code the Standard Positioning Service (SPS) (2σ, 20-30 m). For security concerns the P-code is encrypted (downgraded) to the Y-code so that only authorised users can access the code. This is known as Anti-spoofing (A-S). On the other hand, positioning solutions using carrier phase measurements give a positioning accuracy at the centimetre level (Leick,

2004). This section describes GPS carrier phase observables used in high precision positioning through differential processing of observations.

8.2.1.1 The carrier phase observable

The signals transmitted by GPS satellites consist of two carrier waves (L1 and L2). The L1 carrier has a frequency of 1575.42 MHz and a wavelength of 19 cm. The L2 carrier has a frequency of 1227.60 MHz and a wavelength of 24 cm.

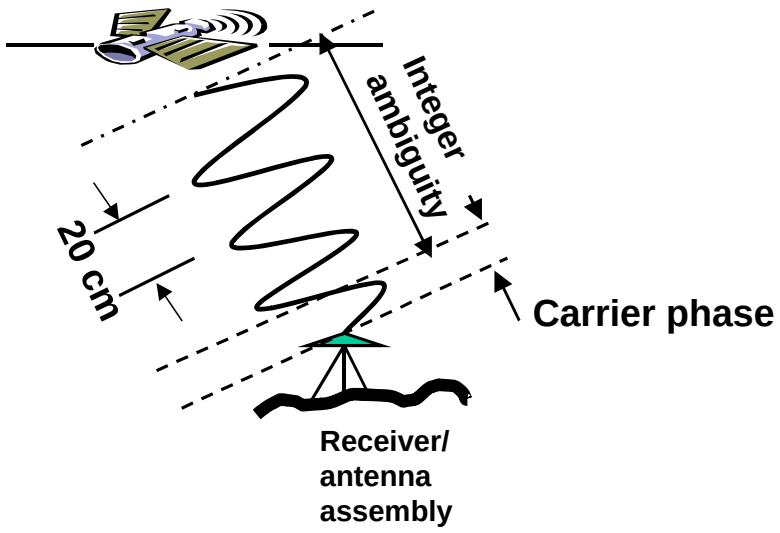

Figure 8.1: Carrier-phase and integer ambiguity

The carrier phase observable is derived from the measurement of the difference between the phase of the signal arriving from the satellite, and the phase of the signal generated locally at the receiver. The direct measurement consists of a phase reading of the fractional part of the whole (integer) number of cycles in the range between the satellite and the receiver (Figure 8.1). Unfortunately, the receiver has no knowledge of the number of whole wavelengths at lock-on (either at the start or after loss of lock) but keeps count of the integer number of wavelengths to be added or subtracted as the receiver to satellite range changes. The unknown whole number of cycles is referred to as integer ambiguity must be resolved in order to determine the range between the receiver and the satellite.

The pure carrier phase observation equation is expressed as follows (Leick, 2004):

$$\Phi_i^p = \rho_i^p + c(\frac{N_i^p}{f_c}) + c\delta_{i,clock} + c\delta_{clock}^p - I_i^p + T_i^p + \delta_{i,orbit}^p + \delta_{i,multipath}^p + \varepsilon_{i,\Phi}^p \quad (8.1)$$

in which $N_i^p = \overline{N}_i^p + (\phi_i - \phi^p)$

where,

Φ_i^p is the measured carrier phase from the i^{th} receiver to p^{th} satellite (m)

ρ_i^p is the geometric distance between the i^{th} receiver to p^{th} satellite in an Earth Centred Inertial (ECI) system (m)

$\overline{N}_i^p$ integer valued ambiguity term (cycles)

ϕ_i initial phase at i^{th} receiver (cycles)

ϕ^p initial phase at p^{th} satellite (cycles)

c speed of light in vacuum (299,729,458 m/sec)

$\delta_{i,clock}$ receiver clock error (m)

δ_{clock}^p satellite clock error (m)

I_i^p range delay due to inospheric refraction (m)

T_i^p range delay due to tropospheric refraction (m)

$\delta_{i,orbit}^p$ satellite orbit error (m)

$\delta_{i,multipath}^p$ multipath delay (m)

f_c carrier frequency (L1=1575.42 MHz, L2=1227.6 MHz)

$\varepsilon_{i,\Phi}^p$ phase measurement noise (m)

The need to determine the integer ambiguity arises from the desire to use carrier phase ranges in the user position solution instead of pseudo-ranges. The use of carrier phase ranges results both in improved accuracy and precision. This improvement is largely due

to different effects of some of the errors that affect the observables. The improvement in precision is mainly due to the difference in the effect of receiver thermal noise on the carrier phase and code phase measurement errors. Improvement in accuracy is the direct result of the effect of multipath errors which are proportional to the wavelength of the signal. With the exception of the multipath bias and ionospheric delay bias which affect code (pseudorange) and carrier phase measurements in an equal but opposite sense, all other measurement biases associated with pseudoranges have an identical affect on the carrier phase range. Hence, well established principles and techniques used to reduce these biases in pseudorange measurements can be applied to carrier phase measurements to allow an accurate resolution of the integer ambiguities. After the treatment of the biases arising from satellite navigation errors, the only unknown that remains in the derivation of the range between the satellite and receiver from carrier phase measurements is the determination of the integer ambiguity.

During the last decade effort has been mainly focused on the use of GPS dual-frequency for a faster and more accurate determination of the integer ambiguity. The modernization of the GPS, primarily through the implementation of a new publicly available PRN ranging code on the L2 signal (known as L2C) and a new civilian signal at the L5 frequency of 1176.45 MHz, and the advent of Galileo will together lead to a *multi-frequency* civil GNSS (a constellation with 24 GPS and 27 Galileo satellites) which will enhance the capability of resolving the carrier phase ambiguities significantly (Tiberius et al., 2002)**.**

Carrier phase data processing is usually carried out in relative mode, between a static receiver at a known location and another receiver that is either static or moving. The effect of relative positioning (for limited baseline lengths) is to eliminate common errors and to significantly reduce other errors. The most commonly used observable in the relative mode is the double differenced (DD) observable where the satellite clock and receiver clock errors are eliminated and satellite orbit and atmospheric errors are largely reduced.

8.2.1.2 Differential carrier phase GPS

The single difference (SD), double difference (DD), and triple difference (TD) are most commonly used differencing techniques in the literature (e.g., Sauer, 2004; Hoffmann-Wellenhof et at., 1997; Leick, 2004). The SD observables are obtained either between

one satellite and two receivers (across receivers) or between one receiver and two satellites (across satellites) at the same epoch. The DD is obtained from differencing between two SD's. The TD involves differencing across receivers, across satellites, and across time. Out of these, the DD is the one usually adopted for high precision positioning applications due to consideration of the noise level and the number of observations. The DD differencing technique is therefore used in this study.

The SD between the satellite *p* and the receivers *i* and *j* can be expressed as:

$$\Delta\Phi_{i,j}^{p} = \Phi_{i}^{p} - \Phi_{j}^{p} \qquad \textbf{(8.2)}$$

The SD between the satellite *q* and the receivers *i* and *j* can be expressed as:

$$\Delta\Phi_{i,j}^{q} = \Phi_{i}^{q} - \Phi_{j}^{q} \qquad \textbf{(8.3)}$$

The satellite clock error of satellite *p* is removed by differencing across receivers *i* and *j* when the corresponding pure carrier phase observation equations (8.1) are substituted into equation (8.2), the satellite clock error of satellite *q* is removed by differencing across receivers *i* and *j* as can be seen in equation (8.2). These two above SDs can be combined to obtain a DD which is given by

$$\Delta\Phi_{i,j}^{p,q} = \Delta\Phi_{i,j}^{p} - \Delta\Phi_{i,j}^{q} \qquad \textbf{(8.4)}$$

From equations (8.1), (8.2), and (8.3), equation (8.4) can be rewritten as:

$$\Delta\nabla\Phi_{i,j}^{p,q} = \rho_{i,j}^{p,q} + c(\frac{N_{i,j}^{p,q}}{f_c}) + I_{i,j}^{p,q} + T_{i,j}^{p,q} + \delta_{multipath} + \varepsilon_{\Phi} \qquad \textbf{(8.5)}$$

in which

$\rho_{i,j}^{p,q} = (\rho_i^p - \rho_j^p) - (\rho_i^q - \rho_j^q)$, $N_{i,j}^{p,q} = (N_i^p - N_j^q) - (N_i^q - N_j^q)$

$I_{i,j}^{p,q} = (I_i^p - I_j^p) - (I_i^q - I_j^q)$, $T_{i,j}^{p,q} = (T_i^p - T_j^p) - (T_i^q - T_j^q)$

$\delta_{multipath} = (\delta_{i,multipath}^{p} - \delta_{j,multipath}^{p}) - (\delta_{i,multipath}^{q} - \delta_{j,multipath}^{q})$,

$\varepsilon_{\Phi} = (\varepsilon_i^p - \varepsilon_j^p) - (\varepsilon_i^q - \varepsilon_j^q)$

Since equation (8.5) is a differencing across satellites and across receivers, both the receiver clock error and the satellite clock error are eliminated and other errors are reduced. Integer ambiguity (in this case, the DD-ambiguity, $N_{i,j}^{p,q}$) still needs to be resolved.

The real-time availability of precise GPS satellite orbit and clock data has facilitated the development of a novel positioning technique known as Precise Point Positioning (PPP) (Heroux et al., 200; Shen and Gao, 2002). PPP, which is a new area of research in the field of positioning and navigation, is based on the processing of un-differenced pseudorange and carrier phase observations from a single GPS receiver. It has the potential to provide global position accuracy at the level of decimetres to centimetres in stand-alone kinematic and static modes. A number of researchers and institutions around the world are developing models for predicting ephemeris and satellite clock correction, which would help to make the real-time PPP possible. However, the PPP method is not yet available and hence cannot apply in this research.

8.2.1.3 Ambiguity resolution

The key to the use of the carrier phase observables is the correct determination of integer ambiguity. As long as the connection between the receiver and the satellite is not broken, integer ambiguity remains constant while the fractional phase which changes over time can be measured by the receiver. The loss of signal lock between a GPS satellite and a receiver is referred to as 'cycle slip'. If signal lock is re-established, a new ambiguity exists and must be solved for separately from the original ambiguity. The complexity of ambiguity determination depends on the type of application e.g., whether the positioning mode is static or kinematic. A fuller description of ambiguity determination can be found in Sauer (2004). In this research kinematic positioning with carrier-phase data is used to determine the vehicle trajectory using the SkiPro GPS post-processing software™ by Leica Geosystems AG (2001). The key processing parameters used by SkiPro are elevation cut-off angle, standard models for compensations of tropospheric and ionospheric biases, baseline length, and precise ephemeredes or broadcast ephemeredes for the computation of satellite positions.

Unsuccessful ambiguity resolution, when passed unnoticed, may lead to unacceptable errors in the positioning results. Normally, when processing an individual baseline, two

types of double differenced solutions result. One is a float solution in which the ambiguities are solved as real numbers, instead of integers, and the other is a fixed solution in which the ambiguities are fixed by basically exploring those integers close to the float solution of the ambiguities. Under normal circumstances, a fixed solution is better than a float solution. In open spaces and in static positioning, a fixed solution should be routine. However, float solutions cannot be avoided in kinematic positioning, especially in built-up urban areas. The variance-covariance matrix of the least squares estimation of the ambiguities contains the information necessary to infer the quality and reliability of ambiguity estimation. The SkiPro GPS post-processing package gives a number of quality indicators for each position estimate, including the variance from the variance-covariance matrix. A threshold value for the standard deviation of the horizontal positioning can be used to select the float solution position estimates to use as reference or truth alongside ambiguity fixed position estimates.

8.2.2 Methodology for Validation

The input to map matching algorithms is the positioning data (easting, northing), speed, heading, and error variances obtained either from GPS or GPS/DR. The output of a map matching algorithm is the link on which the vehicle is travelling and the physical location of the vehicle on that link. In order to validate the results of a map matching algorithm, a higher accuracy reference (truth) of the vehicle trajectory is essential. The reference of the vehicle trajectory is determined by the carrier phase observables from GPS with a high degree of precision as explained in the previous section. From this reference trajectory, the actual (truth) link on which the vehicle is travelling and the correct physical location (at the centimetre level) of the vehicle on that link are then determined.

The methodology used to validate the algorithm is to compare the results (both the identification of the link and the physical location of the vehicle) obtained from the map matching algorithm and the reference trajectory obtained from the carrier phase observables. Since the location data used in the map matching algorithms and the reference trajectory are obtained from two different receivers, time synchronization is a crucial issue. This can be resolved if both sensors are based on the same time reference, such as, GPS time or Coordinated Universal Time (UTC). It should be noted that GPS time is 13 seconds ahead of UTC in 2004. Once time synchronization is achieved between the receivers, the comparison can be performed.

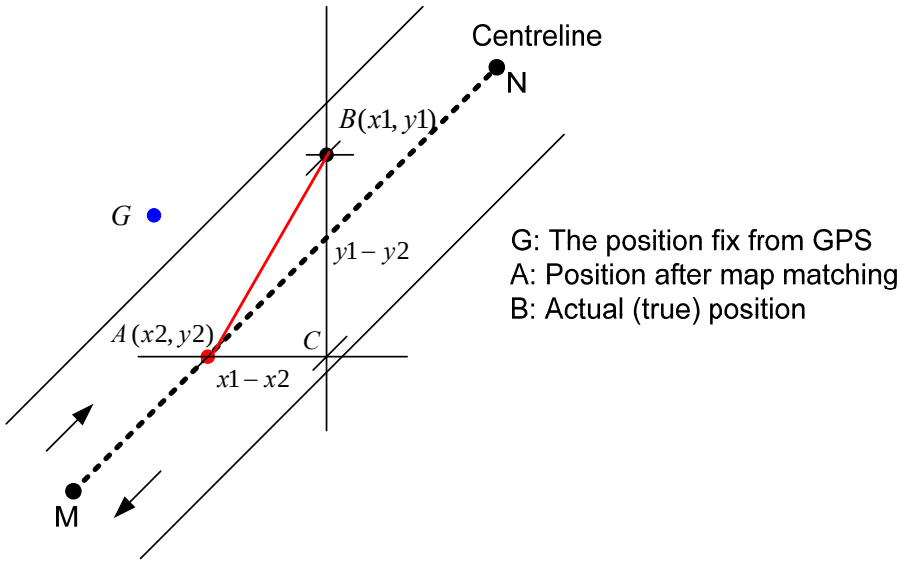

Figure 8.2: Determination of error in map matching

Figure 8.2 shows a road segment in which the vehicle position from GPS (C/A code-ranging) is denoted by the point G, the corresponding position estimated using the map matching algorithm (on the road centreline) is represented by the point A (x2, y2) and the true position of the vehicle from GPS (carrier-phase observable) is indicated by the point B (x1, y1) for a particular epoch *t*. Since the actual position of the vehicle at epoch *t* is at the point B, the error in the easting coordinate is AC and the error in the northing component is BC. Assuming a plane rectangular Cartesian coordinate system, the horizontal error at epoch *t* (HE_t) is given by

$$HE_t = \sqrt{(x1 - x2)^2 + (y1 - y2)^2} \qquad \textbf{(8.6)}$$

A series of such horizontal errors can be derived using equation (8.6) for all epochs. The associated statistics derived from these errors (e.g., mean, standard deviation) can be used to determine the relative performance of the map matching algorithms.

Most of the road network map data contains only road centreline information. In this case map matching algorithms use the centreline of the road segment as a reference and subsequently match the vehicle location to it. Since the vehicle's actual position is not always constrained to be on the road centreline, it is necessary to calculate the bias introduced by the algorithm from matching the vehicle position on the road centreline.

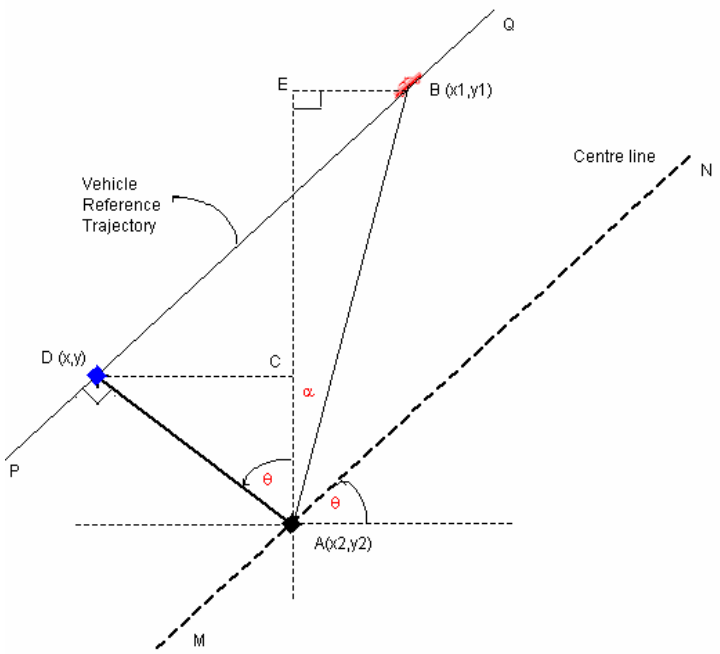

Figure 8.3: Bias introduced by matching on road centreline

In Figure 8.3, the line MN represents a road centreline on which the map matching process matches a vehicle position to point A(x2, y2) at a particular epoch *t*. The corresponding true position of the vehicle at the same epoch is at point B(x1, y1). Line PQ (parallel to line MN) is drawn through point B. Point A is then perpendicularly projected onto line PQ. Therefore, the final location of the vehicle position is at D (x, y) on the line PQ. Now the task is to determine the new easting, x, and northing, y, coordinates of the point D.

The new easting coordinate is given by

$$x = x2 - CD = x2 - AB\cos(\theta + \alpha)\sin\theta \qquad \textbf{(8.7)}$$

The new northing coordinate is given by

$$y = y2 + AC = y2 + AB\cos(\theta + \alpha)\cos\theta \qquad \textbf{(8.8)}$$

where θ can be derived from the heading of the road segment MN and can be obtained from the map data. The line AB is the known distance between A and B and α can be derived from ΔAEB. The equations (8.7) and (8.8) are derived for a particular orientation

of A and B (i.e., the true position and the position estimated from the map matching results). These equations can easily be derived for other orientations of A and B.

The horizontal error after adjusting for the road centreline at epoch *t* (HE_{at}) is therefore given by

$$HE_{at} = \sqrt{(x - x1)^2 + (y - y1)^2} \qquad \textbf{(8.9)}$$

The difference between equations (8.6) and (8.9) can be viewed as the bias introduced by the map matching algorithms when matching the location data to the road centreline.

8.2.3 Results

The validation technique explained in the previous section was tested using the probabilistic map matching algorithm developed in Chapter 6 as an example. Chapter 9 describes the validation of all three map matching algorithms using different inputs. The positioning data to validate the map matching algorithm was obtained from a comprehensive field test in London on the 5 July 2004. The test vehicle was equipped with a single frequency high sensitivity GPS receiver (a *GPSi-AVL unit* which is fully described in Chapter 5, section 5.6). In order to obtain the reference (truth) trajectory, the vehicle was also equipped with a 24-channel dual-frequency *Leica SR9500* geodetic receiver. High accuracy local measurement of 3-D offsets between the two antennae was undertaken in order that the position information was referenced to a single point. The test route had a good mixture of different roadway characteristics such as one-way, two-way, dual carriage-way, motorway, roundabout, merging and diverging sections. The route was a circular loop and about 80km long and was chosen carefully to have good satellite visibility as GPS carrier-phase observables require observations from a large number of GPS satellites for reliable and correct ambiguity resolution. Therefore, it was also expected that the navigation data from stand-alone GPS would be quite good because of fewer effects of signal masking.

The positioning data (easting and northing), speed and heading were collected at one second intervals directly from both GPS receivers. The duration of data collection was about 2 hrs. In order to implement the map matching algorithm, the positioning data from

GPS was augmented with DR. A high-resolution (1:2500) digital road network base map was used in the map matching algorithm. As an example, the probabilistic map matching algorithm was considered to test the methodology described in section 8.2.2. The test route and the results after applying the map matching algorithm are shown in Figure 8.4.

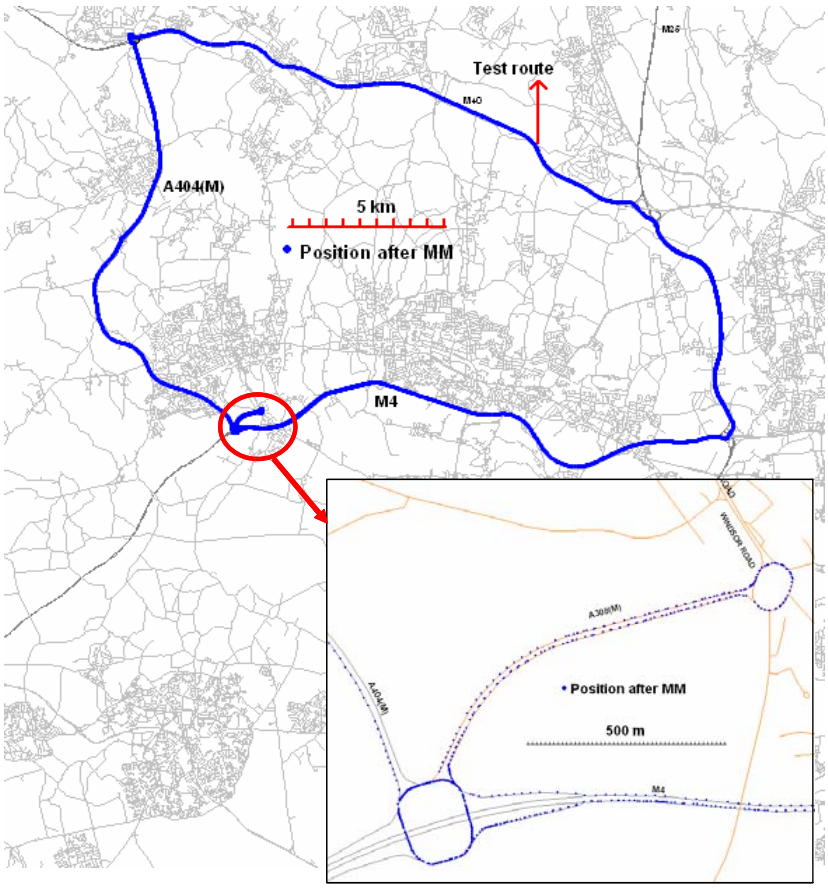

Figure 8.4: Test route with positions after map matching

The GPS carrier-phase observables were processed in relative mode to reduce errors. Therefore, the raw data was needed from both a reference (static) station and also from the geodetic receiver (roving). The applicable static station for this study was 'LOND' (located in London) which is an Ordnance Survey (OS) active station operating within the *UK National GPS Network* (http://www.gps.gov.uk). The raw data from this station for the 5 July 2004 (available at a 15 second sampling interval), was extracted from the OS internet enabled data archives. All available data sets from the geodetic receiver and the reference station were processed in a post-processing mode using the *SkiPro GPS post-*

processing package. The satellite positions were computed using precise Ephemeredes [32]. Integer ambiguities (for GPS kinematic positioning) were resolved for all baselines involving all satellites in view (elevation angle cut-off 10^{O}), having detected and resolved all cycle slips. A standard tropospheric model (Hopfield model[33]) and ionospheric model (Klobuchar model[34]) were used for compensations of tropospheric and ionospheric biases.

On the test route, both fixed and float solutions were obtained corresponding largely to open and built-up areas respectively. The positioning quality indicator in the form of the standard deviation of the horizontal position given by the *SkiPro GPS post-processing package* was used to select good float solutions which were used together with the fixed solutions to provide the reference (truth) of the vehicle trajectory. It was found that the values of the standard deviation of the horizontal position were always less than 0.03m for the ambiguity fixed solutions. In the case of the float solutions, this value varied from 0.1m to 26.0m. To select a threshold value for the standard deviation, which could identify good carrier-phase observations from the float solutions of the ambiguities, the position fixing data from both solutions was overlaid onto a high resolution digital base map (Figure 8.5) of scale 1:2500. The positioning fixes from the float solutions were sometimes offset by more than 20m from the road centreline when the standard deviation was large. It was found that the positioning fixes identified by a threshold value of 0.5m agreed reasonably with the positioning fixes from the fixed solutions relative to the road centreline. Therefore, this threshold value of the standard deviation was employed to select all good carrier phase observations from GPS. The total number of good reference positions (where the standard deviation is below the threshold 0.5m) of the vehicle was then found to be 408.

[32] Ephemeredes are a set of parameters acquired by the receiver from the GPS signals to calculate the satellite position and clock offset. Precise Ephemeredes were obtained from the international GNSS service (http://igscb.jpl.nasa.gov)
[33] Hopfield (1969)
[34] Klobuchar (1987)

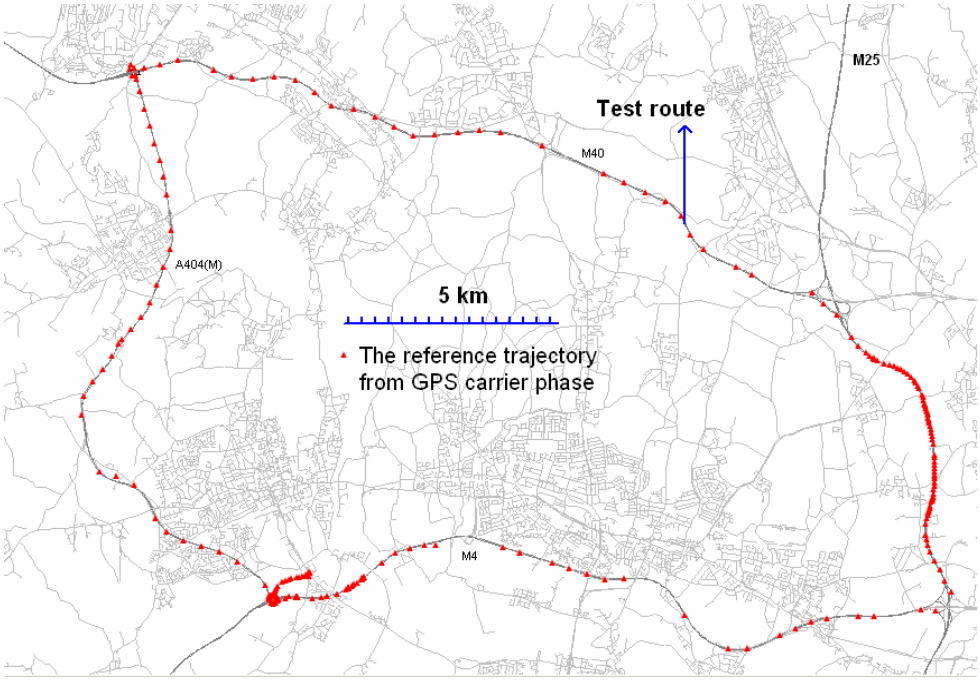

Figure 8.5: The reference trajectory of the vehicle from GPS carrier-phase observables

One section of the test route (a roundabout) is shown in Figure 8.6. This includes the reference positions from the GPS carrier-phase observables (round dots) and the corresponding positions estimated from the map matching results ((triangular symbols). In this section of the route, the vehicle was travelling from point 1 through point 8. In the real-world and for driving in the left side of the road, the true positions of the vehicle should lie on the right side of the road centreline within points 1 to 5 and on the left side of the centreline within points 6 to 8. The reference positions (truth) from GPS carrier phase observations (triangular symbols) agreed with the real-world positions, confirming the quality of carrier phase data.

The discrepancies between the actual vehicle positions and the road centreline map are clearly apparent in Figure 8.6. None of the carrier phase observables correspond exactly to the road network as drawn from the map database.

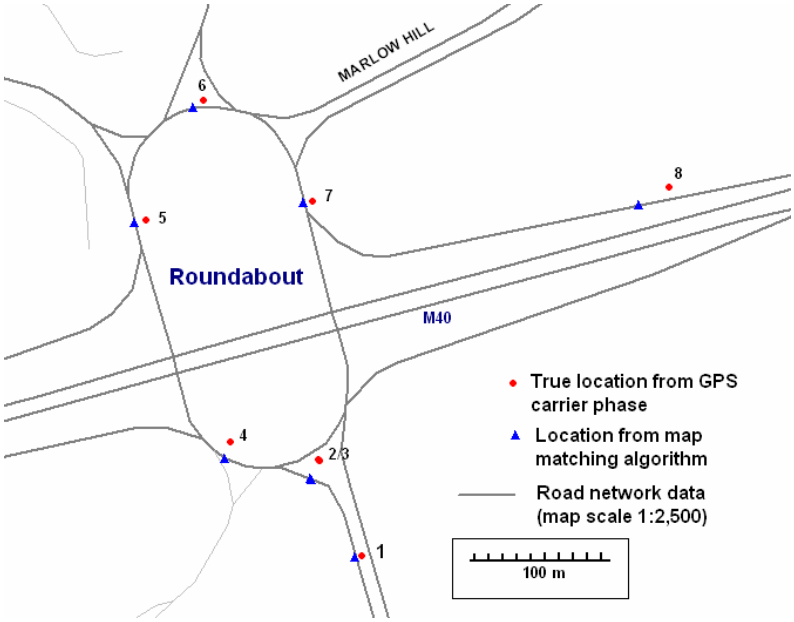

Figure 8.6: Map matching results and the truth reference for a particular section of test route

Based on the reference of the vehicle trajectory obtained from the GPS carrier-phase measurements, a set of correct links on which the vehicle was travelling was identified. Another set of links was identified for the corresponding epochs from the map matching results. From this a 98.1% correct link identification was achieved by the probabilistic map matching algorithm for this example. A more detailed performance assessment is made in chapter 9. In terms of physical location of the vehicle, different categories of horizontal positioning errors could be derived. The errors associated with the positions from the stand-alone GPS C/A code-ranging or the GPS C/A code-ranging augmented with DR, are shown in Figure 8.7. The maximum horizontal error of this category was 34m i.e., all GPS positions were within 34m of the true positions. The 2-D horizontal accuracy was 13.5m (2σ). The root mean square (RMS) of the easting component of this error was 12.5m and the northing component was 10.4m.

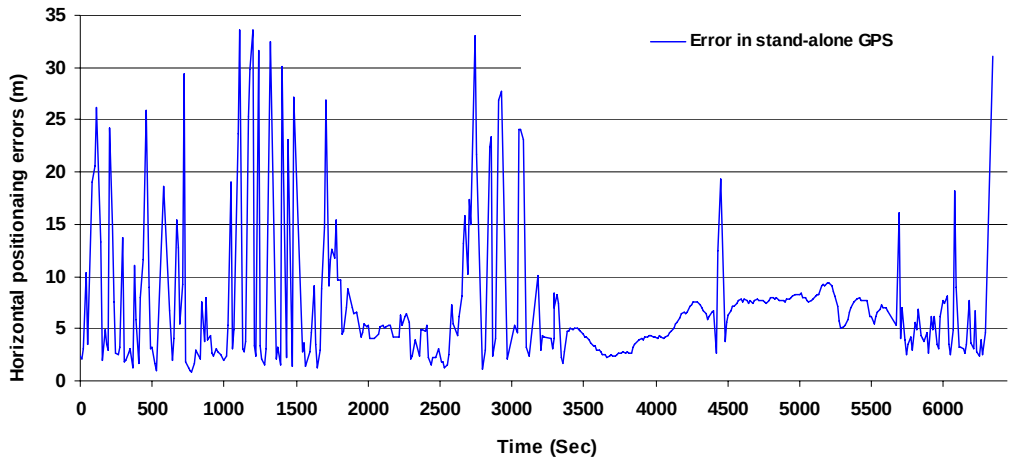

Figure 8.7: Horizontal errors of stand-alone GPS positions relative to the reference (truth) of the vehicle trajectory

The next step was to compute the horizontal errors associated with the positions estimated from the map matching results. This is shown in Figure 8.8. The errors were calculated using equation (8.6). It was found that all map-matched positions on the road centreline were within 11m (maximum error) of the truth positions of the vehicle. The 2-D horizontal accuracy was then increased to 9m (2σ) whereas the RMS of the easting component of the error was 9.5m and the northing component of the error was 6.4m. Therefore, a significant improvement in the estimation of the vehicle positions on the map was achieved by the map matching algorithm.

The horizontal errors were also calculated after correction for the biases introduced by road centreline using equation (8.9). This is also shown in Figure 8.8. The maximum horizontal error was only 6m implying that the final positions of the vehicle were within 6m of its true position. The 2-D horizontal accuracy was 5.1m (2σ). The RMS of the easting component of this error was only 3.03m and the northing component was 4.03m. Therefore, a further improvement in the estimation of the vehicle position could be achieved after adjustment for the road centreline biases introduced by the digital map.

Clearly the quality of vehicle positions estimated from the map matching algorithm largely depends on the quality of the digital base map. If an accurate digital network map is not used in the map matching process, the positions estimated by the map matching

algorithm may be less accurate than the positions obtained from stand-alone GPS. Chapter 9 discusses this issue in more detail.

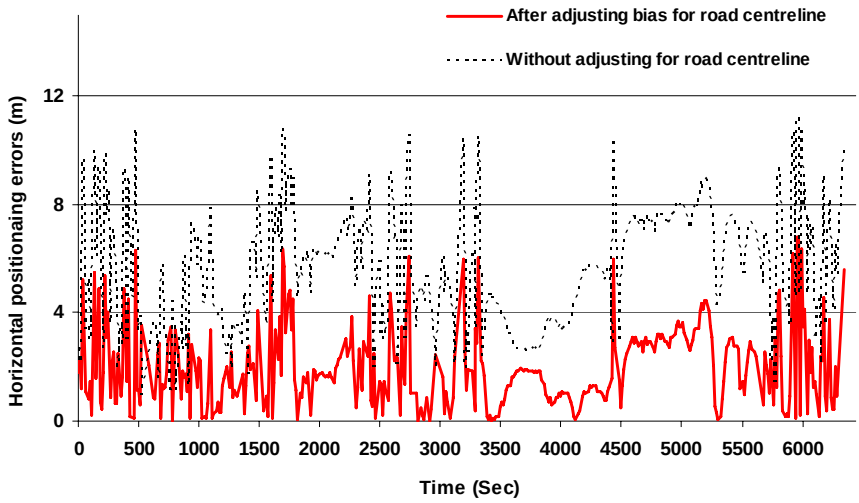

Figure 8.8: Horizontal errors of positions from the mm results relative to the reference (truth) of the vehicle trajectory

The majority of the map matching algorithms in the literature (e.g., Greenfeld, 2002, White et al., 2000, Quddus et al, 2003) use epoch-by-epoch heading information from GPS in order to identify the correct link among the candidate links. Therefore, one can compare the GPS/DR heading with the actual link heading which is calculated from the map data where the actual link is identified by the GPS carrier phase observations. The results are shown in Figure 8.9.

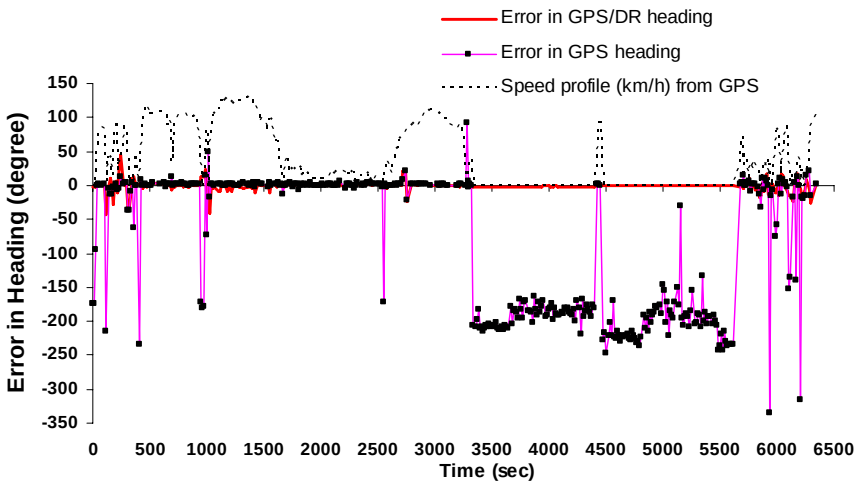

Figure 8.9: Errors in GPS and GPS/DR heading relative to the truth link heading

It was found that the heading from the stand-alone GPS was significantly different from the true heading even at low speed. The difference was higher when the speed of the vehicle was very low. On the other hand, the vehicle heading from the integration of GPS/DR was very close to the true heading. Therefore, the heading derived from stand-alone GPS SPS should be used with caution within map matching algorithms as incorrect heading data could lead to the incorrect selection of links.

8.3 Integrity of Map Matching Algorithms

To increase the level of confidence in the map-matched locations, the map matching algorithm should deliver a quality indicator for each position solution. A threshold for the quality indicator can be established using a real input/output dataset. If the quality indicator exceeds a pre-defined threshold it can then be regarded as an incorrect position solution and the algorithm should then provide a warning to the driver not to depend on the information provided by the algorithm at that time. This concept is usually known as "*integrity"* in the navigation literature. The definition of "*integrity"*, the factors affecting it and the quantification of the "*integrity"* of a map matching algorithm are presented below.

8.3.1. Definition of Integrity

This section gives a clear definition of the term "*integrity"* both in general and in the context of a navigation system. A distinction is made between the integrity performance of a navigation system such as GPS, and that of a map matching algorithm.

8.3.1.1. General definition

Several English dictionaries give the following definitions for the term "*integrity"*:

- the state or quality of being entire or complete; wholeness; entireness; unbroken state
- the entire, unimpaired state of anything, particularly of the mind; moral soundness or purity; incorruptness; uprightness; honesty
- moral soundness; honesty; freedom from corrupting influence or motive
- unimpaired, unadulterated, or genuine state

Therefore, integrity can be regarded as quality (of a person or a method) expressed in terms of several key words including uprightness, honesty, rectitude, sincerity, and trustworthiness. The integrity of any system refers to a measure of quality expressed in terms of these words.

8.3.1.2. Integrity in the context of navigation systems

Integrity is a measure of the trust that can be placed in the correctness of the information provided by the total system. Ochieng et al (2003a) defined integrity in the contexts of aviation as "*the ability of the navigation system to provide timely and valid warnings to users when the system must not be used for the intended operation or phase of flight. Specifically, a navigation system is required to deliver a warning (an alert) of any malfunction (as a result of a set of alert limit being exceeded) to users within a given period of time (time-to-alarm) with a given probability (integrity risk)".* Monitoring the integrity of a navigation system such as GPS is essential to ensure that the error in navigation solution is within tolerable limits. Ideal integrity monitoring involves the detection, isolation and the removal of faulty measurement sources from the navigation solution. Various external and autonomous (receiver-based) integrity monitoring methods are available for GNSS. External monitoring of GNSS relies on a number of ground-based stations, positioned at known locations (Fernow and Loh, 1994). In this method, individual satellites are monitored by comparing the measured pseudoranges with those computed from the coordinates of the satellites and within the monitoring stations. A fault is indicated when a measurement error exceeds a predefined threshold, and then a warning is sent to the users within the time-to-alarm. The Receiver Autonomous Integrity Monitoring (RAIM) method, on the other hand, is applied within the user receiver to allow it to autonomously establish system integrity (Ochieng et al., 2003a). RAIM addresses two basic concerns: (1) the existence of an unreliable "bad" measurement, and (2) the identification of the affected satellite.

The overall objective of measuring integrity is to protect a system against excessive positioning error. Therefore, the integrity of a map matching algorithm must detect an event when the horizontal error goes beyond a certain threshold, within a specified level of confidence. It should also detect whether the map matching algorithm selects as incorrect link. The integrity can then be used to deliver a warning to the driver (just as it does in the case of RAIM) that the map-matched location is not trustworthy for

positioning or navigation. This is particularly important at a junction in highly dense areas where a number of candidate road segments fall within the error ellipse around the position fix. As discussed in Chapter 3, the purpose of a map matching algorithm is twofold: (1) the identification of a link among the possible links in the vicinity of the vehicle, and (2) the determination of the correct vehicle location on that link. Consequently, the integrity of a map matching algorithm can be defined as its ability to correctly identify a link and to accurately determine the vehicle location on the link for a particular epoch. In the quantification of integrity, therefore, emphasis must be given to how correctly a map matching algorithm identifies a link and how closely the algorithm estimates the vehicle location compared to the actual location. A high integrity map matching algorithm means that its location estimation capability can be trusted or believed. Therefore, a criterion is needed to judge whether the new map matching algorithms can be trusted. This section introduces a simple way to determine "*integrity"*.

8.3.2. Factors Affecting the Integrity of a Map Matching Algorithm

The uncertainty (i.e., σ_e and σ_n) associated with a map-matched position as estimated by the equation (6.31) can be used to derive the integrity of a map matching algorithm. A larger uncertainly usually indicates less confidence in the position solution and vice versa. Moreover, both the quality of the position fix obtained from the navigation sensors and the quality of the digital map may also affect the integrity of a map matching algorithm. This involves the uncertainties associated with the raw GPS or GPS/DR measurements determined from the variance-covariance matrix, the bias introduced by the road centreline and the systematic error associated with the calculation of link heading due to errors in the map data. By taking into account these factors, a metric can be specified for measuring the quality (and level of confidence) of map matching and the detection of anomalies in map-matched locations.

8.3.2.1 Integrity based on the uncertainty associated with the position solution

Assume that P represents the vehicle position fix for a particular epoch and M denotes the corresponding map-matched location of the vehicle on the link AB (Figure 8.10). In this case link AB will have been selected as the correct link for the position fix P by a map matching algorithm. R refers to the true location of the vehicle for the same epoch.

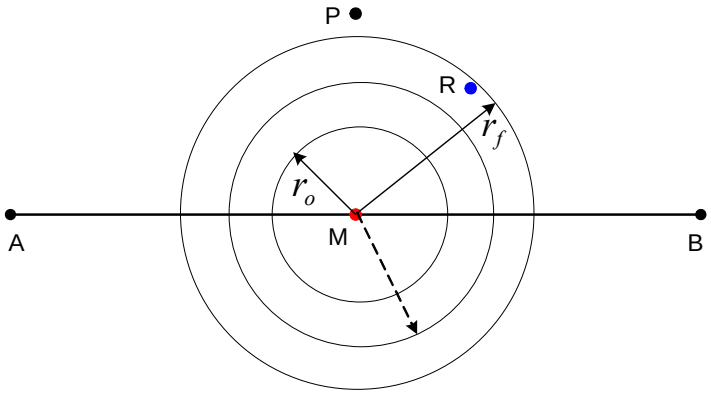

Figure 8.10: Derivation of the expansion factor

According to the equation (6.31), the easting and northing components of uncertainties (i.e., σ_e and σ_n) associated with M can be given as

$$\sigma_e = \sqrt{\frac{\sigma_{map,e}^2 \sigma_{gps,e}^2}{\sigma_{map,e}^2 + \sigma_{gps,e}^2}} \qquad \textbf{(8.10)}$$

$$\sigma_n = \sqrt{\frac{\sigma_{map,n}^2 \sigma_{gps,n}^2}{\sigma_{map,n}^2 + \sigma_{gps,n}^2}} \qquad \textbf{(8.11)}$$

In which $\sigma_{map,e}$ and $\sigma_{map,n}$ are the standard deviation of the errors (easting and northing components respectively) associated with the map data. $\sigma_{gps,e}$ and $\sigma_{gps,n}$ are the standard deviation of the errors (easting and northing components respectively) associated with the navigation sensors. Assuming that there is no correlation between the easting and northing components of the position solution, the uncertainty associated with the horizontal position at M is

$$\sigma = r_o = \sqrt{\sigma_e^2 + \sigma_n^2} \qquad \textbf{(8.12)}$$

The real (true) position of the vehicle, R, may not fall inside the circle of radius r_o drawn at M as can be seen in Figure 8.10. Therefore, the value of σ may not always represent the uncertainty associated with the map-matched position. The probability that the true

position, R, is within a circle of radius σ is about 63% (Kaplan, 1996). Moreover, a map matching algorithm essentially places the vehicle position fixes on the road centreline. This may introduce bias in the map-matched positions. Moreover, a map matching algorithm may identify a wrong link and hence the map-matched location fails for the true position of the vehicle.

Consequently, the confidence level associated with a map-matched position should be $k\sigma$ where k is a growth factor and $k \geq 1$. An empirical study was conducted to derive the value of k. The basic idea is to increase the radius r_o so that the circle includes the real position, R. The minimum radius of a circle that includes R is denoted by r_f. Therefore, the value of k can be given by

$$k = \frac{r_f}{\sigma} \qquad \textbf{(8.13)}$$

The value of r_f (i.e., $k\sigma$) can be used as the uncertainty or the level of confidence associated with the map-matched positions. A large value of $k\sigma$ may indicate a lower confidence level and vice versa.

To implement the above concept, a series of map-matched positions with their corresponding true positions is needed. Therefore, the dataset used in the validation technique (section 8.2.3) can also be employed to derive a relationship between k and σ. Figure 8.11 shows the observed relationship between them. The fuzzy logic map matching algorithm is applied to the navigation data from GPS/DR and the map data from the map of scale 1:2500 to obtain the map-matched positions. The corresponding true positions of the vehicle are obtained from the GPS carrier-phase observables using the fixed solutions only[35]. This gives a total of 217 true positions of the vehicle.

[35] The float solutions for ambiguity resolution are not considered in order to have more accurate vehicle positions

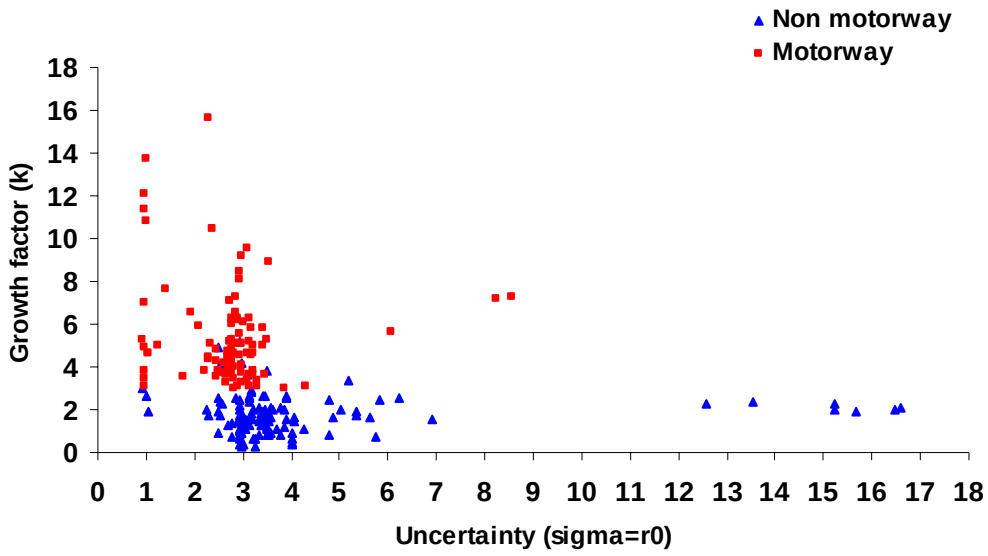

Figure 8.11: Observed relationship between k and σ

The growth factor can be as high as 16 as seen in Figure 8.11 meaning that the minimum radius of a circle which includes the real position of the vehicle is 16σ. It seems that the map-matched position is far away from the true position indicating a wrong selection of link or an incorrect location determined by the map matching algorithm. However, the higher values of *k* may not necessarily be due to the identification of wrong links by the map matching algorithm. The error introduced by the road centreline may also give a higher growth factor. Usually, a wider roadway (e.g., a motorway) produces a larger error. Figure 8.11 indicates that the relationship between *k* and σ for a motorway is different from that of a non-motorway. Therefore, two types of relationships can be modelled: one for roadways with more than 2-lane (in each direction) and the other for all other roadways.

Since the value of *k* is always non-negative, an additive model can be considered unsatisfactory. Therefore, a log-linear relationship between *k* and σ is suggested:

$$\ln k_t = \theta D + \beta \sigma_t + \varepsilon_t \qquad \textbf{(8.14)}$$

where *D*=1 if the vehicle travels on a motorway and *D*=0 otherwise, θ and β are the parameters to be estimated, and ε is the identically and independently distributed error

term. The parameters are estimated using Ordinary Least Square (OLS) using 217 observations. The goodness-of-fit (adjusted R^2) is found to be 0.80.

Table 8.1: The parameter estimation results

Parameters	Coefficients	*t*-statistics	*p*-value	*95% confidence intervals*	
				Lower limit	*Upper limit*
Error sigma (β)	1.3295	21.14	0.00	1.205	1.454
Dummy variable (θ)	0.0706	6.20	0.00	0.048	0.093

Therefore, the growth factor (k) can be calculated from the following equations.

For roadways with more than 2-lane:

$$\hat{k} = \exp(1.3295 + 0.0706\sigma) \quad \textbf{(8.15)}$$

For all other roadways:

$$\hat{k} = \exp(0.0706\sigma) \quad \textbf{(8.16)}$$

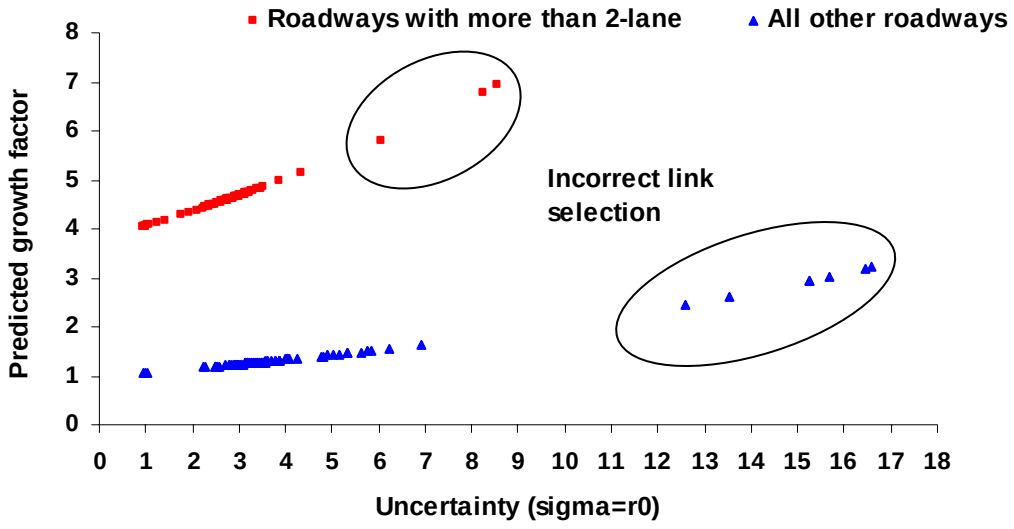

Figure 8.12: Estimated relationship between k and σ

Once σ is estimated by the map matching algorithm, the corresponding value of k can then be calculated using either equation (8.15) in the case of the vehicle travelling on a roadway with more than 2-lane (in each direction) or equation (8.16) in the case of all other roadways. Then the corrected uncertainty (i.e, $k\sigma$) associated with each map-

matched position can easily be obtained. Figure 8.12 shows the estimated relationship between *k* and σ. The points surrounded by the ellipses are all incorrect map-matched positions associated with higher values of uncertainty. However, there are incorrect map-matched positions even when *k* is small. This suggests that other factors influencing the integrity of a map matching algorithm also need to be taken into account.

8.3.2.2 Integrity based on the ability to identify the correct link

The vehicle direction, θ, (i.e., heading relative to the north) for a particular position fix can be obtained from the outputs of the navigation sensors (GPS or GPS/DR). The road network data can also be used to acquire vehicle direction. This is because a map matching algorithm identifies a link for a position fix and therefore, the direction of the link, β, should be the direction of the travelling vehicle. The absolute difference between these two directions, (i.e., $|\theta - \beta|$) can be used to derive an integrity measure of a map matching algorithm in terms of link identification. For example, if a map matching algorithm identifies the correct link for a position fix, then the $|\theta - \beta|$ should be close to zero and the identification of the link may be trusted for the fix. However, the uncertainties associated with both direction measurements need to be considered before inferring any conclusion. If the vehicle heading is obtained from stand-alone GPS, then the heading is not accurate when the vehicle travels at a low speed (Chapter 6, section 6.3.1.2). Although heading from GPS/DR is quite good, it may sometimes provide inaccurate results. The uncertainty in heading can be detected by the error variance for heading (σ_h^2) from the variance-covariance matrix. In order to have a 99% confidence level, the true heading (θ_{true}) from the navigation system is:

$$\theta_{true} = \theta \pm 3\sigma_h \qquad \textbf{(8.17)}$$

The error associated with the heading of a road link can be obtained from the quality of the map data. If the heading of a link AB of length *L* is denoted by β and the map scale is $1:m$ then the maximum error (3σ, a 99% confidence level) associated with β can be given by $\Delta\beta$ as shown in Figure 8.13. This is because the position of nodes A or B can be anywhere within a circle of radius *m*. In the worst-case scenario, the position of the node A may be at *a* and the position of the node B may be at *b*.

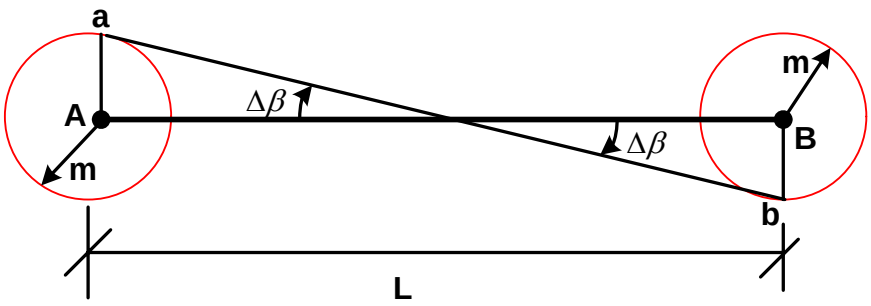

Figure 8.13: Error associated with the heading of a link

Therefore, the link *ab* has the largest heading error ($\Delta\beta$) relative to the original link AB. This can be derived as

$$\Delta\beta = \arctan(\frac{m}{L/2}) \tag{8.18}$$

Therefore, the true heading of the link AB is

$$\beta_{true} = \beta \pm \arctan(\frac{m}{L/2}) \tag{8.19}$$

The maximum error associated with θ is $3\sigma_h$, and β is $\Delta\beta$. Using an error propagation theorem, the combined heading error (*HE*) can be given by the following equation:

$$HE = \sqrt{(3\sigma_h)^2 + (\arctan(\frac{m}{L/2}))^2} \tag{8.20}$$

The identification of the link is said to be reliable if the difference between θ and β (i.e., the observed difference) is less than or equal to the combined heading error, *HE*. In other words, if the difference between $|\theta - \beta|$ and HE is less than or close to zero, then it can be said that the identification of the link by the map matching algorithm is more reliable. This difference can be termed as *the heading residual* (ΔH) and is given by:

$$\Delta H = \left|\theta - \beta\right| - HE \leq 0 \quad \textbf{(8.21)}$$

8.3.2.3 Integrity based on the ability to accurately estimate vehicle location

The proximity between the raw position fix and the corresponding map-matched location on a link can be used to derive the integrity of a map matching algorithm in terms of location determination. If a position fix and the map-matched location are close to each other then the map matching algorithm is normally assumed to be quite trustworthy given that the map matching algorithm takes into account both the road network connectivity and the recent history of the vehicle trajectory. However, the quality of the position fix and the error associated with the road width need to be taken into account.

Two-dimensional (2-D) horizontal positional accuracies are normally estimated and reported using distance root mean square (DRMS) radial error statistics (Kaplan, 1996). The DRMS error measures are approximations to the error ellipses that are computed for measured position fixes fully described in Chapter 6 (section 6.2.1.1). This DRMS error statistic is related to the variance-covariance matrix associated with the outputs of the navigation sensors. This can be defined as

$$DRMS = \sqrt{\sigma^2_{gps,e} + \sigma^2_{gps,n}} \quad \textbf{(8.22)}$$

where $\sigma^2_{gps,e}$ and $\sigma^2_{gps,n}$ are the error variances associated with the easting and northing components of a position fix.

DMRS statistics can have variable confidence levels. The probability that the measured position fix falls within circle of radius DRMS from the true position largely depends on the ratio between $\sigma^2_{gps,e}$ and $\sigma^2_{gps,n}$. If, for instance, the 2-D error distribution is close to being a circular (i.e., $\sigma^2_{gps,e} = \sigma^2_{gps,n}$), the probability of falling inside this circle is about 63%. If $\sigma^2_e = 10\,\sigma^2_n$, then the probability is about 68%. A circle twice this radius i.e., 2DMRS represents 95% to 98% positional probability based on the ratio between σ^2_e and σ^2_n. The probability that the true position is within a circle of radius 3DRMS is more than 99% (Kaplan, 1996).

The 3DRMS error statistic can be used to deduce integrity for a map matching algorithm. A map-matched vehicle location is said to be trustworthy if this location is very close to its actual (true) location. Therefore, a good map-matched location for an epoch should be within a circle of radius 3DRMS drawn at the corresponding position fix. The distance between the raw position fix and the map-matched location is necessarily less than 3DRMS if a 99% or more confidence level is desired. Since the road network data only contains road centreline data and a map matching algorithm takes road centreline as the true reference for vehicle positioning, then an adjustment is essential for road width. This adjustment, which largely depends on the types of roadways (i.e., motorway, major road, minor road etc), can be regarded as the correction for road centreline ($\Delta R_{centreline}$). The expanded radius of a circle can then be given by the following equation:

$$R_{3drms} = 3DRMS + \Delta R_{centreline} \quad \textbf{(8.23)}$$

Assuming that a vehicle equipped with a navigation sensor travels on a two-way road with 2-lane in each direction as shown in Figure 8.14, P represents a position fix for an epoch *t* and T stands for the corresponding true location. AB is the road centreline which is a network representation of the two-way 2-lane road of width *W*. A map matching algorithm identifies link AB as the correct link for the position fix P. Q is the vehicle location on the link estimated by the algorithm. Although the true location of the vehicle (T) falls inside a circle of radius 3DRMS (i.e., r_{3drms}), the map-matched location falls outside. This is due to the fact that the map-matched location is always on the road centreline whereas the true location does not necessarily have to be on the centreline. However, the map-matched location, Q, is positioned within the confidence area of an expanded circle of radius R_{3drms} which includes the correction for road width, is used.

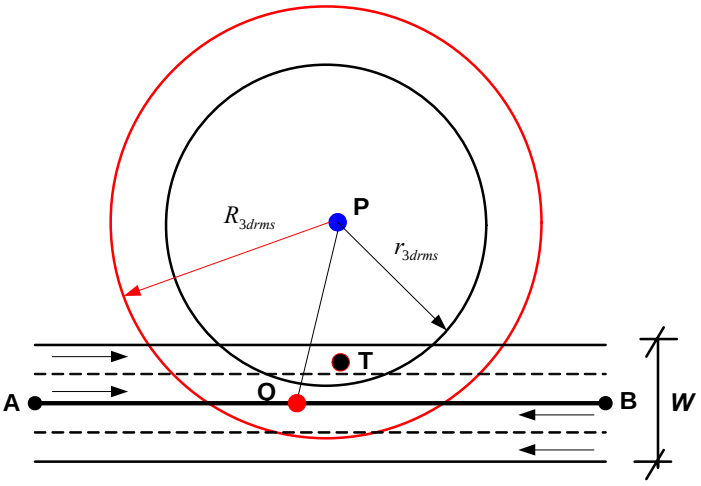

Figure 8.14: Correction for road width

The correction for road centreline, $\Delta R_{centreline}$, is normally the deviation of the actual location of the vehicle relative to the centreline, i.e., the shortest distance from T to AB as can be seen in Figure 8.14. The deviation largely depends on the number of lanes associated with the roadway. For instance, the value of $\Delta R_{centreline}$ will normally be higher for a motorway than a minor road. With navigation data from a low-cost GPS receiver, it is impossible to determine the particular lane on which the vehicle is travelling. Therefore, the maximum deviation can be considered as the correction for road centreline. Assuming a lane width of 3.5m, the maximum deviation of the actual vehicle location from the road centreline for roads with various numbers of lanes is shown in Table 8.2.

Table 8.2: Correction for road centreline

The number of lanes	**The maximum deviation ($\Delta R_{centreline}$), m**
5	7
4	5.25
3	3.5
2	1.75
1	0

For the UK, data on the number of lanes is not readily available in GIS format at this moment. However, UK Ordinance Survey is working towards the development of an integrated transport network (ITN) layer which will include road attributes such as road width and the number of lanes. For the use of this study, a value of 3.5m for $\Delta R_{centreline}$ is assumed for all roads. Therefore, equation (8.23) becomes

$$R_{3drms} = 3\sqrt{\sigma_e^2 + \sigma_n^2} + 3.5 \quad \textbf{(8.24)}$$

The map-matched location is said to be good if the distance between the raw position fix (P) and the map-matched position (Q) is less than R_{3drms}. The difference between PQ and R_{3drms} can be termed as *the distance residual*, ΔD, which can be defined as

$$PQ - R_{3drms} = \Delta D \leq 0 \quad \textbf{(8.25)}$$

Therefore, the key variables required to derive a metric for measuring the quality of map matching are $k\sigma$, ΔD and ΔH. The integrity of a map matching algorithm can be regarded as high if:

- $k\sigma$ is small
- ΔD is less than or close to zero
- ΔH less than or close to zero

All the above conditions are linguistic statements. Therefore, the metric can superiorly be derived using a qualitative decision-making process rather than a mathematical process. Hence, a fuzzy logic model is a good choice to deal with these linguistic terms. This is explained below.

8.3.3 The Derivation of an Integrity Metric using Fuzzy Logic

A detailed description of fuzzy logic models can be found in Chapter 7. Here a Sugeno fuzzy inference system (FIS) is used to derive a metric (0 to 100) representing the integrity of the results of a map matching algorithm based on the parameters $k\sigma$, ΔD and ΔH.

The three state input variables of this FIS are: (1) the corrected uncertainty associated with the map-matched position, $k\sigma$ (m), (2) the distance residual, ΔD (m), and (3) the heading residual, ΔH (degree). The fuzzy subsets associated with the $k\sigma$ are *small, medium,* and *high*. The fuzzy subsets associated with the ΔD are *positive* and *negative.*

The fuzzy subsets related to ΔH are also *positive* and *negative*. The fuzzification of these inputs is shown in Figure 8.15.

The single output of this FIS is the integrity of the map-matched position (denoted as *L4*). A zero-order Sugeno fuzzy model is considered which takes five constants for the output. These values are selected initially as e.g., *very low (Z1)* = 0, *low (Z2)* = 50, *average (Z3)* =70, *high (Z4)=90,* and *very high (Z5)=100.* The next step is to formulate the fuzzy rules which are related to the number of system state variables. Twelve rules comprising the fuzzy knowledge are applied to this FIS (see Table 8.3). The rules are established based on human knowledge and experience in interpreting the variables.

Table 8.3: Fuzzy rules used in the fuzzy inference system

R1: if $k\sigma$ is high and ΔD is positive and ΔH is positive then the integrity associated with map-matched location (*L1*) is very *low (Z1)*
R2: if $k\sigma$ is high and ΔD is positive and ΔH is negative then the *L1* is *low (Z2)*
R3: if $k\sigma$ is high and ΔD is negative and ΔH is positive then the *L1* is *low (Z2)*
R4: if $k\sigma$ is high and ΔD is negative and ΔH is negative then the *L1* is *average (Z3)*
R5: if $k\sigma$ is medium and ΔD is positive and ΔH is positive then the *L1* is *low (Z2)*
R6: if $k\sigma$ is medium and ΔD is positive and ΔH is negative then the *L1* is *average (Z3)*
R7: if $k\sigma$ is medium and ΔD is negative and ΔH is positive then the *L1* is *average (Z3)*
R8: if $k\sigma$ is medium and ΔD is negative and ΔH is negative then the *L1* is *high (Z4)*
R9: if $k\sigma$ is small and ΔD is positive and ΔH is positive then the *L1* is *average (Z3)*
R10: if $k\sigma$ is small and ΔD is positive and ΔH is negative then the *L1* is *high (Z4)*
R11: if $k\sigma$ is small and ΔD is negative and ΔH is positive then the *L1* is *high (Z3)*
R12: if $k\sigma$ is small and ΔD is negative and ΔH is negative then the *L1* is *very high (Z5)*

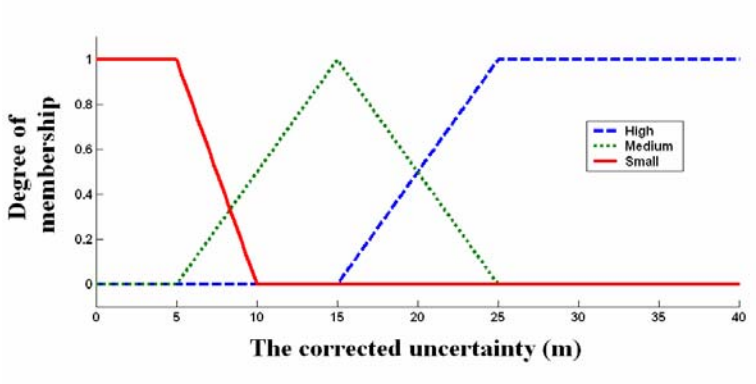

(a)

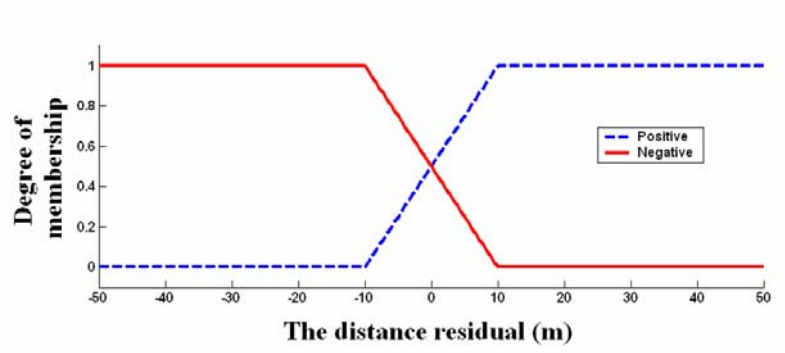

(b)

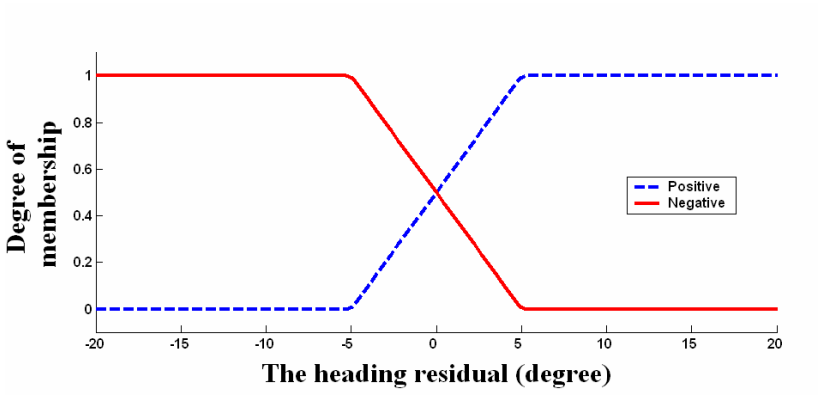

(c)

Figure 8.15:Membership functions for (a) the corrected uncertainty, (b) the distance error, and (c) the heading error

8.3.4. Statistical Performance of Integrity

The integrity derived above has to be transformed into quantifiable parameters in order to assess its performance. Three parameters are suggested: (1) false alarm rates, (2) missed detection rates, and (3) overall correct detection rates. The procedures to determine these parameters are given below:

- Determine the integrity value (0 to 100) for each observation using the fuzzy logic method described in section 8.3.3.
- Determine a threshold for the integrity in order to represent a wrongly map-matched location (see section 8.3.4.1 below).
- Identify epochs where the integrity value falls below the threshold. These epochs (denoted as set A) can be regarded as the incorrect matches identified by the integrity method.
- Select epochs associated with the incorrect matches based on the reference trajectory (see section 8.2.2). These epochs (denoted as set B) are the true incorrect matches.
- Identify epochs which can be found in set A but cannot be found in set B. The total number of such epochs is termed as *m*. This means that the integrity method gives an incorrect warning for *m* epochs which can be regarded as total false alarms (*FA*).
- Identify epochs which can be found in set B but cannot be found in set A. The total number of such epochs is termed as *n*. This indicates that the integrity method fails to give a warning for *n* epochs which can be regarded as total missed detections (*MD*).

If the total number of observations is denoted by *r*, then the false alarm rates (*FAR*) can be given as:

$$FAR = \frac{total\ \ false\ alarms\ (m)}{total\ observations\ (r)} \tag{8.26}$$

The missed detection rates (*MDR*) can be given as:

$$MDR = \frac{total\ missed\ detections\ (n)}{total\ observations\ (r)} \tag{8.27}$$

The overall correct detection rates, *OCDR*, which is the overall performance of the integrity method, can be given as:

$$OCDR = 1 - FAR - MDR \tag{8.28}$$

8.3.2.1 Derivation of the integrity threshold

In any integrity assessment it is necessary to define a threshold level below which the measurement should be discarded. In order to derive the threshold for the integrity metric previously described, the fuzzy logic-based integrity method was applied in combination with the fuzzy logic map matching algorithm. This analysis was done for the example case using navigation data obtained from GPS/DR and digital map data obtained from a map of scale 1:2500. The navigation data was a subset of the data used in section 8.2.3, including only observations associated with the ambiguity fixed solutions. For each of the map-matched locations obtained from the map matching algorithm, three input variables ($k\sigma$, ΔD *and* ΔH) to the Sugeno FIS were calculated. The corrected uncertainty ($k\sigma$) was calculated using either equations (8.15) or (8.16). The distance residual (ΔD) was estimated using the equation (8.25) and the heading residual (ΔH) was obtained from the equation (8.21). For each of the inputs, the corresponding crisp output, which is the integrity of the map-matched location, was achieved from the Sugeno FIS.

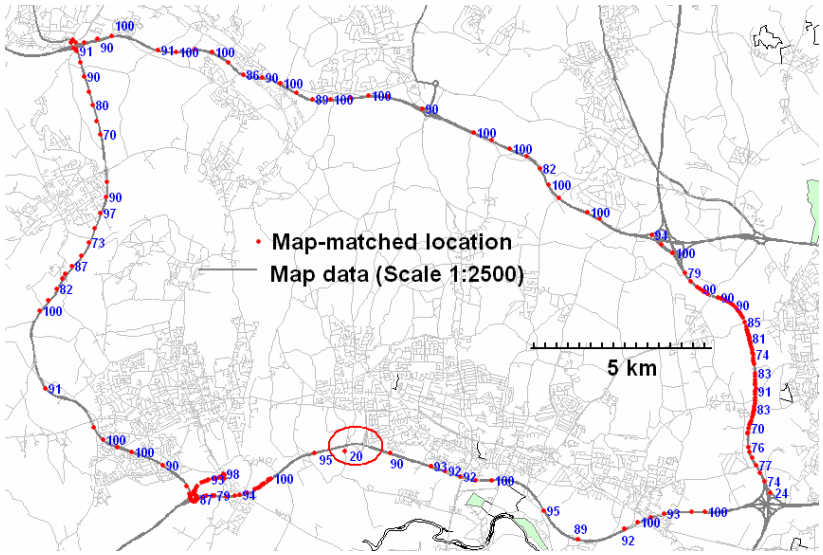

Figure 8.16: The level of confidence for the map-matched locations

Figure 8.16 shows the results of the metric representing the integrity of the map-matched locations. The value of the metric (level of confidence) varies from 0 to 100 where 0 means the map-matched location is not reliable at all and 100 means the map-matched location is very reliable. The level of confidence associated with each of the map-matched locations is then evaluated against the true location of the vehicle. A very good agreement between these two has emerged. For instance, in the example in Figure 8.16, it

is noticeable that the fuzzy logic map matching algorithm selects a wrong link for one of the position fixes (indicated with a circle) and the corresponding integrity value is 20.

Figure 8.17 shows the relationship between the frequency for the correct and incorrect matches for the different bins of integrity values. It can be observed that larger values of the integrity are related to the correct map-matched locations. The frequency of the correct matches is close to zero when the integrity value is below 70 for the fuzzy logic map matching algorithms. The topological and probabilistic map matching algorithms also give the similar results. This suggests that the incorrect map-matched locations are usually associated with metric values of less than 70 which correspond to the middle *L4* output constant from the Sugeno FIS. This was chosen to represent an "average" level of integrity. For this example values below 70 can therefore be seen as having below average integrity and 70 can be taken as being an appropriate threshold value. In other words, if the value of the metric is below 70, then we are not confident that the map-matched location is reliable.

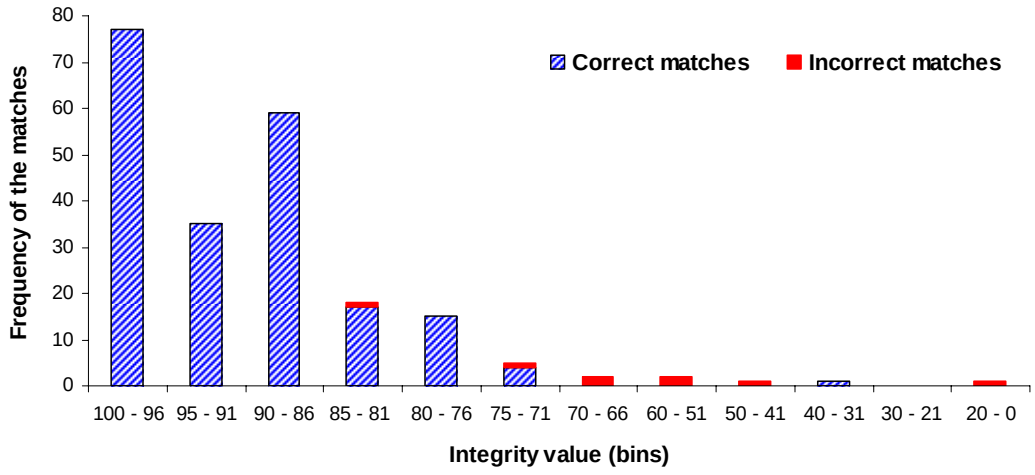

Figure 8.17: Frequencies of the matches vs integrity values (bins)

It should be noted however that there is always a certain level of integrity risk associated with a threshold. The risk can be seen as representing the acceptable trade-off between the probabilities of *MD's* and *FA's*. Some transport telematics services, such as emergency services, route guidance should have a low level of integrity risk and hence the threshold should be increased (e.g., >70 in our example). Integrity risk may not be too critical for some services such as public transport operations. In these cases the threshold for the integrity measure can be decreased (i.e., <70 in our example).

8.3.5. Performance Evaluation using the Integrity Method

As discussed earlier, one of the applications of integrity monitoring is to deliver a warning to the driver that the map-matched location identified by the map matching algorithm is not reliable. Following the detection of the failure, the map matching algorithm aims to quickly recover from the failure. For our example in the previous section, it was found that an integrity value below 70 indicates a failure for all map matching algorithms.

This section describes the performance of the integrity method developed in section 8.3.3. This is accomplished using a new dataset of GPS carrier-phase observables which has not been used to determine the criteria for the integrity method. This new dataset was obtained from a field campaign in the West of London (near Reading) on the 18 August 2005. The nearest Ordnance Survey (OS) active station is *AMER* (located in Amersham). The raw data for this station is available at a 30 second sampling interval. This makes it difficult to use this data for the carrier-phase processing.

A reference station (R) was therefore created at Silwood Park near Reading (see Figure 8.18**)** in order to obtain continuous raw data at one second intervals**.** A *Leica SR9500* geodetic base station GPS receiver was used to record the data at the reference station. Another *Leica SR9500* geodetic receiver was used to collect GPS carrier phase data when the vehicle was travelling on the test route shown in Figure 8.18 for about an hour**.** The test route is within 15km of the reference station meaning that the length of the baseline is always less than 15km. All available datasets from the two receivers were then processed in a kinematic post-processing mode using the Leica SkiPro package. The satellite positions were computed using precise ephemeredes. Both fixed and float solutions were obtained but only fixed solutions (840 epochs) were used in this analysis.

The *GPSi-AVL* unit[36] was used to collect GPS and DR sensor data along the test route at one second intervals. The navigation data from GPS/DR and the digital map data from a map of scale 1:2500 were used to implement the fuzzy logic map matching algorithm.

[36] See Chapter 5 (section 5.6) for a description of this unit

For each of the map-matched locations obtained from the fuzzy logic map matching algorithm, the input variables $k\sigma$, ΔD *and* ΔH were calculated in order to feed into the Sugeno FIS that derives the integrity measure. Although σ, ΔD *and* ΔH were obtained from the observed data, k was estimated from equations (8.15) or (8.16). In order to examine whether the coefficients in these equations were trustworthy, equation (8.14) was re-estimated using the new dataset described above. It was found that the newly estimated coefficients (β=1.41 and θ =0.052) fell within the confidence limits shown in Table 8.1. Therefore, equations (8.15) and (8.16) were directly used to estimate k. It should be noted that the output of the FIS was also calculated when k was obtained from β=1.41 and θ =0.052. The means of these two outputs were not found to be statistically different.

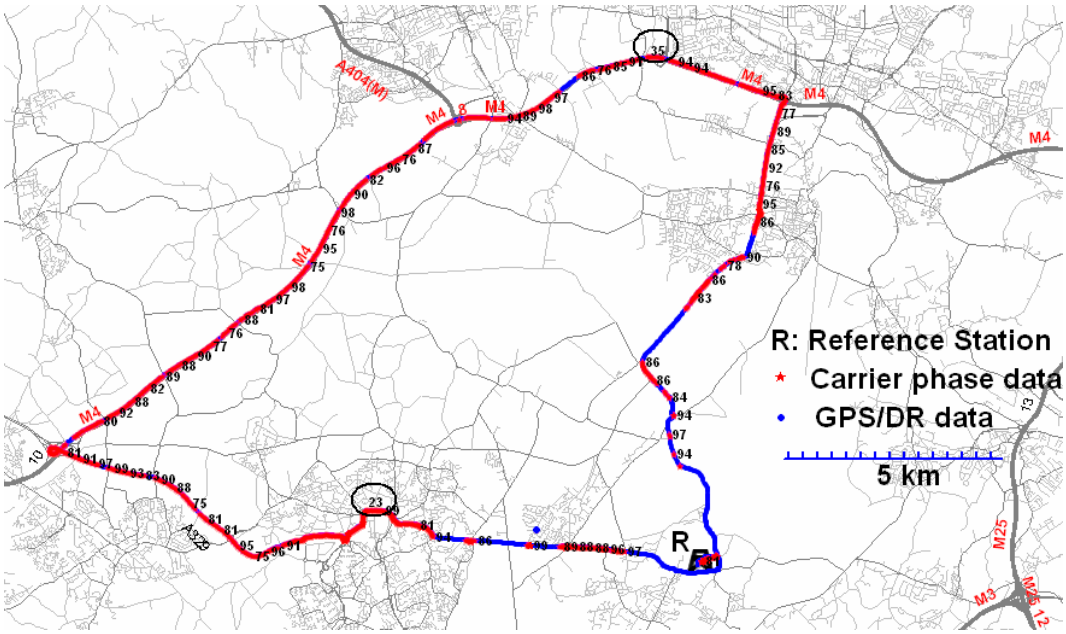

Figure 8.18: The test site used to validate the integrity method

In order to assess the performance of the integrity method for the fuzzy logic map matching algorithm, the step-by-step procedure presented in section 8.3.4 was implemented. The total number of valid observations was 840 (ambiguity fixed solutions only), the threshold to determine the parameters representing the statistical performance of integrity was taken as 70. Therefore, the total number of false alarms (*FA*) was found to be 9, and the total number of missed detections (*MD*) was found to be 6. This gives a *FAR* of 0.011, a *MDR* of 0.007, and an *OCDR* of 0.982. It can be said that the integrity method developed in this chapter is capable of providing a valid warning to the driver

98.2% of the time when the fuzzy logic map matching algorithm is used. After detecting each failure mode (i.e., when the integrity value falls below 70), the map matching algorithm goes back to the MPJ (in the case of probabilistic map matching algorithm) or the SMP-junction (in the case of fuzzy logic map matching algorithm) to acquire a correct fix.

Although the integrity value for an average output of the FIS is 70, it is possible that selection of different thresholds could affect the performance of the integrity method. It is envisaged that higher number of *FA* is associated with higher thresholds and vice versa. On the other hand, higher *MD* is related to lower thresholds and vice versa. Figure 8.19 confirms the above assertion for the fuzzy logic map matching algorithm when the navigation data is obtained from GPS/DR and the digital map data is obtained from a map of scale 1:2500. The number of *FA* is increased rapidly when the thresholds are higher than 70 and for these thresholds, the number of *MD* are small.

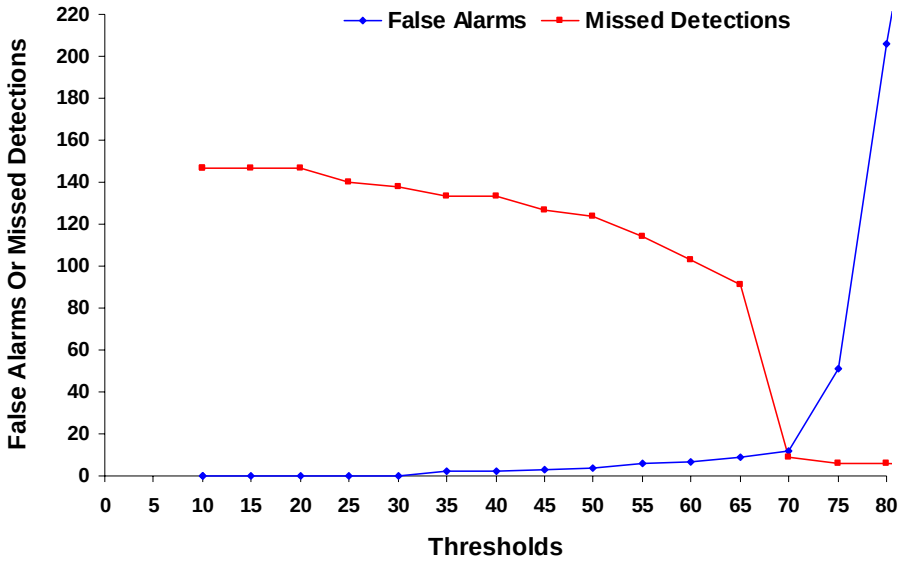

Figure 8.19: The variation of FA and MD with thresholds

Figure 8.20 shows how the selection of threshold affects the overall performance of the integrity method. *OCDR* (%) increases with an increase in threshold level. This is because the *MDs* are decreased. The *OCDR* is significantly reduced when the thresholds are above 70. This is because the *FAs* are increased. The optimal performance of the integrity

method is associated with the threshold of 70, which is based on the average *L4* from the Sugeno FIS.

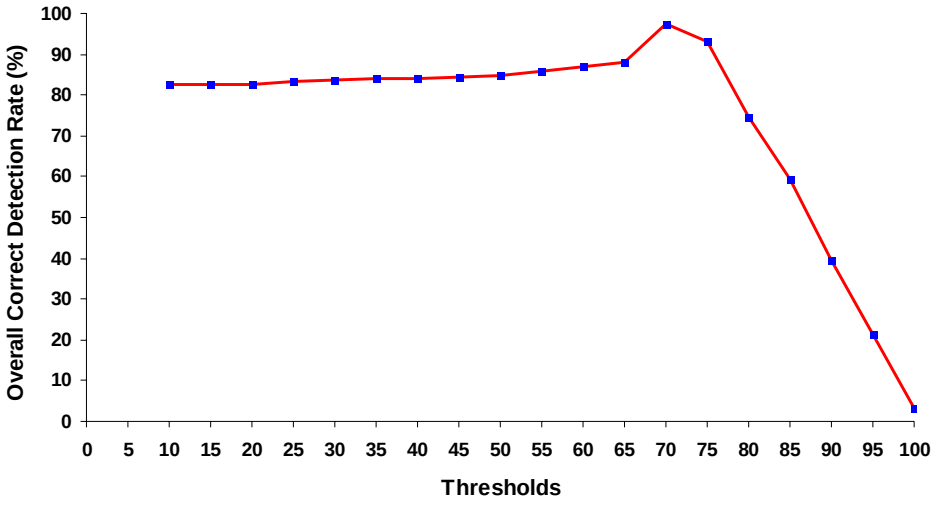

Figure 8.20: The variation of OCDR with thresholds

The performance of the integrity method for different map matching algorithms using inputs from various navigation sensors and digital maps is described in Chapter 9 in detail.

8.4 Summary

The validity and integrity of map matching algorithms was discussed in this chapter. In order to validate the map matching algorithms, the validation methodology was developed and applied as an example to the probabilistic map matching algorithm. It was found that the algorithm identified 98% of the links correctly when the navigation data was obtained from GPS/DR and the digital map data was obtained from a map of scale 1:2500. The horizontal accuracy (2-D) was 9m for 95% of the time. It should be noted that the validation technique developed in this chapter was generic and could be applied to any of the map matching algorithms.

Integrity is essential to quickly recover from a failure of the navigation system. A metric (0 to 100) to represent the integrity of the map-matched locations was developed based on various error sources associated with the position fixes and map data using a fuzzy logic

technique. A threshold is derived, which is essential to determine the statistical performance of the integrity measure. It was found that the integrity method was capable of providing valid warnings to the driver 98.2% of the time when the fuzzy logic map matching algorithm was used.

The next chapter will describe the effects of navigation sensors and the digital map quality on the performance of map matching algorithms and integrity. The chapter will also include the results of map matching algorithms applied to urban areas.

CHAPTER 9

PERFORMANCE EVALUATION

9.1 Introduction

As discussed in Chapter 3, the required navigation performance (RNP) for some advanced transport telematics (ATT) services cannot be achieved with a standalone GPS in areas with urban canyons, streets with dense tree cover, and tunnels. Deduced Reckoning (DR), with the aid of an odometer and a gyroscope, is commonly used to bridge any gaps in GPS positioning, but its positioning error grows rapidly if not controlled by other sensors or systems. A GPS unit may be used to recalibrate a DR device giving an integrated navigation system capable of more robust performance, despite remaining prone to errors. These errors are discussed and characterised in Chapter 3.

Another essential element for land vehicle positioning and navigation is a digital map of the road network but these are also prone to errors (Noronha and Goodchild, 2000). For example, roads are normally represented as a single "centreline" and curvatures are represented as piecewise linear lines (for gentle curves) or as a polyline (for sharp curves). This generalisation alters the features on the ground and potentially introduces significant bias (NRC, 2002). Goodwin and Lau (1993) emphasised the need for accurate electronic map data for vehicle navigation. Their study distinguished two types of errors associated with a digital map, geometric error and topological error. Both errors could potentially confuse an en-route guidance system.

Bullock and Krakiwsky (1994) analysed the use of digital maps in vehicle navigation. They found that most of the existing land vehicle navigation systems used digital maps simply to display the vehicle's position without taking into account the errors associated

with them. Kim et al. (2000) described the efficient use of digital road maps in various positioning and navigation systems for ATT applications. Their study concluded that an accurate digital road map can effectively improve positioning accuracy.

Due to errors associated with the navigation data and the digital map data, there is always a level of uncertainty associated with map matching algorithms. Previous chapters described the development of three map matching algorithms, and techniques for their validation. However, the performance of the map matching algorithms largely depends on the nature of the application and the types of data inputs. Both the quality of digital maps and the types of navigation data may affect the performance of a map matching algorithm.

This chapter describes the effects of navigation sensor and digital map quality on the performance of the developed map matching algorithms. The effects are quantified separately for suburban and urban road networks. The integrity method developed in Chapter 8 is also analysed in this chapter. The performances of the new map matching algorithms are then evaluated against those of existing map matching algorithms reviewed in Chapter 4 (Bernstein and Kornhauser, 1998; White et al., 2000; Greenfeld, 2002; Yu et al., 2002; Srinivasan et al. 2003, Yang et al., 2003; Fu et al., 2004; and Syed and Cannon, 2004).

9.2 Effects of Navigation Systems and Digital Map Quality

The quality of a digital map largely depends on the accuracy of the map. The map scale is normally considered as a good indicator for the accuracy of a digital map. Three map algorithms developed in this study can be tested with a choice of digital maps and navigation systems. The performance of a map matching algorithm can be evaluated for each pair of digital map and navigation system. The performance of GPS and GPS/DR is different in built-up areas as shown in Chapter 5. In suburban road networks the system performance may be therefore different from urban road networks with physical obstructions. Consequently, suburban and urban road networks are treated separately below.

9.2.1 Suburban Road Networks

Suburban areas are typically open and expansive with wide roads in predominantly open and clear areas where GPS signal blockage is minimal. The method adopted to quantify the effects of the quality of the digital map and navigation systems in suburban environments is presented below.

9.2.1.1 Methodology

Two types of navigation systems (GPS and GPS/DR) and three types of digital maps of different map scales (1:1250, 1:2500 and 1:50000) are taken as inputs to the map matching algorithms in order to assess their performance. As discussed in Chapter 3, the purpose of a map matching algorithm is twofold: (1) the identification of a link among the possible links, and (2) the estimation of the vehicle location on that link. Therefore, the performance of a map matching algorithm needs to be assessed in terms of both link identification and location estimation. Consequently, a higher accuracy reference (truth) of the vehicle trajectory is necessary to confirm the results of a map matching algorithm. The true link on which the vehicle is travelling and the actual physical location of the vehicle on that link can be determined using the carrier-phase observables from GPS (see Chapter 8, section 8.3). This process creates a reference trajectory.

The primary task is to compare the results (both the identification of the link and the physical location of the vehicle) obtained from the map matching algorithm and the reference trajectory. For a particular position fix, for example, if a link determined by the reference of the vehicle trajectory (true link) is the same as the link determined by the map matching algorithm then it can be said that the map matching algorithm identifies the link correctly. Based on this criterion, a percentage of correct link identification from all fixes can be calculated which gives a good indication for the assessment of the map matching algorithm in terms of link identification.

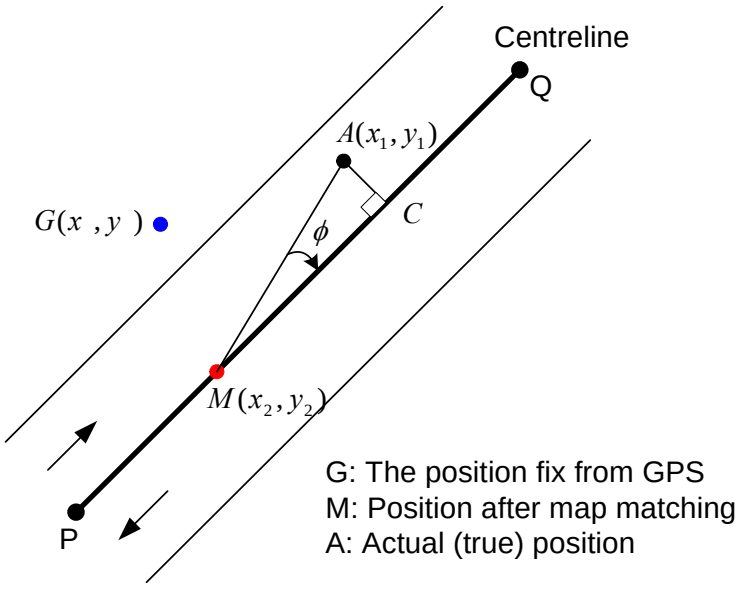

Figure 9.1: Determination of Error in map matching

Figure 9.1 shows a road segment in which the vehicle position from GPS/DR is denoted by the point *G (x, y)*, the corresponding map-matched location on the road centreline is represented by the point $M(x_2, y_2)$ and the actual (true) position of the vehicle from the true reference trajectory is indicated by the point $A\ (x_1, y_1)$ for a particular epoch *t*. Since the actual position of the vehicle at the same epoch *t* is at the point A, the map matching error in the easting coordinate is (x_2-x_1) and the error in the northing component is (y_2-y_1). The horizontal error (2-D) at epoch *t* (*MA*), therefore, is given by,

$$MA = \sqrt{(x_2 - x_1)^2 + (y_2 - y_1)^2} \qquad \textbf{(9.1)}$$

A series of such horizontal errors can be derived from this equation for all position fixes. The associated accuracy statistics derived from these errors (e.g., mean, standard deviation) can be used to determine the relative performance of the map matching algorithms. The along-track component of the horizontal error *MA* is *MC* and the cross-track component is *AC*. The angle ϕ can easily be derived from the absolute heading differenced between the line *MA* and the link *PQ*. The along-track and the cross-track errors can then be calculated from

$$MC = MA\cos\phi \qquad \textbf{(9.2)}$$

$$AC = MA\sin\phi \qquad \textbf{(9.3)}$$

The percentage of the correct link identification, the 2-D horizontal error (*MA*), along-track error (*MC*) and the cross-track error (*AC*) are used in the analysis that follows to compare the performance of the map matching algorithms based on the digital map quality and navigation sensor error.

9.2.1.2 Data processing

In order to assess the performance of the various map matching algorithms, a higher accuracy reference (truth) of the vehicle trajectory is essential. Therefore, the data obtained from the field tests in the west of London on the 5 July 2004 (see section 8.2.3 for details) and on the 18 August 2005 (see section 8.3.5 for details) were used to analyse the performance of the algorithms. Only good carrier-phase observations from GPS were used to derive the reference trajectory of the vehicle. This was achieved using a threshold for the standard deviation of the horizontal position solution as discussed in Chapter 8. A total of 2040 observations were obtained. The positioning data was then available from three sources: GPS carrier phase observables (2040 epochs), stand-alone GPS (9290 epochs), and GPS/DR (9290). Data from stand-alone GPS and GPS/DR was used as input to each of the map matching algorithms.

In order to investigate the effects of digital map quality on the performance of the map matching algorithms, three digital maps with different map scales were used. Two of these were obtained from the UK Ordnance Survey (UKOS) with map scale 1:1250 and 1:50000. The other digital map was obtained from Navigation Technologies (NavTech) which has a scale of 1:2500.

9.2.1.3 Results

The performance of the map matching algorithms can be assessed using the methodology explained in section 9.2.1.1. A total of 18 analyses (2 navigation systems, 3 digital maps and 3 map matching algorithms) were carried out. For each case, the percentage of correct link identification was calculated. Two dimensional (2-D) horizontal, along-track and cross-track positioning errors were also estimated for each of the 2040 truth observations using equations (9.1), (9.2) and (9.3).

Importance of Topological Data:

This section addresses the implication of topological information on the performance of map matching algorithms. Detailed results for the fuzzy logic map matching process are presented to show the variation in how the vehicle position fixes (before and after map matching) were plotted on different maps with dissimilar topological data. The results for a part of the test route are shown in Figure 9.2 for the map scale 1:50000, Figure 9.3 for the map scale 1:2500, and Figure 9.4 for the map scale 1:1250. In all cases, the navigation data were obtained from GPS/DR. Each of the round dots represents the vehicle position before map matching. The arrow symbols show direction of travel of the vehicle. Each of the triangular symbols represents the vehicle location on the links as estimated by the map matching algorithm.

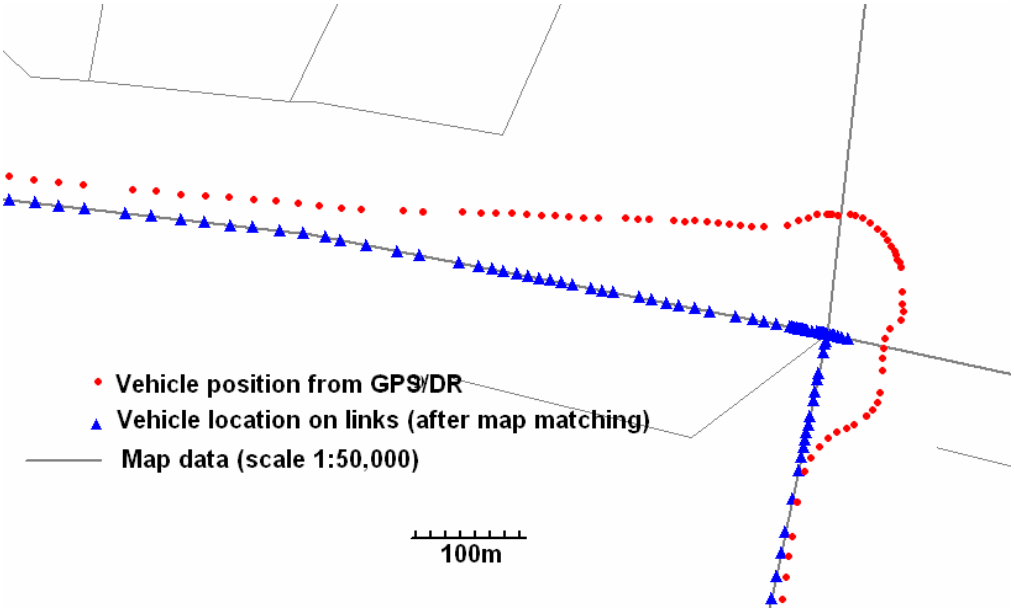

Figure 9.2: Fuzzy logic map matching results for positioning data from GPS/DR and digital map data from map scale 1:50000

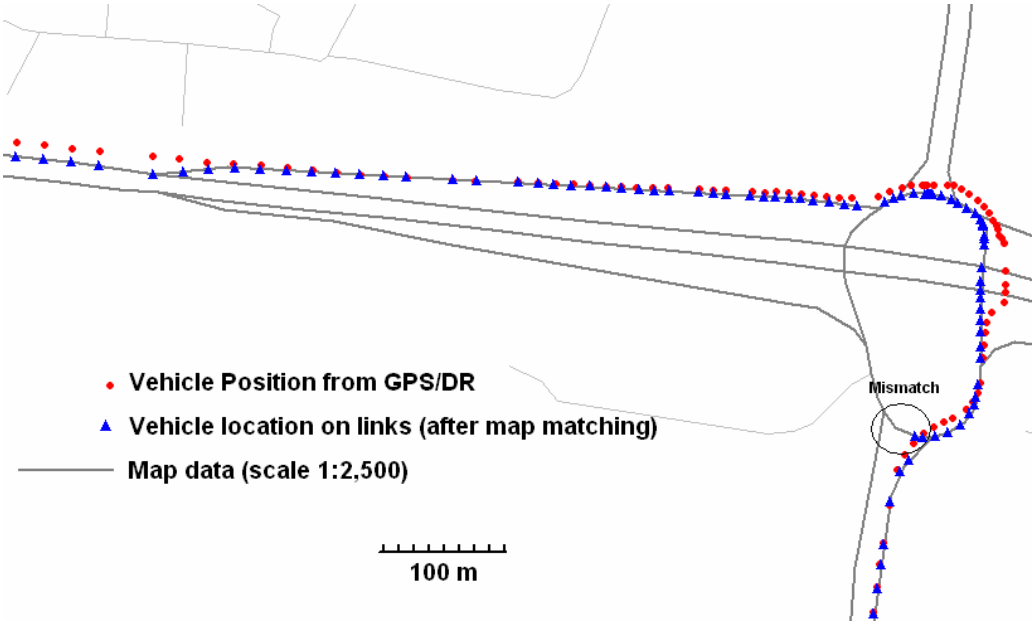

Figure 9.3: Fuzzy logic map matching results for positioning data from GPS/DR and digital map data from map scale 1:2500

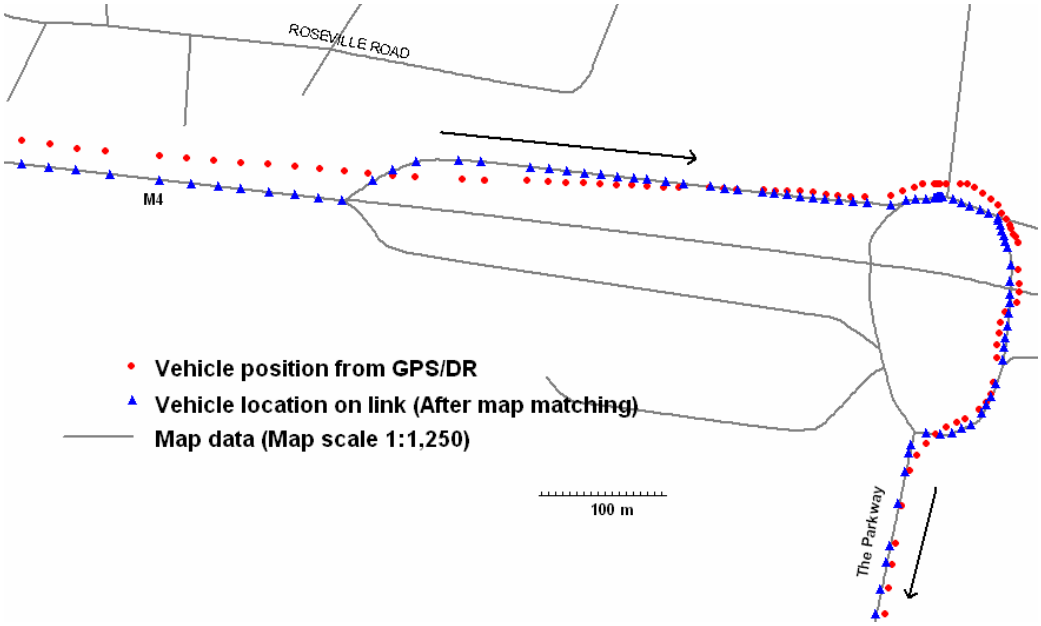

Figure 9.4: Fuzzy logic map matching results for positioning data from GPS/DR and digital map data from map scale 1:1250

From the layout of the digital maps presented in Figures 9.2, 9.3, and 9.4, it is apparent that the map data in Figure 9.2 has the most significant topological and geometric errors: many links are omitted compared to the other maps (Figure 9.3 and 9.4) and the vehicle trajectory derived from the positioning system deviates more from the road centreline. Therefore, one would expect that this map data (map scale 1:50000) will result in higher

map matching errors compared with the other maps. The digital map in Figure 9.4 has the highest map scale (1:1250) but the map in Figure 9.3 (1:2500) seems to have more topological information. For example, the motorway (M4) and dual carriage-way (The Parkway) are represented by two centrelines in Figure 9.3 - one for each direction of travel, whereas they are represented as just a single centreline in Figure 9.4. This should reduce map matching errors in terms of location estimation in Figure 9.3.

General Description of the Results:

Since all three map matching algorithms were tested using navigation data from both positioning systems and map data from three digital maps for the whole test road network, each map matching algorithm provides six sets (3x2) of different results. The results are shown in Table 9.1. The fourth column represents the percentage of correctly matched links. If a link ID estimated by a map matching algorithm for a particular position fix is the same as the link ID estimated by the higher accuracy GPS carrier phase for the same fix, then it is taken that the algorithm identifies the link correctly. The fifth, sixth and seventh columns (see Table 9.1) show horizontal accuracy (2σ), along-track accuracy (2σ) and cross-track accuracy (2σ) respectively. Horizontal accuracy was estimated using equation (9.1) and the along-track and cross-track accuracies were computed from the equations (9.2) and (9.3).

Table 9.1: The performance of map matching algorithms for various positioning systems and digital map data for the test road network

Map Matching Algorithms	Positioning Systems	Map Scale of Digital Maps	Correct Identification of Links (%)	Horizontal Accuracy (2σ, m)	Along-track Accuracy (2σ, m)	Cross-track Accuracy (2σ, m)
Improved Topological Approach	GPS	1:1250	88.7	20.3	19.5	4.7
		1:2500	87.5	20.0	19.1	4.8
		1:50000	75.5	42.8	41.8	9.8
	GPS/DR	1:1250	88.9	18.9	18.1	4.3
		1:2500	88.6	18.5	17.6	4.8
		1:50000	76.2	40.1	39.2	9.2
Probabilistic Approach	GPS	1:1250	97.6	10.5	9.8	4.1
		1:2500	97.8	9.2	8.1	4.5
		1:50000	83.2	30.2	28.9	8.1
	GPS/DR	1:1250	98.0	9.5	8.6	4.2
		1:2500	98.1	9.0	8.2	4.0
		1:50000	84.1	29.5	28.5	7.8
Fuzzy Logic Approach	GPS	1:1250	98.3	7.1	6.0	3.6
		1:2500	99.0	6.5	5.6	3.4
		1:50000	83.5	25.9	24.6	7.7
	GPS/DR	1:1250	99.1	5.5	4.3	3.5
		1:2500	99.2	5.5	4.2	3.2
		1:50000	84.1	24.0	22.8	7.7

Effects of Map Quality:

Table 9.1 shows that both positioning systems and the digital map quality affects the performance of the map matching algorithms. In particular, the effects of the quality of digital maps are quite apparent. The conventional topological map matching algorithm identifies about 88% of the links correctly if the digital map of map scale 1:1250 or 1:2500 are used. The identification of the correct links decreases to 76% if the map scale 1:50000 is utilised. The horizontal accuracy (2σ) is about 20m for map scale 1:1250 and 1:2500. However, this accuracy decreases to 43m for the map scale 1:50000. Along-track and cross-track errors also exhibit similar results. The condition improves in all cases to some extent once the navigation data is derived from the GPS/DR. However, the effects of digital maps remain considerable in the performance of the topological map matching algorithm. The results follow a similar pattern for the probabilistic and fuzzy logic map matching algorithms (see Table 9.1).

There is also not a major difference in the performance of the map matching algorithms when the digital map data come from either scale 1:1250 or scale 1:2500 (see Table 9.1). This is surprising as one would expect that a higher scale digital map (e.g., 1:1250) would give better map matching results. However, a higher scale map does not necessarily imply fewer geometric and topological errors, as shown in Figures 9.3 and 9.4. The map data of scale 1:2500 sometimes gives better results in terms of both correct link selection and location determination. The fuzzy logic map matching algorithm, for instance, identifies 99% of the link correctly with a horizontal accuracy of 6.5m (2σ) if the navigation data is from stand-alone GPS and map data is from a map scale of 1:2500. This is reduced to 98.3% with a horizontal accuracy of 7.1m (2σ) if map data comes from a map scale of 1:1250. One likely explanation for this is the single-centreline representation of multi-lane roads in the 1:1250 scale map. This suggests that correct topological information content is more important than map scale alone.

Effects of Navigation Sensors:

Interestingly, the effects of positioning systems (GPS and GPS/DR) on the performance of a map matching algorithm for a particular digital map is found to be minor both in terms of link identification and location estimation. The probabilistic map matching algorithm, for instance, identifies 97.6% of the links correctly when the navigation data comes from stand-alone GPS and the digital map data comes from a map of scale 1:1250. This is only increased to 98% when the navigation data comes from GPS/DR using the

same scale digital map. This is perhaps due to the fact that the test road network is within a suburban area which is predominately open and clear where the effect of multipath error is relatively low. The GPS/DR gives 100% coverage whereas GPS gives 99% coverage for the whole test road network, with a maximum GPS outage of only 5 seconds. Therefore, the position solutions from GPS and GPS/DR do not vary markedly. The situation might be different in built-up urban areas where GPS signal masking is a common phenomenon (see section 9.2.2). Taylor et al. (2005) found a substantial improvement in the horizontal accuracy of bus position when they utilised positioning data from GPS integrated with vehicle odometers in Central London. For a particular bus route, they showed that the integrated system provided a mean error of 8.8m compared with 53.7m for raw GPS without odometer.

Other Observations:

Along-track accuracies (between 4 m and 42 m, 2σ) are larger than cross-track accuracies (between 3 m and 10 m, 2σ) in all 18 cases presented in Table 9.1. This is an expected result as cross-track error is significantly reduced by the projection of the position fix on the road, provided the map matching algorithm can select the link correctly. The results are also consistent with those described in Kim et al. (2000).

The techniques used in the map matching algorithm also play an important role in the identification of the correct link and the determination of vehicle location. The topological map matching algorithm identifies about 76% of the links correctly with an accuracy of 40m (2σ) when the worst digital map (map scale 1:50000) is used. This increases to 84% with an accuracy of 24m (2σ) when the probabilistic map matching is applied.

For the given suburban test road network and for a particular positioning system and digital map, the fuzzy logic map matching algorithm is found to perform better compared to the topological and the probabilistic map matching algorithms. The fuzzy logic algorithm gives the best results when the positioning data is from GPS/DR and the map data is from a digital map of scale 1:2500. In this case, the map matching algorithm identifies 99.2% of the links correctly with a horizontal accuracy of 5.5 m (2σ), along-track accuracy of 4.2 m (2σ) and cross-track accuracy of 3.2 m (2σ).

Quality of Navigation Data:

To gain a full picture of the assessment, it is also essential to investigate how the quality of the navigation data affects the performance of the map matching algorithms. For this purpose, the epoch-by-epoch standard deviation (variance) of the errors associated with the map matching algorithm (calculated using equation (6.31)) and the navigation sensors (obtained from the variance-covariance (*vcv*) matrix) are examined.

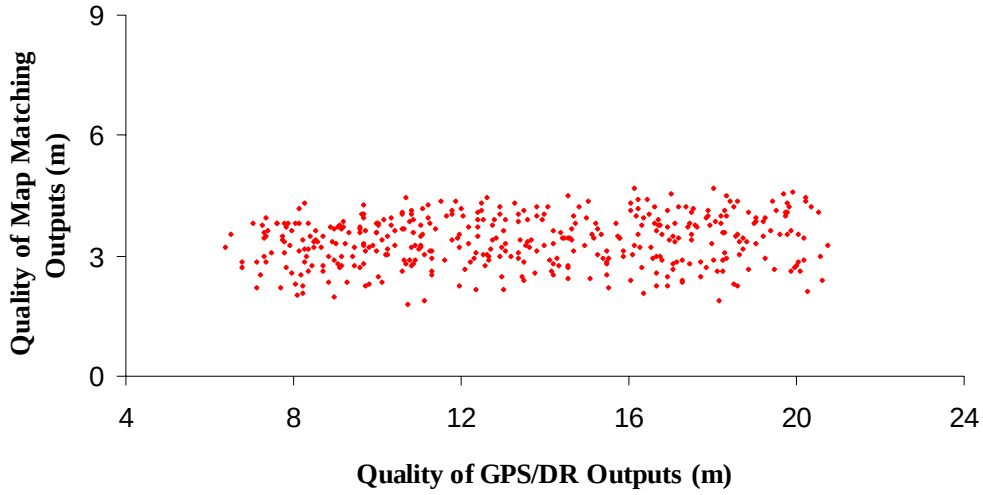

Figure 9.5: The sensitivities of GPS/DR on the performance of the fuzzy logic map matching algorithm

Figure 9.5 shows how the quality of the navigation sensors (GPS/DR) varies with the quality of the map matching algorithm (the fuzzy logic map matching algorithm) for a particular digital map (1:2500). The uncertainties involved with GPS/DR are between 5m and 22m as expected from data collection in an open area. The quality spread of the map matching algorithm is quite stable at (3m ± 1m). The results are relatively similar for other map matching algorithms. However, it is envisaged that the situation should be different in the built-up areas where the effects of multipath error and signal masking usually result in larger uncertainties associated with the GPS or GPS/DR (see section 9.2.2).

Computational speed:

All three map matching algorithms are designed to support ATT services in real-time. In other words, the estimation of map-matched vehicle location at the current epoch does not depend on the information from future epochs. However, in this research the algorithms

were implemented in a post-processing mode to allow the use of precise satellite ephemeredes in deriving the high quality validation datasets.

Computational performance is strongly influenced by the system hardware and the degree to which the code has been optimised. However, it was found that the computational time generally varies across algorithms and across digital road maps. Among the three map matching algorithms, the topological map matching algorithm is found to be the quickest for a given digital map. As a very rough guide, this algorithm takes approximately 5 seconds of CPU time (Pentium 4 CPU 2.66 GHz) to estimate the map-matched locations for 2040 seconds of positioning fixes on the suburban test route when the digital road network data comes from a map of scale 1:2500. This is reduced to 4 seconds when the digital map data comes from a map of scale 1:50000. For the same number of position fixes, the probabilistic and the fuzzy logic map matching algorithms take 7 and 9 seconds respectively when the map data comes from a scale of 1:2500.

Assessment of the Integrity Method:

The integrity of the map matching algorithms described in Chapter 8 was also analysed for each of the 18 cases shown in Table 9.1. The methodology to derive integrity was then applied to the dataset described in Chapter 8 (section 8.3.4). The integrity of the map matching algorithms for various navigation sensors and digital maps data is shown in Table 9.2. The threshold for the integrity is taken as 70 as discussed in Chapter 8. If the integrity associated with a map-matched location falls below 70, the algorithm gives a warning to the driver and the map matching algorithm re-identifies the vehicle location. The fifth, sixth, and seventh columns represent the false alarm rates (*FAR*), the missed detection rates (*MDR*), and the overall correct detection rates (*OCDR*) which were estimated using equations (8.26), (8.27), and (8.28) respectively. The *MDR* ranges between 0.7% and 8.5%. Better map matching algorithms (probabilistic and fuzzy logic) increase *OCDR*. No significant difference in *FAR, MDR, and OCDR* between the probabilistic and the fuzzy logic map matching algorithms is observed. The highest *OCDR* is found to be 98.2% when the fuzzy logic map matching was employed using the navigation data from GPS/DR and the map data from the map of scale 1:2500. The lowest *OCDR* of 84.2% is achieved with the topological map matching algorithm when the navigation data is from GPS/DR and the map data is from a map of scale 1:50000.

Table 9.2: The performance of integrity for map matching algorithms using various positioning systems and digital map data

Map Matching Algorithms	Positioning Systems	Map Scale	False Alarm Rates (%)	Missed Detection Rates (%)	Overall Correct Detection Rates (%)
Topological	GPS	1:1250	5.6	3.5	91.0
		1:2500	5.8	3.0	91.2
		1:50000	9.8	7.9	82.4
	GPS/DR	1:1250	5.7	3.6	90.7
		1:2500	6.0	3.0	91.1
		1:50000	10.2	8.5	81.3
Probabilistic	GPS	1:1250	1.5	1.0	97.5
		1:2500	1.3	1.2	97.5
		1:50000	3.1	4.3	92.6
	GPS/DR	1:1250	1.4	1.0	97.6
		1:2500	1.4	1.1	97.5
		1:50000	3.5	3.6	93.0
Fuzzy Logic	GPS	1:1250	1.3	1.0	97.7
		1:2500	1.3	0.7	98.0
		1:50000	2.5	3.0	94.5
	GPS/DR	1:1250	1.2	0.7	98.1
		1:2500	**1.1**	**0.7**	**98.2**
		1:50000	3.0	2.6	94.4

9.2.2 Urban Road Networks

It is essential that the navigation systems satisfy the RNP in urban areas due to the fact that a lot of benefits can be achieved by solving transport problems in these environments. As discussed in Chapter 2, this is difficult given the characteristics of urban areas, where physical obstructions are imposed due to buildings, urban canyons, narrow streets, tree canopies, tunnels, and very active electromagnetic interference, all of which can interfere with GPS signals.

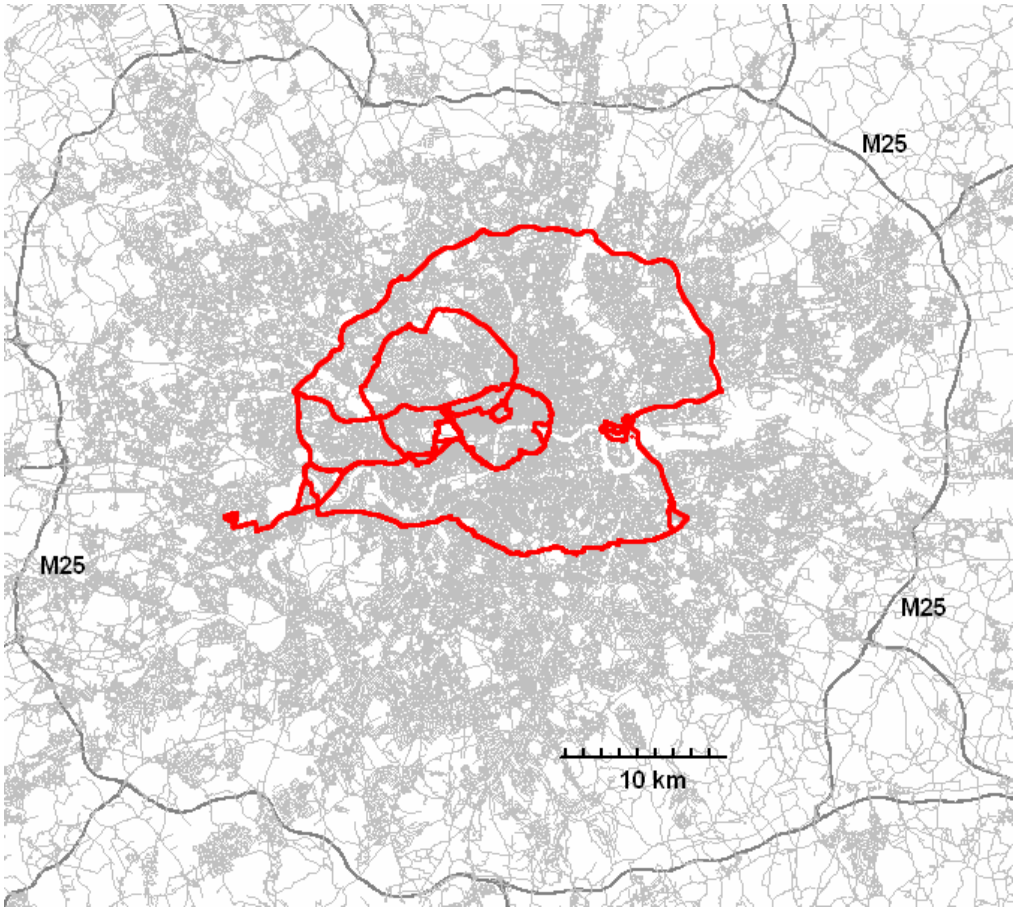

Figure 9.6: The urban test route in Inner London

In order to assess the performance of the map matching algorithms in an urban area, a large amount of navigation data (about 60,000 seconds) was used. This data was obtained from a series of comprehensive field trials in London between 2002 and 2005 (see Chapter 5 for a detailed description of the processing of these data) (Figure 9.6). The GPS coverage, as defined in Chapter 5, was found to be 95.5% for along the test route within the Inner London shown in Figure 9.6. The topological, probabilistic, and fuzzy logic map matching algorithms were applied to three types of digital maps of different map scales (1:1250, 1:2500 and 1:50000) together with two types of navigation systems (GPS and GPS/DR) in order to assess their performance for this test area.

The results of the fuzzy logic map matching algorithm on a complex part of the test route are shown in Figure 9.7 as an example. Some of the other complex parts of the test network have already been presented in Chapters 5, 6, and 7.

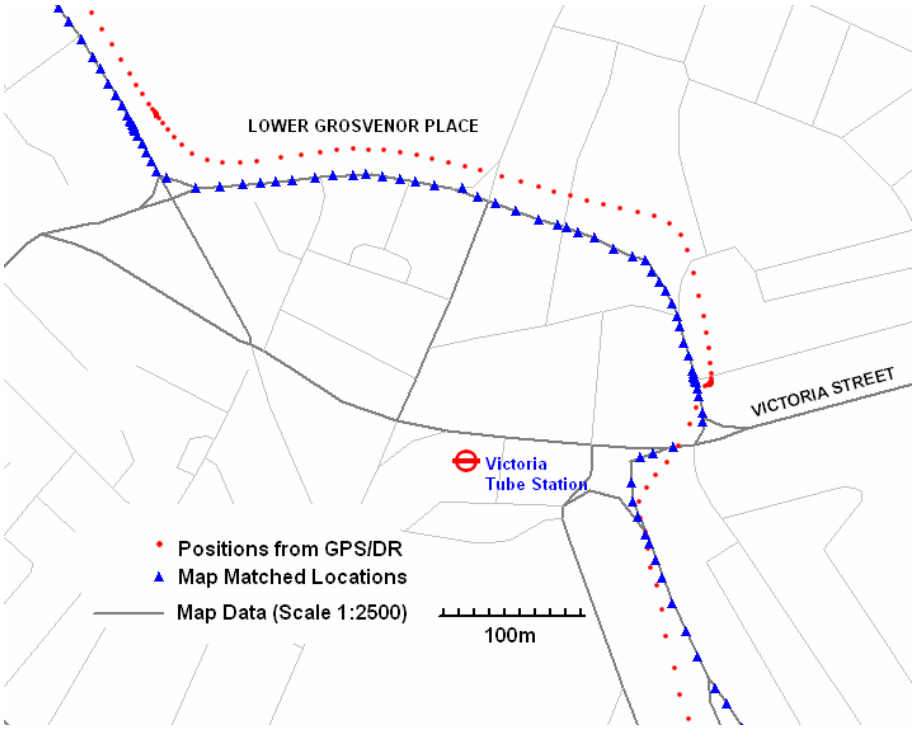

Figure 9.7: A complex part of the test route

The statistics generated from the results for the complete route are shown in Table 9.3. The fourth column represents the percentage of unfixed positions. The vehicle position is considered as unfixed when the stand-alone GPS does not provide a position fix and the map matching algorithm cannot fix the vehicle position during this period. The fifth column represents the percentage of correctly matched links. The sixth column indicates the average integrity value (level of confidence) of the map-matched positions calculated by the metric discussed in Chapter 8 (section 8.3). Because of frequent satellite loss-of-lock in built up areas, an effort to obtain the true vehicle position using GPS carrier phase data was unsuccessful. As a result, the determination of 2-D horizontal accuracy together with the cross-track and along-track errors offered by the map matching algorithms was not possible to estimate due to the lack of true vehicle positioning information. It was also not possible to evaluate the performance of the integrity method in terms of the false alarm rates (*FAR*), the missed detection rates (*MDR*), and the overall correct detection rates (*OCDR*) for an urban road network due to the same reason. The higher accuracy GPS carrier phase observations coupled with a high-grade inertial navigation system (INS) will potentially facilitate the measurement of reference (true) positioning data in urban areas. However, the performance of the map matching algorithms in terms of correct link identification could still be evaluated as the test vehicle travelled on a known route.

Table 9.3:The performance of map matching algorithms in urban road networks

Map Matching Algorithms	Positioning Systems	Map Scale of Digital Maps	Unfixed (%)	Correct Identification of Links (%)	Integrity (Average Level of Confidence) (%)
Geometric	GPS	1:1250	4.5	74.8	82
		1:2500	4.5	75.6	83.5
		1:50000	4.5	68.9	78.6
	GPS/DR	1:1250	0	79.1	83.8
		1:2500	0	80.1	82
		1:50000	0	76.5	77
Probabilistic	GPS	1:1250	4.5	91.1	85.4
		1:2500	4.5	90.2	90
		1:50000	4.5	77.1	79.8
	GPS/DR	1:1250	0	96.8	91.2
		1:2500	0	97.1	90.1
		1:50000	0	83.2	81.5
Fuzzy Logic	GPS	1:1250	4.5	92.2	92
		1:2500	4.5	93.1	92
		1:50000	4.5	78.9	81
	GPS/DR	1:1250	0	97.8	92.5
		1:2500	0	98.5	93
		1:50000	0	84.3	84

Table 9.3 shows that both positioning systems and digital maps affect the performance of the map matching algorithms in urban road networks. The effects of the quality of digital maps are quite similar to the effects that were observed for the suburban road networks shown in Table 9.1. However, the effects of navigation systems (GPS and GPS/DR) on the performance of the map matching algorithms in urban areas for a particular digital map are found to be quite significant in terms of correct link identifications. The probabilistic map matching algorithm, for instance, identifies 91% of the links correctly when the navigation data comes from stand-alone GPS and the digital map data comes from a map of scale 1:1250. This is increased to about 96.8% when the navigation data is obtained from GPS/DR. Due to inherent problems associated with the satellite signal masking along the test route, the stand-alone GPS is unable to provide position fixes 4.5% of the time. The positioning data from GPS are not fixed if the number of satellites is less than 4, or the HDOP is greater than 5. This has a significant impact on the performance of the map matching algorithms.

For a particular navigation system and digital map, the fuzzy logic map matching algorithm outperforms the topological and probabilistic map matching algorithms for the test route. Similar to the suburban road networks as shown in Table 9.1, the fuzzy logic

algorithm also gives the best results in the urban areas when the navigation data is obtained from GPS/DR and the map data is obtained from a digital map of scale 1:2500. In this case, the map matching algorithm identifies 98.5% of the links correctly. The average integrity value is high for all map matching algorithms.

9.3 Performance Compared with Existing Map Matching Algorithms

The performance of the map matching algorithms developed in this research can be evaluated against the performance of other existing map matching algorithms. The most utilised existing map matching algorithms in the literature are point-to-point matching (Bernstein and Kornhauser, 1998), point-to-curve matching (White et al., 2000), improved point-to-curve matching (Srinivasan et al. 2003), weighted topological analysis (Greenfeld, 2002), advanced weighted topological analysis (Yu et al., 2002), Dempster-Shafer's (D-S) theory of evidence (Yang et al., 2003), and fuzzy logic model (Fu et al., 2004; Syed and Cannon, 2004). The description of these eight algorithms can be found in Chapter 4.

Table 9.4: Performance of map matching algorithms

Map matching algorithms	**Correct link Identification** (%)	**Horizontal Accuracy** (2σ, m)	**Along-track errors** (2σ, m)	**Cross-track errors** (2σ, m)
Bernstein and Kornhauser (1998)	70.5	46.0	45.2	10.3
White et al. (2000)	76.8	32.0	29.5	10.1
Srinivasan et al. (2003)	80.2	21.2	18.3	10.3
Greenfeld (2002)	85.6	18.3	15.5	8.6
Yu et al. (2002)	86.3	19.5	19.1	6.9
Yang et al. (2003)	82.5	25.0	24.1	7.2
Fu et al. (2004)	80.5	23.0	22.0	8.5
Syed and Cannon (2004)	92.5	16.1	15.1	5.1
Topological (from this research)	**88.6**	**18.1**	**17.6**	**4.8**
Probabilistic (from this research)	**98.1**	**9.1**	**8.2**	**4.0**
Fuzzy logic (from this research)	**99.2**	**5.5**	**4.2**	**3.2**

The suburban route data described in section 9.2.1.2 are used to examine the performance of these algorithms in terms of the identification of correct links and the determination of 2-D horizontal accuracy together with the along-track and the cross-track errors. The methodology discussed in section 9.2.1.1 is utilised to quantify the performance of the map matching algorithms. The navigation data used to evaluate the performance of the algorithms is from GPS/DR and the digital map data is from the map of scale 1:2500. The results are shown in Table 9.4. The second column represents the percentage of correctly matched links. The third, fourth and fifth columns (Table 9.4) show horizontal accuracy (2σ), along-track errors (2σ, m) and cross-track errors (2σ, m) respectively. 2-D horizontal accuracy was estimated using equation (9.1) and along-track and cross-track errors were computed from the equations (9.2) and (9.3).

The results show that the probabilistic and fuzzy logic map matching algorithms developed in this study outperform all existing algorithms in terms of correct links identification, horizontal accuracy, along-track, and cross-track errors. The topological map matching algorithm also outperforms all existing algorithms except the fuzzy logic map matching algorithm developed by Syed and Cannon (2004). The fuzzy logic map matching algorithm gives the best results among all map matching algorithms evaluated for the test road networks.

9.4 Impact of the Research Findings on the Application Domains

This section describes the implication of the research findings on the performance of the navigation systems to support ATT services and requirements presented in Tables 2.1 and 2.3 respectively. This is to see whether the enhanced map matching algorithms developed in this thesis have the potential to support the RNP of ATTS.

The enhancements to the existing algorithms exploits all of the relevant data available from the key elements in this process i.e., GPS, DR, and map data. This research identifies a number of extra data not exploited in the previous research and uses these to enhance performance. As no extra data from other sensors are required, the improved algorithms can be implemented at no additional cost due either to the navigation sensors or map data.

High integrity map matching algorithms developed in this research have the potential to meet the RNP parameters for many ATT services listed in Tables 2.1 and 2.3. Among the three algorithms, the topological map matching algorithm is the simplest, fastest, and easiest to implement. This can be applied to ATT services where the requirement of positioning accuracy is about 20m (95%) and the integrity for these services is not critical. Integrity of a navigation system need to be expressed in terms of integrity risk, alert limits, time-to-alert, probability of missed detection, and probability of false alarm. As can be seen, Table 2.3 shows integrity in terms of the time-to-alarm only. Assuming the value of accuracy is the lowest allowable error in the navigation solution, the accuracies in Table 2.3 can be taken as the alert limits. Because there is no specification of others, these parameters derived empirically in this research using these alert limits. A range of such ATT services that can be supported by the improved topological map matching algorithm are *stolen vehicle recovery*, *fleet management* (parcel delivery services, taxi services, and haulage companies), *traveller services information*, and *on-board emissions monitoring*. The navigation data can be obtained from stand-alone GPS for a suburban area or GPS/DR for an urban area. However, a large scale digital map (usually 1:2500 or larger) is required. It is worth noting that a small scale map (e.g., 1:50000) cannot be used for such ATT services as this could lead an error up to 42m (95%).

The enhanced probabilistic map matching algorithm is appropriate for ATT services where the positioning requirement is about 10m (95%) and the availability of the integrity function is important. In addition to the above services that can also be supported by the probabilistic map matching algorithm, the additional services may include *route guidance*, *automatic vehicle location, accident and emergency service*, *rail position location, electronic payment system, and fleet management* (secure transport services). This algorithm has the capability to deliver the correct location information up to 97.5% of the time for a 2-hour trip (see Table 9.2). Given the importance of these services, it is suggested that the navigation data should be obtained from GPS/DR and the digital map data should be obtained from a map of scale 1:2500 or higher. This is because the performance of this algorithm is severely degraded when the navigation data comes from GPS alone (especially in urban areas) and the digital map data comes from a map of scale 1:50000.

As discussed in Chapter 2, there are potential economic, social, and environmental benefits in solving transport problems in urban areas. For this reason, higher accuracy as well as integrity may be required in urban areas compared to suburban or rural areas. Consequently, the fuzzy logic map matching should be employed for ATT services operating within urban areas as this algorithm can effectively identify the correct links 99.2% of the time with a positioning accuracy of 5.5m (95%). The integrity offered by this algorithm suggests that it is capable of providing the correct navigation solution up to 98.2% of the time. The additional potential ATT services that can be supported by this algorithm include *route guidance*, *bus priority at a junction*, *accident and emergency services*, and *automatic announcement of bus stops*. However, this algorithm is not capable of supporting the above services if the digital map data is obtained from a map of scale 1:50000 or smaller and the navigation data comes from stand-alone GPS (especially in urban areas).

Besides the above ATT services, there are many Location Based Services (LBS) that can be supported by the enhanced map matching algorithms. LBS builds upon two well-established areas of information technology: (1) wireless communication, and (2) spatial data management. While the primary role of the first technology is to provide a connection between a subscriber and a control centre, its proper function requires knowledge of the position of each subscriber to some degree of accuracy (Wong and Leung, 2000). New application domains for real-time LBS are emerging. These applications are largely driven by the expanding use of mobile phones. Another major push factor for implementing mass LBS markets is the two directives by the U.S. Federal Communications Commission (FCC) and the European Commission (EC) on emergency calls. Both the directives oblige wireless network operators to automatically communicate to the authorities the location of a user making an emergency call with a certain accuracy and integrity requirement. Today, mobile phone operators have a choice of half a dozen technologies for location determination, each with distinct power consumption, handset compatibility, time-to-first-fix, and in-building coverage characteristics. The most accurate and reliable positioning module could be the integration of GPS, DR and map data using a map matching algorithm. This is particularly feasible due to the recent development in MEMS-based small-sized and light-weight gyros. Although the RNP parameters for LBS applications are not clearly defined at the time of writing, it is envisaged that the developed map matching algorithms can effectively support many LBS applications including *location-based billing*, *emergency caller location*, *location of*

petrol stations, *tourist information* (museums, libraries, and monuments) and *location of other points of interest (*hotels, restaurants, and hospitals*)*.

Tables 9.1 and 9.3 suggest that the best performance can be achieved using the fuzzy logic map matching algorithm for both urban and suburban areas. This means that the enhanced map matching algorithms cannot support the navigation module of ATT services where an accuracy of greater than 5m (95%) is required. For this reason, some ATT services listed in Table 2.1 cannot be supported by the map matching algorithms developed in this research because of the requirement of high accuracy (1m, 95%) and high integrity. Examples include *longitudinal collision avoidance* and *intersection collision avoidance*.

An intersection collision avoidance system, for instance, determines the probability of collision at an intersection and provides timely warnings to approaching vehicles so that avoidance actions can be taken. This service builds on the Intersection Collision Warning infrastructure and in-vehicle equipment and adds equipment in the vehicle that can take control of the vehicle in emergency situations. The same monitors in the roadway infrastructure are needed to assess *vehicle locations* and speeds near an intersection. This information is determined and communicated to the approaching vehicle using a dedicated short-range communications (DSRC) system. The vehicle uses this information to develop control actions which alter the vehicle's speed and steering control and potentially activate its pre-collision safety system (ITS America, http://www.itsa.org). Although an intersection collision avoidance system has not been in-operation yet, the algorithms developed in this research may not be suitable to support the navigation module of this type of ATT service as it requires both vehicle-based and infrastructure-based technologies of higher accuracy to help drivers approaching an intersection understand the state of activities within that intersection. An alternative navigation module for such a service could be the integration of enhanced DGPS (phase smoothed code or differential carrier phase), high-grade INS, and large scale digital map data.

The map matching algorithms developed in this research need second-by-second GPS data (i.e., sampling rate of 1 Hz). A high capacity processor is not required to store these data. The argument is that some ATT services do not need fast information updates hence do not require a higher sampling rate. For example, public transport services may need to update the information at bus stops only every 10 seconds or so. Although the map

matching algorithms use a second-by-second input data, they can be assigned to give outputs at any interval greater than 1s. Since the on-board map matching enabled processor does not need to store all historical data, on-board memory capacity is not an issue. The storing of historical data in the on-board system largely depends on how frequently the information (location, speed, and heading) needs to be updated. If the information, for instance, needs updating every 1 minute, then the on-board system may need to store historical data for about 2 minutes (120 epochs).

9.5 Impact of Galileo and EGNOS on the Developed Algorithms

The potential impacts of Galileo (the new European global navigation satellite system) and EGNOS (the European Geostationary Navigation Overlay Service) on the performance of the map matching algorithms developed in this research are discussed below.

9.5.1 The impact of Galileo

As discussed in Chapter 2, the Galileo System will be an independent, global, European-controlled, satellite-based navigation system which will provide a number of services to users equipped with Galileo-compatible receivers. The Galileo system will provide the following navigation and Search and Rescue (SAR) services globally (ESA, 2002).

- *Open Service (OS)*: providing positioning, navigation and timing services, free of charge, for mass market navigation applications (like future GPS - SPS). Table 9.5 shows the service performances for the Galileo OS.

Table 9.5: Service performances for the Galileo OS (positioning)

Type of receivers	Carriers	Single frequency	Dual frequency
	Computes Integrity	No	
	Ionospheric corrections	Based on simple model	Based on dual frequency measurements
Coverage		Global	
Accuracy (95%)		H: 15m	H: 4m
		V: 35m	V: 8m
Integrity		Not applicable	
Availability		99.80%	

- *Commercial Service (CS)*: Generate revenue by providing added value over the *OS* such as dissemination of encrypted navigation related data (1 KBPS), ranging and timing for professional use with service guarantees.

- *Safety of Life Service (SoL)*: comparable with "Approach with Vertical Guidance" (APV-II) as defined in the ICAO Standards and Recommended practices (SARPs), and includes Integrity. Table 9.6 presents the service performance for the Galileo *SoL* service.

Table 9.6: Service performances for the Galileo Safety of Life Service

Type of receivers	Carriers	Three frequencies	
	Computes Integrity	Yes	
	Ionospheric corrections	Based on dual frequency measurements	
Coverage		Global	
Accuracy (95%)		Critical Level	Non-critical Level
		H: 4m	H: 220m
		V: 8m	V: 556m
Integrity	**Alarm limit**	H: 12m V:20m	H: 556
	Time-to-alarm	6 seconds	10 seconds
	Integrity risk	3.5x10-7 / 150 s	10-7/hour
Continuity risk		10-5/15 s	10-4/hour – 10-8/hour
Cetification/liability		Yes	
Availability of integrity		99.50%	
Availability of accuracy		99.80%	

- *Public Regulated Service (PRS)*: for applications devoted to European/National security, regulated or critical applications and activities of strategic importance - Robust signal, under Member States control.

- *The Search and Rescue (SAR) Service:* broadcasts globally the alert messages received from distress emitting beacons. It will contribute to enhance the performances of the international COSPAS-SARSAT Search and Rescue system.

It is envisaged that most ATT services will be supported by the combination of Galileo Open Service (OS) and the commercial service (CS) which will provide a horizontal positioning accuracy of 4m 95% of the time when a dual frequency Galileo receiver is used (Table 9.5). Given that stand-alone GPS provides an accuracy of 13m (95%), the integration of Galileo with DR will provide better positioning fixes. Therefore, the performance of a map matching algorithm will improve if the map quality allows.

The United States and the European Union (EU) signed an agreement to harmonize their respective satellite navigation systems: the existing U.S. GPS system and the planned European Galileo system during the U.S.-EU summit in Ireland (http://www.useu.be/Galileo). As a result, this opened the door for some future navigation receivers using both systems. This will provide the capability of computing the receiver location using a total of 54 satellites (both GPS and Galileo constellations). Therefore, the deployment of Galileo and the modernization of GPS over the next few years or so will have a profound impact on future GNSS receiver design. Currently in transport telematics applications, single frequency GPS receivers are used. However, in the future it will be possible to have affordable multi-frequency receivers. Such receivers will provide higher positioning accuracy, will be less susceptible to RF interference, and will be able to acquire and track lower strength signals than the current single frequency GPS receivers. In general, the cost of a future integrated GNSS receiver (GPS + Galileo) will be of the order of 10-20% more than a single-system receiver (Rizos, 2005). However, the navigation module of an ATTS will still require to be supported by a robust map matching algorithm. This is because:

- the positioning fixes obtained from an integrated GNSS receiver will still need to be placed on a known-road network where a spatial digital map is used as a physical reference for the vehicle.

- although the availability of satellites from a particular point on the earth will be increased, the effect of multipath and satellite blockage (including weak satellite configurations) on the performance of the quality of navigation solutions will remain a critical issue, especially in urban areas. The implication of this will be that augmentation with other sensors such as DR will still be required. A good example of this is the urban canyon where although more satellites will be visible, the geometry of the satellites with respect to the receiver will still be relatively weak. In such cases, a map matching algorithm will be required not only to identify the physical location of the vehicle but also to improve accuracy and availability of the positioning service.

It can be concluded that the navigation module of an ATTS with a high RNP requirement will still require a detailed map matching algorithm even when both GPS and Galileo are integrated. This will be particularly true for urban areas.

9.5.2 The impact of EGNOS

Although GPS provides users with their locations and other derivates in real-time, limitations on system performance and political considerations suggest that stand-alone GPS cannot always meet all the requirements of a range of ATT services and other safety-of-life (SOL) applications. Moreover, the US DoD, which operates GPS, does not guarantee the Standard Positioning Service (SPS). One solution to this is to develop an augmentation to GPS to improve accuracy, integrity, continuity, and availability (Ledinghen and Auroy, 2001). Therefore, Europe is developing a satellite-based regional augmentation system, known as the European Geostationary Overlay Service (EGNOS). The development of EGNOS started in the early nineties initiated by the Tripartite Group (ETG), comprising the European Space Agency (ESA), European Community (EC), and EUROCONTROL. The initial operation of EGNOS started in July 2005 (http://www.essp.be), with full operational capability expected in 2006. EGNOS has designed to provide the potential users with the following services (Sauer, 2004).

- GEO Ranging: Under this service, 3 GEO satellites transmit GPS-like L1 band signals which improve the availability.

- Integrity Channel: GPS/EGNOS integrity information is available in this service. This is expected to satisfy the integrity requirement for civil aviation up to Category I (*CAT I*) *Precision Approach*.

- Wide Area Differential: This service includes the broadcast of differential correction data to users. This enhances the accuracy of GPS/EGNOS.

Ledinghen and Auroy (2001) provide an overview of how Europe-wide civil aviation can benefit from EGNOS. Other transport sectors, especially land transport can also benefit from the use of EGNOS. The following scenarios are considered to discuss the potential impact of EGNOS on the performance of the map matching algorithm.

Scenario 1 (GPS + DR + Map Matching): This is the basic scenario on which this research is based. In this scenario, a map matching algorithm takes inputs from an integrated GPS/DR and a road map. The quality of the position solution from the GPS/DR depends among other things on the duration of GPS outage. In such cases, the

performance of a map matching algorithm depends on the performance of DR sensors, especially in a dense urban area where the visibility of GPS satellites is bad.

Scenario 2 (GPS+ EGNOS + DR+ Map Matching): In this scenario, a GPS receiver will be capable of receiving data as transmitted by the different services provided by EGNOS. This will facilitate to obtain a good quality GPS data due to the availability of differential corrections and marginally better geometry due to the additional data (GEO L1) for some instances where the EGNOS GEO satellites will be visible. These will lead to a marginally better positioning accuracy. Therefore, the improvement in the performance of the map matching algorithm is going to be marginal, especially in urban areas.

Scenario 3 (GPS + EGNOS(SISNet) + DR + Map Matching): In this scenario, the problem of the unavailability of GEO satellites in urban areas (scenario 2) is addressed to some extent by the development of an internet solution called SISNeT[37] which provides the wide-area differential correction data via the internet. SISNeT gives access to the corrections and the integrity information of EGNOS. Any user with access to the internet (usually through wireless networks i.e., GSM or GPRS) can access EGNOS through SISNeT. This will provide EGNOS differential correction data continuously. Therefore, it will be possible to have better quality GPS data for visible satellites at all times. This will always lead to the better quality positioning data. However, note that although with SISNet, visibility to the GEO will not be required, the GEO L1 data is effectively lost and that there will not be any improvement in satellite geometry. Therefore, there will be significant improvement in positioning accuracy when the geometry allows. Consequently, the improvement in the performance of the map matching algorithm will be significant and only constrained by the map quality.

Scenario 4 (GPS + EGNOS (conventional + SISNet) + DR + Map Matching): This is the combination of scenarios 2 and 3. In this scenario, a GPS receiver will be capable of receiving both differential correction data via SISNet and the additional data (GEO L1) directly from EGNOS. This will lead to a better GPS data at all times and a marginal improvement in geometry for some instances. The performance of the map matching algorithm will be significant if the map quality allows.

[37] http://esamultimedia.esa.int/docs/egnos/estb/sisnet/sisnet.htm

9.6 Constraints and Limitations

The map matching algorithms developed in this research overcome various shortcomings of existing algorithms. As a result, these algorithms possess the capability to support the navigation module of many ATTS listed in Table 2.1. These algorithms are validated and their performances are evaluated. It is found that a positioning accuracy up to 5.5m (95%) is achievable. An assessment of the integrity of these algorithms suggests that the integrity method has the ability to provide valid warnings to the driver up to 97.5% of the time. Among the three algorithms, the fuzzy logic map matching algorithm provides the best performance both in urban and suburban areas. However, the developed algorithms have some weaknesses that should be discussed. Therefore, some considerations for further improvement of map matching algorithms are reported in this section.

- a variety of thresholds were used to make the correct decision during various decision-making processes within the map matching algorithms. The threshold values were derived empirically from a series of field observations. Therefore, these values could vary in different operational environments. For example, the values of *a* and *b* (as shown in equation 5.6 in Chapter 5) were derived using the data from London. These values may be different when they are derived using the data from another city even with the same sensors. Therefore, it is suggested that a user needs to derive these values using the procedure outlined in section 5.3.1.4 prior to implementing the algorithm.

- the developed map matching algorithms may fail to identify the correct road segment in a section of roadway such as shown in Figure 9.8 Given that a map matching algorithm identifies the correct link, AB, for the position fixes P1 and P2, the identification of the correct link for the fix P3 may be incorrect if the perpendicular distance from P3 to link BC and BD is *equal*, and the heading of the vehicle from the navigation sensor is 90 degrees. This type of hypothetical road network may be observed in motorway diverging scenarios. Further improvement of map matching algorithms should focus on this type of scenario.

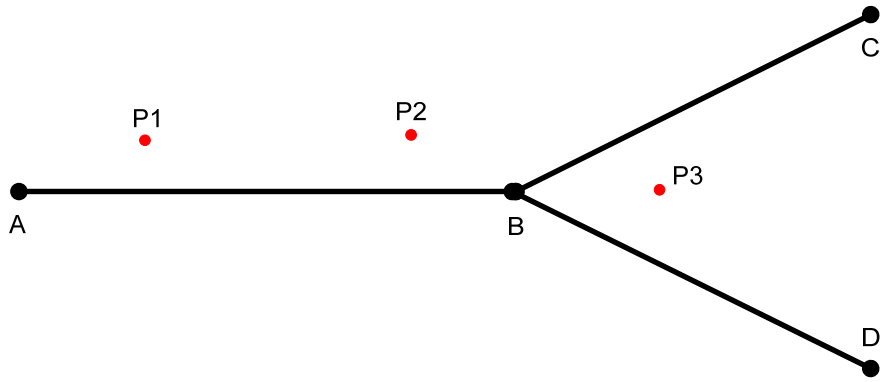

Figure 9.8: A hypothetical road network

- this research does not make use of height data from a navigation sensor[38]. This height data together with the data from a 3-D digital road network map can effectively identify the correct road segment at a section of roadway with flyovers. However, this will largely depend on the accuracy of height data and the availability of a high-quality 3-D road map.
- an examination is undertaken to see why a map matching algorithm fails to identify the correct links about 5-6% on average in the case of the probabilistic and fuzzy logic algorithms and 15-16% on average for the case of the topological algorithm. Although the preliminary results show that this is due to the error in map data (especially in a map of scale 1:50000), a number of mismatches are found at roundabouts. Therefore, future research should investigate in more detail the conditions upon which the algorithms fail and how to correct this.

- this research uses an empirical study to determine the *minimum speed* at which the heading of the vehicle from stand-alone GPS is incorrect. A more analytical approach may be needed to improve this value.

- the integrity method derived in the research is based on an empirical study. A more statistical approach can be used to detect outliers in the navigation solution.

[38] Note that height data from GPS is not as accurate as horizontal positioning data.

- the performance of the developed map matching algorithms in terms of positioning accuracy is not evaluated in this research. This is because the unavailability of high accuracy GPS carrier-phase observations in central London. Future research may utilize a high-grade INS integrated with GPS that may have the potential to provide the true vehicle trajectory in urban areas.

- the effects of the digital road network map on the performance of the map matching algorithms are evaluated using a map scale of 1:1250, 1:2500, and 1:50000. Clearly there is a large gap between map scales 1:2500 and 1:50000. It might be useful to include a map of scales 1:5000, 1:10000, and 1:25000. I addition to this, it would be interesting to see how the topological features of road map affect the performance of a map matching algorithm.

9.7 Summary

This chapter discussed the effects of navigation systems and digital maps on the performance of the three map matching algorithms developed in this research. This was achieved by testing the algorithms using inputs from two navigation systems (GPS and GPS/DR) and three digital maps of different map scales (1:1250, 1:2500, and 1:50000). The percentage of correct link identification and the determination of vehicle location by a map matching algorithm were found to be dependant on the map scale of digital maps. However, the difference in the performance of a map matching algorithm is small when the digital map data was taken from a large scale map (1:1250 or 2500). It was found that the digital map data of map scale 1:2500 gave better results in most cases. This is because this digital map has more topological features than the digital map of scale 1:1250. Therefore, both accurate road geometry and detailed road attributes (i.e., error related to topology) are equally important. Interestingly, the types of navigation data had very little effect on the performance of the map matching algorithm in the case of the suburban road network. This may be due to the fact that the test route is from a suburban area which is predominately open and clear where the effect of multipath error is relatively low.

The performance of the integrity measure was also evaluated for the map matching algorithms developed in this research. The results suggested that while the average integrity value is quite high for all map matching algorithms, the fuzzy-logic based integrity method has the highest potential to provide valid warnings to the driver.

On the other hand, both the navigation system and the digital map quality affected the performance of a map matching algorithm in urban road networks. The probabilistic map matching algorithm, for example, identified about 90.2% of the links correctly when the navigation data was obtained from GPS and the digital map data was obtained from a map of scale 1:2500. This was increased to about 97.1% when the navigation data came from GPS/DR. These differences in the performance are largely due to the unavailability of GPS signal in some urban areas. The navigation data from GPS/DR offers an improvement in the performance of all the map matching algorithms in urban areas. Of the three map matching algorithms tested, the fuzzy logic map matching process outperformed other map matching algorithms in urban areas.

The performance of the developed map matching algorithms was evaluated against the performance of some widely cited map matching algorithms. The developed algorithms outperformed all existing algorithms both in terms of correct link identification and location determination.

The impact of the research findings on the application domains presented in Chapter 2 is also discussed in this chapter. Moreover, the implications of the Galileo and EGNOS on the performance of the map matching algorithms are presented. This chapter ends with the limitations of the enhanced map matching algorithms developed in this research.

The next chapter ends the thesis with conclusions and recommendations for further research.

CHAPTER 10

CONCLUSIONS AND RECOMMENDATIONS

The primary aim of this thesis was to develop high integrity map matching algorithms in order to support the navigation module of a wide range of Advanced Transport Telematics Systems (ATTS). This section summarises the main conclusions and results obtained from the research. Furthermore, some recommendations based on the findings of this thesis for future research in the field of map matching algorithms are discussed.

10.1 Conclusions

This thesis has developed high integrity map matching algorithms suitable for supporting the navigation module to deliver a wide variety of advanced transport telematics (ATT) services. The conclusions are divided into several parts and are presented below.

10.1.1. Positioning Systems for the Navigation Module of ATTS

A review of the literature showed that a number of potential ATT services require the spatial and temporal positioning information of a vehicle or a fleet of vehicles. The RNP parameters of these ATT services indicated that the required 2-D horizontal positioning accuracy ranges from 5m to 50m (95%) with availability 99.7% of the time. Most of the existing navigation modules of ATTS used GPS and a digital road network map to locate the vehicle on the road segments. Such navigation modules are inadequate to support the navigation function of some ATT services requiring high positioning accuracy, especially in urban areas.

In order to attain continuous navigation data, especially in urban road environments, GPS data can be augmented with DR data using an Extended Kalman Filter (EKF) algorithm.

The results showed that GPS coverage in Inner London was 95.5% for the 60,000 seconds mission duration, while that of the integrated (GPS/DR) system was 100% (see Chapter 9). Therefore, stand-alone GPS could not be used for the navigation module of an ATTS in an urban area, but GPS/DR was found to be a good alternative. Although GPS/DR increased coverage in urban areas, it did not increase the positioning accuracy (see Chapter 5). Therefore, a *map matching algorithm* is an essential component of a navigation module of ATTS such as en-route guidance, fleet management, accident and emergency response, road user charging, public transport operations, traffic control and management, and on-board emissions monitoring systems.

10.1.2. Existing Map Matching Algorithms

This thesis reviewed an extensive literature on existing map matching algorithms and suggested that these algorithms were not appropriate to support the navigation function of some important ATT applications, for instance, accident and emergency management, en-route guidance, and public transport operations in which relatively high accuracy of positioning information is essential. Most authors also did not provide a meaningful validation technique to assess the performance of the map matching algorithms. None of the algorithms gave a quality indicator (level of confidence) for map-matched locations. Therefore, three map matching algorithms were developed in this research to overcome the limitations of the existing algorithms.

10.1.3. Enhanced Map Matching Algorithms

The first algorithm developed in this thesis was an improved topological map matching algorithm. This algorithm was designed to take inputs from GPS or GPS/DR. Data on the historical trajectory of the vehicle was used to avoid sudden switching of mapped locations between unconnected road links. The topological aspects of the road network such as link connectivity and curvature allowed improvements in performance of the algorithm, especially at junctions. Heading and speed data from the positioning system were also taken into account. The performance of the algorithm was evaluated against the performance of a widely cited map matching algorithm developed by Greenfeld (2002) for a typical road network configuration. The results showed that there was an improvement in performance for the new algorithm in terms of link identification. The algorithm was tested using positioning data from GPS/DR and road network data from a large scale digital map (1:1250). The results suggested that there was very good

agreement between the vehicle trajectory derived from the map-matched locations and the actual path taken by the vehicle. The algorithm was also applied to other road networks with varying levels of complexity. Although the performance of the algorithm was found to be superior compared to other existing algorithms, it was not always reliable in more complex road networks.

A probabilistic map matching algorithm was then developed to eliminate some of the problems associated with the topological map matching algorithm. This algorithm took all links as candidate links that fell within an error ellipse around a position fix. The error ellipse was formed from the error variance-covariance matrix associated with the positioning system. This eliminated the problem of outliers in the positioning data. The topology of the map, the orientation of the position fix relative to the link, the proximity of the fix to the link, the connectivity of the links at a junction and the historical trajectory of the vehicle were used to identify the correct link for a particular position fix. The field tests carried out in this research suggested that if the vehicle speed was less than 3 m/sec (10.8 km/hr) then GPS derived vehicle headings were not reliable. Most existing map matching algorithms including the algorithm developed in Chapter 5 use an orthogonal projection from the position fix to the link to estimate the vehicle location. Because of network mapping and GPS positioning errors, this is not a robust estimation of vehicle location as explained by Greenfeld (2002). An optimal estimation method was introduced in this research to determine vehicle location. This estimation took into account error sources associated with the network map and the navigation system. The probabilistic algorithm was then tested in complex urban road networks including a 5-legged roundabout. Results showed a good agreement between the vehicle trajectory acquired from the map-matched locations and the true path taken by the vehicle.

It was seen that the vehicle trajectory derived from the navigation system was quite different from the actual route due to the inherent problems associated with GPS in urban canyons as well as imperfections of the map database. Therefore, the error ellipse used in the probabilistic map matching algorithm to identify the correct link was relatively larger and contained a higher number of links. The topological and probabilistic map matching algorithms could not always distinguish precisely on which particular link the vehicle was travelling, as discussed in Chapter 7. Therefore, a fuzzy logic map matching algorithm was developed to deal with such uncertainties. In this algorithm, a set of knowledge-based IF-THEN rules were built based on consideration of the speed, heading and

historical trajectory of the vehicle, the connectivity and the orientation of the links, and the satellite geometric contribution to the positioning error (HDOP). A Sugeno-type fuzzy inference system was used where the membership functions were trained and modified using a sample dataset. The developed map matching algorithm was then tested in different road networks of varying complexity. The results showed that the map-matched locations agreed well with the known route along which the vehicle had travelled.

10.1.4. Validation and Integrity

The next step was to develop a validation strategy to assess the performance of the map matching algorithms. High precision positioning using GPS carrier-phase observables was employed in the validation methodology. Although the validation technique was generic, it was tested with the probabilistic map matching algorithm. The validation results revealed that a 98.1% correct link identification was achieved by this map matching algorithm. It was found that the horizontal position of the vehicle estimated from GPS C/A code-ranging deviated at most by 34m from its true position. The maximum horizontal position error of the vehicle was 11m from its true position after the application of the map matching algorithm, indicating that map matching improved the mapping of vehicle positions on a link. The estimate was further improved to within 6m in the estimation of the vehicle positions after adjusting map matching results to account for the fact that the digital map represents a road by its centreline. One of the interesting findings was that the matching of the vehicle positions on the road centreline introduced additional error. Consequently, if an accurate digital map is not used in map matching algorithms, the estimation of the vehicle positions may become worse than the positions from GPS C/A code-ranging. Another finding was that the vehicle heading derived from stand-alone GPS was significantly different from the true heading of the link especially at very low speed. Therefore, when headings are derived from GPS, they must be used carefully in map matching algorithms.

In order to quickly recover from a failure of the map matching algorithm, a measure of integrity (level of confidence) of a map matching algorithm was developed. A metric (0 to 100) to represent the integrity of the map-matched locations was developed based on various error sources associated with the position fixes, the digital map, and the uncertainty associated with the map-matched locations using a fuzzy logic method. It was found that an incorrectly map-matched location was usually related to integrity values of less than a threshold value (in this case, 70). The performance of the integrity measure

was evaluated for a suburban road network employing the three map matching algorithms developed in this research. The statistical parameters used to measure the integrity were the false alarm rates, the missed detection rates, and the overall correct detection rates. The performance of the integrity measure was found to be dependent on the map matching algorithms. The highest correct detection rate was found to be 98.2% when the fuzzy logic map matching algorithm was used. However, the performance of the integrity measure could not be evaluated for urban areas due to frequent satellite loss-of-lock which makes it difficult to obtain the true vehicle positions using GPS carrier phase data. The average integrity values of the developed map matching algorithms were then estimated and found to be between 78.2 (topological map matching) and 93 (fuzzy logic map matching) for the test route in the urban area.

10.1.5. Performance Evaluation

The effects of navigation sensors and digital map quality on the performance of three different map matching algorithms were investigated. Suburban and urban road networks were treated separately due to inherent problems associated with GPS signal masking in urban areas. The navigation sensors used for this purpose were stand-alone GPS and GPS/DR. Three digital maps of different map scales (1:1250; 1:2500; and 1:50,000) were used. The map matching algorithms were then tested in different road networks with varying complexity. These included complex roundabouts, merging or diverging sections of a motorway and complex road networks.

In the case of the suburban road networks, the accuracy of the map matching algorithms was validated against the high accuracy GPS carrier phase observables to determine the variation in performance based on these different criteria. It was found that the percentage of correct link identifications and the estimation of vehicle location (horizontal accuracy) by a map matching algorithm largely depended on the scale of the digital maps. The topological map matching algorithm, for instance, only identified about 76% of the links correctly with a horizontal accuracy of 43m (95%) when the digital map data of map scale 1:50,000 were used. The correct link identification increased to about 88% with a horizontal accuracy of 20m (95%) when the digital map data of map scale 1:1250 or 1:2500 were used. Similar results were obtained using the other map matching algorithms. However, the difference in the performance of the map matching algorithms was small when the digital map data were taken from a large scale map (1:1250 or 2500). The digital map data of map scale 1:2500 gave better results in most cases. This is

probably because this digital map had more topological features than the digital map of scale 1:1250. Therefore, one should not only rely on the map scale of the digital map as a measure of quality if a precise vehicle location is desired. More accurate road geometry as well as more detailed and accurate attributes (i.e., error related to topology) are important. Interestingly, the types of navigation data had very little effect on the performance of the map matching algorithm. This may be because that the test route is from a suburban area which is predominately open and clear where the effect of multipath error is relatively low. Of the three map matching algorithms tested, the fuzzy logic map matching process outperformed other map matching algorithms.

In the case of the urban road networks, it was not possible to derive the accuracy of the map matching algorithms due to an inability to obtain true vehicle positions in urban areas. However, the performance of the map matching algorithms was evaluated in terms of correct link identification. The results suggested that the quality of positioning systems and digital maps affected the performance of the map matching algorithms in urban road networks. The effects of the quality of digital maps were quite similar to the effects that were obtained for the suburban areas. However, the effects of navigation systems (GPS and GPS/DR) on the performance of the map matching algorithms in urban areas for a particular digital map were found to be quite different in terms of correct link identifications. The probabilistic map matching algorithm, for instance, identified about 90% of the links correctly when the navigation data was obtained from GPS and digital map data was obtained from a map of the scale 1:2500. This was increased to about 97% when the navigation data was obtained from GPS/DR using the same road map data. Similar to the suburban road networks, the fuzzy logic map matching algorithm gave the best results in urban road networks with an average integrity metric value of 93.

10.1.6. Comparison to Existing Map Matching Algorithms

The performance of the map matching algorithms developed in this research was also evaluated against the performance of the existing map matching algorithms identified in the case of this research. The results showed that the probabilistic and fuzzy logic map matching algorithms developed in this study outperformed all existing algorithms in terms of correct link identification, along-track, and cross-track errors. The fuzzy logic map matching algorithm gives the best results. The performance of the topological map matching algorithm was also found to be superior compared to the other existing map matching algorithms, excluding the algorithm proposed by Syed and Cannon (2004).

10.1.7. General Comments

If the navigation data comes from stand-alone GPS, then all the new map matching algorithms will be unable to match position fixes when GPS suffers signal masking.

Finally, it is important to note that although this research has made a significant contribution to the realisation of a robust and high integrity map matching algorithm, the validation of the map matching algorithms in terms of accuracy under harsh urban environments remains difficult to accomplish. Further research is still required in the areas discussed in the next section.

10.2 Recommendations

As a result of the experience gained during the course of this thesis, the following issues are recommended for further research in the field of map matching algorithms:

10.2.1. Integration of GPS and DR in the Measurement Domain

The integration of GPS and DR was achieved in the position domain (the *loosely coupled* approach). However, the integration can be performed in the measurement domain which is usually known as the *tightly coupled* approach where the height variable from a Digital Terrain Model (DTM) can be used as a known parameter in the Least Squares estimation of a position solution. For this purpose, the height data needs to be reasonably good. This will give a position solution from only three satellites and increases availability in urban areas when stand-alone GPS is used.

10.2.2. Validation of Map Matching Algorithms in Dense Urban Areas

Due to inherent problems associated with GPS signal masking and multipath error in dense urban areas, it was not possible to obtain the true vehicle positions from the GPS carrier phase observations and hence the accuracy offered by the developed map matching algorithms could not be estimated. However, a *tightly coupled* integrated navigation system employing GPS and a high-grade Inertial Navigation System (INS) may be used to obtain true vehicle trajectory in urban areas at the centimetre level. The cost of such a system prevented its use in this research.

10.2.3. Consideration of Road Design Parameters in Map Matching

Road design parameters such as turn restrictions at junctions, roadway classification (one-way or two-way) and overpass and underpass information were not included as inputs in the developed map matching algorithms as the data was not readily available. This information could potentially improve the performance of the map matching algorithms especially at junctions where the map matching sometimes gave unexpected results.

10.2.4. Improvement in the Derivation of Integrity

A simple method was used to derive the *"integrity"* of a map matching algorithm. Although the performance of the integrity method developed in this study is quite good for the test route, it is essential to investigate further the performance of the integrity method in other test routes, especially in urban areas. There are also ways to improve the integrity method. One way would be to consider the Receiver Autonomous Integrity Monitoring (RAIM) approach. However, the quality of the digital road network data needs to be incorporated in the RAIM process if the concept is to be applied to map matching algorithms.

10.2.5. Sensitivity Analysis using Different Digital Maps

This research set out to investigate a sample of existing map data (map scale 1:1250, 1:2500, and 1:50000 obtained from two different vendors) together with whatever topological data was attached to them. It should be noted that there are a variety of sensitivity-type analyses that could be carried out. An example is to investigate the effects of the digital map quality on the performance of map matching algorithms employing the digital maps with the same topological data but with varying map scales (for example, various maps from a particular vendor with map scales 1:1250, 1:2500, 1:5000, 1:10000, and 1:50000).

REFERENCES

Abraham, A. 2001. *Neuro-fuzzy systems: state-of-the-art modelling techniques, connedtionist models of neurons, learning process, and artificial intelligence.* Springer-Verlag Germany, Jose Mira and Alberto Prieto (Eds), Granada, Spain, pp.-269-276.

Anderson, J.M., Mikhail, E.M., 1998, *Surveying: theory and practice*, 7th edition, WCB/McGraw-Hill.

Abdel-Aty, M., Kitamura, R., Jovanis, P., 1995, *Investigating effect of travel time variabilityon route choice using repeated measurement stated preference data*. Transportation Research Record, 1493, 39 - 45.

Arnott, R., De Palma, A., Lindsey, R., 1991, *Does providing information to drivers reducetraffic congestion*, Transportation Research A, 25(5), 309 - 318.

ATIP, Asian Technology Information Program, 2002, *REPORT: ATIP02.022: Mobile Internet Navigation Services*, May 29.

Bentley, J.L., Mauer, H.A., 1980, *Efficient worst-case data structures for range searching*. Acta Inf. 13, 155-168.

Bernstein D., Kornhauser A., 1996, *An introduction to map matching for personal navigation assistants*. http://www.njtude.org/reports/mapmatchintro.pdf. Accessed June 19, 2002.

Bernstein, D., Kornhauser, A., 1998, *Map matching for personal navigation assistants*. In proceedings of the 77th annual meeting of the Transportation Research Board, 11-15 January, Washington D.C.

Bouju, A., Stockus, A., Bertrand, F., Boursier, P., 2002, *Location-based spatial data management in navigation systems*, IEEE Symposium on Intelligent Vehicle, 1, 172-177.

Brunner, F.K., Welsch, W.M., 1993, *Effect of the troposphere on GPS measurements*. GPS World, 4(1), 42-51.

Bullock, J.B., Krakiwsky, E.J., 1994, *Analysis of the Use of Digital Road Maps in Vehicle Navigation*. Position Location and Navigation Symposium, 1994., IEEE, 11-15 April, pp. 494 - 501, Las Vegas, NV.

Buxton, J.L., Honey, S.K., Suchoweskyj, W.E., Temoelhof, A., 1991, The Travelpilot: a second-generation automatic navigation system, IEEE Transactions on Vehicular Technology, Vol., 40, No. 1.

Catling, I., 2000, *Road user charging using vehicle positioning systems*, Tenth International Conference on Road Transport Information and Control**,** London.

Chadwick, D., 1994, *Projected navigation system requirements for intelligent vehicle highway systems*. In: Proceedings of Institute of Navigation GPS-94, 485–490.

Chen, W., YU, M., Li, Z.-L., Chen, Y.-Q. 2003. *Integrated Vehicle Navigation System for Urban Applications*. GNSS 2003, Graz, April , CD-ROM, 15 pp.

Collier, W.C., 1990, *In-vehicle route guidance systems using map-matched dead reckoning*. Position Location and Navigation Symposium, IEEE, 359-363, 20-23 March, Las Vegas, NV.

Czerniak, R.J. and Reilly, J.P., 1998, *NCHRP Synthesis of Highway Practice 258: Applications of GPS for Surveying and Other Positioning Needs in Departments of Transportation*, Transportation Research Board, National Research Council, Washington, D.C.

DETR, 1999, *Traffic Advisory Leaflets 07/99: The "SCOOT" Urban Traffic Control System*, UK.

DoT, 1998, *Intelligent transportation systems: real world benefits*, FHWA-JPO-98018, USA.

Drane, C.R., Rizos, R., 1998, *Positioning systems in intelligent transportation systems*, Norwood MA: Artech House.

Elliot, S.D., Darley, D.J., 1995, *Wireless communications for intelligent transportation systems*, Norwood, MA: Artech House.

Ericsson, E., 2001, I*ndependent driving pattern factors and their influence on fuel-use and exhaust emission factors*, Transportation Research Part D: Transport and Environment: 6(5), 325-345

ESA (European Space Agency), 2002, Galileo: mission high level definition. Available at: http://www.esa.int.

Farrell, J.A., Barth, M. 1999. *The Global Positioning System & Inertial Navigation*. McGraw-Hill, New York.

Ferman, M.A., Blumenfeld, D.E., Xiaowen, D, 2003, *A simple analytical model of a probe-based traffic information system*, Intelligent Transportation Systems, Proceedings 2003 IEEE, Vol. 1, 12-15 October.

Fernow, J. and Loh, R., 1994, *Integrity Monitoring in a GPS Wide-Area Augmentation System (WAAS)*. *DSNS 94*, London, UK. 1-8.

Fontana, R., Cheung, W., Stansell, T., 2001, The modernised L2 civil signal, GPS World, 12(9), 28-32.

Foster, M.R., 1989, *Vehicle Location for route guidance*. Vehicle Navigation and Information Systems Conference, IEEE, pp. 11-16, 11-13 September. Toronto, Ontario, Canada.

French, R.L., 1989, *Map matching origins, approaches, and Applications*, In Proceedings on the Second Symposium on Land Vehicle Navigation, 91-116.

Frey, H.C., Rouphail, N.M., Unal, A., Colyar, J.D., 2001. *Measurement of on-road tailpipe CO, NO and hydrocarbon emissions using a portable instrument*. In Proceedings

of the Annual Meeting of the Air and Waste Management Association, June 24-28, Orlando, Florida.

FRP, 2001, *Federal radionavigation plan*. http://www.navcen.uscg.gov/pubs/frp2001/, accessed August 2004.

Fu, M., Li, Jie, Wang, M., 2004, *A hybrid map matching algorithm based on fuzzy comprehensive Judgment*, IEEE Proceedings on Intelligent Transportation Systems, 613-617.

Fuchs, H., Kedem, Z.M., Naylor, B.F., 1980, *On visible surface generation by a priori tree structures*. Comput. Graphics, 14, pp. 124-133.

Gelb, A., 1979, *Applied Optimal Estimation*. The MIT Press.

Goodwin, C. and Lau, J. 1993. *Vehicle Navigation and Map Quality.* In Proceedings of the IEEE-IEE Vehicle Navigation & Information Systems Conference, pp. 17-20, Ottawa.

Greenfeld, J.S., 2000, *Automatic vehicle locations for transit operation*, In Processings of the 10th Mediterranean Electrotechnical Conference, 2, 656-659.

Greenfeld, J.S., 2002, *Matching GPS observations to locations on a digital map.* In proceedings of the 81st Annual Meeting of the Transportation Research Board, January, Washington D.C.

Grewal, M.S., Weill, L.R., Andrews, A.P., 2001, *Global positioning systems, inertial navigation, and integration*, John Wiley and Sons.

Hansen, M. and Yuanlin, H., 1997, *Road supply and traffic in California urban areas*, Transportation Research A, 31: 205-218.

He, X.F., Law, C.L., King, K.V., 2001, *GPS based IPS for ERP vehicles*, IEEE Magazine on Aerospace and Electronic Systems, 16(9), 10-14.

Heroux, P, Kouba, J., Collins, P., Lahaye, F., 2001, *GPS Carrier-phase point positioning with precise orbit products*, Proceedings of the KIS 2001, Banff, Alberta, Canada, June 5-8, CD-ROM.

Hofmann-Wellenhof, B., Lichtenegger, H., Collins, J., 2001, *GPS theory and practice*. SpringerWien, Nework.

Holmen, B.A., Niemeier, D.A., 1998, *Characterizing the effects of driver variability on real-world vehicle emissions*. Transportation Research D, 3(2), pp.117-128.

Honey, S.K., Zavoli, W.B., Milnes, K.A., Phillips, A.C., White, M.S., Loughmiller, G.E., 1989, *Vehicle navigational system and method*, United States Patent No., 4796191.

Hopfield, H., 1969, *Two-quartic tropospheric refractivity profile for correcting satellite data*, Journal of Geophysical Research, 74(18).

Hotchkiss, N.J. 1999. *A comprehensive guide to land navigation with GPS.* Alexis Pub, 3rd Edition, ISBN: -187.

Huang, L.-J., Kao, W.W., Oshizawa, H., Tomizuka, M., 1991, *A fuzzy logic based map matching algorithm for automotive navigation systems*, IEEE Roundtable Discussion on Fuzzy and Neural Systems, and Vehicle Applications, Paper No., 16.

ICAO, 1997, *All Weather operations panel, advanced surface movement guidance and control systems*, Draft 4, January.

ICD-GPS-200C, 2000, *Interface control document ICD-GPS-200C, Revision C*, IRN-200C-004, April 12, ARINC, Incorporated, EI Segundo, CA.

ITS America, 1992, *Strategic plan for intelligent vehicle highway systems in the United States*, Washington, D.C.

Jackson, P., 1995, *How will route guidance and navigation systems affect cognitive maps?* Proceedings of the PTRC, the 23rd European Transport Forum, Warwick University, 11-15 September, UK.

Jo, T., Haseyamai, M., Kitajima, H., 1996, *A map matching method with the innovation of the Kalman filtering*. IEICE Trans. Fund. Electron. Comm. Comput. Sci. E79-A, pp 1853-1855.

Joppe, M., 2000, *The Research Process* on www.ryerson.ca/~mjoppe/rp.htm
Kaplan E.D., 1996, *Understanding GPS: Principles and Applications*, Artech House, London.

Kao, W.W., Huang, L.-J., 1994, *System and method for locating a travelling vehicle*, United States Patent No., 5283575.

Kelly, K. T., 1996, *The logic of reliable inquiry*. New York: Oxford University Press.

Kim, J.S., Lee, J.H., Kang, T.H., Lee, W.Y., Kim, Y.G., 1996, *Node based map matching algorithm for car navigation system*, Proceeding of the 29th ISATA Symposium, Florence, 10, 121-126.

Kim, S., Kim, J., 2001, *Adaptive fuzzy-network based C-measure map matching algorithm for car navigation system*, IEEE Transactions on industrial electronics, 48 (2), 432-440.

Kim., S., Kim, J.-H, Hyun, I.-H, 1998, *Development of a map matching algorithm for car navigation system using fuzzy Q-factor algorithm*. In proceedings of the World Congress Intelligent Transport System, October, Seoul, Korea.

Kim, W., Jee, G, Lee, J., 2000, *Efficient use of digital road map in various positioning for ITS*, IEEE Symposium on Position Location and Navigation, San Deigo, CA.

Kirson, A, 1992, *ATIS-a modular approach Position Location and Navigation Symposium*, IEEE, 528-533, 23-27 March, Monterey, CA.

Klein, L.A., 2001, *Sensor technologies and data requirements for ITS*, Artech House.

Klobuchar, J.A., 1987, *Ionospheric time-delay algorithm for single-frequency GPS users,* IEEE Transactions on Aerospace and Electronic Systems, AES-23(3), 325-331.

Klobuchar, J.A., 1991, *Ionospheric effects on GPS*, GPS World, 2(4): 48-51.

Klobuchar, J.A., 1996, *Ionospheric effects on GPS*, In: Parkinson, Spilker (eds), Vol. 1, Chap 12: 485-515.

Krakiwsky, E.J, 1993, The diversity among IVHS navigation systems worldwide, IEEE-IEE Vehicle Navigation and Information Systems Conference, Ottawa, 433-436.

Krakiwsky, E.J., Harris, C.B., Wong, R.V.C., 1988, *A Kalman filter for intrgrating dead reckoning, map matching and GPS positioning*. In: Proceedings of IEEE Position Location and Navigation Symposium, 39-46.

Lachapelle, G., 1990, *GPS observables and error sources for kinematic positioning*. In: Schwarz KP, Lachapelle G (eds): Kinematic system in geodesy, surveying, and remote sensing, Springer, 17-26.

Leica Geosystems AG, 2001, *User guide v 2.1: SkiPro GPS post-processing software*, Roosendaal, The Netherlands.

Leick, A., 2004, *GPS Satellite Surveying*, Third Edition, John Wiley & Sons.

Ledinghen, N., Auroy, J., 2001, EGNOS: European Satellite Navigation System, *Alcatel Telecommunications Review*, 4th Quarter, 279-284.

Li, J., Fu, M., 2003, *Research on route planning and map-matching in vehicle GPS/dead-reckoning/electronic map integrated navigation system*, IEEE Proceedings on Intelligent Transportation Systems, 2., 1639-1643.

Liu, H.X., Recker, W., Chen, A., 2004, *Uncovering the contribution of travel time reliability to dynamic route choice using real-time loop data*, Transportation Research A, 38(6), 435-453.

Mamdani, E.H., S. Assilian. 1975, *An experiment in linguistic synthesis with a fuzzy logic controller*. International Journal of Man-Machine Studies, Vol. 7, No. 1, pp. 1-13, 1975.

MathWorks, 2000, *Fuzzy logic toolbox user's guide*. The Mathworks inc., Natick, MA.
Mazzoleni, R, 2001, *Electronic toll collection (ETC) in Dulles corridor*, in Stough, R. (eds) , Intelligent transport systems: cases and policies, Edward Elgar Publishing, pp.47-72.

McDonald, K., 1999, *Opportunity knocks. Will GPS Modernization Open Doors?* GPS World, 10(9), 36-46.

McLellan, J.F., Krakiwsky, E.J., Schleppe, J.B., Kanpp, P.L, 1992, *The NavTrax fleet management*, Position Location and Navigation Symposium, IEEE, Monterey, CA.

McQueen, B., McQueen, 1999, *Intelligent transportation systems*, Artech House.

Meng, Y., Chen, W., Chen, Y., Chao, J.C.H., 2003, *A simplified map-matching algorithm for in-vehicle navigation unit*. Research Report, Department of Land Surveying and Geoinformatics, Hong Kong Polytechnic University.

Mohring, H., 1999, *Congestion*, in Jose A. Gomez-Ibanez, William B. Tye, Clifford Winston (eds), *Essays in transportation economics and policy*, Washington, D.C.: Brookings Institution Press, pp. 181-221.

Montenbruck, O., Gill, E., 2000, *Satellite, orbits, models methods applications*, Springler, Berlin, Heidelberg, New York.

Nam, E.K., Gierczak, C.A., Butler, J.W., 2003, *A comparison of real-world and modelled emissions under conditions of variable driver aggressiveness*. Paper presented at the 82nd Annual Meeting of the Transportation Research Board, January 12-16, Washington D.C.

Najjar, M.E., Bonnifait, P., 2003, *A roadmap matching method for precise vehicle Localization using belief theory and Kalman filtering*. The 11th International Conference in Advanced Robotics, Coimbra, Portugal, June 30 - July 3.

Nijkamp, P., Pepping, G., Banister, D., 1996, *Telamatics and transport behaviour*, Springer-Verlag.

Noland, Robert B., 2001, *Relationships between highway capacity and induced vehicle travel*, Transportation Research A, 35(1): 47-72.

Noland, R.B., Cowart, W.A., 2000, *Analysis of metropolitan highway capacity and the growth in vehicle miles of travel*. Transportation 27: 363-390.

North, R.J., Ochieng, W. Y., Quddus, M.A., Noland, R.B., and Polak, J.W., 2005, *Validation and Characterisation of a Vehicle Performance and Emissions Monitoring System*, Transport: Proceedings of the Institution of Civil Engineers, 158: 167-177.

Noronha, V., Goodchild, M.F., 2000, *Map accuracy and location expression in transportation reality and prospects*. Transportation Research C, 8, 53-69.

NRC, National Research Council, 2002, *Collecting, processing and integrating GPS data with GIS*. NCHRP Synthesis 301. National Academy Press; Washington D.C.

NRC, National Research Council, 2004, *Development and deployment of standards for intelligent transportation systems: a review of the federal program*, Special Report 280, Transportation Research Board, National Academy Press; Washington D.C.

Ochieng, W.Y., 2004, *The Global Positioning System (GPS): an overview and data processing models.* MSc. (Transport) Lecture Notes, Centre for Transport Studies, Imperial College London.

Ochieng, W.Y., Flament, D., 1996, *The EGNOS baseline design handbook.* European Space Agency. Toulouse, France.

Ochieng, W.Y., Sauer, K., 2002, *Urban Road Transport Navigation: Performance of GPS after Selective Availability*, Transportation Research C, 10 (3), pp.171-187.

Ochieng, W.Y., Shardlow, P.J., Johnston, G., 1999, *Advanced transport telematics positioning requirements: an assessment of GPS performance in greater London*. Journal of the Institute of Navigation, 52 (3), 342–355.

Ochieng, W.Y., Sauer, K., Walsh, D., Brodin, G., Griffin, S., Denney, M., 2003a, *GPS integrity and potential impact on aviation safety*, The Journal of Navigation,56, 51-65.

Ochieng, WY., Polak, JW., Noland, RB., Park, J-Y, Zhao, L., Briggs, D., Gulliver, J,. Crookell, A., Evans, R., Walker, R., Randolph, W., 2003b, *The Development and Demonstration of a Real Time Vehicle Performance and Emissions Monitoring System*, Traffic Engineering and Control, 44 (6), pp.352-356.

Ochieng, WY., Polak, JW., Noland, RB., Park, J-Y, Zhao, L., Elliott, P., Briggs, D., Gulliver, J, Crookell, A., Evans, R., Walker, R., Randolph, W., 2003c, *Integration of GPS and Dead Reckoning for Real Time Vehicle Performance and Emissions Monitoring*, GPS Solutions Journal, 6 (4), 229-241.

Ochieng, W.Y., Quddus, M.A., Noland, R.B., 2004, *Integrated positioning algorithms for transport telematics applications*. In proceedings of the Institute of Navigation (ION) annual conference, 20-24 September, California, USA.

Parkinson, B.W., Spilker, Jr., Axelrad, P, 1996, *Global positioning system: theory and applications*, Volume 1-2, AIAA, Washington, D.C.

Phuyal, B., 2002, *Method and use of aggragated dead reckoning sensor and GPS data for map matching*, In proceedings of the Institute of Navigation (ION) annual conference, 20-27 September, Portland, OR.

Pyo, J., Shin, D., Sung, T., 2001, *Development of a map matching method using the multiple hypothesis technique*, IEEE Proceedings on Intelligent Transportation Systems, 23-27.

Quddus, M.A., Ochieng, W.Y., Zhao, L., Noland, R.B., 2003, *A general map matching algorithm for transport telematics applications*. GPS Solutions, 7(3), 157-167.

Raquet, J.F., 1998, *Development of a method for kinematic GPS carrier-phase ambiguity resolution using multiple reference receivers*, Ph.D. thesis, University of Calgary, Department of Geomatic Engineering.

Ried, D.B., 1979, *An algorithm for tracking multiple targets*, IEEE transactions on Automatic Control, AC-24, 843-854.

Rizos, C., 2005, *Trends in geopositioning for LBS, navigation, and mapping*, Working paper, School of Surveying and Spatial Information Systems, The University of New South Wales.

Ruimin, L.,Qixin, S., 2003, *Study on integration of urban traffic control and route guidance based on multi-agent technology*, IEEE Proceedings of Intelligent Transportation Systems, 2, 1740-1744.

Sandhoo, K., Turner, D., Shaw, M., 2000, *Modernization of the Global Positioning System*, In Proceedings of the 13th International Technical Meeting of the Satellite Division of the Institution of Navigation, 2175-2183, Institute of Navigation, Salt Lake City, Utah.

Sauer, K., 2004, *Integrated high precision kinematic positioning using GPS and EGNOS observations*, PhD dissertation, Imperial College London, UK., 2004.

Scott, C.A., 1994, *Improved GPS positioning for motor vehicles through map matching*, In proceedings of the Institute of Navigation (ION) annual conference, 20-23 September, Salt Lake City, Utah.

Scott, C.A., Drane, C.R., 1994, *Increased accuracy of motor vehicle position estimation by utilizing map data, vehicle dynamics and other information sources*. In: Proceedings of the Vehicle Navigation and Information Systems Conferences, 585-590.

Seeber, G., 2003, *Satellite geodesy*, De Gruyter, New York.

Shen, X., Gao, Y., 2002, Kinematic processing analysis of carrier phase based precise point positioning, FIG XXII International Congress, Washington D. C. USA, Arial 19-26.

Sheridan, K., 2001, *Service requirements document (SRD) for vehicle performance and emissions monitoring system (VPEMS)*, Centre for Transport Studies, Department of Civil and Environmental Engineering, Imperial College London.

Spilker, J., 1996, *Satellite constellation and geometric dilution of precision*. In: Parkinson, Spilker (eds.), Vol. 1, Chap. 5: 177-208.

Srinivasan, D., Cheu, R.L., 2003, *Development of an improved ERP system using GPS and AI techniques*, IEEE Proceedings on Intelligent Transportation Systems, 554-559.

Sugeno, M., 1985., *Industrial applications of fuzzy control*, Elsevier Science Pub. Co.

Syed, S., Cannon, M.E., 2004, *Fuzzy logic-based map matching algorithm for vehicle navigation system in urban canyons*. In proceedings of the Institute of Navigation (ION) national technical meeting, 26-28 January, California, USA.

Tanaka, J., Hirano, K., Itoh, T., Nobuta, H., Tsunoda, S., 1990, *Navigation system with map-matching method*. Proceeding of the SAE International Congress and Exposition, pp 40-50.

Taylor, G., Blewitt, G., Steup, D., Corbett, S., Car, A., 2001, *Road Reduction Filtering for GPS-GIS Navigation*, Transactions in GIS, ISSN 1361-1682, 5(3), 193-207.

TfL (Transport for London), 2004, *London Busses-Countdown.*
http://www.tfl.gov.uk/buses/ini_countdown.shtml, accessed July 2004.

Tiberius, C., Pany, T., Eissfeller, B., Joosten, P., Verhagen, S., 2002, 0.99999999 confidence ambiguity resolution with GPS and Galileo, GPS Solutions 6, 96-99.

Tsui, J.B., 2000, *Fundamentals of global positioning system receivers: a software approach*, John Wiley and Sons.

US DoA., 2003, *Engineering and design: NAVSTAR global positioning system surveying*, EM 1110-1-1003, US Army Corps of Engineers, Washington, D.C.

US DoD., 2001, *Global Positioning System Standard Positioning Service Performance Standard.* Assistant secretary of defense for command, control, communications, and intelligence.

Vickrey, W., 1969, *Congestion theory and transport investment*, American Economic Review, 59(3), 251-260.

Wang, J., Yang, G., 2004, *Identification of GPS positioning solutions deteriorated by signal degradations using a fuzzy inference system,* GPS Solutions, 8(5): 245-250.

Westmeyer, P., 1981, *A guide for use in planning and conducting research projects*. Springfield, IL: Charles C. Thomas.

Weymann, J., Farges, J.-L., Henry, J.-J., 1995, *Dynamic route guidance, congestion and disobedience*, Control Eng. Practice, 3(4), 525-533.

White, C.E., Bernstein, D., Kornhauser, A.L. ,2000, *Some map matching algorithms for personal navigation assistants*. Transportation Research Part C 8, 91-108.

Wong, W.S., Leung C.M, 2000. *Location management for next generation personal communication networks*. *IEEE Network*, 14(5):18-24.

Xu, A.G., Yang, D.K., Cao, F.X., Xiao, W.D., Law, C.L., Ling, K.V., Chua, H.C., 2002, *Prototype design and implementation for urban area in-car navigation system*, IEEE 5th International Conference on Intelligent Transportation Systems, 3 - 6 September, Singapore.

Yang, D., Cai, B., Yuan, Y., 2003, *An improved map-matching algorithm used in vehicle navigation system*, IEEE Proceedings on Intelligent Transportation Systems, 2, 1246-1250.

Zadeh, L.A., 1965, *Fuzzy sets, Information and Control*, 8, 338-353.

Zadeh, L.A., 1973, *Outline of a new approach to the analysis of complex systems and decision processes*. IEEE Transactions on Systems, Man, and Cybernetics, 3 (1), 28-44.

Zadeh, L.A., 1989, *Knowledge representation in fuzzy logic*. IEEE Transactions on Knowledge and Data Engineering, 1, 89-100, 1989.

Zhao, Y., 1997, *Vehicle Location and Navigation System*. Artech House, Inc., MA.

Zhao, L., Ochieng, W.Y., Quddus, M.A, Noland, R.B., 2003, *An Extended Kalman Filter algorithm for Integrating GPS and low-cost Dead reckoning system data for vehicle performance and emissions monitoring.* The Journal of Navigation, 56, 257-275.

Frequently Used Acronyms

ANFIS : Adaptive Neuro Fuzzy Inference System

APTS : Advanced Public Transportation Systems

ATIS : Advanced Traveller Information Systems

ATMS : Advanced Transportation Management Systems

ATT : Advanced Transport Telematics

ATTS : Advanced Transport Telematics Systems

AVL : Automated Vehicle Location

AVCS : Advanced Vehicle Control Systems

AS : Anti Spoofing

CAD : Computer Aided Dispatch

CVO : Commercial Vehicle Operations

CCTV : Closed Circuit Television

DD : Double Difference

DETR : Department of the Environment, Transport and the Regions

DoD : Department of Defence

DGPS : Differential Global Positioning System

DOP : Dilution of Precision

DoT : Department of Transportation

DSRC : Dedicated Short Range Communications

DR : Deduced Reckoning

DRMS : Distance Root Mean Square

DTM : Digital Terrain Model

EDINA : Edinburgh Data and INformation Access

EFC : Electronic Fare Collection

EKF : Extended Kalman Filter

FIS : Fuzzy Inference System

ERP : Electronic Road Pricing

FAR : False Alarm Rate

FOC : Full Operational Capability

FRP : Federal Radio-navigation Plan

GDF : Geographic Data File

GDOP : Geometric Dilution of Precision

GIS : Geographic Information Systems

GLONASS : GLObal NAvigation Satellite System

GNSS : Global Navigation Satellite Systems

GPRS : General Package for Radio Service

GPS : Global Positioning Systems

GSM : General System for Mobile

HDOP : Horizontal Dilution of Precision

HFOM : Horizontal Figure of Merit

ICAO : International Civil Aviation Organization

IGS : International GNSS Service

IMP : Initial Map-matching Process

IMU : Inertial Measurement Unit

INS : Inertial Navigation Systems

ITS : Intelligent Transportation Systems

KOF :Kinematic on the Fly

MDR : Missed Detection Rate

MEMS : Micro-Electro Mechanical Systems

MF : Membership Function

MMT : Multiple Hypothesis Technique

MPJ : Matching Process at Junctions

NAVSTAR : NAVigation System with Timing And Ranging

NRC : National Research Council

OCDR : Overall Correct Detection Rate

OLS : Ordinary Least Squares

OS : Ordnance Survey

PDOP : Position Dilution of Precision

PNR : Pseudo Random Noise

PPP : Precise Point Positioning

PPS : Precise Positioning Service

RAIM : Receiver Autonomous Integrity Monitoring

RF : Radio Frequency

RMS : Root Mean Square

RNP : Required Navigation Performance

RS : Reference Station

SA : Selective Availability

SCOOT : Split Cycle Offset Optimisation Technique

SD : Single Difference

SIS : Signal in Space

SMP : Subsequent Map-matching Process

SMPL : Subsequent Matching Process on a Link

SOL : Safety of Life

SPS : Standard Positioning Service

TD : Triple Difference

TDOP : Time Dilution of Precision

TfL : Transport for London

TOA : Time of Arrival

TSE : Total System Error

TTFF : Time-to-first fix

UERE : User Equivalent Range Error

UKOS : UK Ordnance Survey

USGS : United States Geological Survey

UTC : Coordinated Universal Time

VDOP : Vertical Dilution of Precision

VPEMS : Vehicle Performance and Emissions Monitoring System

Publications

1. Quddus, M.A., Noland, R.B., Ochieng, W.Y., 2004, Validation of map matching algorithm using high precision positioning with GPS. *Journal of Navigation* 58, 257-271.

2. Ochieng, W.Y., Quddus, M.A., Noland, R.B., 2004, Positioning algorithms for transport telematics applications. *Journal of Geospatial Engineering* 6 (2), 10-30.

3. Quddus, M.A., Ochieng, W.Y., Lin, Z., Noland, R.B., 2003, A general map-matching algorithm for transport telematics applications, *GPS Solutions* 7(3), 157-167.

4. Ochieng, W.Y., Quddus, M.A. and Noland, R.B., 2003, Map matching in complex urban road networks, *Brazilian Journal of Cartography* 55 (2), 1-18.

5. Zhao, L., Ochieng, W.Y., Quddus, M.A., Noland, R.B., 2003, An extended Kalman filter algorithm for integrating GPS and low cost dead reckoning system data for vehicle performance and emissions monitoring, *Journal of Navigation* 56 (2), 257-275.

6. Ochieng, W.Y., North, R., Quddus, M.A., Noland, R., Polak, J., 2005, Developing an integrated Vehicle Performance and Emissions Monitoring System, *Transactions of Nanjing University of Aeronautics and Astronautic,* 22(2), 39-43.

7. Quddus, M.A., Noland, R.B., and Ochieng, W.Y, 2005, A fuzzy logic-based map matching algorithm for road transport. Presented at the 37th Annual Universities' Transport Study Group (UTSG) conference, Bristol, UK and submitted to *Journal of Intelligent Transportation Systems: Technology, Planning, and Operations*.

8. Quddus, M.A., Noland, R.B., and Ochieng, W.Y., 2005, The effects of navigation sensors and digital map quality on the performance of map matching algorithms, Submitted to *Computer-aided Civil and Infrastructure Engineering Journal.*

9. Quddus, M.A., Noland, R.B., and Ochieng, W.Y., 2005, Integrity for the navigation module of advanced transport telematics systems (ATTS), Submitted to *Transportation Research C.*

10. North, R.J., Ochieng, W.Y., Quddus, M.A., Noland, R.B., Polak, J.W., 2005, Validation and characterisation of a vehicle performance and emissions monitoring system, *Transport: Proceedings of the Institution of Civil Engineers* 158: 167-177.

11. Ochieng, W.Y., Quddus, M.A. and Noland, R.B., 2004, Integrated positioning algorithms for transport telematics applications. Proceedings of the Institute of Navigation (ION) *GNSS 2004* Conference, Long Beach, California.

12. Quddus, M.A., 2004, An enhanced map matching algorithm for vehicle performance and emissions monitoring system. Presented at the 36th Annual *Universities' Transport Study Group (UTSG) conference*, Newcastle, UK.